An experimental investigation of the scale effects observed in mine waste rock

Thesis presented in fulfilment of the requirements for the degree of Master of Engineering in the Faculty of Engineering at Stellenbosch University

By

Shane Tabor Teek

Supervisor: Mrs Nanine Fouché (Stellenbosch University)

Co-supervisor: Professor Thomas Pabst (Polytechnique Montréal, RIME, Canada)

Department of Transport and Geotechnical Engineering

Faculty of Engineering (Civil)

Stellenbosch University

March 2021

Stellenbosch University https://scholar.sun.ac.za

UNIVERSITEIT•STELLENBOSCH•UNIVERSITY
jou kennisvennoot • your knowledge partner

Plagiaatverklaring / Plagiarism *Declaration*

1 Plagiaat is die oorneem en gebruik van die idees, materiaal en ander intellektuele eiendom van ander persone asof dit jou eie werk is.
Plagiarism is the use of ideas, material and other intellectual property of another's work and to present is as my own.

2 Ek erken dat die pleeg van plagiaat 'n strafbare oortreding is aangesien dit 'n vorm van diefstal is.
I agree that plagiarism is a punishable offence because it constitutes theft.

3 Ek verstaan ook dat direkte vertalings plagiaat is.
I also understand that direct translations are plagiarism.

4 Dienooreenkomstig is alle aanhalings en bydraes vanuit enige bron (ingesluit die internet) volledig verwys (erken). Ek erken dat die woordelikse aanhaal van teks sonder aanhalingstekens (selfs al word die bron volledig erken) plagiaat is.
Accordingly all quotations and contributions from any source whatsoever (including the internet) have been cited fully. I understand that the reproduction of text without quotation marks (even when the source is cited) is plagiarism.

5 Ek verklaar dat die werk in hierdie skryfstuk vervat, behalwe waar anders aangedui, my eie oorspronklike werk is en dat ek dit nie vantevore in die geheel of gedeeltelik ingehandig het vir bepunting in hierdie module/werkstuk of 'n ander module/werkstuk nie.
I declare that the work contained in this assignment, except where otherwise stated, is my original work and that I have not previously (in its entirety or in part) submitted it for grading in this module/assignment or another module/assignment.

Studentenommer / *Student number*	**Handtekening / *Signature***
S. T. Teek **Voorletters en van / *Initials and surname***	5 February 2021 **Datum / *Date***

Stellenbosch University https://scholar.sun.ac.za

Plagiarisim Declaration

By submitting this thesis/dissertation electronically, I declare that the entirety of the work contained therein is my own, original work, that I am the sole author thereof (save to the extent explicitly otherwise stated), that reproduction and publication thereof by Stellenbosch University will not infringe any third party rights and that I have not previously submitted in its entirety or in part submitted it for obtaining any qualification.

March 2021

Copyright © 2021 Stellenbosch University All rights reserved

Stellenbosch University https://scholar.sun.ac.za

Abstract

The Direct Shear test remains a cornerstone of the geotechnical industry, despite the well-known inherent drawbacks presented by this test method. The primary objective of this dissertation was to systematically investigate the effects of Shear Mould size, particle shape and specimen gradation on the resultant Direct Shear strength parameters, shedding light on the scale effects present in the Direct Shear Test.

Experimentally it has been found that the peak shear strength measured in Direct Shear tests on a given material decreases with the length and increases with the height scales of the test specimen. The aspect ratio provided a unique lens through which to study the opposing effects of the Shear Mould length and height scales on the macromechanical shear behaviour of granular materials. By assessing the combined effects of the specimen length and height scales, by means of the aspect ratio, an inflexion point was identified where the macromechanical (i.e. shear strength and related) behaviour became less uniform and more difficult to predict.

Grain shape and particle regularity are important factors that may determine the repeatability of direct shear tests conducted near the maximum box scale ratios suggested by ASTM D3080-11, e.g. increased uniformity in the particle shapes of test specimens seemingly reduced the errors associated with test results.

Other key findings of the present study include observations made on the effects of grain size distributions and the Shear Mould aspect ratio and their effects. Well-graded grain size distributions yielded greater strength parameters, but only at smaller box length scales; when the box length scale was increased, the poorly-graded grain size distribution yielded greater peak strength parameters. The peak stress ratio is typically inversely proportional to the aspect ratio of the Shear Mould size and has been shown to fit an exponential function.

Stellenbosch University https://scholar.sun.ac.za

Opsomming

Die Direkte Skuifboks Toets bly die hoeksteen van die geotegniese industrie, ten spyte van die bekende erkende nadele van hierdie toetsmetode. Die primêre doel van hierdie skripsie is om stelselmatig ‘n ondersoek te voltooi wat die effek van die ‘Shear Mould’ grootte, partikel vorm en gradering van ‘n monster op die gevolglike Skuifboks sterkteparameters te kan verduidelik en lig te werp op skaal-effekte wat voorkom in die Direkte Skuifboks Toets.

Dit is eksperimenteel bewys dat die piekspanningsparameters wat gemeet is gedurende Direkte Skuifboks Toetse verminder met die lengte en vermeerder met die hoogte-skale van die toetsmonster. Die beeldverhouding voorsien ‘n unike lens waardeur die opponerende gevolge van die ‘Shear Mould’ lengte- en hoogte-skale op die makromeganiese skuifgedrag van korrelmateriale kan bestudeer word. Deur die gekombineerde effekte van monster lengte- en hoogte-skale te beoordeel met die gebruik van die beeldverhouding, was ‘n infleksiepunt geidentifiseer waar die mikromeganiese (d.w.s. skuifsterkte en verwante) gedrag minder eenvormig word, en moeliker om te voorspel.

Die korrelvorm en partikel-reëlmaat is belangrike faktore wat die herhaalbaarheid van die Skuifboks Toetse naby die maksimum voorgestelde ASTM D3080-11 boksskaalverhoudings bepaal. So, byvoorbeeld, verminder die verhoogde eenvormigheid in korrelvorms van proefmonsters die foute wat geassosieer word met eksperimentele toetsresultate.

Ander kernbevindings van die huidige studie sluit in waarnemings van die effekte wat die verspreiding van verskillende korrelgroottes en ‘Shear Mould’ beeldverhoudings het. Goed gegradeerde korrelgrootte-verspreiding het groter sterkte parameters opgelewer, maar net op kleiner skaallengtes. Wanneer die bokslengte-skaal verhoog is, het die swak gegradeerde korrelgrootteverspreiding groter piekspanningsparameters opgelewer. In hierdie studie is die beeldverhouding tipies omgekeerd proporsioneel tot die piekspanningsverhouding, en dit pas by 'n eksponensiële funksie.

Stellenbosch University https://scholar.sun.ac.za

Acknowledgements

The following individuals and institutions are acknowledged and thanked for their respective contributions to this project, without them this dissertation would not have been possible:

- Mrs Nanine Fouché
- Professor Thomas Pabst
- Mr Leon Croukamp
- Dr Charles MacRobert
- Members of the geotechnical laboratory at Stellenbosch University - Dion, Eric and Gavin
- Mrs Vessela Hobson
- Ms Tahnee Otto
- Mrs Lynette Faber
- Mr Jerome Webster & Mrs Pamela Webster
- Mr Bernard Besseling & Mrs Katrien Besseling
- Mr Dirk van Rooyen
- Mrs Marjo Hofman (of Control Geosciences, Cape Town)
- The students in the S477 office at Stellenbosch University
- The students and Staff at Polytechnique Montréal, who taught me so much and gave me many great memories
- Last, but not least: The Teeks - Alan, Andy, Angeles, Emma, Kae, Justin and Olivia

Stellenbosch University https://scholar.sun.ac.za

"We wish to pursue the truth no matter where it leads — but to find the truth, we need imagination and scepticism both. We will not be afraid to speculate, but we will be careful to distinguish speculation from fact. The cosmos is full beyond measure of elegant truths; of exquisite interrelationships; of the awesome machinery of nature." – Carl Sagan

Stellenbosch University https://scholar.sun.ac.za

Table of Contents

Stellenbosch University https://scholar.sun.ac.za

Stellenbosch University https://scholar.sun.ac.za

Stellenbosch University https://scholar.sun.ac.za

Stellenbosch University https://scholar.sun.ac.za

List of Figures

Stellenbosch University https://scholar.sun.ac.za

Stellenbosch University https://scholar.sun.ac.za

Stellenbosch University https://scholar.sun.ac.za

Stellenbosch University https://scholar.sun.ac.za

Stellenbosch University https://scholar.sun.ac.za

List of Tables

Stellenbosch University https://scholar.sun.ac.za

Nomenclature and Technical Abbreviations

USCS – Unified Soil Classification System

WRG – West Rand Group

DEM – Discrete Element Method

WR – Waste Rock

CRG – Central Rand Group

ASTM – American Society of Testing and Materials

GP – Poorly-Graded Gravel

GW – Well-Graded Gravel

D_{max} – Maximum particle size diameter

D_{min} – Minimum particle size diameter

PSD – Particle Size Distribution

SU – Stellenbosch University

DS – Direct Shear

H – Height of Shear Box

L – Length of Shear Box

Gs – Specific gravity of soil particles

Particle-box ratio – Ratio between either the box length or the box height and the D_{max}

ϕ’ – Drained friction angle (˚) and/or peak friction angle (˚), or in the case of the direct shear test the undrained friction angle (˚)

c’ – Drained cohesion (kPa)

Python – Freely-available and universal, high-level scientific computing program

Residual – The difference between the expected value (as predicted by a model or fitted curve) and the experimentally observed value

LVDT – Linear variable differential transformer

Stellenbosch University https://scholar.sun.ac.za

Oversize fraction – Particles with diameters that exceed the permissible size for a given Direct Shear apparatus

Box scale ratio – The ratios recommended in ASTM 3080 – 11 which are to be implemented during the undertaking of a direct shear test, between the particle diameter and the box length, and the box height, as well as the ratio between the box length and the box height

Shear Box mould (or Shear Mould) – The components associated with a set of dimensions for a particular Shear Box setup (e.g. 100[L] x 24.5[H] mm requires the appropriately-sized upper and lower Shear Box halves, two alignment screws, a load cap, and an upper and lower grip plate)

Convolution – A moving average function available in the data science software package Python

Stellenbosch University https://scholar.sun.ac.za

Chapter 1 – Introduction

1.1 Background

Despite waste rock piles being complex geotechnical structures, little information exists on the shear strength of mine waste rock (Blight, 2010). The lack of understanding of shear behaviour coupled with poor mine waste rock management practises can compromise mine resource recovery, mine safety and result in environmental consequences (Kainthola *et al.*, 2011). The lack of information exists mainly as a consequence of waste rocks lack of economic significance in the mining cycle (Spitz and Trudinger, 2003; Azam *et al.*, 2007, 2009; Martin *et al.*, 2017). Due to the coarse-grained nature of the particle sizes, conventional laboratory shear strength testing equipment cannot be used.

A limited number of studies have been conducted based on field tests using a constructed *in situ* direct shear (DS) box (Fakhimi and Hosseinpour, 2008; Gao *et al.*, 2017). Other studies have obtained information on the shear strength of waste rock by modifying the grain size distribution (Azam *et al.*, 2009; Zou *et al.*, 2018). Furthermore, shear strength data has been derived from large-scale laboratory or *in-situ* DS apparatus to comply with the box scale ratios defined by ASTM 3080 – 11 (ASTM, 2011). The maximum allowable particle size to be used in any DS test apparatus has been recognised to be too conservative (Cerato and Lutenegger, 2006; Wang and Gutierrez, 2010).

More information needs to be acquired to understand the effects of the ASTM box scale ratios on the returned shear strength of soils. A better understanding of these box-scale ratios, i.e. particle size (D_{max}) with respect to the Shear Box mould, would generate more reliable shear strength data, which ultimately limits failures in waste rock piles (Hicher, 2012).

1.2 Problem Statement

There is general disagreement in the literature with the internal box length (L) and height (H) scale and aspect ratios (L/H) in the DS test outlined in the ASTM D3080-11 standard. Recently, numerous authors have argued that stricter box scale ratios (i.e. the allowable L/Dmax and H/Dmax ratios should be increased) and should be employed when determining soil strength parameters (Jacobson, Valdes and Evans, 2007; Wu, Matsushima and Tatsuoka, 2007; Wang and Gutierrez, 2010; Wen-Jie, Qiang and Rui-Lin, 2011; Moayed, Alibolandi and Alizadeh, 2016). The need for accurate and reliable soil strength data derived from the DS test is critical to safe long-term management and stability of (among other applications) mine waste rock piles (Cerato and Lutenegger, 2006; Chang, Cerato and Lutenegger, 2010; Wang and Gutierrez, 2010; Hicher, 2012). Due to the scrutiny of the box-scale ratios presented in the ASTM 3080 standard, there is a need for determination of the most suitable box-scale ratios to be employed to gain the most reliable shear strength results.

Stellenbosch University https://scholar.sun.ac.za

1.3 Objectives

The main objective of this project is to investigate whether the recommended limiting maximum particle size to box ratio and aspect ratios (or box scale ratios) specified in the ASTM D3080-11 standard are reasonable when intending to diminish the scale effects present in the DS test. To achieve this aim, several smaller sub-objectives were identified:

1. Determine the macromechanical effects of the systematic variation of the DS box-length scale and -height scale, to assess their independent effects on the peak shear strength parameters of crushed Witwatersrand waste rock.
2. Assess the macromechanical effect of the aspect ratio (the combined effects of box length and height scale) on the DS test peak strength parameters.
3. Investigate the effect of the particle size distribution (PSD) on the macromechanical strength behaviour when exceeding the recommended box scale ratios in the ASTM D3080-11 standard.
4. Investigate the variations in particle shape of the Witwatersrand mine waste rock after collection and after crushing.
5. Assess the variation of particle shapes of the crushed Witwatersrand mine waste during preparation and after shear tests have been conducted.

1.4 Scope of the Present Study

To achieve the first objective, an experimental testing program was proposed to systematically vary the Shear Box length and height scale independently of one another in the commercially available DS apparatus at Stellenbosch University (SU). Two unique particle size distributions (PSD) classified as well-graded gravelly-sand (GW) and a poorly-graded gravelly-sand (GP) was generated by making use of random numbers in the Microsoft Excel software package. This PSD was generated to ensure that the maximum and minimum particle size diameters (of the PSD), in ratio to the box length and height-scales, exceeded the ASTM D3080-11 box scale ratio recommendations in the conventional Shear Box mould. This PSD was reconstituted and tested in the SU laboratory using the available DS apparatus, and crushed Witwatersrand mine waste rock was used as a study medium. The second objective was achieved by generating several graphs that displayed the trends in peak stress ratio and shear strength, with changes in the aspect ratio of the DS test box (i.e. the variation of the length- and height-ratio, as the box scales changed). The third objective was achieved by modifying the original well-graded PSD in a way that the maximum particle size diameter remained constant but the minimum particle size diameter was increased. This resulted in a poorly-graded gravelly-sand material, which was tested following the same protocol as the original material. The fourth and fifth objectives were achieved by classifying and comparing grain samples of the field-derived waste rock and the crushed, untested, well- and poorly-graded sample specimens according to a grain classification chart devised by Krumbein and Sloss (1963).

Stellenbosch University https://scholar.sun.ac.za

1.5 Limitations of Research

The limitations of this study relate to the fixed dimensions of the industry-grade Shear Box device, which Stellenbosch University (SU) presently has available for use. The Shear Box apparatus at SU had sample lengths (*L*) of 60 mm and 100 mm. The nature of the DS test devices for both the box sizes available at SU allowed for a minor variation in the height (*H*) of the specimen. These limitations were overcome by designing and implementing an 'insert' into the 60 mm DS sample housing, allowing for a reduction of the DS box's internal length to 20 mm (L). The implementation of the 'insert' was ensured a full-transgression (and beyond) of the scope of the prescribed ASTM D3080-11 box scale ratios. This included samples which conformed to and those which did not conform to the recommended box scale ratios proposed by ASTM D3080-11, i.e. $L/D_{max}>10$, $H/D_{max}>6$ and L: H > 2: 1 (ASTM, 2011). The internal design length of the insert was based on three preliminary designs which were ultimately designed based on what was possible to be fabricated using what was available in the SU mechanical engineering department's workshop. Moreover, considering that physical experiments were conducted, the present study only assessed the macromechanical shear behaviour.

1.6 Report Layout

This dissertation is divided into six distinct chapters:

1. The first chapter serves as an introduction to the project, defining the scope of the project by highlighting the key aim, objectives and limitations of the project.
2. The second chapter involves a detailed literature review of waste rock pile construction and characteristics of granular soils shear strength, i.e. the factors which inherently affect the strength of a granular media. Moreover, a review of several crucial past works conducted to delineate the respective origins of scaling effects presented in the DS test is provided. This consists of a review of the factors which affect the DS test results, and includes, where and how scaling effects arise in the DS test and the background information necessary to understand the DS test.
3. The third chapter describes the test methodology of the DS tests that were conducted during this study. Moreover, the sample preparation for the tests conducted and the locality of origin of the test materials are described.
4. The fourth chapter presents a summary of the results and their interpretation.
5. The fifth chapter is a discussion of the DS test results from the crushed Witwatersrand waste rock. In this chapter, the scaling effects which arise from variations in box scale ratios are discussed.
6. The sixth chapter concludes the research, summarizing the major findings of the study and proposes recommendations for further research on the topic.

Stellenbosch University https://scholar.sun.ac.za

Chapter 2 – Literature Review

This chapter introduces mine waste, associated production and presents an overview of the common geotechnical parameters for waste rock piles. Thereafter, an appraisal of the geotechnical parameters governing the shear strength of granular materials is given, this includes an overview of the DS test and its shortcomings, and a review of the sample scaling techniques. Finally, the variables and their controls on the scale effects associated with the DS test are identified.

2.1 Mine Waste

Waste generation during the mining process is inevitable (Spitz & Trudinger, 2003). To meet global resource demands; increasing quantities of mine wastes are being generated; this coupled with increased volumes of waste, there is also pressing environmental concern. There is a need for characterisation of site-specific mine waste to effectively manage and store it sensibly and sustainably (Blight, 2010; Vallero & Blight, 2019). Mining produces several types of waste, the amount generated globally is complex to quantify; in 1996, the International Committee on Large Dams (ICOLD) estimated that globally the mining industry generated over 5 thousand million tonnes of waste per annum (ICOLD, 1996; Vallero & Blight, 2019). Given that globally the demand for resources is increasing, the need for mining prevails; encouraging the mining of lower-grade ores, which elevates the accompanying quantity of waste that is produced (Vallero & Blight, 2019). The amount of mine waste generated at a particular mine site is determined by the stripping ratio and the principal components of mine waste can be divided into waste rock and tailings (Figure 2-1).

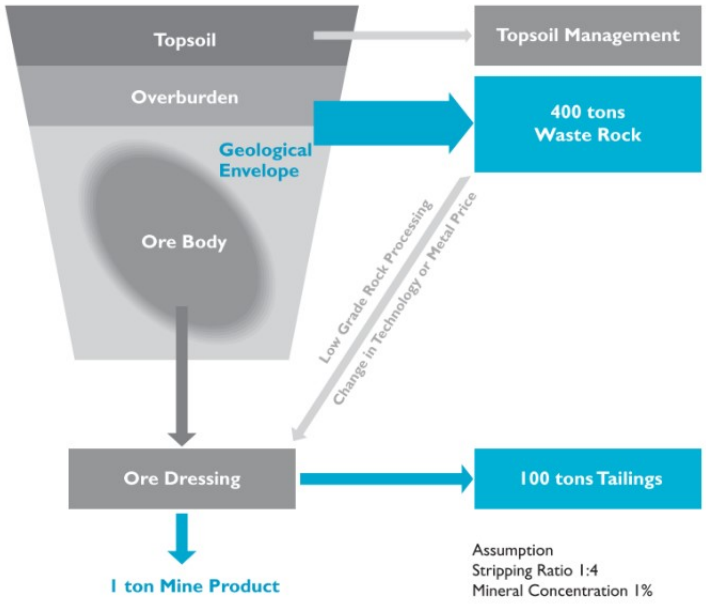

Figure 2-1. Schematic of mining waste streams (Spitz and Trudinger, 2003)

Stellenbosch University https://scholar.sun.ac.za

Broadly, mine waste is stored based on the material's size, and typically two distinct size-fractions exist: i) finer mine tailings and industrial-type wastes, and ii) often much coarser mine waste rock (Blight, 2010). The fine material is stored in tailings dams and the coarse fraction is stored in stockpiles. The derivation of waste rock results as a by-product of mining, it is generally derived from overburden or barren country rock that overlies (or surrounds) the orebody and is devoid of any mineralization. The waste rock component is usually stockpiled and may later be processed, depending on the grade and the composition of the waste rock material (Spitz & Trudinger, 2003; Figure 2-1).

The material used for the present study is mine waste rock and was sourced from Witwatersrand Basin, South Africa, a well-known gold mining region, boasting reserves that are unlike any other on the planet (Frimmel, 2019). Approximately 33% (~53, 000 t) of the world's gold production has originated in this basin to date and it represents almost a third of the worlds remaining gold reserves, much of which, is currently unattainable due to the depths at which the ore was emplaced. The great depths at which these valuable metals are hosted within the Witwatersrand basin has lead to some of the world's deepest mines, the record holder; however, is always subject to change (Potvin, Hadjigeorgiou & Stacey, 2007; Hudyma & Potvin, 2010; Tynan *et al.*, 2017). Despite the challenges associated with ores emplaced at great depth, considerable amounts of waste were generated in less than 10 years (1997 – 2006) a cumulative 74 x 10^4 tons of mine tailings were generated (Chamber of mines, 2006). Moreover, in the last century approximately 6 x 10^9 tons of gold mine tailings alone was produced in South Africa (Sutton, *et al.,* 2006).

Mine waste in the greater Witwatersrand region has caused a considerable amount of contaminants to be released into the surrounding environment (Chevrel *et al.*, 2003). No baseline studies were conducted before the inception of mining on the Witwatersrand began and often mine waste facilities were established on areas of land that had previously been deemed 'environmentally sensitive' (Sutton, Galpin & Heller, 2006). Shortly after mining of the Witwatersrand began, waste repositories (areas of mine waste storage) were erected on areas of known karst terrains as they were assumed to offer a high permeability and this ensured that the mechanical and chemical stability of the waste repository was increased (Sutton, Galpin & Heller, 2006). Unfortunately, this has subsequently been disproved and the now inexorable effects of acid mine drainage and acid rock drainage; have caused for stability and subsidence problems to develop beneath the aforementioned mine waste repositories (Sutton, Galpin & Heller, 2006).

Stellenbosch University https://scholar.sun.ac.za

2.2 Waste Rock Management

These coarse-grained stockpiles are widely referred to as waste rock- or overburden piles, and in Australia and New Zealand are sometimes termed a 'mullock' (Piteau, 1991; Spitz & Trudinger, 2003). For a comprehensive list of terms used in present and past literature refer to Fakhimi *et al.*, (2008) and Mclemore *et al.*, (2009). In any mining scenario, whether open-cast or underground, the generation of mine waste rock (by blasting and excavating) is unavoidable, as its removal grants access to the orebody (Figure 2-1). During mining, subeconomic material that is too low-a-grade to be put through beneficiation that is generated, is also sometimes referred to as 'waste rock' and is stockpiled in waste rock piles (Piteau, 1991). Once the blasted and/or excavated, the resultant waste rock is transported by mean of rubber-tyred tip-trucks or rail-tracked conveyor belts to the designated location where it is discarded or physically 'dumped' (Mclemore *et al.*, 2009). Waste rock is most often deposited in a moist or semi-dry state (Blight, 2010).

There are many factors to be considered when establishing the most favourable location for the establishment of a waste rock pile (Mclemore *et al.*, 2009). The factors can be summarised as follows, after Hawley *et al.*, (2017): Regulatory and social, mining (or operational), terrain and basement geology, environmental, geotechnical considerations, fill material quality; and, mine closure. Once the location has been selected, there are a few methods of constructing the waste rock pile and the method of construction selected is largely based on the prevailing topography (Mclemore *et al.*, 2009; Blight, 2010).

If these factors are not dealt with at length during the conceptual design phase of a mining project, in one or another way, the waste rock pile will affect the immediate environment through geotechnical or environmental hazards, or both. Numerous publications have pointed out safety and environmental problems, such as slope failures (Brawner & Broughton, 1991; Stormont & Farfan, 2005), acid rock drainage (Martin *et al.*, 2017a) and leaching of other toxic metals into the surrounding environment and ultimately water resources (often collectively termed: acid mine drainage or AMD) (Lapakko, 2002; Blight, 2010). Despite the available information in the literature, mine waste is generally an under-researched topic due to lack of economic significance, which only draws an estimated 1 – 3 % of an average mines total budget (EU Report cited in Hitch, 2010)

Stellenbosch University https://scholar.sun.ac.za

2.3 Waste Rock Pile Characteristics

2.3.1 Construction and Geometric

Once the factors for site selection have been considered, the waste dump is erected. The employed method of construction and the waste rock pile's geometry determine its shear behaviour, therefore, a review of these methods and geometric characteristics are considered appropriate. The selected method of construction and ultimately the geometry of the waste rock pile is based on the prevailing topography and location selected for the site of construction (Mclemore *et al.*, 2009).

When the topography of the rock dumpsite has been established, a method of dumping must be employed, the material dumped in five different ways namely; end dumping, push dumping, free dumping, drag-line spoiling or co-mixing of waste rock and tailings (Mclemore *et al.*, 2009). End, push and free dumping are the common methods employed in metal mining operations. When the waste rock material is either end-dumped (by truck) or push-dumped (by a bulldozer) the material follows the slope of the dump's sides (Figure 2-2); both methods favour particle segregation and internal layering of the constructed pile causing an accumulation of the coarsest particles at the base and finest at the top of the rock pile, this is known to cause zones of higher permeability (Mclemore *et al.*, 2009). During plug or free dumping, small piles of waste are dumped in laterally continuous layers that form new benches that successively raise the overall dump height, during this process the layers are compacted (Figure 2-2) (Blight, 2010; Hawley *et al.*, 2017).

Often, topography surrounding mines is mountainous, in which case, the waste rock pile may be erected on a ridge-top, on the side of a hill or may fill a valley; however, in the case of mines on the Witwatersrand the topography is generally flat and the waste rock is typically end-dumped in a 'heaped' configuration (Figure 2-3) (Blight, 2010). Waste rock piles, as a whole, prove to be complex geotechnical structures due to the lateral and vertical variation in properties, which is a consequence of the variety of materials with a range of engineering properties, that are stockpiled (Hitch, Ballantyne & Hindle, 2010). When this is not considered at length, or on-going monitoring/management of waste rock piles is not implemented, the waste rock pile may fail; the most remarkable example being the Aberfan disaster in Wales (Blight, 2010).

Field-based research has revealed that the mechanism of waste rock pile failure, develops as a 'double wedge'. The development of the double wedge is often a result of the settlement of loose material in the rock dump, consequently, several 'shear surfaces' develop, i.e. there is more than one active 'wedge' that contributes to the successive failure of the waste rock pile (Blight, 2010). The development of multiple planes in the waste rock pile causes localised increases in permeability, which enlarges the size of the surface seepage zone in the waste rock pile, especially during high rainfall periods (Figure 2-4). The development of these shear planes and the associated increased permeability phenomenon, along

Stellenbosch University https://scholar.sun.ac.za

with several often poorly characterised/misinterpreted geotechnical parameters for any site, can result in catastrophic failures (Blight, 2010; Hawley *et al.*, 2017; Zevgolis, 2018).

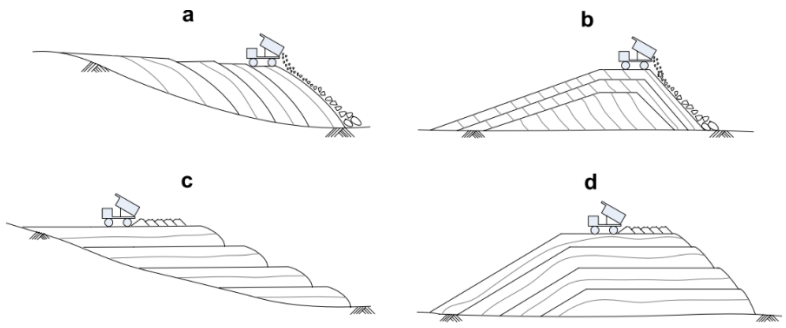

Figure 2-2. Typical methods of constructing mine waste rock piles with changes in topography: End dumping on a) inclined topography, and b) horizontal topography. Plug or free dumping on c) inclined topography, and d) horizontal topography (image retrieved from Zevgolis, 2018; modified after blight, 2010)

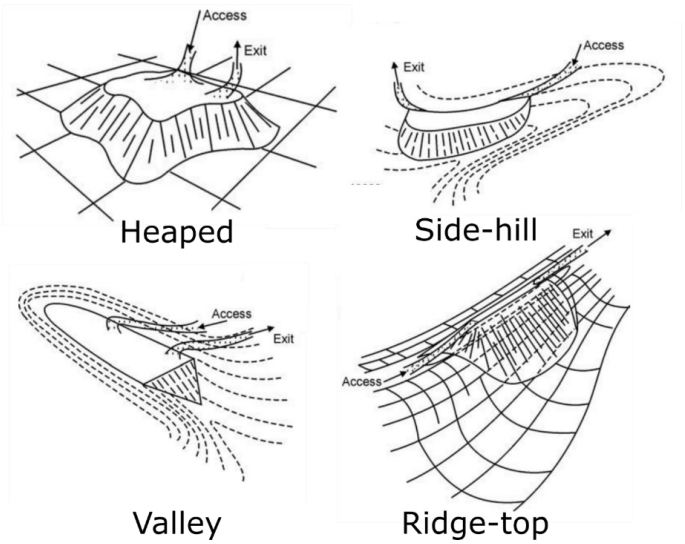

Figure 2-3. Waste rock pile geometry with prevailing topography (after Blight, 2010)

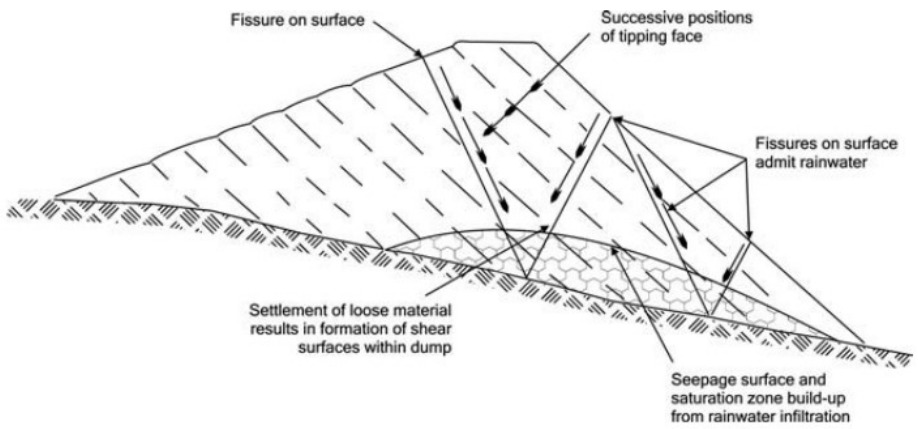

Figure 2-4. Fissure or failure development and seepage surface in an end-tipped waste rock pile (after Blight, 2010)

Stellenbosch University https://scholar.sun.ac.za

2.3.2 Geotechnical

Waste materials can be classified and assessed similarly to other geotechnical materials by making observations and undertaking tests on *in situ* materials, and by performing laboratory tests. The parameters that are often required for design purposes are as follows (after Blight, 2009):

1. Particle Characteristics and Size Distribution (PSD) or Granulometry,
2. Compaction characteristics,
3. Consolidation characteristics,
4. Bulk density,
5. Permeability or hydraulic conductivity,
6. Particle density, and
7. Shear strength parameters.

As the present study makes use of material from a mine waste rock pile as a study medium, a list of the typical parameters of waste rock piles is considered useful. Characteristics 1 - 7, as highlighted in subsequent sections, all influence the shear strength parameters of the material.

2.3.3 Typical Geotechnical Waste Rock Parameters

Waste rocks typically display wide gradations, ranging from the boulder size down to the clay fractions (Figure 2-5) (Blight, 2010). Waste rock is typically highly heterogeneous, with a wide variation in PSD, and may exhibit variation in one or another characteristic from the mine locality-scale to the meter scale within a single waste dump (Blight, 2010; Hawley *et al.*, 2017).

Typically, geotechnical properties used to characterise waste rock piles are highly variable, on and between sites, this is a consequence of the materials mined and the methods used vary widely between mine sites (Blight, 2010; Hawley *et al.*, 2017; Vallero and Blight, 2019). For example, the dry density of waste rock can vary anywhere between 1500 to 2650 kg/m^3 (Table 2-1). Consequentially, these parameters yield a wide spread in the strength parameters of waste rock material, for example, the friction angles and cohesion values of waste rock typically vary between 21˚ to 55˚, and 0 to (Table 2-2). No single geotechnical parameter directly governs the friction angle and cohesion of a given waste rock material.

It has, however, been shown that several parameters contribute to the magnitude of each of these properties in fine-grained materials, such as shales. For example, the friction angle is affected by the clay mineralogy (i.e. composition, absorption and adsorption of ions), and the Atterberg limits. Whereas, the cohesion is most affected by the clay mineralogy and the slake durability (Dick, Shakoor & Wells, 1994; Hajdarwish, 2006; McLemore, Fakhimi, van Zyl, Ayakwah, Anim, Boakye, Ennin, Felli, Fredlund, Gutierrez, Nunoo, Tachie-Menson & Viterbo, 2009).

Stellenbosch University https://scholar.sun.ac.za

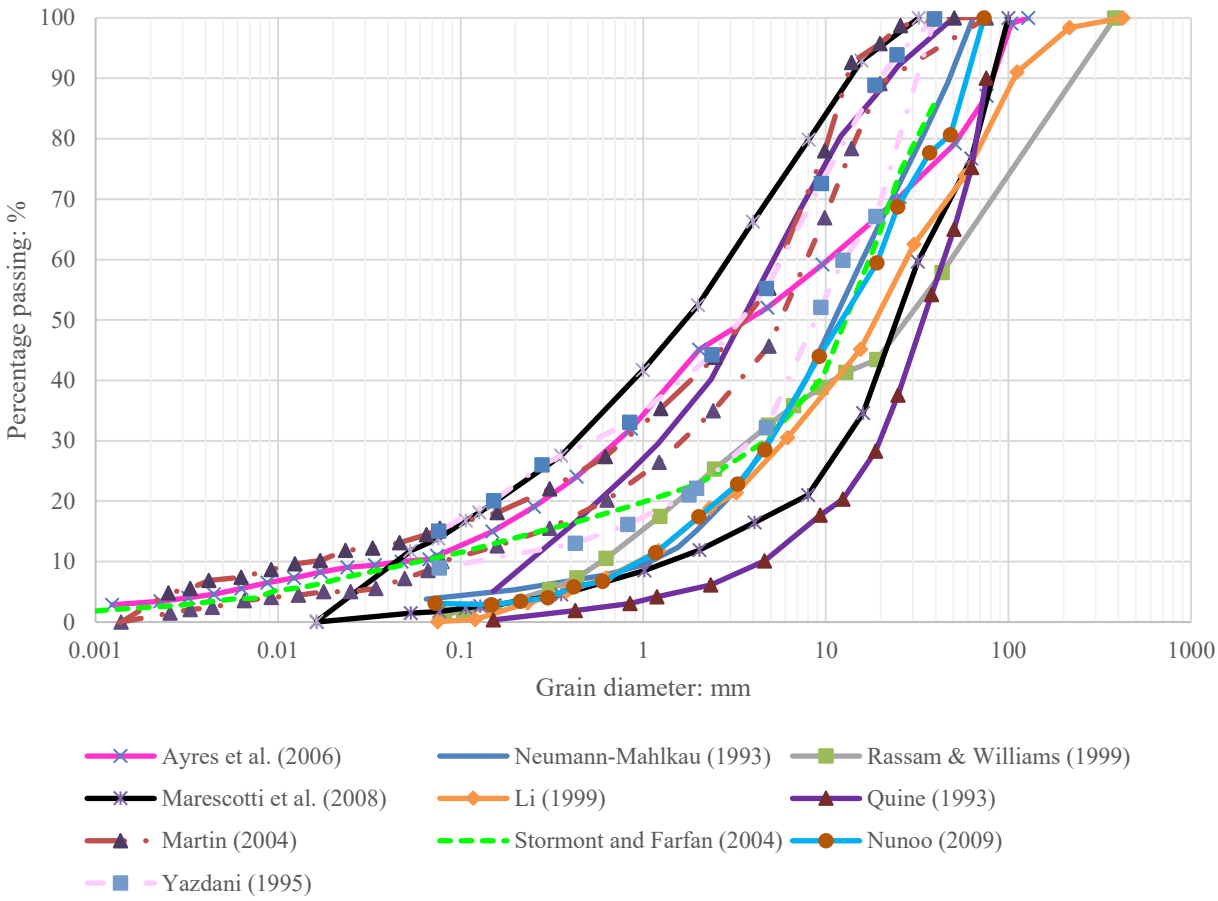

Figure 2-5. Several grain size distributions; in some cases, only upper and lower bounds are indicated, from waste rock piles found in the literature. The source of each curve can be found in the figure legend

Stellenbosch University https://scholar.sun.ac.za

Table 2-1. Characteristic geotechnical properties of waste rock from various mine sites (modified after McLemore *et al.*, 2009)

Mine	Mine rock material	Porosity (-)	Dry Density kg/m^3	Specific gravity	LL	PL	PI	Moisture Content (%)	USCS soil group	References
Tyrone, NM (heap leach)	Porphyry, granite	-	-	2.64 - 2.78	28 - 40	15 - 18	8 - 23	-	GC; GW - GC; SC	Earley *et al.* (2003)
Chino, NM (heap leach)	Porphyry, granite	-	1780 - 1930	2.63 - 2.75	26; 36	-	8; 13	4.2 - 15.1	GW - GC; GC	URS Corp. (2003)
Davis mine, Mass.	Schist, quartzite	0.35 - 0.55	2650	-	-	-	-	-	-	Adams *et al.* (2007)
Heath	Greenschist	-	2350	-	-	-	-	-	-	Nolan, Davis and Associates Limited (1991)
Stratmat, New Bruswick	Greenschist metamorphic rocks	0.264	2064 - 3250	-	-	-	-	-	-	Li (1999)
Ajo, Arizona	Volcanic rocks, monzonite	-	1610 - 2060	-	-	-	-	0.5 - 7	-	Savci and Williamson (2002)
Bonner, CO		-	1650 (*in situ*)	-	-	-	-	6 - 10	GP - GM	Stormont and Farfan (2005)
Golden Sunlight, Montana	Latite and diameter breccia pipe	0.221 - 0.335	1050 - 2100	2.63 - 2.78	-	-	-	4 - 39	SW; GP; GW	Azam *et al.* (2006)
Central Pit, Turkey	Sedimentary rocks	-	-	-	35	24	11	-	GC	Kasmer and Ulusay (2006)
Lignite Creek, Alaska	Sedimentary rocks	-	1500	-	19 - 20	15 - 18	2 - 4	-	SM	Kroeger *et al.* (1991)
Aberfan, England	Sedimentary rocks	-	1600 - 1940	2.1	-	-	-	-	-	Lucia (1981)
Equity		-	-	-	-	-	-	-	-	Saretzky (1998)
Kidston, Australia		0.4	-	2.65	-	-	-	-	-	Bews *et al.* (1997)
Midnight, WA (uranium)	Metamorphic rocks	-	1520 - 2000	2.75 - 2.84	19 - 52	-	1 - 29	-	-	URS Corp. (2003)
Lichtenbergpit, Germany		0.24	2100	2.75	-	-		-	-	Hockley *et al.* (2003)
Ohio coal dumps	Sedimentary rocks	-	1690 - 2130	-	24 - 43	15.0 - 26.2	4.5 - 19.6	4.4 - 18.2	GW; SW; GP; CL	Shakoor & Ruof (1989)
Yorkshire coal mine	Coarse discard	-	1500 - 1900	2.04 - 2.63	23 - 44	16 - 25	-	8 - 13.6	-	Bell (1996)
Brancepath coal mine	Coarse discard	-	1060 - 1680	1.81 - 2.54	23 - 42	0.00 - 35.0	-	5.3 - 11.9	-	Bell (1996)
Wharncliffe coal mine	Coarse discard	-	1390 - 1910	2.16 - 2.61	25 - 46	14 -21	-	6 - 13	-	Bell (1996)
Bogdanka coal mine, Lubelskie, Poland		-	1690 - 1750	-	-	-	-	11 - 21	-	Filipowicz & Borys (2005)
Sukinda Mine, India	Weathered ultrmafic mass, overlain by ferruginous laterite	0.4 - 0.61	1300 - 1630	2.935	-	-	-	2.5 - 27.64	-	Verma *et al.* (2017)
Diavik Mine, Canada	Granite, pegmatitic grainite (massive), biotite shist xenoliths	0.24	-	-	-	-	-	7 - 27	-	Smith *et al.* (2013a), (2013b), (2013c); Neuner *et al.* (2013)
Key Lake Mine, Canada	Hydrothermally altered quartz–chlorite–'sericite'–graphite schist regolith	-	-	-	-	-	-	15 - 30	-	Stockwell. *et al* (2006); Stockwell (2002)
Cluff Lake Mine, Canada	Aluminous and quartzo-feldspathic gneisses	-	1660 - 2300	-	-	-	-	-	-	Nichol (2002), (2005)
Lac Tio	Massive hematite–ilmenite ore band, massive anorthosites	0.27 - 0.30	1860 - 2230	2.75 - 4.23	-	-	-	-	SP - SW	Martin *et al. 2017*

Stellenbosch University https://scholar.sun.ac.za

Table 2-2. Strength properties of waste rock from various mine sites (modified after McLemore *et al.*, 2009)

Mine	Mine rock material	Internal friction angle (°) φ	Apparent cohesion (kPa) C	Normal stress range (kPa)	Comments	References
Tyrone, NM (heap leach)	Porphyry, granite	34.1 - 36.9	-	2.8-15.2		Earley *et al*. (2003)
Chino, NM (heap leach)	Porphyry, granite	34	0	234-819	Hoek-Brown method	URS Corp. (2003)
Lubelskie, Poland	Coal	Fresh: 32 - 55; 5 yrs old: 34 - 35; 7 yrs old: 27-37	20 - 32; 21 - 35; 25 - 40	-	With age: friction angle decreases and cohesion increases	Filipwicz & Borys (2004)
Upper Silesian, Poland		Fresh: 36-41; 8 yrs old: 21-29	18 - 23; 27 - 37	-	With age: friction angle decreases and cohesion increases	
Bouganville Copper Ltd., Papua, New Guinea	Fractured rock (Panguna andesite)	29 - 45	0	-	Triaxial test 15.24 mm diameter, Dmax=1.905 mm, samples comprise of moderately to slightly weathered rock with 20% fines	URS Corp. 2003
Endako, B.C., Canada	Molybdenum in quartz monzonite	36	490	766	Material properties: 30% >300 mm, 2% < no. 200 sieve	B.C. Mine Waste Rock Research Comm. (1991), URS Corp. (2003)
Bald Mountain, Nevada	Gold in Dundrberg Shale	39	172	-	Direct shear test, shear box 38.1 mm x 38.1 mm, Dmax=7.62 mm	Quine (1993)
Barrick Nevada	Gold in argillized granodiorite	38 - 40.3	83 - 139	-	Direct shear test, shear box 38.1 mm x 38.1 mm, Dmax=7.62 mm	Quine (1993)
Big Springs, Nevada	Gold in argillaceous siltstone	47 - 50	206 - 239	-	Direct shear test, shear box 38.1 mm x 38.1 mm, Dmax=7.62 mm	Quine (1993)
Candelaria, Nevada	Gold in siltstone and shale	43 - 47	90 - 239	-	Direct shear test, shear box 38.1 mm x 38.1 mm, Dmax=7.62 mm	Quine (1993)
Newmont, Nevada	Gold in siltstone/sandstone	35 - 51	69 - 205	-	Direct shear test, shear box 38.1 mm x 38.1 mm, Dmax=7.62 mm	Quine (1993)
Round Mountain, Nevada	Gold in rhyolite tuff	40 - 41.5	77 - 96	-	Direct shear test, shear box 38.1 mm x 38.1 mm, Dmax=7.62 mm	Quine (1993)
PT Freeport Grasberg, Indonesia	Gold porphyry and skarn	37 - 42.2; 39.6 - 40.4	34 - 64	-	Direct shear, Triaxial compression, consolidated, undrained	Walker and Johnson (2000); Infomine (2007)
Bonner, Colorado		37	5	-	Direct shear test, in situ shear box 76.2 mm x 76.2 mm x 40.6 mm	Stormont and Farfan (2005)
Equity Silver		37.5	-	345 - 800		URS Corp. (2003)
Midnight, Washington	Uranium in quartz monzonite, marble, and	32.6 - 43.7	0-29	-	Triaxial test: 10.16 mm diameter, Dmax=1.905 mm	URS Corp. (2003)
	calc-silicate rock	37	31	-	Triaxial test: 15.24 mm diameter, Dmax= 3.81 mm	
Brancepath coal mine	Coarse discard	31.5 - 35	19.44 - 21.41	-		Bell (1996)
Wharncliffe coal mine	Coarse discard	27.5 - 39.5	3.65-39.03	-		Bell (1996)
Bogdanka coal mine, Lubelskie, Poland	Coarse discard	29 - 37	16 - 40	-		Bell (1996)
Sukinda Mine, India	Weathered ultramafic mass, overlain by ferruginous laterite	44.56 (mean)	5.62 (mean)	-		Verma *et al*. (2017)
Not disclosed	-	37.67	1.67	-	Direct shear test: 100 x 100 x 30 mm, Dmax = 4.75	Azam *et al*. (2009)

Stellenbosch University https://scholar.sun.ac.za

2.4 Mohr-Coulomb Failure Criterion

The shear behaviour of waste rock is controlled by the granular characteristics of the material (Azam *et al.*, 2009). The most frequently used model to describe the shear strength of granular soils is the Mohr-Coulomb Failure criterion. Coulomb's main findings, among other things, were that there are two main contributing factors to the strength of soil, the cohesion and the friction of the soil. He noted that the friction within the soil (f) was equal to what today is denoted as $\tan \phi$ (where ϕ is the symbol describing the ratio between shear stress and normal stress). Coulomb also identified the position of the failure surface behind a retaining wall (Rengach, 1973).

A more general theory was developed by Christian Mohr, in 1900, to graphically display material stresses and their rupture with nonlinear behaviour (Nadai, 1950). Today, the integration of the theories developed by Coulomb (in 1776) and Mohr (in 1900) describe and model soil as a continual mass and approximate the non-linear relationship between shear-stress and normal-stress, or effective normal stress on a failure plane as a failure envelope (Figure 2-6). The relationship is initially non-linear as the strength of the soil is controlled by friction and the interlocking of particles, and thereafter it is only determined by friction alone (Craig and Knappett, 2012). This nonlinear relationship is approximated by the linear function:

$$\tau = c + \sigma \tan \phi \tag{2.1}$$

where c is the cohesion of the soil (kPa), σ is the total normal stress (kPa), and ϕ is the angle of the internal friction of the soil (measured in degrees) (Das, 2010). Equation (2.1) is usually modified by the removal of the pore water pressure (u_w) from the total stress, to account for the fact that shear stress cannot be resisted by water and that soil is a three phase material (Terzaghi, 1943; Terzaghi, Peck and Mesri, 1948; Powrie, 1997). The description of shear strength, when accounting for the effective stress principle, is governed by the substitution of Equation (2.2) into Equation (2.1).

$$\sigma' = \sigma - u_w \tag{2.2}$$

Yielding:

$$\tau = c' + \sigma' \tan \phi' \tag{2.3}$$

where c' is the effective cohesion (kPa), σ' is the effective stress within the soil (kPa), and ϕ' is the effective friction angle of the soil (˚). According to the British System of classification (BS 1377-2: 1990), a material which possesses particles larger than 0.075 mm in diameter is considered a coarse, or granular material with no cementation between particles (Mitchell and Soga, 2005). In this case, the cohesion term may be neglected as is most often the case with coarse granular materials which possess no plasticity, (Das, 2010):

Stellenbosch University https://scholar.sun.ac.za

$$\tau = \sigma' \tan \phi' \quad (2.4)$$

The shear strength of granular materials is primarily a result of the frictional resistance, and cohesion between particles (Burland, 2012b; Craig and Knappett, 2012; Powrie, 2012). There is a multitude of variables which affect the strength of soil, all of which may not vary independently of one another (Mitchell and Soga, 2005). Six main factors are influence coarse-grained materials behaviour, which includes the sample's overburden pressure; water content; relative density (or void ratio); gradation; and the soil particle's size, strength, and shape (Hawley, 2001; Holtz and Kovacs, 2003; Yu *et al.*, 2006).

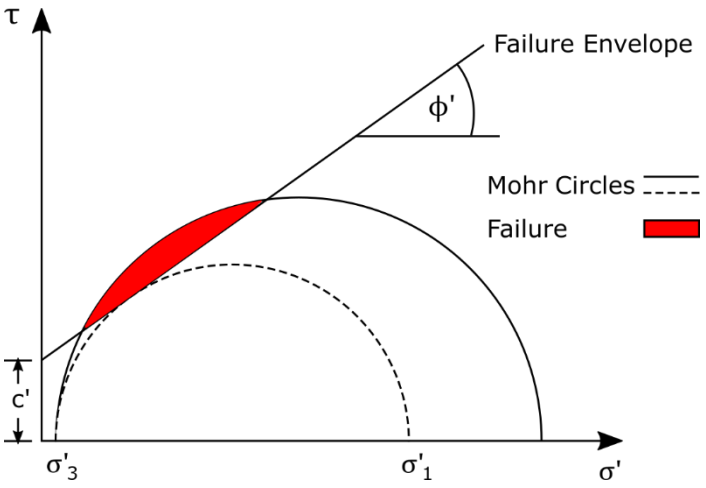

Figure 2-6. Graphical representation of Mohr-Coulomb failure criterion (after Das, 2010)

2.5 Factors Influencing Shear Strength

A summary of the main influencing parameters that affect the shear strength of granular material is listed in Table 2. Essentially, any characteristic that increases the interparticle contact area, will increase the resultant maximum shear resistance for a given soil (Hicher, 2012).

Table 2-3. Summary of factors affecting the shear strength of granular materials (after Holtz & Kovacs, 1981)

Factor	Effect
Void Ratio, *e* (relation to density – See Section 2.4)	*e*↑, ϕ↓
Water content (or saturation ratio), *w (Sr)*	*w*↑, ϕ↓ (slight)
Particle angularity, *A*	*A*↑, ϕ ↑
Surface roughness, *R*	*R*↑, ϕ ↑
Particle size	No effect (provided, *e* is constant)
Grain size distribution (PSD) classification, *Cu*	*Cu*↑, ϕ ↑
Overconsolidation or prestress	Negligible

Stellenbosch University https://scholar.sun.ac.za

Density is the primary parameter that influences the shear strength behaviour of soil, this parameter is controlled by several other variables (Terzaghi, Peck and Mesri, 1948; Simoni & Houlsby, 2006; Burland, 2012a). The void ratio reflects the packing, or closeness of particles within a given soil profile, and can be expressed as:

$$e = {}^{V_v}/_{V_s} \tag{2.5}$$

Where Vv is the volume of the voids (m^3) and Vs is the volume of the solids (m^3). Because of the nature of granular soils structure, soil particles rest upon one another in a soil mass (Figure 2-7). The frictional resistance of a soil mass is controlled by the friction between adjacent soil particles (Hicher, 2012). The friction between soil particles is a function of the contact area between the particles. (Terzaghi, Peck & Mesri, 1948). The tighter the packing of particles in a soil mass, the lower the volume of the voids, and consequently, the lower the void ratio. The lower the void ratio of the soil ultimately the higher the bulk density of the soil becomes:

$$\rho = {}^{[G_s \cdot \rho_w \cdot (1+w)]}/_{[1+e]} \tag{2.6}$$

Where G_s is the specific gravity of the individual soil particles (-), ρ_w is the density of water ($1000 kg/m^3$) and w is the water content of a soil, which is the ratio of the mass of water, to the mass of soil particles in a unit volume of soil.

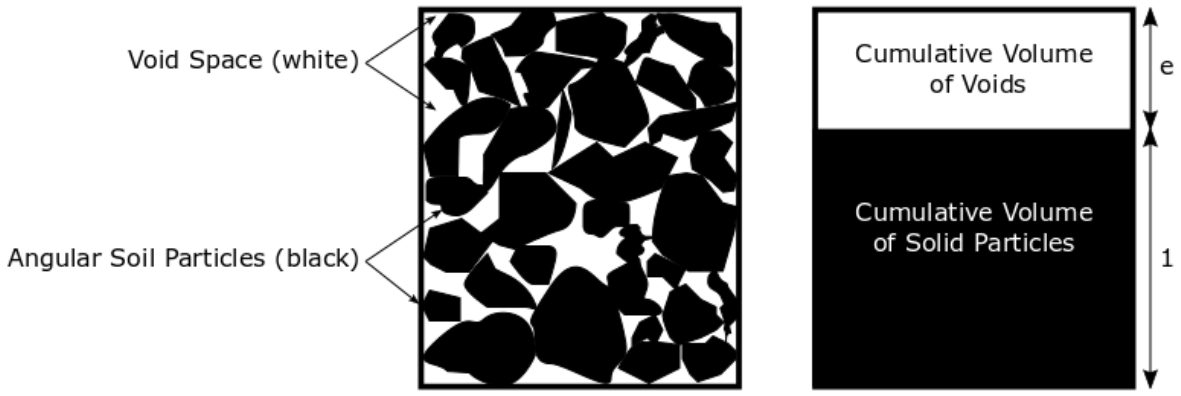

Figure 2-7. The particulate nature of soil. Depicts the void ratio as soil particles (left) and as one mass (right) in the same volume (after Burland, 2012)

2.5.1 Mineralogy

The mineralogy of a soil governs the shearing resistance of the said soil (Coduto, 2001; Terzaghi, Peck & Mesri, 2009). From equation 2.6, it is apparent that the density of soil particles plays a role in the bulk density of soil. The mean grain density (or G_s) of a soil is determined by the mineraology of the aggregate of particles hosted within the soil coloumn (Terzaghi, Peck & Mesri, 1948; Blake, 2008). It

Stellenbosch University https://scholar.sun.ac.za

is challenging to quantify the contribution to strength by individual grains of varying mineralogy, an attempt was made to define relations between mineralogy and sample strength by Terzaghi, (1943).

The results that Terzaghi, (1943) presented, indicated that varying the mineralogy, or composition of the material yields different shearing resistances at varying normal stresses. For example, the maximum shearing resistance at a normal stress of 300 kPa of basaltic rockfill is 267 kPa, as opposed to sodium montmorillonite clay which is only 33 kPa (Figure 2-8). It is important to mention that the void ratios and grain size distributions of the materials were distinctly different, i.e. 0.37 and 3.71, respectively.

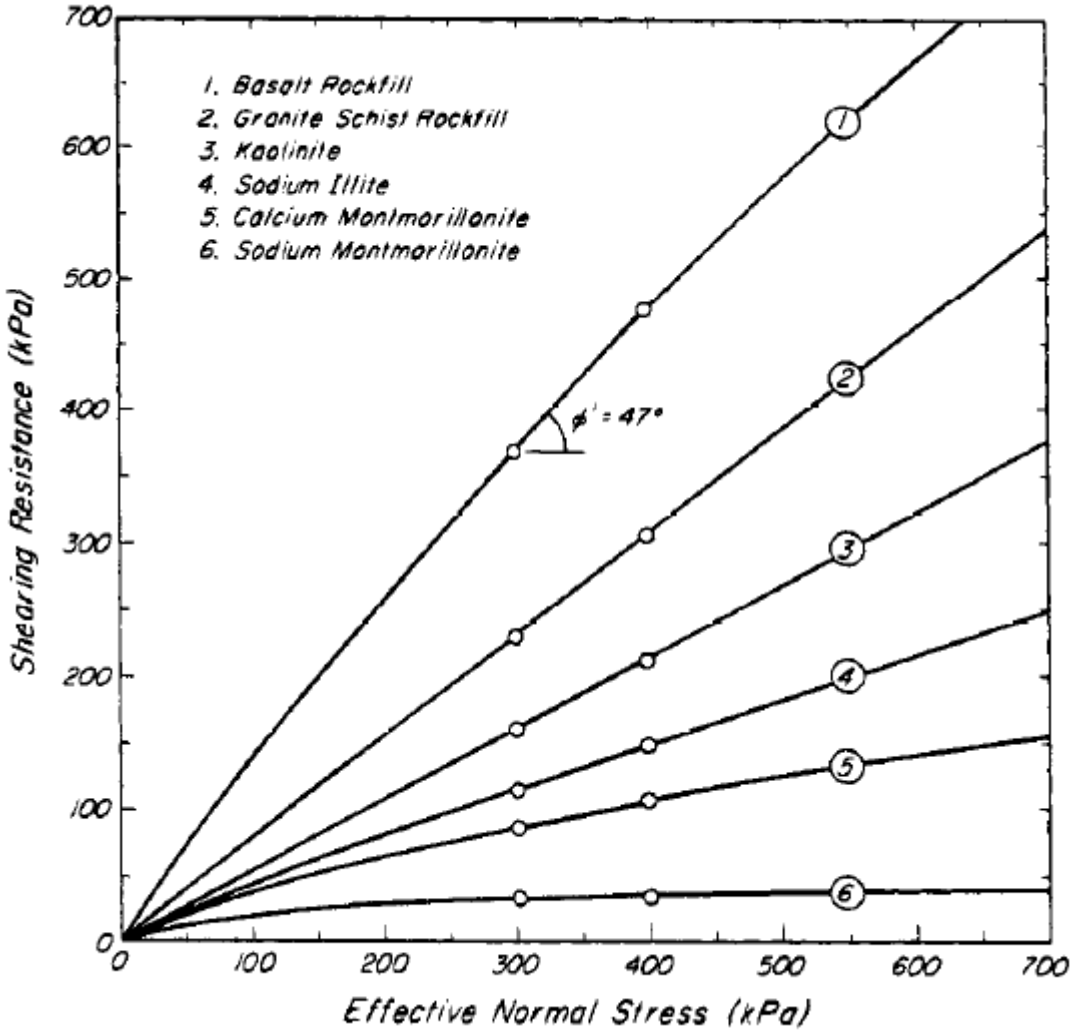

Figure 2-8. Shear Strength variation of various material types, (after Terzaghi, Peck & Mesri, 1948)

2.5.2 Material Density

As mentioned, the most significant factor that contributes to the shear strength of a soil is the density of the soil; this is a measure of the 'closeness of packing' of soil particles. The 'closeness of packing' can be expressed as the void ratio (Craig and Knappett, 2012). Typically, for a given soil, a range of densities can be achieved. The maximum and minimum void ratios (-) can indicate the relative density of soil, i.e.

Stellenbosch University https://scholar.sun.ac.za

the loosest and densest state of that particular soil. The relative density of a particular soil is given by the following equation:

$$I_D = {e_{max} - e}/{e_{max} - e_{min}} \tag{2.9}$$

where, e is the void ratio (-), and the subscripts max and min, refer to the maximum and minimum attainable void ratio for a given material.

The relative density determines the soil elements response to shearing (Das, 2010). The shearing resistance of dense material is increased by an increased degree of interlocking taking place between particles over and above the conventional friction between particles (Knappett and Craig, 2012). This interlocking between particles causes soil particles to dilate. This dilation in shear results in the points of contact between the respective soil particles to dislodge, and the particles move up and over their neighbouring particles at an inclined angle which is termed the dilation angle, this was first identified by (Bolton, 1986). The dilation angle (˚) is denoted by the symbol ψ, and can be expressed as (after Powrie, 1997):

$$\psi = \tan^{-1}\left({-\delta\varepsilon_{vol}}/{\delta\gamma}\right) \tag{2.10}$$

Where,

$$\varepsilon_{vol} = {\Delta x}/{h_0} \tag{2.11}$$

And,

$$\gamma = {\Delta y}/{h_0} \tag{2.12}$$

In the above equations (2.11 – 2.12) the Δx and Δy terms refer to change in the horizontal and vertical directions (mm), respectively. The term h_0 refers to the initial height of the sample (mm). Equations 2.11 and 2.12 approximate the horizontal and vertical strain (%) in the soil sample (Bolton, 1986). The negative sign in equation 2.10, stems from the convention of taking compressional forces as positive (Bolton, 1979, 1986; Burland, 2012a; Craig and Knappett, 2012; Powrie, 2012). The dilation angle (˚) can represent dilation or contraction of a soil sample, with a positive or negative magnitude, respectively.

Once a soil with a low relative density is exposed to a shear force, the particles tend to fill the voids in the soil profile (Figure 2-9a). This phenomenon is known as the slip down effect or soil contraction (Dafalias, 1993). Conversely, the volume of a high-density soil (particles with numerous particle contacts, also termed a high co-ordination number) will increase in volume with exposure to shear stress (Figure 2-9,b). Increased energy, or shear stress, is required to shear the material of a higher density, which results in a more pronounced peak stress ratio, as compared to a material of lower relative density

Stellenbosch University https://scholar.sun.ac.za

(Figure 2-9). The observed contractile or dilative behaviour of particles, subject to shear in a soil mass, is to some degree also influenced by the shape of the particles (Santamarina and Cho, 2004; Cho, Dodds and Santamarina, 2006; Lu *et al.*, 2019).

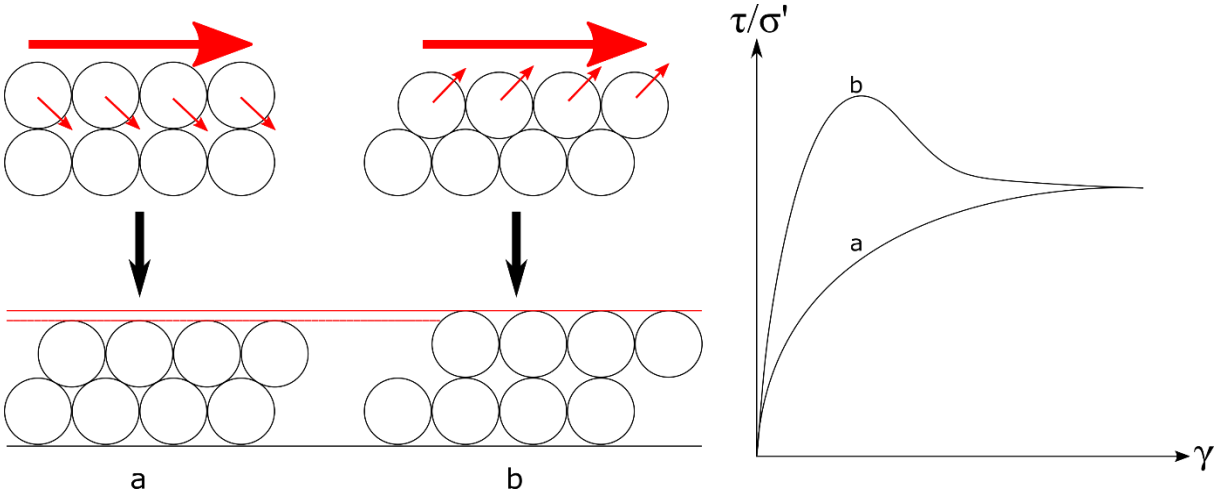

Figure 2-9. Left: graphical depiction of a coarse grain soils particle vectors in (a) contraction, and (b) dilation of loose and dense soil, respectively (After Powrie 1997; Knappet & Craig 2012). Right: corresponding trends of peak stress ratio behaviour for granular soils (a) and (b), after (Roscoe, 1953). Note: the shear force direction is represented by the larger red arrows and the resultant contraction or dilation vector is annotated by the smaller red arrows

2.5.3 Particle and Particle Aggregate Characteristics

When assessing the strength of soil, it is important to understand and consider the interactions taking place at the grain-scale (Hicher, 2012). The shape and surface characteristics of the particles, in a soil mass, influences the strength by increasing or decreasing the friction between adjacent particles (Terzaghi, Peck and Mesri, 1948; Santamarina and Cho, 2004). Three main characteristics describe particle shape (at varying scales), which are: 1) the eccentricity of the particle (global particle shape); 2) the surface roughness of the particle, and: 3) the angularity of the particle (Figure 2-10).

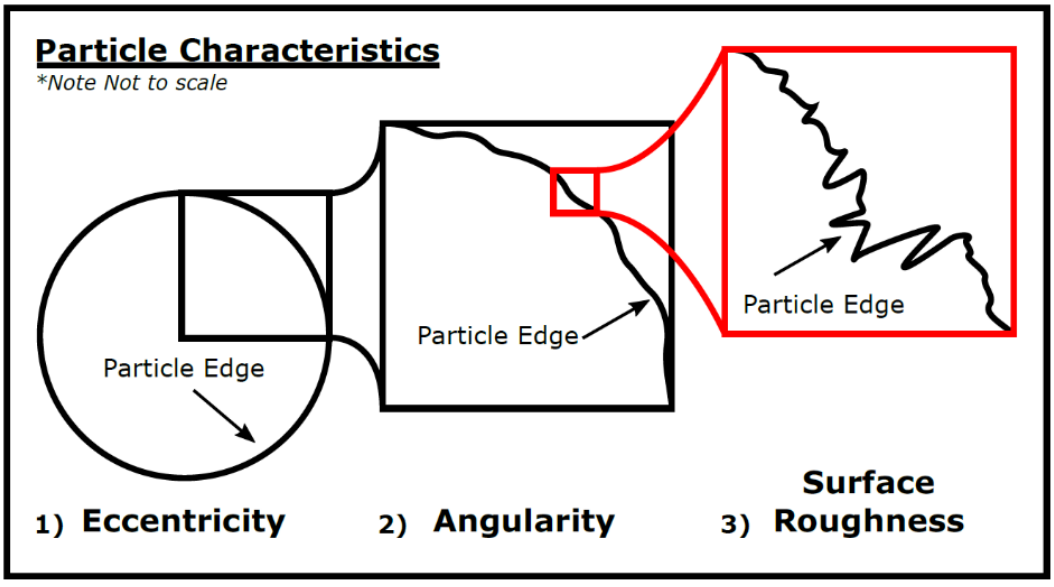

Figure 2-10. Particle shape and characteristic components of particle shape, (after Krumbein and Sloss 1963; Cho, Dodds and Santamarina 2006)

Stellenbosch University https://scholar.sun.ac.za

The effects of the respective particle characteristic components can be summarised as:

1. Eccentricity (also known as sphericity) is the global shape of particles, this has a direct influence on the packing efficiency of particles, and affects the density of the individual particle (Kyrylyuk and Philipse, 2011);
2. The angularity (also known as roundness) has a significant influence on the frictional contacts between soil particles. Increasing the angularity usually increases the frictional resistance between particles (Guo & Su, 2007; Das, 2010; Craig and Knappett, 2012). This will also increase interlocking and thus dilation (Rowe, 1962);
3. The surface asperities (or surface roughness) of the particle's surface affect the contact points between particles. Increasing surface roughness contributes to increasing friction between particles (Guo and Su, 2007);

Using two of these three components (the sphericity and the angularity), Krumbein and Sloss (1963), devised a classification system for particle shape (Figure 2-11). This method has been widely accepted by the scientific and engineering communities and has been adopted by several authors (Bear, 1975; Santamarina and Cho, 2004; Cerato and Lutenegger, 2006; Cho, Dodds and Santamarina, 2006) to quantify the particle shape in various studies of soils and particulate materials.

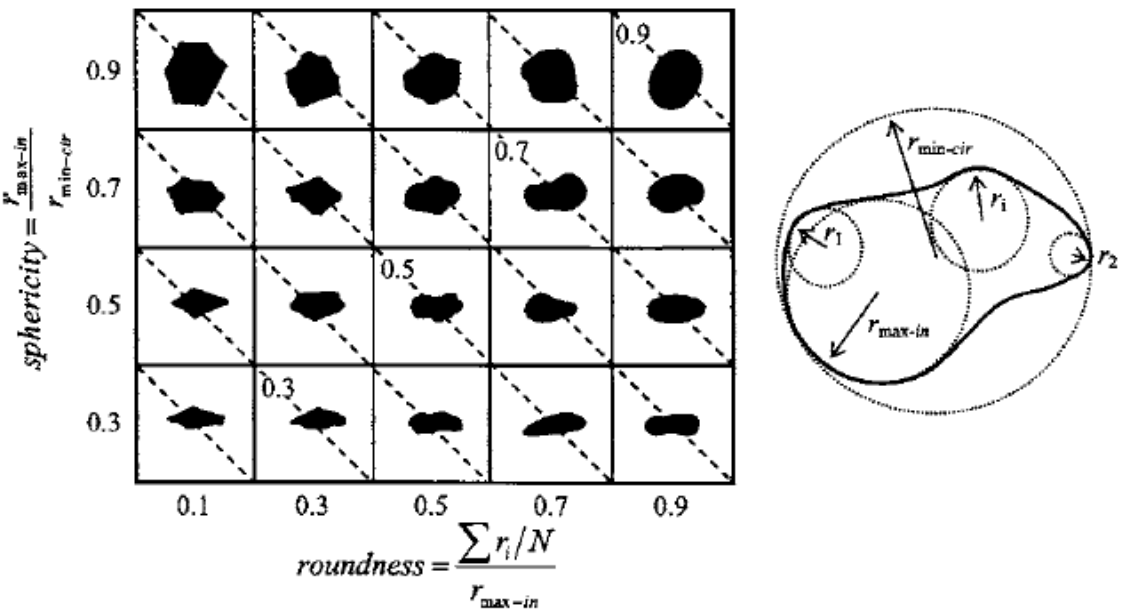

Figure 2-11. Depiction of the main features used in the classification of particle shape, roundness and sphericity (after, Krumbein and Sloss, 1963)

Given that the mechanics governing granular media's shear strength is merely based on friction (Mitchell and Soga, 2005), intuitively, the more irregularly shaped the soils particles the more resistance between adjacent particles there will be. Lu *et al.*, (2019) made use of discrete element models to simulate numerically regularly-shaped (spherical) and irregularly-shaped granular soil particle's

Stellenbosch University https://scholar.sun.ac.za

strength. It was identified that shape irregularity can be distinguished by two distinct contributions to soil strength: a) the contribution made by interparticle contact friction which is caused largely by the surface roughness of the particle; and b) the dilatancy contribution, which stems mainly from both the eccentricity and angularity of the aggregate of particles (Lu *et al.*, 2019).

Several authors have identified that with an increase in the eccentricity of particles (and decrease in sphericity) the maximum and minimum achievable void ratios (and the difference between the two) become greater, (Bolton, 1986). Conversely, Lu *et al.*, (2019) noted that with decreasing sphericity, particles formed a denser packing than that of round soil particles. Dense soils with irregularly shaped particles also exhibited a lower peak shear strength than that of regular-spherical particles. This increase in strength for spherical particles was attributed to an increase in the dilational contribution of the spherical particles (Lu *et al.*, 2019).

Dependant on the origin of the material, the shape and size of a granular particle are controlled by the mechanical processes that brought it to its current state (Margolis and Krinsley, 1974; Mitchell and Soga, 2005). For natural materials, these mechanical processes are mainly, but not limited to, abrasion and attrition, during transportation in a medium (water, wind). It is important to note that, in the mining context, these particle characteristics are derived through several processes that are dominated by blasting and crushing of rock and rock particles (Blight, 2010; Hawley *et al.*, 2017). Depending on the blasting technique employed, the material fragments in many different ways, often generating a collection of irregularly sized and shaped particles.

Generally, it is accepted that with increased maximum particle size diameter leads to an increase in the strength of the soil, this will be elaborated upon later (Mitchell and Soga, 2005). The particle size distribution has also a significant effect on soil shear strength (Terzaghi, Peck and Mesri, 1948; Powrie, 1997; Burland, 2012b; Craig and Knappett, 2012). There are two main parameters used to characterise and describes the slope and shape of a grain size distribution: the coefficient of uniformity (Cu) and the coefficient of curvature (Cz) can be expressed as (after, Craig and Knappett, 2012):

$$C_u = {}^{D_{60}}/_{D_{10}} \tag{2.13}$$

$$C_z = {}^{(D_{30})^2}\Big/_{D_{10} \times D_{60}} \tag{2.14}$$

A given particle size diameter can be denoted by the script D (mm) and the accompanying subscript for a given particle size distribution indicates the mass percentage (%) of the soil, that is finer than the specified grain size diameter. Typically, the grain size distribution of particles in a particular waste rock pile is highly variable and can range from well to poorly sorted (Table 2-1).

Stellenbosch University https://scholar.sun.ac.za

2.5.4 Environmental Conditions

It should be mentioned that the environmental conditions of a granular soil can have a significant role in the behaviour of the material, particularly the degree of saturation coupled with the atmospheric pressure (Fredlund and Rahardjo, 1993), which is much the same for waste rock piles (Azam *et al.*, 2009). There is a typical variation of the degree of saturation with depth in a conventional soil profile (Figure 2-12), and in the case of a mine waste rock pile, this is known to develop differently and less uniformly (e.g. Figure 2-4). There is an increase in the peak shear force required to shear a soil sample with increasing saturation, until the point at which the soil is entirely saturated (Blight, 2013).

The shear strength of water is zero, when stationary or moving at slow velocities, and may only experience the effects of isotropic compression (Powrie, 1997). Depending on the field scenario, when assessing the shear strength of a granular soil mass, it is pertinent to delineate solely the strength of the soil skeleton, as the water is allowed to drain away freely (as in a granular soil sample within the field). This is replicated in the laboratory by shearing the soil at a slow enough rate so that there is no buildup of pore water pressure inside the voids of the soil structure; suggested shear rates are listed in Table 2-4. Even when saturated, granular material that is sheared at too high a velocity results in the material behaving in an unsaturated manner (Craig and Knappett, 2012).

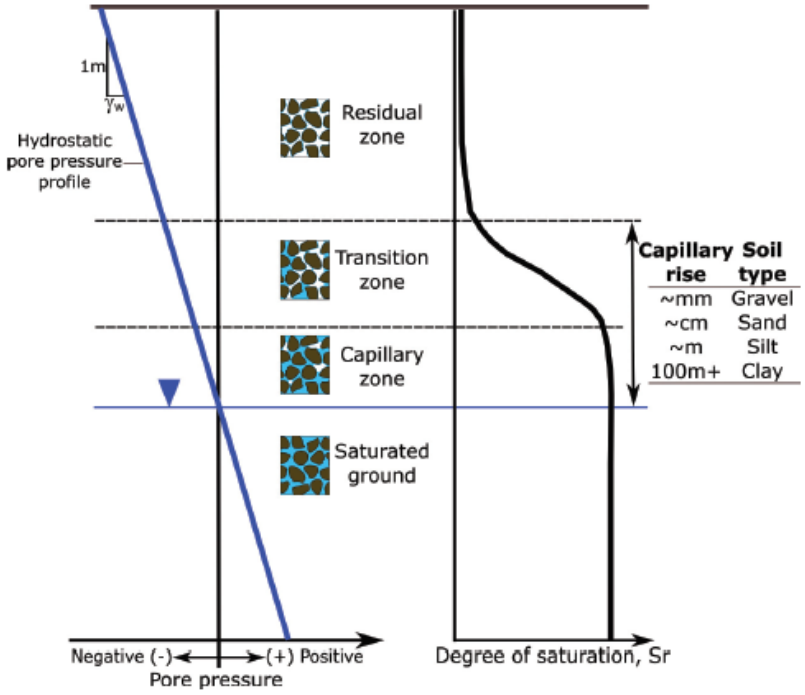

Figure 2-12. Pore water pressure distribution and saturation as a function of depth. The profile is depicted in a state of zero flow and hydrostatic equilibrium (Siemens, 2018)

Stellenbosch University https://scholar.sun.ac.za

Table 2-4. Shear rates for various grain sizes (Bolton, 1979)

Grain Size	Max Shear Rate (mm/min)
Sand	1
Silt	0.01
Clay	0.001

Over time, increasing amounts of waste rock are dumped on waste rock piles, this increases the thickness of the waste rock soil profile, and this corresponds to an increase in density because of increased confining pressure with depth (Terzaghi, Peck and Mesri, 1948; Burland, 2012b). The confining pressure in a waste rock pile is known to be variable and often very large in magnitude, particularly at the base of the structure, especially when the waste rock dump is extremely tall (Valenzuela *et al*., 2008). These high pressures can have implications such as a reduction in the maximum particle size diameter of the material, which affects the material gradation, and ultimately, the shear behaviour of the waste rock pile (Valenzuela *et al*., 2008; Hicher, 2012).

2.6 The Direct Shear Test

Shear strength can be measured via *in situ* testing or laboratory testing (Craig and Knappett, 2012). The DS test is conducted in the laboratory, which provides a means of rapid acquisition of shear strength parameters and is therefore routinely used in research and the industry (Shibuya, Mitachi & Tamate, 1997; Lings & Dietz, 2004). When the acquisition of strength parameters of coarse-grained materials is required, e.g waste rock or rockfill, a challenge is presented, which is a consequence of the large particle size often contained in these materials. The ASTM 3080-11 standard limits the maximum permissible particle size that may be tested within a shear box mould of given dimensions (ASTM, 2011).

Some studies suggest that i*n situ* tests offer a more precise reflection of a soils shear strength as they are undisturbed, and especially when some of the particles exceed the gravel size fraction as this can be accounted for by designing appropriately sized test apparatus (e.g. mine waste rock: Fakhimi *et al.*, 2008 and Rai & Shrivastva, 2012; landslide materials: Fannin, Eliadorani & Wilkinson, 2005; soil-rock mixtures: Xu, Xu & Hu, 2011). It is a difficult task to test shear strength *in situ* so two approaches were proposed to try and replicate natural conditions within the laboratory, by reconstitution and by remoulding (ASTM, 2011). Reconstitution involves tamping a soil specimen into laboratory apparatus, to replicate the field specimen density, whereas the desired density by remoulding is typically achieved by 'cutting' a specimen out of a Proctor/Modified Proctor mould, where the specimen has been subject to a certain compactive effort (ASTM, 2011).

Stellenbosch University https://scholar.sun.ac.za

2.6.1 Apparatus Configuration

In the laboratory two types of DS apparatus exist and are employed on the grounds of, i) the measurement of flow properties in particle technology (this apparatus is circular in cross-section and is known as the Jenike shear cell), and; ii) the strength properties of granular media in geotechnical engineering (square in cross-section and is known as the Direct Shear test). Essentially, the DS test allows for the drained frictional resistance of a soil to be delineated, i.e. cohesion (c') and internal friction angle (φ'), by relating the shear stress, at failure, to the applied normal stress (Das, 2010). The box (or Shear Mould) that hosts the soil sample, has two distinct halves, one of the halves moves relative to the other forcing a shear plane to develop horizontally between the box halves (Holtz and Kovacs, 1981; Craig and Knappett, 2012). The other crucial element of the DS test is the ability to induce a normal load on the sample during the shearing, such that a shear force is generated during displacement (of one the box halves). The displacement of one of the halves relative to the other of the Shear Mould results in the shearing of a sample along a pre-defined shear plane, which may not be the weakest plane present in the soil (Das, 2010).

The other main drawbacks to be considered when making use of the DS test are related to stress and strain localization (or non-uniformity/heterogeneity) due to boundary effects (the Shear Box confining the soil specimen deformation). These boundary effects were brought to light experimentally by Morgenstern, (1967), and were later confirmed by numerical analyses (Potts, Dounias and Vaughan, 1987). They showed that the propagation of the shearing followed a horizontal direction from the leading edges of the DS box halves (i.e. boundary effects). In addition to these boundary effects, the principal stress axes rotate along with the rotation of the topcap and/or upper half of the Shear Box, as the shear test progresses (Powrie, 1997), this exacerbates the non-unitformity of stresses (Fredlund and Rahardjo, 1993). Apart from this, the area of shearing does not remain constant throughout the test as one half of the box is displaced and therefore, this needs to be accounted for when calculating the normal and shear stress generated by the shearing of the sample (Craig and Knappett, 2012). While the sample is sheared, the sample's resistance to shearing is measured by data loggers which are typically connected to an LVDT and load cell in the horizontal direction and an LVDT in the vertical direction (Holtz and Kovacs, 1981).

The determination of which of the two halves of the prism that moves remains dependent on the design and the manufacturer of the Shear Box (Shibuya, Mitachi and Tamate, 1997; Lings and Dietz, 2004). Three types of DS test apparatus setups exist and are commonly used in laboratories globally, regardless of which, the same set of parameters are determined (Figure 2-13a-c). Each of the distinct types of DS apparatus allows for variable degrees of freedom in movement/rotation of the shear box. 'Type a' permits the most rotation of the upper Shear Mould (also termed the "archetype" shear box and is the often considered the original design); 'type b' aims to limit rotations of the Shear Mould while allowing for free particle movement (referred to in the literature as the DS apparatus with "induced" rotational

Stellenbosch University https://scholar.sun.ac.za

restraint), and; 'type c' negates any movement of the top DS frame (referred to as the DS with "enforced" rotational restraint) (Lings and Dietz, 2004).

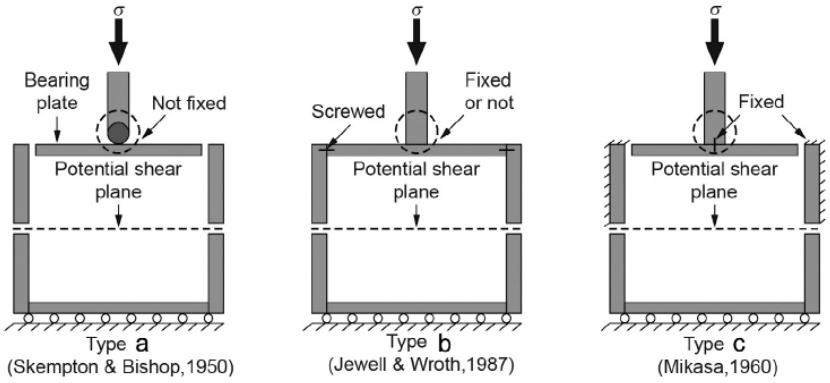

Figure 2-13. Three types of modern DS test apparatus (after Fu *et al.*, 2015)

The "type c" DS apparatus induces vertical movement of particles along the vertical boundaries of the DS inner wall. As a result, increased friction is generated along the vertical boundaries of the Shear Mould, ultimately increasing the error associated with the resultant shear stress parameters derived from the "type c" apparatus (Shibuya, Mitachi and Tamate, 1997). The free-rotation of the top wall and shear box half associated with the "type a" DS apparatus, allows for no excess particle-boundary friction, it does, however, cause progressive rotation of both the shear box top wall and top box half. This results in non-uniformity of the applied stresses and strains during the undertaking of the test, e.g. progressive rotation causes proportionately more eccentric (i.e. less) normal loading, and thus less shear stress is observed for the "type a" DS apparatus (Wu, Matsushima & Tatsuoka, 2007; Craig and Knappett, 2012).

The effects of the DS apparatus design extremities and the levels of restraint on components can be demonstrated by the laboratory DS results obtained by Hong *et al.*, (2015). The material used during the undertaking of the study was and subject to varying degrees of normal stress (50 to 400 kPa) and sheared at 0.5 mm/min. The results indicate that the "type a" DS apparatus 'with rollers' yield greater friction angles than those that do not possess rollers (Figure 2-14). The "type a" apparatus without rollers yields the lowest friction angle result as compared to the "type c" DS apparatus, which adopts total restraint of box movement. The study reveals that the 'type a' apparatus may over-or underestimate the strength parameters depending on the boundary conditions imposed by the SB apparatus, i.e. whether the apparatus is fixed or operated using rollers/bearings. The "type c" DS test provides a more consistent set of parameters (Hong *et al.*, 2015).

Stellenbosch University https://scholar.sun.ac.za

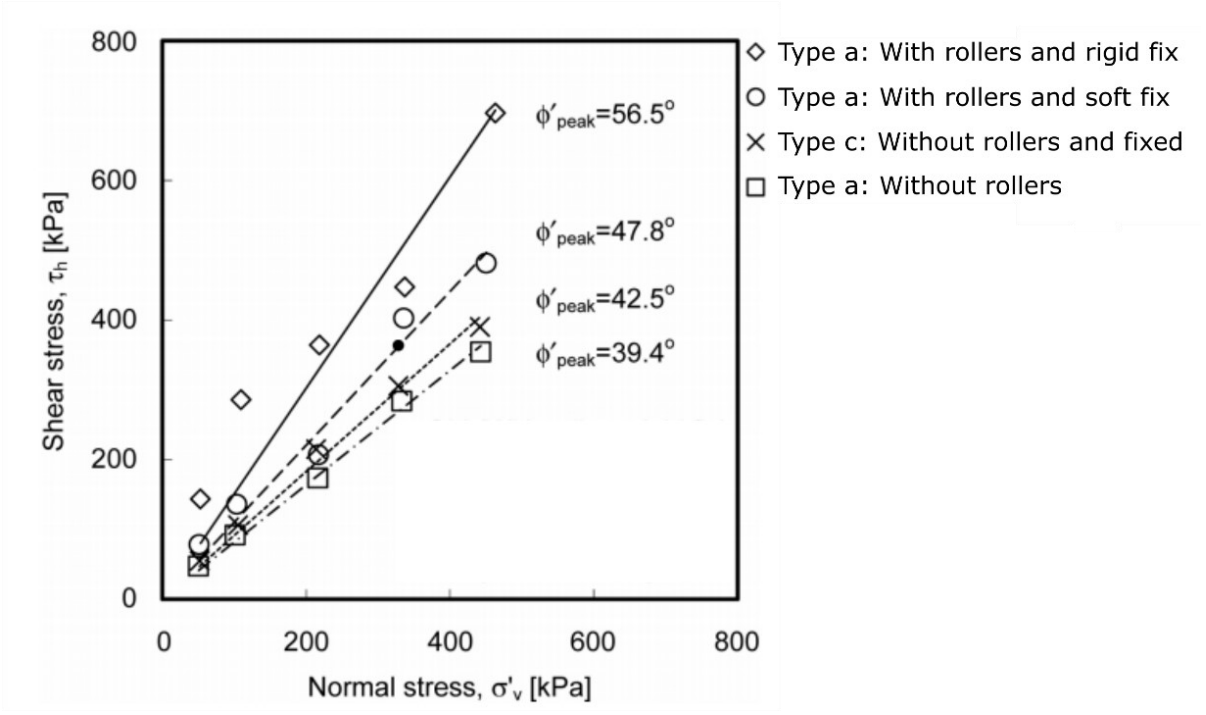

Figure 2-14. Friction angle of sand derived from various shear box apparatus types (after Hong *et al*., 2015)

The type of Shear Box employed for a given project is generally determined either by the DS apparatus available for use and its associated dimensions or by the maximum particle size of the material that is to be tested (Bareither, Benson and Edil, 2006; Alias, Kasa and Taha, 2014).

2.6.2 Strength Computation

There are several means of displaying and interpreting the results derived from the DS test. The following equation describes the derivation of drained Mohr-Coulomb internal angle of friction (or friction angle) mentioned during the undertaking of the present study:

$$\phi = \tan^{-1}(\tau_p/\sigma) \tag{2.13}$$

Where,

τ_p: Observed peak shear stress (kN/m^3)

σ: Initially applied normal stress (kN/m^3)

ϕ: Angle of internal friction (˚)

The above equation (2.13) is a simple reworking of the latter half of equation 2.4. Presenting the strength results in the form of the stress ratio (τ/σ) with displacement can be beneficial when establishing trends in the strength and dilation behaviour of granular media (e.g. Wang and Gutierrez, 2010; Harehdasht *et al.*, 2019). The advantage of presenting the data in this form is that the effects of sample area reduction during shearing are negated, and an indication of the instantaneous or tangential angle of friction with horizontal/shear displacement (mm), or with the shear strain (%), can be presented (e.g. Figure 2-20).

Stellenbosch University https://scholar.sun.ac.za

2.7 ASTM Shear Box Scale Ratios

American Society for Testing and Materials (ASTM) D 3080-11 details the procedure for conducting the direct shear test. Several further, or "added" requirements are listed in Section 6.2.1 to 6.2.3 of ASTM 3080-11. The added requirements specify that two specific particle-box ratios and an aspect ratio that are implemented during the undertaking of the test: i) the ratio between L and the D_{max} be greater than ten; ii) the ratio between H and the D_{max} be greater than six; and, iii) the ratio between L and H be greater than two (ASTM, 2011).

Often, granular materials used in the construction of civilian structures contain large particle size diameters, this poses a challenge when considering the ASTM 3080-11 added requirements. As the access to DS equipment with sufficiently large dimensions is typically a challenge, the present study adopts a systematic approach in assessing the Shear Box to particle size ratios (or scale effects) in conventional laboratory equipment, i.e. the 60 x 60 mm^2 and 100 x 100 mm^2 DS test apparatus (Azam *et al.*, 2007, 2009; Hicher, 2012). Moreover, an insert was designed to fit into the ordinary DS box sample mould to reduce the sample size to 20 x 20 mm to further assess the shear behaviour of crushed mine waste rock, i.e. when $L/D_{max} << 10$, $H/D_{max} << 6$, and $L: H << 2:1$.

2.8 Scaling Down Techniques

Although not a main focus in the present study, this subchapter provides an overview of the methods for manipulating the particle size distribution of materials that contain particles of large diameters to obtain strength parameters, while upholding the added requirements of the ASTM 3080-11 standard. The methods described, all aim to reduce the maximum particle size diameter of a granular material to allow for strength testing in conventional and available laboratory apparatus. The most commonly adopted methods for "scaling down" grain size distributions are the "Parallel gradation" method (Lowe, 1964), the "Scalping" technique (Zeller and Wullimann, 1957); and, the "Scalp and Replace" technique (Frost, 1973). Some examples of material that often possess oversized particles and may require grain size distribution 'scaling' are waste rock piles (Li, 1999), backfill material (Bareither, Benson and Edil, 2006); and, coarse rockfills that are routinely used in dam construction (Ovalle *et al.*, 2015).

When making use of the parallel gradation method to alter a field sample, the entire grain size distribution is essentially shifted 'parallel' (along the x-axis) to the original field samples graduation, such that the relative percentage of each size fraction remains the same, while each size fraction of the field sample (Dfs) is reduced by a factor (R) to ensure that the largest grain diameter in the test sample (Dts) meets the specified maximum admissible particle size diameter of the laboratory apparatus (Figure 2-15) (Lowe, 1964). This is also sometimes called a homothetic grain size distribution (Ovalle *et al.*, 2014). This method preserves the Cu and Cz parameters of the soil (Lowe, 1964).

$$Dts = Dfs/R$$

Stellenbosch University https://scholar.sun.ac.za

The “Scalping” and the “Scalp and Replace” techniques, rely on the same concept of simply removing the mass fraction of the oversized particles in the PSD. This produces a distinctly different and unique set of coefficients of curvature, and uniformity, as compared to that of the original field grain size distribution curve (Hicher, 2012). When deriving a “Scalped” curve, the resultant curve is achieved by removing (via screening out or sieving in practice) the oversized material which was sampled in the field (Zeller and Wullimann, 1957). This results in a sample test curve which is steeper than the original field curve, and the curve “lifts” off of the original curve (Figure 2-15).

The “Scalp and Replace” method; on the other hand, the oversized fraction is removed (same process as Scalping) and is replaced with an equivalent mass of the largest size fraction available in the field sample, which respects the ASTM D3080 – 11 recommendations (Frost, 1973). Thus, the resultant test sample curve derived by the “Scalp and Replace” method initially mimics the original field gradation followed by a sharp increase in the percentage passing of the largest available (and permissible) size fraction.

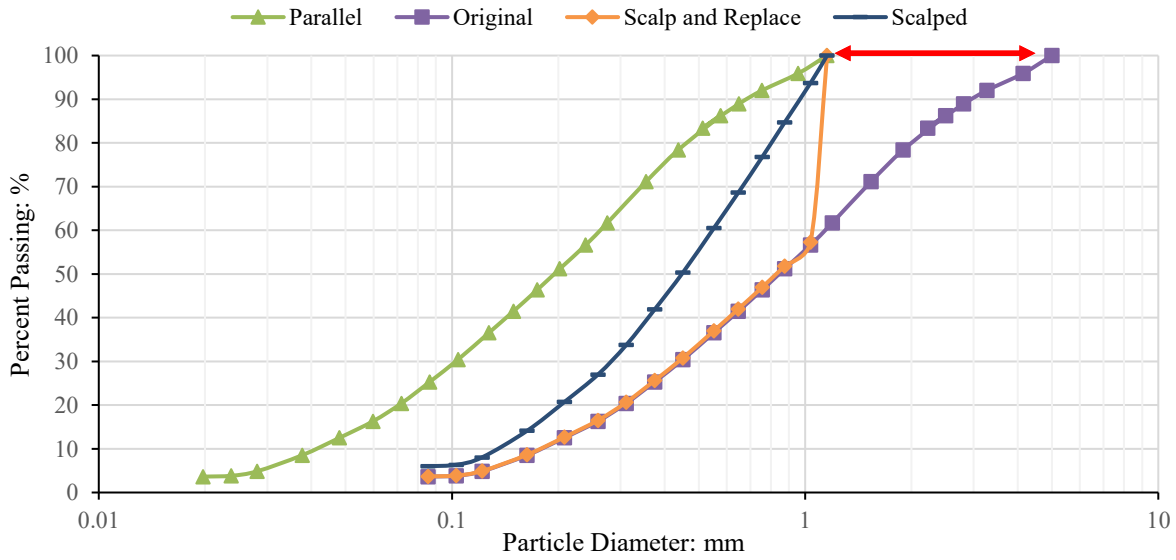

Figure 2-15. Examples of most common gradation modification techniques

Several studies have been conducted to assess the effects of the grain size distribution manipulation on the behaviour of granular materials by utilising the scalping technique (e.g. Xu, Williams & Serati, 2017; Zeller & Wullimann, 1957); the parallel method (e.g. Lowe, 1964; Bagherzadeh-khalkhali & Mirghasemi, 2009; Gupta, 2009); and the scalp and replace technique (e.g. Donaghe & Torrey, 1979).

Stellenbosch University https://scholar.sun.ac.za

2.9 Review of Scale Effects of DS Test

Scale effects (or specimen size effects) arise from the inaccurate representation of forces and/or boundary effects within a model of a real life-system, for example, the DS test apparatus (Cerato & Lutenegger, 2006; Heller, 2011). The smaller the Shear Mould of the DS test, the less volume in which deformation of the granular material may take place. This was first observed by Parsons in 1936, he observed that variations in DS Shear Mould dimensions yielded differences in the resultant friction angles for the same soil. More recently, an example of the scale effects of the direct shear test indicated that the friction angle obtained from a 60 x 60 mm shear mould (L), may be up to 10˚ higher than the results derived from a 305 x 305 mm shear mould (L), for the same material (Figure 2-16) (Cerato & Lutenegger, 2006).

The causes of scaling effects in the DS test may emerge due to reductions in the inner dimensions of the Shear Mould (e.g. Parsons, 1936; Palmeira & Milligan, 1989; Cerato & Lutenegger, 2006; Chang, Cerato & Lutenegger, 2010), when the inner dimensions of the Shear Mould height dimensions are varied (e.g. Wang & Gutierrez, 2010), when the ASTM 3080-11 suggested aspect ratio (L/H) and/or box-scale ratios between the grain size distribution and the dimensions of the Shear Box are not maintained/implemented (i.e. L/D_{max} and H/D_{max}) (Wu, Matsushima & Tatsuoka, 2007; Bagherzadeh-khalkhali & Mirghasemi, 2009).

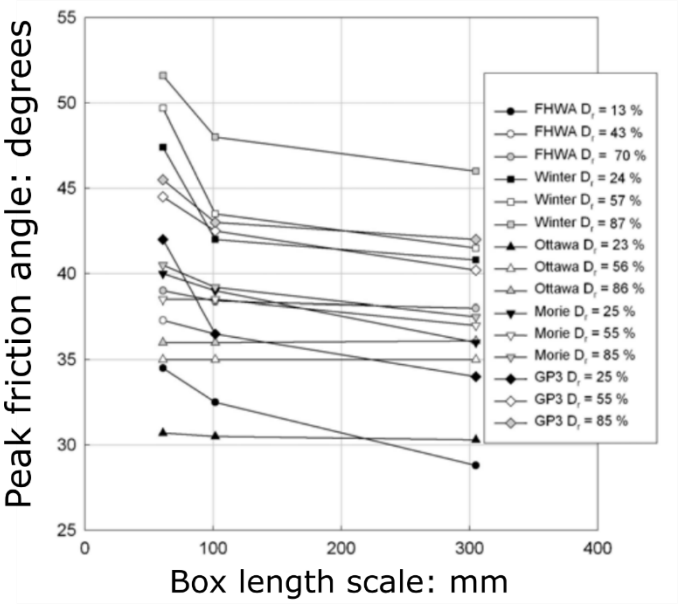

Figure 2-16. Effect of box length on peak friction angle for several soil types and densities (after, Cerato and Lutenegger, 2006)

Stellenbosch University https://scholar.sun.ac.za

2.9.1 Effects Shear Mould Dimensions

Wang and Gutierrez (2010) conducted a series of DEM DS tests, to study the effects of systematic variation of the Shear Box length and height scales on the maximum peak stress ratio $(\tau/\sigma)_{max}$ (Figure 2-16). An inversely proportional relationship exists between the maximum peak stress ratio and the box length scale; for example, an increase in the peak stress ratio can be observed with decreasing box length scale (specimen height scale constant: 14 mm) (Figure 2-17a). In contrast, a directly proportional relationship can be observed for the maximum peak stress ratio and the box height scale; for instance, the maximum peak stress ratio increases with increasing box height scale (specimen length scale constant: 88 mm) (Figure 2-17,b).

Additional effects of the Shear Mould, i.e. the variation of box length and height scale, on the stress ratio (τ/σ) can be recognised when assessing the stress ratio variation with shear displacement (Figure 2-18). Immediately, it is clear that as the box length scale increases, the resultant peak stress ratio is decreased (Figure 2-18a). The peak stress ratio is reached at similar, but progressively larger, shear displacements with decreasing box length scale. As an example, when the box length scale is 80 mm the peak stress ratio was reached at approximately 1,0 mm of shear displacement; and when box length scale is 35 mm the peak stress ratio is reached at approximately 1,2 mm of shear displacement (Figure 2-18a).

A clear distinction can be made for the Shear Mould height scale, that is that as the box height scale decreases, so too does the peak stress ratio; furthermore, with increasing box height scale the peak stress ratio is reached at higher magnitudes of shear displacement (Figure 2-18b). For example, when the DS test is conducted with a height scale of 14 mm, the resultant peak stress ratio occurs at approximately 1,0 mm, and when the box height scale is 56 mm, the resultant peak stress ratio occurs at approximately 2,5 mm (constant length scale: 88 mm). Additionally, it would appear that variations observed in the peak shear stresses, with variations in box height scale, were considerably smaller for the samples tested with box height scales of 14 and 28 mm, as compared to the sample tested with a box height scale of 56 mm (Figure 2-18b).

Additional conclusions made by Wang and Gutierrez (2010) were that with increasing sample height scales, the absolute dilation (or volume increase) taking place inside the sample decreased; for example, the 56 mm sample experienced less dilation as compared to the smaller sample heights (14 and 28 mm). Finally, as the box height scale increases, the total volumetric strain required to bring the sample to failure decreases.

Stellenbosch University https://scholar.sun.ac.za

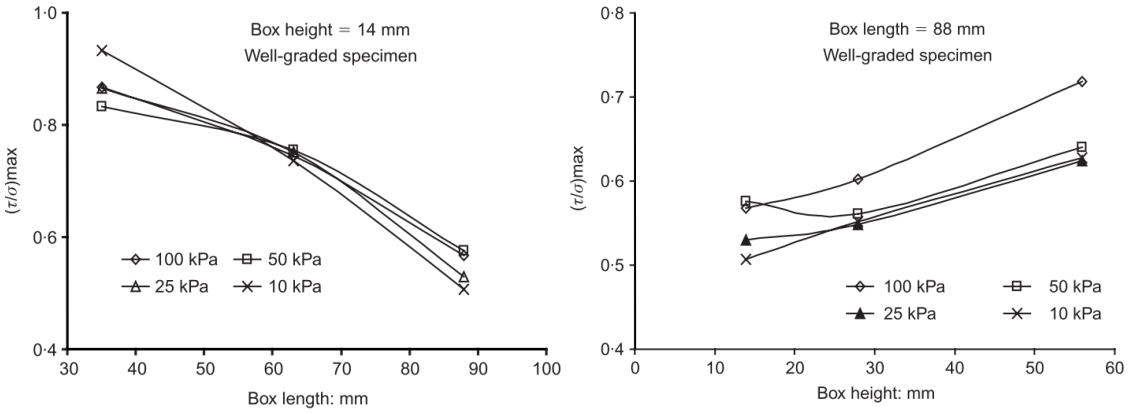

a b

Figure 2-17. Effects of systematic variation of a) box length scale, and: b) box height scale, on the peak stress (after, Wang and Gutierrez, 2010)

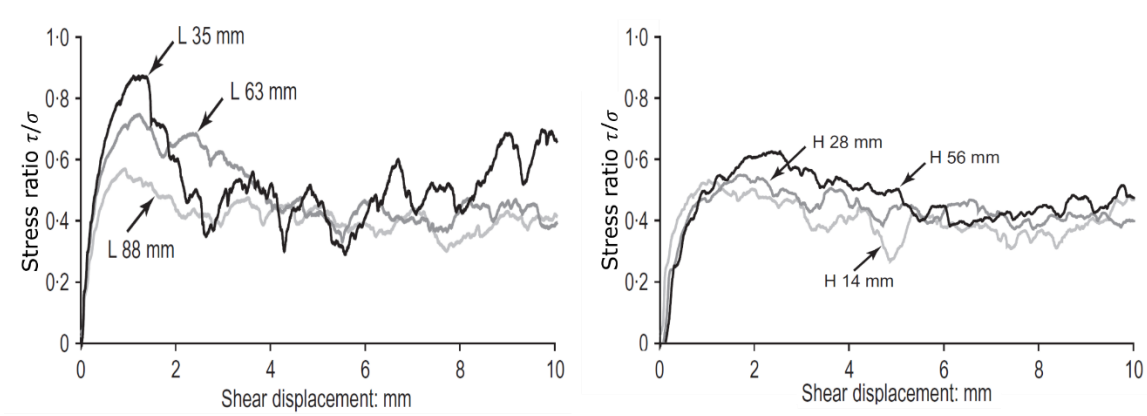

a b

Figure 2-18. Effects of variation in a) length scale, and; b) height scale, on the stress ratio with shear displacement (by DEM simulations) (modified after, Wang and Gutierrez, 2010)

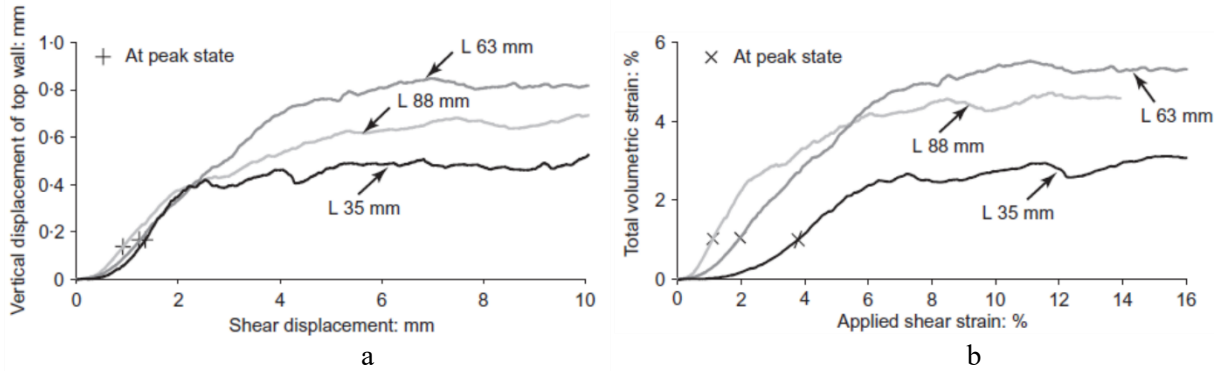

a b

Figure 2-19. Variation effects of length scale on a) vertical displacement of shear box top wall, and; b) total volumetric strain of a direct shear specimen (by DEM simulations) (after, Wang and Gutierrez, 2010)

2.9.2 Effects Aspect Ratio

Another important factor to be considered when aiming to diminish the inherent scale effects of the DS test is the aspect ratio (L/H). One of the earlier works that indicated the effect of the aspect ratio on the shear behaviour of granular soils was conducted by Hight and Leroueli (2003). The DS tests conducted revealed that when the Shear Mould length scale is kept constant and the height scale is progressively reduced (simultaneous reduction of the aspect ratio) the peak stress ratio of the granular material is increased proportionately (Figure 2-20). Some years later, Wang and Gutierrez (2010) assessed the

Stellenbosch University https://scholar.sun.ac.za

impact of the Shear Mould's aspect ratio (*L/H*) on the results of the direct shear test. The results of the study, too indicated, that when decreasing the box height scale (and thereby reducing the aspect ratio), in most cases the peak stress ratio increased (Figure 2-21). Here, it is important to mention that the ASTM 3080-11 recommendations (L: H > 2:1) were made to limit the effects of arching induced in the vertical sidewalls of the DS test (ASTM, 2011; BPR, 1958).

Wang and Gutierrez, (2010) further established that when the aspect ratio was increased, i.e. the box length scale was enlarged, the corresponding peak stress ratio increased proportionately (Figure 2-21). An elevated rate of change in the peak stress ratio is observed when the height scale is kept constant and the length scale is changed, as this trend suggests, the length scale has a principal control on the macromechanical behaviour of granular material.

As a result, Wang and Gutierrez (2010) termed the aspect ratio a "critical shape factor" in the determination of the mechanics responsible for the mechanism of failure of a DS test specimen. They postulated that two fundamental modes of failure prevail when testing granular materials while altering the length and height scales of the DS test: i) global (or bulk) failure, and; ii) local (or progressive) failure. These processes were identified and further described through a micromechanical analysis of the test results.

Based on the findings of the micromechanical analysis, Wang and Gutierrez, (2010) made recommendations that are somewhat, contrary to the aspect ratio, and are aligned with the box scale and recommendations made by AST (2011). Wang and Gutierrez (2010) found that the suggestions made by ASTM (2011) on the maximum particle size to box ratios were far too liberal; it was suggested that to ensure the mitigation of the inherent scale effects of the DS test, the aspect ratio (*L/H*) for a given sample should be between 1.5 and 2, the height scale ratio (H/D_{max}) should be greater than 40 and that the length scale ratio (L/D_{max}) should exceed 60.

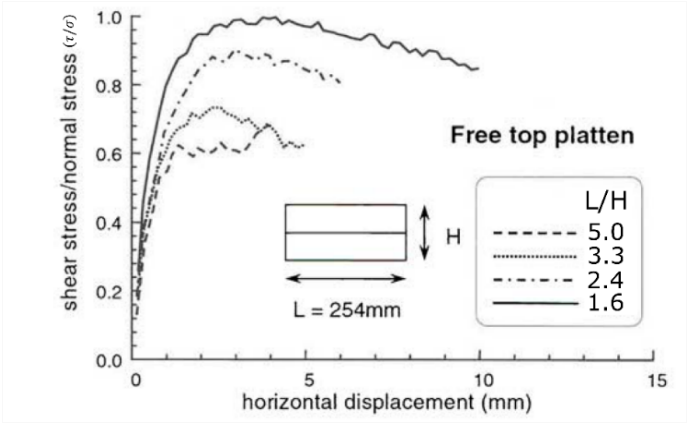

Figure 2-20. Effect of aspect ratio on the stress ratio (from Hight & Leroueli, 2003; modified after Cerato and Lutenegger, 2006)

Stellenbosch University https://scholar.sun.ac.za

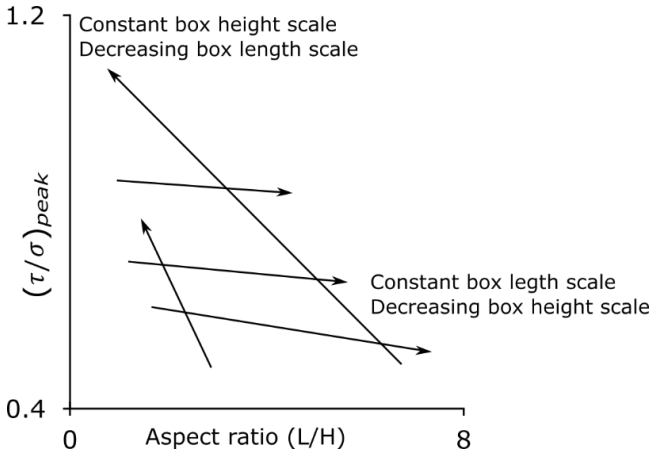

Figure 2-21. General effects of variation in aspect ratio on peak stress ratio of granular materials (after Wang and Gutierrez, 2010)

2.9.3 Effects of Particle Size and Gradation

As indicated in Section 2.9.2, as the length scale of the DS box decreases relative to the maximum particle size, so the strength of the material increases; similarly, as the maximum particle size of a granular material increases the strength of the material increases proportionately (Holtz & Kovacs, 1981). Experimentally, there have been several studies that have assessed the effects of increasing particle size on the resultant shear strength. A summary of tests conducted using direct shear apparatus has revealed that as the maximum particle size of a material increases, relative to the direct shear test in which strength tests are being conducted, the magnitude of the resultant strength parameters increase (Table 2-5).

Table 2-5. Effect of increasing maximum particle size diameter on friction angle results obtained by direct shear test

Source	Maximum particle size diameter tested (mm)	Result of increasing Dmax on friction angle:
Bishop, 1948	6.350 - 25.40	No effect
Lewis, 1956	25.40	Increase
Simoni & Houlsby, 2006	0.075 - 20	Increase
Bareither, Edil, Benson & Mickelson, 2008	0.4 - 60	Increase
Fakhimi & Hosseinpour, 2008	19 - 6.6	Increase
Xu, Williams & Serati, 2017	2.36 - 75	Increase

The average grain size diameter may also play a role in the shear behaviour and strength parameters of granular media. As an example, Wang *et al.* (2013), assessed the effects of the median particle size (D_{50}), the overall PSD characteristics (i.e. C_u), and the amount of gravel contained within the sample on the shear strength of an accumulation soil derived from the 2008 Schian earthquake (Richter scale magnitude = 8.0). It was established that an increase in the median particle size diameter (Figure 2-22a), or increased gravel contents (C_t) (Figure 2-22b), when assesing strength with a direct shear test (or triaxial apparatus) the maximum angle of shearing resistance (or friction angle) increases. Moroever, Wang *et al*. (2013), found that that, generally, the angle of shearing resistance decreased with an increase in the coefficient of uniformity of a grain size distribution; this suggests a gradation with a broader range

Stellenbosch University https://scholar.sun.ac.za

of particle sizes yields higher strength parameters, i.e. those tending towards well-graded PSDs result in elevated friction angles (Figure 2-23).

Perfectly uniform grain size distributions have been shown to pronounce the effects of fabric anisotropy, as they typically rest in lattice-like structures when aggregated (Einav, Dyskin & Sukumaran, 2006). Another study was conducted by Moayed *et al*. (2017), a practical assessment of the effect of the silt content of soil (along with variations of the inner box dimensions) on the observed friction angle. It was established that the percentage of silt in Firoukook sand decreased the observed scale effects of Shear Mould dimensions on the returned strength parameters, this further eludes to the idea that scale effects are a function of the grain size distribution coefficients of curvature and uniformity.

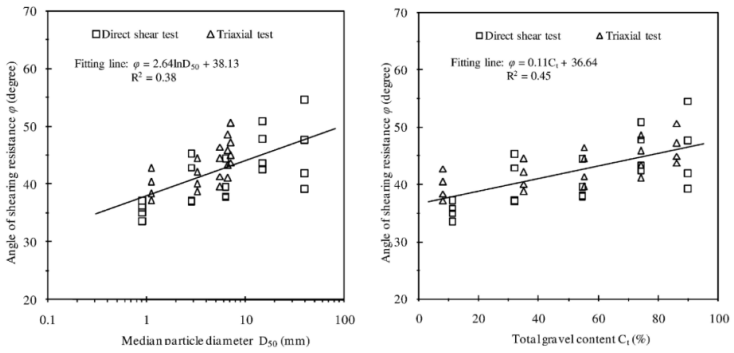

a b

Figure 2-22. Effect of a) median particle diameter, and; b) gravel contents, on the measured friction angle of residual soils (after, Wang *et al.*, 2013)

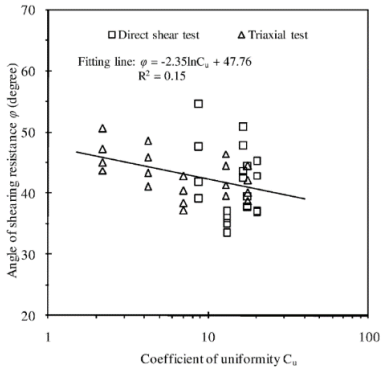

Figure 2-23. Effect of the coefficient of uniformity on the angle of shearing resistance of residual soils (after, Wang *et al.*, 2013)

Stellenbosch University https://scholar.sun.ac.za

2.9.5 Shear Band Development

Upon shearing, regardless of the Shear Mould size, grains contained within a Shear Box specimen are forced to fail along, an irregular, but predefined plane (i.e. initial failure zone; Figure 2-24). It has been shown that failure of the specimen is initiated by grain movements at the boundaries of the Shear Mould, which propagate inward (with shear displacement) toward the centre of the specimen (Wang and Gutierrez, 2010). The individual grain movements within the initial failure zone coalesce to form several shear bands, which comprises a distinct ellipsoidal shear zone (Qin, 2007; Zhou *et al.*, 2009) (Figure 2-25b,c).

The properties of shear band development have been studied both numerically (e.g. Jacobson, Valdes & Evans, 2007), and experimentally (e.g. Wu, Matsushima & Tatsuoka, 2007; Dyer & Milligan, 1984). Numerical simulations have repeatedly proven that shear bands propagate from the boundaries of the direct shear test (Potts, Dounias & Vaughan, 1987; Jacobson, Valdes & Evans, 2007; Wang, Dove & Gutierrez, 2007; Zhang & Thornton, 2007; etc.); yet no quantitative definition of what constitutes the shear band exist.

Several authors have investigated ratios between the maximum grain diameter of the tested material and thickness of the shear band that ensues. For example, it has been indicated that the thickness of the shear band is between 5 and 20 times the maximum particle diameter (Jacobson, Valdes and Evans, 2007 and references therein). Moreover, Jacobson, Valdes and Evans (2007), assessed the shear band development in a simulation-based study of direct shear test, it was concluded that shear band development is very limited to non-existent when the L/D_{max} is smaller than, or equal to 13, and only become distinctly visible when the L/D_{max} is greater than, or equal to 58.

Stellenbosch University https://scholar.sun.ac.za

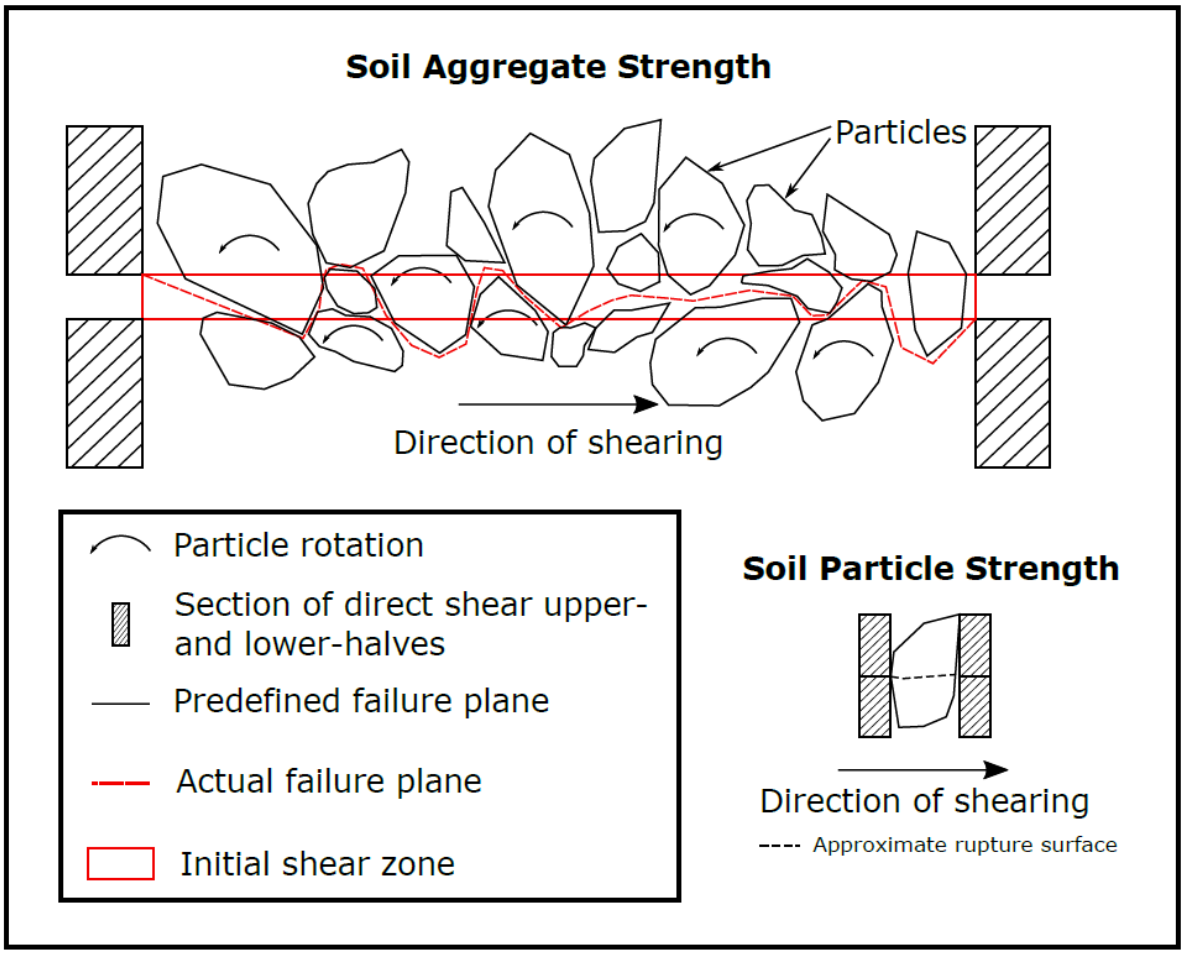

Figure 2-24. Intricacies associated with shear surface/band (after Fu *et al*., 2015)

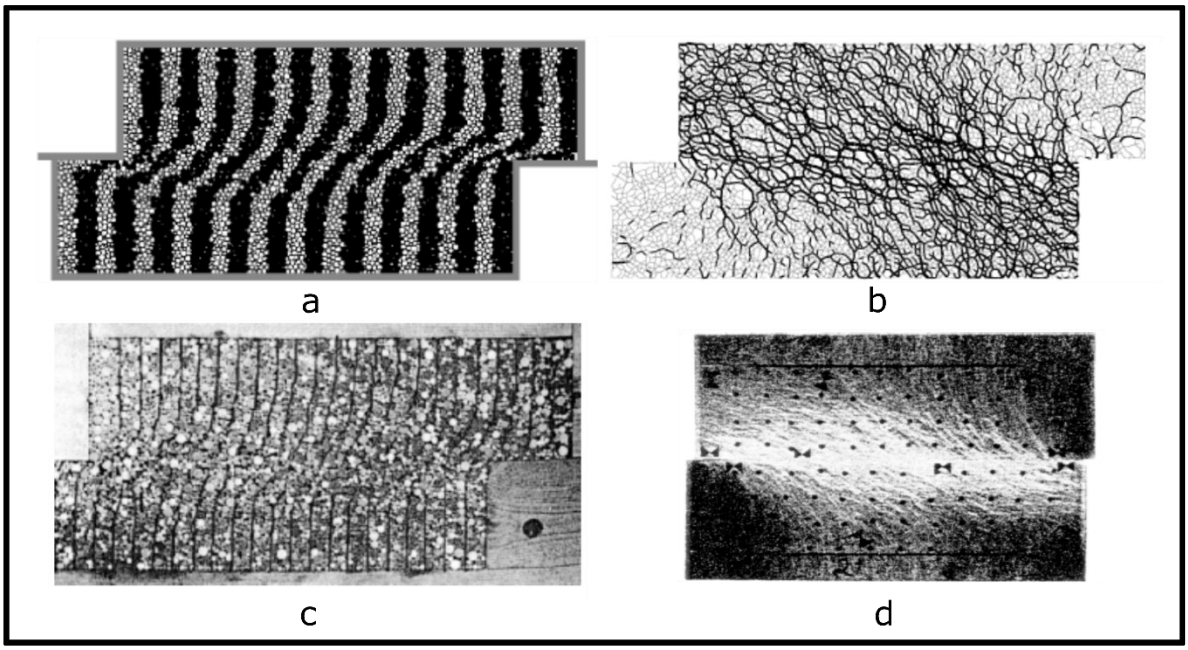

Figure 2-25. Deformation and shear band propagation: a) discrete element method simulation of deformation, and; b) contact force network at peak stress ratio (Zhang and Thornton, 2007); c) shear deformation at the end of shearing (Vardoulakis & Sulem, 1995); d) photoelectric image highlighting the major principal stress direction (Dyer & Milligan, 1984)

Stellenbosch University https://scholar.sun.ac.za

2.9.6 Micromechanical Behaviour and Shear Failure

Micromechanical assessments of shear behaviour can be obtained from DEM tests, this method of assessing the shear behaviour of granular materials has proven to provide deeper insights, especially in the development of the shear band, than ordinary laboratory tests (Jacobson, Valdes and Evans, 2007; Wang, Dove and Gutierrez, 2007). For example, a set of DEM shear box test scenarios with shear strain concentrations as well as associated contact force networks have been selected and presented; this may aid in making inferences about the micromechanical behaviour of the granular assemblies in the tests undertaken for the present study, from Wang and Gutierrez (2010) (Figure 2-26). These scenarios illustrate the transition between two distinctly different mechanisms/modes of failure which are governed by the box scale ratios, and in particular, the aspect ratio employed when conducting direct shear tests.

It is observed that smaller aspect ratios (i.e. an increased height scale relative to the length scale) yield more defined and confined shear bands (especially after post-peak shear stress) (Figure 2-26c). On the other hand, larger aspect ratios (with relatively smaller height scales) produce more wide-spread and discordant shear bands that result in the majority of the test specimen being put under strain, which propagates through/occupies almost the entirety of the shear mould volume (Figure 2-26a). The intermediate box height scale marks a transition from the behaviour observed in largest and the smallest box height scales, with the partial development of the shear band and comparatively less mobilization of the specimen volume (Figure 2-26b).

The main deduction that can be made from the micromechanical work conducted by Wang and Gutierrez, (2010), is that the aspect ratio plays a crucial role in the controlling mode of failure that takes place within the direct shear test: either a bulk failure or a progressive failure. Typically, smaller aspect ratios favour bulk shear failures, which more uniformly mobilize the entire fabric of the granular specimen; and larger aspect ratios are more conducive to progressive failure of specimens, which is induced by locally induced anisotropies propagating inward from the shear box boundaries (Wang and Gutierrez, 2010).

Stellenbosch University https://scholar.sun.ac.za

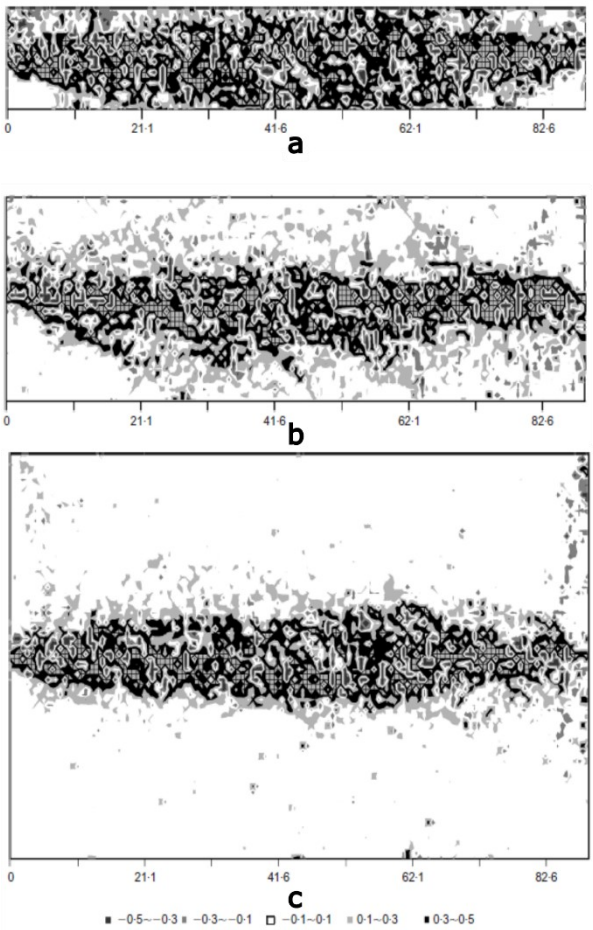

Figure 2-26. Distribution of shear strain inside DEM direct shear test for constant Shear Box length scale (L = 88 mm): a) H = 14 mm; b) HH = 28 mm; c) H = 56 mm

2.9.7 Variations in Experimental and Numerical Observations

The scale effect has been observed to generate disagreeable results between studies which have been conducted on physical models and numerical (or DEM) models. The strength of coarse-grained soils varied significantly when comparing laboratory experiments and DEM simulations conducted on the "same specimens" (Bagherzadeh-Khalkhali & Mirghasemi, 2009). An attempt was made to characterise the variation in the observed friction angle of modified (or scaled) grain size distributions via the parallel and scalping methods (Figure 2-27). The respective tests revealed that the internal angle of friction results derived from the laboratory DS apparatuses, were considerably larger in magnitude, than those derived from the DEM DS models (minimum difference of 3˚).

The effects of scaling grain size distributions on the friction angle were immediately more apparent in the DEM simulation results (Bagherzadeh-Khalkhali and Mirghasemi, 2009). Both the physical and simulation results indicated that friction angles derived from original gradations were greater than those obtained by modified gradations. Typically, friction angles derived using the scalping technique were appreciably greater than those generated by employing the parallel gradation method, despite having the same maximum particle size (Figure 2-27) (Bagherzadeh-Khalkhali and Mirghasemi, 2009).

Stellenbosch University https://scholar.sun.ac.za

The results obtained from DEM simulations displayed more variations in the resultant friction angles, e.g. the difference in the results of the scaled (i.e. parallel vs scalped) PSDs obtained by DEM simulations showed a variation of almost ten degrees, whereas, the difference in the friction angles yielded by physical experiments varied by as little as 3 degrees (Figure 2-27). The variations observed between the DEM software and experimental results were attributed to the limitations of the laboratory equipment and the software (Bagherzadeh-Khalkhali and Mirghasemi, 2009).

Despite the pit-falls of numerical modelling, i.e. simulating granular assemblies, it is an indispensable tool that when utilized during the study of granular materials, allows for deductions to be made about shear behaviour at the particle-particle and particle-boundary scales (Hicher, 2012). That being said, differences exist between shear behaviour results derived by simulations and those acquired in the laboratory; both means provide valuable information but do not necessarily represent the absolute behaviour of a particular granular media.

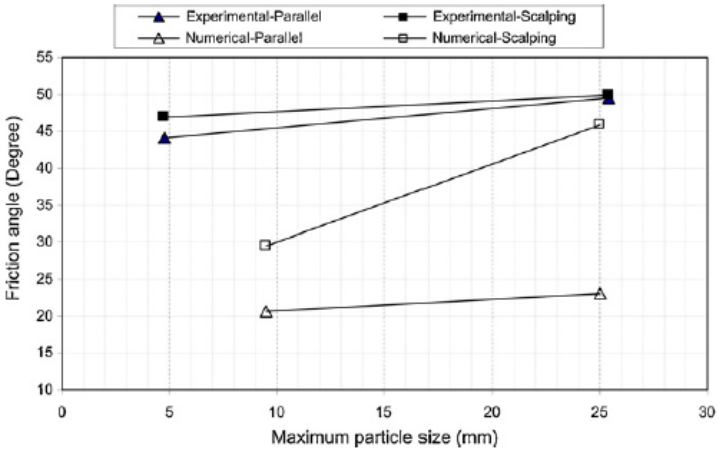

Figure 2-27. Variation in internal angle of friction, for 'the same samples', derived by experimental and numerical methods (after, Bagherzadeh-khalkhali and Mirghasemi, 2009)

Stellenbosch University https://scholar.sun.ac.za

Chapter 3 – Methodology

3.1 Introduction

This chapter can be divided into two broad components: fieldwork and laboratory work. An outline of the conducted fieldwork is given, as well as the experimental design and the methodology that was adopted to address the aforementioned key sub-objectives mentioned in Section 1.3 Objectives of Chapter 1.

3.2 Desk Study and Fieldwork

The fieldwork was carried out in January 2019, entailing three-days of sampling in the East Rand Goldfield, Gauteng, South Africa. The main objective of this field program was to obtain samples of Witwatersrand mine waste rock. The two sampling/collection locations of the mine waste rock were selected based on their accessibility and availability. Both sampling sites were situated approximately 30 km east of Johannesburg central and approximately 4,6 km apart from one another. The sample collection sites, ST02 and ST03 are waste repositories that are associated with Van Ryn and New Modderfontein mines, respectively (Figure 3-1; Table 3-1).

Table 3-1. Sample site locations and sample masses

Sampling Location	Coordinates	Sample Type	Mine	Mass of Sample Collected (kg)
ST02	26°10'19.08"S; 28°21'29.10"E	Waste Rock	Van Rhyn Mine	330
ST03	26°11'03.60"S; 28°24'08.70"E	Waste Rock	New Modderfontein Mine	131

The geological origin dictates the magnitude or behaviour of several geotechnical factors (Blight, 2010). Both of the sampling sites are underlain by sediments of the Johannesburg and Vryheid Formations (Figure 3-1). Given that both mines were underground, the material overlying the orebody that was extracted to sink the shaft was considered waste rock and was the most likely origin of the material that was sampled in the present study.

Stellenbosch University https://scholar.sun.ac.za

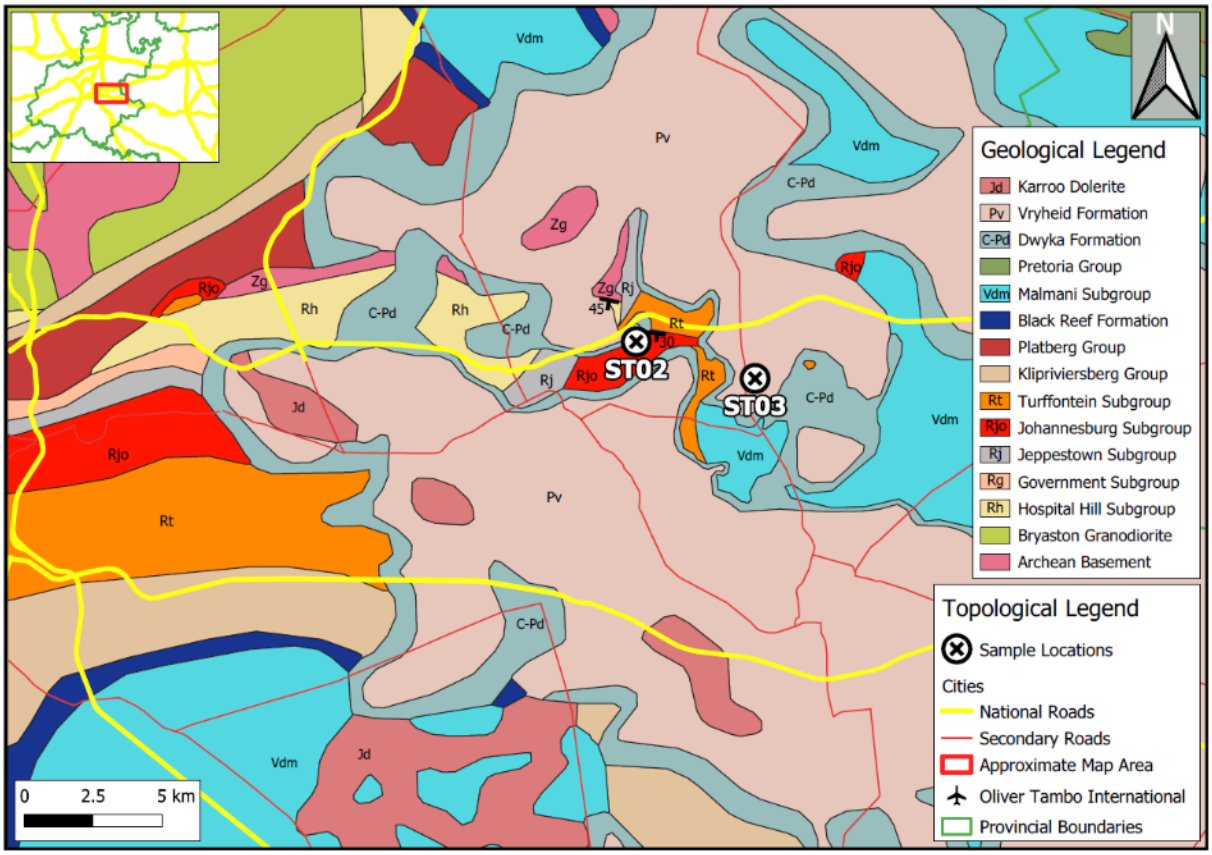

Figure 3-1. Regional Geology of the field area (compiled from CGS, 1985 and CGS, 2019)

3.2.1 Regional Geology

The sediments of the Witwatersrand Supergroup are Meso- to Neoarchean in age and unconformably overlie, in part, the older 3.1 Ga Archean granitoid and greenstone basement, as well as the slightly younger ~3.01 Ga volcano-metasedimentary Dominion Group (Marsh, 2006; McCarthy, 2006; Agangi *et al.*, 2015). Sedimentation within the Witwatersrand Basin begun after a brief hiatus at around 2.914 – 2.970 Ga (Robb and Robb, 1998) and ended between the years of 2.714 – 2.894 Ga (Robb and Meyer, 1995). The Witwatersrand sequence is unconformably overlain by lava, known as the Venterdorp Contact Reef (VCR), of the Ventersdorp Supergroup that is 2,78 – 2,71 Ga (Agangi *et al.*, 2015).

The East Rand goldfield (or basin) has been described in the literature as a continuation of the adjacent Central Rand basin (Robb and Robb, 1998; McCarthy, 2006). The volcano-metasedimentary Witwatersrand Supergroup comprises two principal groups: the West Rand Group (WRG) and the Central Rand Group (CRG). The auriferous horizons are largely present within the overlying CRG, and in the East Rand goldfield mainly in the 'South Reef' (also termed the Nigel Reef Leader or the Main Reef) and forms the divide between the CRG and WRG (Robb and Robb, 1998; McCarthy, 2006) (Figure 3-2).

The CRG constitutes fluvial to fluvio-deltaic quartzites and conglomerates, with minor amounts of interlayered shales (Frimmel, 2019). There is, however, a laterally continuous shale layer referred to as the Booysens Formation that set the precedent for the division of the CRG into two principal subgroups,

Stellenbosch University https://scholar.sun.ac.za

namely the Johannesburg and the Turffontein subgroups (Figure 3-2). The Johannesburg subgroup is primarily comprised of quartzites that represent a fluvial braid plain environment, periodically interrupted by small deposits of conglomerate that indicate periodic cycles of vigorous erosion and deposition. The Turfontein Subgroup is somewhat similar, but with almost equivalent proportions of quartzites and conglomerates (Robb and Robb, 1998). The majority of the waste rock material for both mines would, therefore, is derived from the stratum overlying the basal auriferous horizons in the Johannesburg and Turffontein Subgroups. In the case of the New Modderfontein mine, there may be components of the waste rock derived from the Carboniferous-aged Dwyka Formation, a glacial deposit which includes a series of diamictite horizons and some shales, and the Vryheid Formation that comprises sandstones, shales and (in places) coal beds (CGS, 1985).

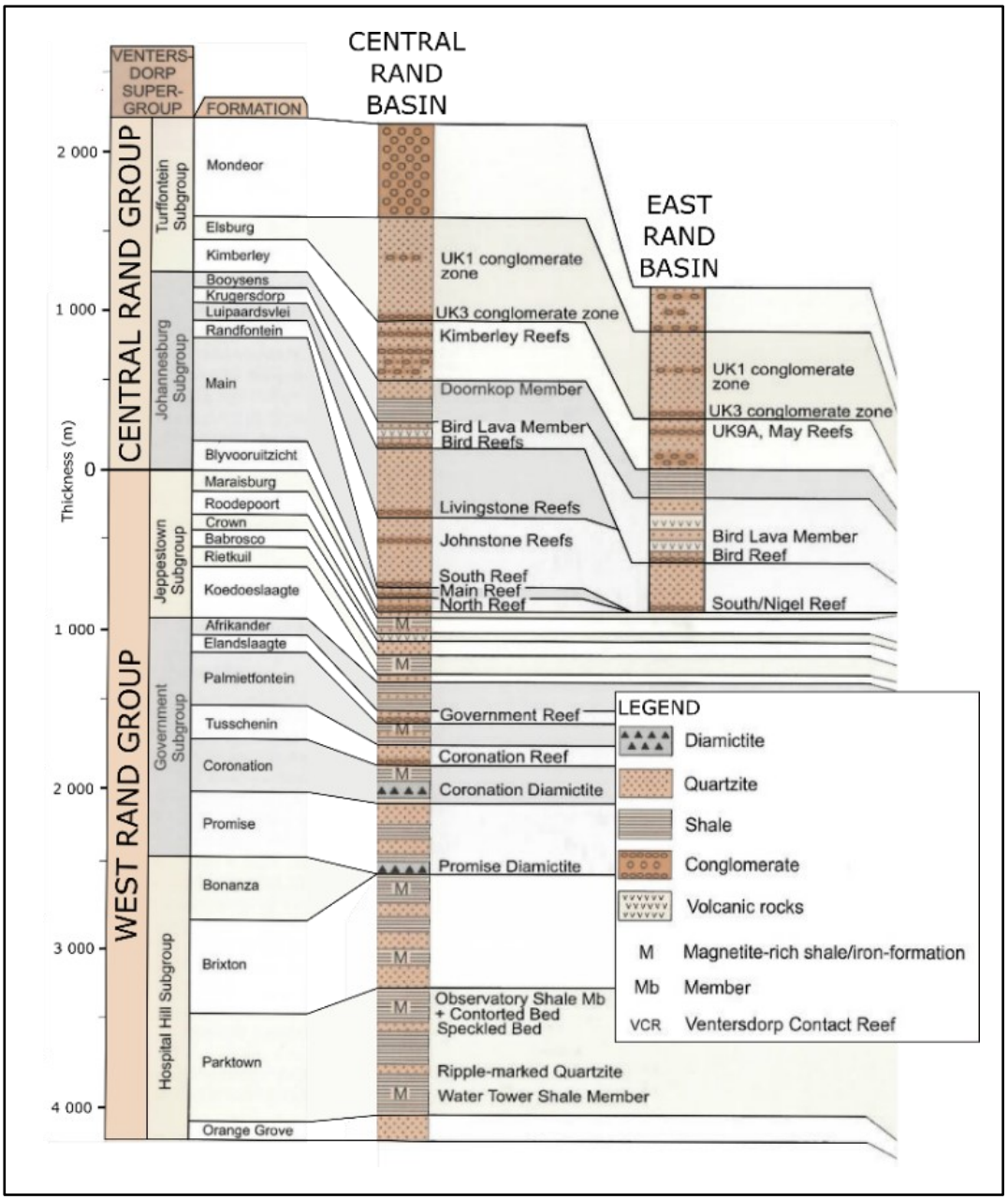

Figure 3-2. Stratigraphic column of the Central and East Rand Gold-baring Sub-basins (Modified after SACS, 2006)

Stellenbosch University https://scholar.sun.ac.za

3.2.2 Sampling Site Locations

Sampling location ST02 is an existing tailings facility, at the decommissioned Van Rhyn Mine. Waste rock fragments were placed on the exterior of the tailings impoundment as cladding to limit the generation of dust (Mphephu, 2002). Waste rocks with a D_{max} greater than 50 mm were hand-picked in a random fashion, within approximately five meters of position ST02 (Figure 3-1). This site was selected based on an above-average accumulation of mine waste rocks, which was a consequence of an existing slip failure that had occurred in a localised area of the tailing facility (Figure 3-3a).

Sampling site ST03 is on the New Modderfontein Mine premises. The effects of acid mine drainage (AMD) are visually clear in the area surrounding site ST03. As can be seen by the ochre-precipitates in a nearby surface water-body with pale-to-dark red colours (Valente & Leal Gomes, 2009) (Figure 3-4a). Even though this mine has been decommissioned, the reworking of the waste of existing tailings facilities is taking place. Waste rock fragments that were originally used as cladding were collected and stockpiled in an approximately ten-meter tall mine waste rock pile (Figure 3-4,b). Sampling was conducted by handing picking waste rocks with a D_{max} greater than 50 mm in a random fashion, within approximately five meters of location ST03.

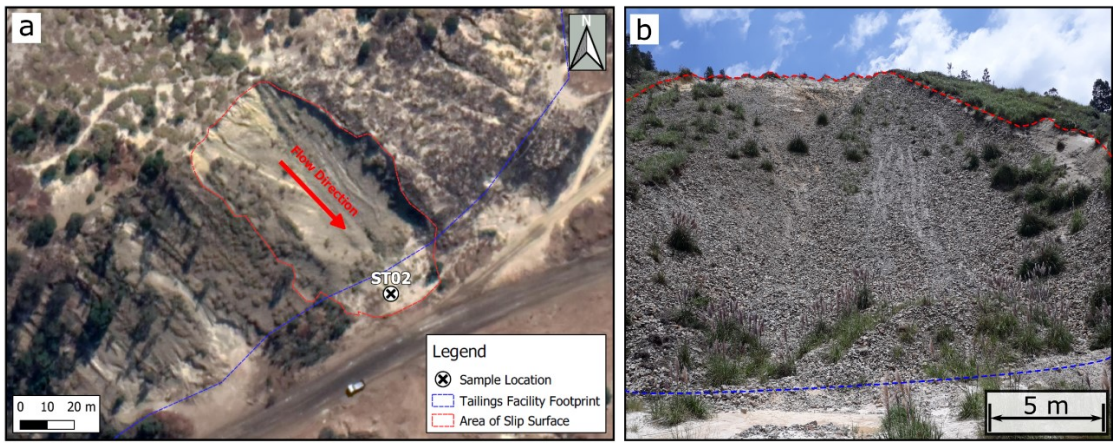

Figure 3-3. Sampling site 'ST02': a) Google Earth Imagery of Sample site and b) sampling site ST02, slip surface indicated

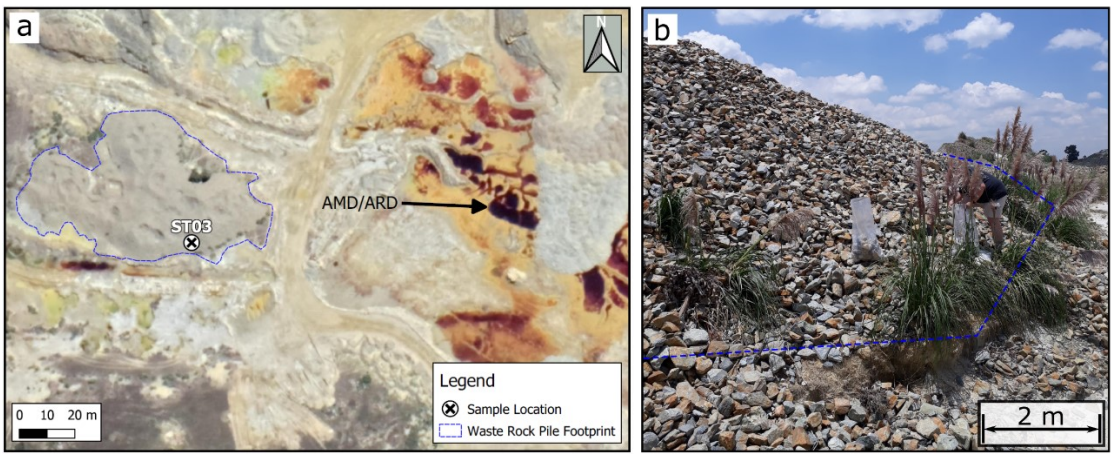

Figure 3-4. Sampling location 'ST03': a) Google Earth Imagery and b) sample collection at site ST03

Stellenbosch University https://scholar.sun.ac.za

3.3 Laboratory Characterisation

3.3.1 Witwatersrand Waste Rock Characteristics

The particle size distribution of the collected mine waste rock samples was assessed as per ASTM D6913M (ASTM, 2017). Particles larger than 75 mm were assessed as per ASTM D5519 (ASTM, 2001). The material from both sampling localities yielded a fairly narrow grading, which mainly fell within the cobble size-fraction (86.1%), few particles fell into the boulder-sized range (3.4% > 200 mm) and some were classified as gravels (10.5% < 60 mm) according to the Unified Soil Classification System (USCS) (Figure 3-5). The uniformity index (C_u) of the grain size distribution of the collected materials (C_u = 1.98) was typical of hard rock mine waste rock produced by blasting (Ovalle *et al.*, 2015). The collected materials were classified as GP according to ASTM D6913M (ASTM, 2017).

During the classification of the collected waste rock PSD, each of the samples were grouped into their respective localities and photographed with a scale to confirm the resultant PSD (Figure 3-6). The waste rock particle shape characteristics were assessed according to Krumbein and Sloss (1963).

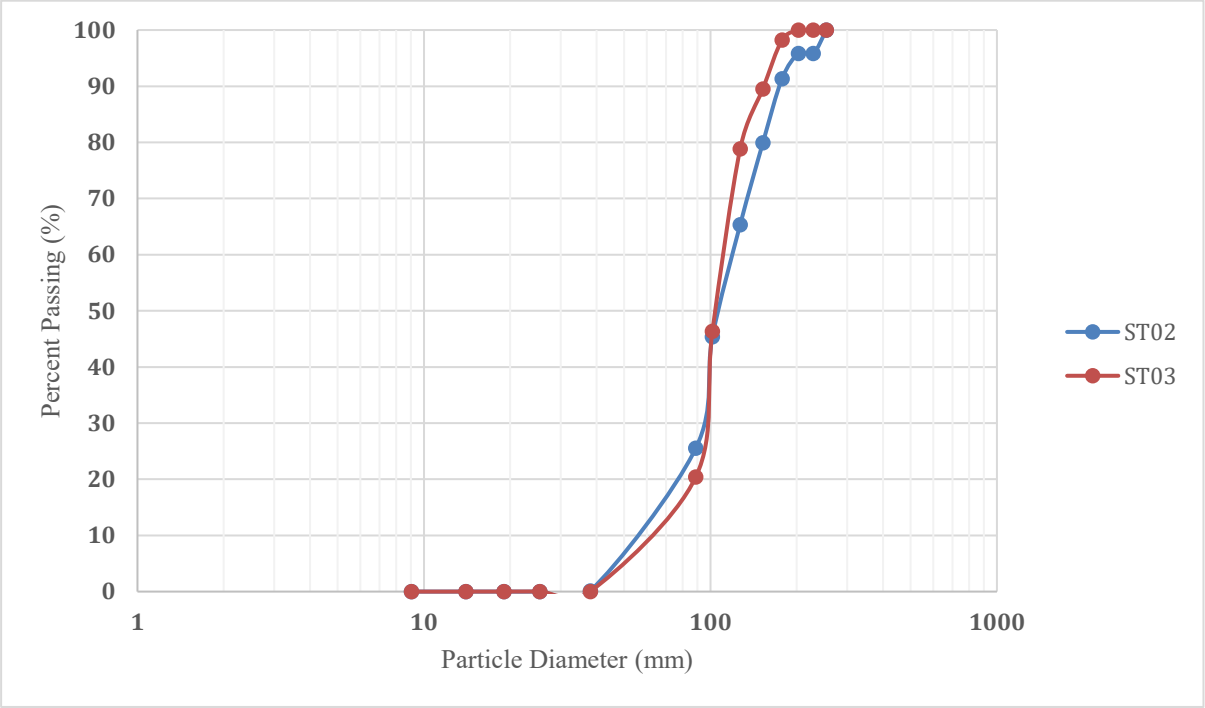

Figure 3-5. Particle size distribution of mine waste rock collected from sample sites ST02 and ST03

Stellenbosch University https://scholar.sun.ac.za

Figure 3-6. A representative example of waste rock particles collected from ST03. A range of shales and sandstones were collected, presumably derived from the Central Rand group

3.3.2 Sample Gradation

The collected waste rock material was crushed several times, using a jaw crusher with a minimum aperture of approximately 10 mm, to give rise to particles that had a D_{max} greater than 4 mm. Two distinct PSDs needed to be defined: a well-graded PSD (GW) and a poorly-graded PSD (GP). Specific constraints/characteristics were selected for the PSDs to achieve the aforementioned objectives: i) the resultant PSDs had to be classified as GW and GP, according to the USCS; ii) when Direct Shear testing specimens with the largest Shear Mould (100 x 100 x 24.5 mm) all of the ASTM D3080 – 11 particle-box ratios were adhered to, and; iii) when testing samples using the smallest Shear Mould (20 x 20 x 12.5 mm) none of the recommended ASTM D3080 -11 particle-box ratios were adhered to (ASTM, 2011).

The D_{max} for the PSD was based on existing Shear Box configurations and the sieves available. It was decided that D_{min} would be limited to the 'medium sand' or material retained on the 0.425 mm sieve as per ASTM 2487 (ASTM, 2006). The C_u is 6.18 (i.e. greater than 6) and the C_z is 1.36 (i.e. between 1 and 3) and can, therefore, be considered a well-graded sandy (34%) gravel (66%) with no fines (USCS; ASTM, 2017). Both the GW and GP grain size distributions are typical of waste rock PSDs encountered in the field (Table 2-1).

Stellenbosch University https://scholar.sun.ac.za

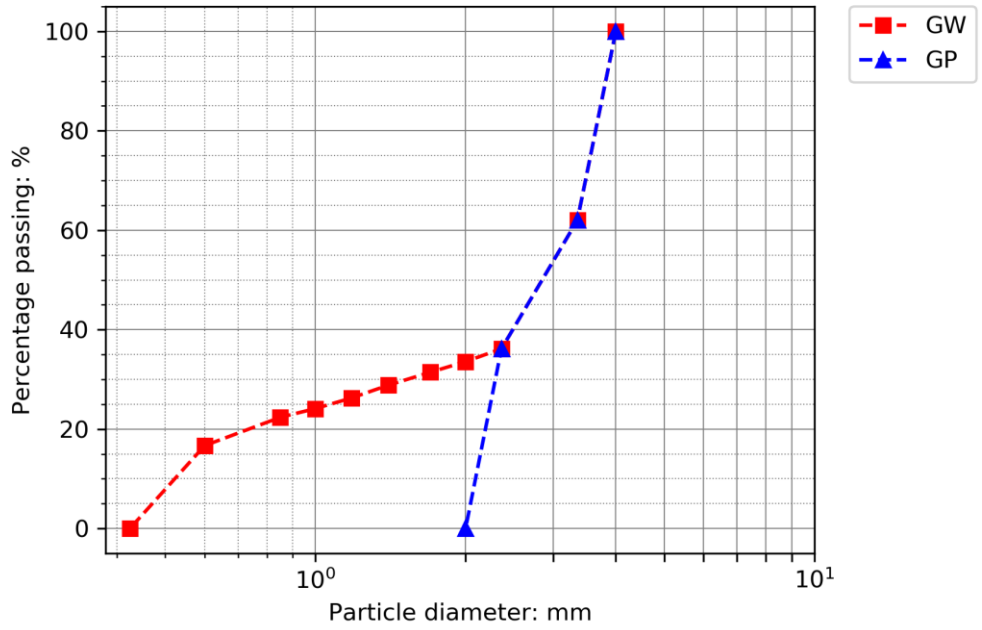

Figure 3-7. Tested particle size distributions: well-graded (GW) and poorly-graded (GP) reconstituted Witwatersrand waste rock specimens

To assess the effects of PSD on the returned strength parameters, a second particle size distribution was selected, and created by modifying the well-graded PSD and applying the reverse of a scalping technique, i.e. instead of decreasing the D_{max}, the D_{min} was increased (Table 3-2). As a consequence, the resulting PSD is narrowly graded and is considered (according to the USCS) as a poorly graded fine gravel (GP), with a D_{max} of 4 mm and a D_{min} of 2 mm (Table 3-2). The D_{50} parameter of the resultant narrowly graded (or GP) PSD was 2.21 mm, which changed from 3.16 mm for GW. A range of box height- and length scales were tested, using the generated PSD composed of reconstituted crushed mine waste rock as a sample medium (Table 3-3). The box-scale ratios were selected to evaluate the independent effects of the box height (H) and length (L) scale ratios on the strength parameters.

Table 3-2. Key characteristics of the well-graded and poorly-graded grain size distribution curves

Characteristic	GW	GP	Unit
D_{max}	4.00	4.00	mm
$D60$	3.27	3.32	mm
$D50$	2.21	3.16	mm
$D30$	1.54	2.30	mm
$D10$	0.53	2.10	mm
D_{min}	0.425	2.00	mm
C_U	6.18	1.58	-
C_z	1.36	0.76	-
$Dmax/Dmin$	9.41	3.30	-

Stellenbosch University https://scholar.sun.ac.za

3.3.2 Box Scale Ratios

A conventional Shear Box testing setup was altered to specific dimensions (length, breadth [L] and height [H]) to address the respective sub-objectives as set out in the – Introduction of this thesis. The length of the sample was varied using two separate sample-moulds respectively, a 100 x100 mm and a 60 x 60 mm, manufactured by Wykeham Farrance. A third box length was added to the experimental program by designing and manufacturing a modular 'insert' that would reduce the length of the 60 mm sample-mould to 20 mm (Figure 3-8b-d). The mould was fabricated not to interfere with the frictional resistance generated by the Shear Box sample-mould. The height of the sample was altered by adding or removing additional porous plates (Figure 3-8a).

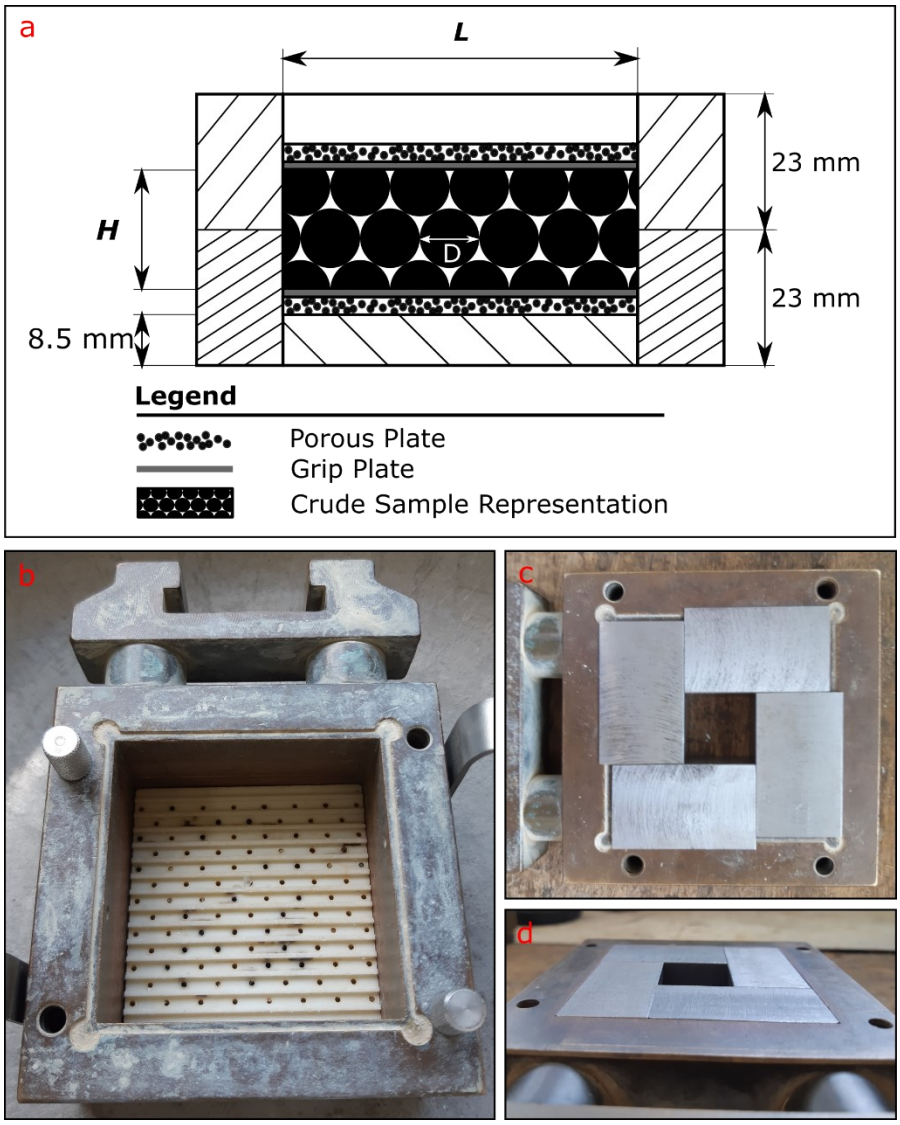

Figure 3-8. Shear Box sample moulds: a) schematic of shear box setup; b) 60 x 60 mm assembled sample mould with vies of grip plate; c) top view of the 60 x 60 mm sample-mould fitted with the manufactured 'insert', and; d) the underside of the 60 x 60 mm sample mould fitted with the 'insert'

Stellenbosch University https://scholar.sun.ac.za

3.4 Shear Box

In total, 162 DS tests were performed using 6 separate Shear Box Shear Mould sizes to assess the effect of box-scale on the shear behaviour of crushed mine waste rock. The selected box length- and height scale ratios allowed for simultaneous testing of several sample aspect ratios (Table 3-3). The recommended aspect ratio of 2:1 (ASTM, 2011) was respected when the box length scale was 60 mm and 100 mm, but was not when the box length scale is 20 mm (Table 3-3). The tests were conducted on reconstituted samples of crushed and blended Witwatersrand Mine waste rock samples from locations ST02 and ST03. The samples were reconstituted according to a typical well-graded and poorly-graded particle size distribution (Figure 3-7).

3.4.1 Experimental Apparatus

The DS test apparatus used during this investigation is a Wykeham Farrance Digishear, which is hosted in the Pavement Laboratory at SU (Figure 3-9). This model of the Wykeham Farrance Digishear is manufactured to allow for an interchangeable sample-box area, with capabilities for samples with a surface area of 3 600 mm^2 and 10 000 mm^2, respectively. Conventionally, the tests are conducted with a fixed sample height of 20 mm. All of the Shear Moulds utilized in this study are square prisms (i.e. equal length and breadth).

Figure 3-9. Wykeham Farrance Digishear used in this study

3.4.2 Test Preparation and Experimental Procedure

The preparation for each shear test can be divided as follows: i) the relevant Shear Box mould was selected; ii) the top half of the Shear Box was fastened to the lower half by two alignment screws; iii) the appropriately sized base plate, number of porous disks and grip plate were added to the bottom of the now fastened shear box halves, and; iv) the depth(s) to the bottom grip plate (in each corner of the box) were measured using a veneer (Figure 3-8,b).

Stellenbosch University https://scholar.sun.ac.za

The experimental procedure consisted of two distinct components: a layer preparation phase, and a specimen reconstitution phase. Each specimen was comprised of three layers of the same mass. The first component, the layer preparation phase, consisted of weighing out of the masses required for each size fraction of each layer (Figure 3-10). Once weighed out, the individual layers were saturated in air-tight 'sealable' bags for 24 hours. The second component, the sample reconstitution phase, involved the transferring (or reconstitution) of the sample layers into the relevant Shear Box sample-mould resulting in a specimen with a constant dry density of 1 600 kg/m^3. This density is typical of waste rock densities commonly encountered in the field (Table 2-1 and references therein; Williams, 2000). Specimens were reconstituted in three layers; each waste rock layer was prepared to a known mass and was hand tamped/compacted until a specific layer thickness, thereby the target density was achieved. The top of each layer was scarified in two directions (parallel and perpendicular to the shearing direction) to ensure binding between layers.

Figure 3-10. Material preparation station. Each container represents one layer of one specimen, as seen the containers are grouped and each group (of three containers) represents one sample

This process was repeated for each of the respective layers. The thicknesses of each layer were recorded. The top grip plate was added to the top of the third layer and the relevant number of porous disks were placed on top of the top grip plate (depending on the target height of the sample). Finally, the load cap was placed on top of the final porous plate (or, in the case of the largest sample height, directly onto the grip plate). The reconstituted sample in the Shear Box sample mould was placed into the Shear Box bath and was filled with distilled water. The appropriate dead load was applied in a single increment; it was assumed that no excess pore pressure developed in response to the applied loading. The alignment screws that initially fastened the box halves together were removed and used to part (i.e. create a gap between) the shear box halves (of 1.5 mm).

Most of the DS tests were conducted following the guidelines set out in the ASTM D3080-11 standard. Deviations were made only to assess the effects of the box length and height scales of the DS test, that is some of the tests contravene the stated ASTM 3080 box scale ratios. The Shear Box tests were

Stellenbosch University https://scholar.sun.ac.za

conducted under three normal stresses (50 kPa, 100 kPa and 150 kPa). Each test was repeated three times to generate a more statistically robust dataset that accounts for minor test/procedure and interpretation inaccuracies (Table 3-3). The selected target porosity was 0.407 (corresponding to a dry density of 1 600 kg/m^3). Most of the pre-shear porosities deviated slightly from this target value, the mean pre-shear porosity for the well- and the poorly-graded specimen was 0.387 (1658.19 kg/m^3) and 0.390 (1650.09 kg/m^3), respectively. The minimum initial porosity (and maximum densities) for the well- and poorly-graded samples was 0.329 (1815.07 kg/m^3) and 0.318 (1844.81 kg/m^3), respectively (Table 3-3). As to be expected, the pre-shear density was never less than that of the target value of 1600 k/gm^3.

Stellenbosch University https://scholar.sun.ac.za

Table 3-3. Summary of conducted shear tests and associated parameters

L: mm	H: mm	L/H	L/Dmax	H/Dmax	Well graded material: SW			Poorly graded material: SP		
					σ: kPa	Triplicates	Initial porosity: P_0	σ: kPa	Triplicates	Initial porosity: P_0
20	**12.5**	1.60	5	3.125	50	A; B; C (3)	0.406; 0.405; 0.405	50	A; B; C (3)	0.406; 0.407; 0.406
20	**12.5**	1.60	5	3.125	100	A; B; C (3)	0.400; 0.398; 0.399	100	A; B; C (3)	0.405; 0.406; 0.406
20	**12.5**	1.60	5	3.125	150	A; B; C (3)	0.394; 0.395; 0.399	150	A; B; C (3)	0.404; 0.401; 0.404
20	**18.5**	1.08	5	4.625	50	A; B; C (3)	0.407; 0.405; 0.403	50	A; B; C (3)	0.407; 0.407; 0.407
20	**18.5**	1.08	5	4.625	100	A; B; C (3)	0.402; 0.405; 0.400	100	A; B; C (3)	0.405; 0.405; 0.407
20	**18.5**	1.08	5	4.625	150	A; B; C (3)	0.397; 0.400; 0.398	150	A; B; C (3)	0.405; 0.405; 0.407
20	**24.5**	0.82	5	6.125	50	A; B; C (3)	0.405; 0.406; 0.407	50	A; B; C (3)	0.407; 0.406; 0.407
20	**24.5**	0.82	5	6.125	100	A; B; C (3)	0.404; 0.403; 0.405	100	A; B; C (3)	0.407; 0.407; 0.406
20	**24.5**	0.82	5	6.125	150	A; B; C (3)	0.402; 0.402; 0.398	150	A; B; C (3)	0.405; 0.405; 0.407
60	**12.5**	4.80	15	3.125	50	A; B; C (3)	0.387; 0.383; 0.390	50	A; B; C (3)	0.393; 0.397; 0.393
60	**12.5**	4.80	15	3.125	100	A; B; C (3)	0.368; 0.374; 0.378	100	A; B; C (3)	0.390; 0.383; 0.393
60	**12.5**	4.80	15	3.125	150	A; B; C (3)	0.371; 0.366; 0.374	150	A; B; C (3)	0.393; 0.386; 0.369
60	**18.5**	3.24	15	4.625	50	A; B; C (3)	0.390; 0.389; 0.396	50	A; B; C (3)	0.398; 0.397; 0.394
60	**18.5**	3.24	15	4.625	100	A; B; C (3)	0.387; 0.377; 0.393	100	A; B; C (3)	0.391; 0.367; 0.388
60	**18.5**	3.24	15	4.625	150	A; B; C (3)	0.388; 0.337; 0.383	150	A; B; C (3)	0.391; 0.397; 0.365
60	**24.5**	2.45	15	6.125	50	A; B; C (3)	0.396; 0.397; 0.398	50	A; B; C (3)	0.402; 0.401; 0.397
60	**24.5**	2.45	15	6.125	100	A; B; C (3)	0.392;0.392;0.399	100	A; B; C (3)	0.400; 0.401; 0.398
60	**24.5**	2.45	15	6.125	150	A; B; C (3)	0.386; 0.388; 0.391	150	A; B; C (3)	0.395; 0.395; 0.378
100	**12.5**	8.00	25	3.125	50	A; B; C (3)	0.369; 0.368; 0.368	50	A; B; C (3)	0.376; 0.369; 0.330
100	**12.5**	8.00	25	3.125	100	A; B; C (3)	0.345; 0.376; 0.370	100	A; B; C (3)	0.346; 0.355; 0.355
100	**12.5**	8.00	25	3.125	150	A; B; C (3)	0.329; 0.350; 0.344	150	A; B; C (3)	0.360; 0.318; 0.363
100	**18.5**	5.41	25	4.625	50	A; B; C (3)	0.381; 0.381; 0.386	50	A; B; C (3)	0.391; 0.390; 0.388
100	**18.5**	5.41	25	4.625	100	A; B; C (3)	0.380; 0.361; 0.387	100	A; B; C (3)	0.378; 0.350; 0.372
100	**18.5**	5.41	25	4.625	150	A; B; C (3)	0.370; 0.356; 0.386	150	A; B; C (3)	0.367; 0.380; 0.380
100	**24.5**	4.08	25	6.125	50	A; B; C (3)	0.398; 0.378; 0.399	50	A; B; C (3)	0.389; 0.380; 0.391
100	**24.5**	4.08	25	6.125	100	A; B; C (3)	0.393; 0.374; 0.391	100	A; B; C (3)	0.395; 0.396; 0.399
100	**24.5**	4.08	25	6.125	150	A; B; C (3)	0.389; 0.387; 0.387	150	A; B; C (3)	0.389; 0.394; 0.392

Stellenbosch University https://scholar.sun.ac.za

3.4.3 Grain Shape Quantification

The shape of the particles was assessed after collection, after crushing, and after conducting the DS tests. A representative sample was obtained for each of these three stages, similar to the process described by Cho, Dodds and Santamarina (2006). The shape of the particles was compared with published shape estimation charts (Figure 2-11; Krumbein and Sloss, 1963).

Each of the particles were laid out on their shortest axis, as this ensured that the longest and intermediate axes were photographed. Of the 536 waste rock particles collected from the field, 140 of them were randomly selected and assessed as a representative sample for the uncrushed waste rock samples. The samples were taken from both sampling sites and were selected to cover the broadest size range.

Subsequently, the waste rock was crushed by a jaw crusher and was cycled through the machine a minimum of five times. The crushed waste rock was randomly sampled, and a minimum of ten particles of various size fractions were selected to assess the particle shape. A similar approach was adopted to assess the particle shapes of the crushed and tested waste rock particles. 185 particles were randomly selected from samples that comprised well-graded specimen, and 108 particles were randomly selected from the poorly-graded specimen.

3.4.4 Statistical Methods

For the most part, analysis of the collected (and presented) data was conducted using ordinary modal statistics, and the standard error associated with the direct shear triplicate test results was determined, all of which is discussed in the subsequent Chapters. Moreover, in assessing the trends of several collected or derived parameters, models were used to describe a number of these trends, which were devised by implementing the 'scipy' package and 'optimise curve fit' module, which is an algorithm that fits curves to experimental data, in the scientific computing program, Python. The 'goodness of fit' of these curves were assessed by examining the difference between the observed values (obtained experimentally) and those which were predicted by the model (i.e. the optimised curve), which is represented in figures in the present study by the residual error. Furthermore, the 'goodness of fit' was assessed and represented as numerical figures, e.g. the r^2 values of the respective modelled curves.

Stellenbosch University https://scholar.sun.ac.za

Chapter 4 – Results

4.1 Data Smoothing

Data logger collected data at a high rate during the DS tests, resulting in very high resolution. This made the extraction of overall trends challenging, especially when assessing tests that were conducted at small box-length scales as a high degree of variability in shear force, and ultimately shear stress (or 'noise'), was observed as the tests progressed. For this reason, Python's "NumPy.convolve" convolution algorithm was employed. The convolution algorithm reduces the significance of the noise by calculating a moving average of measurements; a mode is to be selected, in this case, the mode 'same' was selected this smooths the length of the dataset, but boundary effects may be visible (Figure 4-1). The convolution algorithm that was employed can be found in Appendix A.

When nearing the end of the data range, the algorithm generates a 'tail', i.e. steep drop in shear stress (Figure 4-1), which was removed and excluded from the analysis. The shear stress was the only parameter that was directly smoothed by convolution. Any parameter derived from shear stress (e.g. stress ratio) is consequently also a smoothed trend. It is important to indicate that in the following chapters, the applied shear strain (%) and total volumetric strain (%) have been expressed as a percentage; i.e. the shear displacement normalised with respect to the box length scale, and the shear box vertical wall displacement normalised with respect to the initial height of the test specimen.

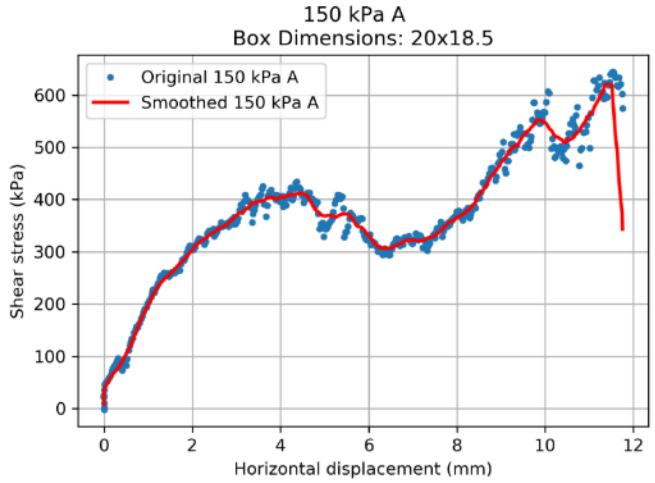

Figure 4-1. Example of raw and resultant 'smoothed' data using convolution function for test using a well-graded sample (dimensions: 20 x 18.5 mm; normal stress: 150 kPa; test label: '150 A')

Stellenbosch University https://scholar.sun.ac.za

4.2 Poorly Graded Specimen Results

One of the primary concerns of the present study was to assess the influence of the Shear Boxes' length and height, on the measured shear strength parameters. In each of the subsequent sections, a set of results is presented with the largest box volume appearing first, and each subsequent curve displaying the results of a shear mould with a reduced volume. In this section, the results of 81 DS tests conducted on reconstituted, poorly-graded specimen are presented. It should be noted that in the present and subsequent sections and chapters, the respective length and height dimensions of the Shear Box moulds utilised in this study are defined as the following: i) the largest length scale is 100 mm and the largest height scale is 24.5 mm; ii) the intermediate length scale is 60 mm and the intermediate height scale is 18.5 mm; and iii) the smallest length scale is 20 mm and the smallest height scale is 12.5 mm.

Additional information regarding the results presented in subsequent sections can be found in the summary table of the conducted shear tests as well as the shear box data summary table (Table 3-3 and Table 4-1).

4.2.1 Stress ratio – displacement curves

The stress ratio-displacement curves for poorly-graded specimens are presented in Figure 4-2 to Figure 4-4. For the majority of the stress ratio curves, the higher the normal stress, the lower the stress ratio. For example, when carrying out tests using the largest box dimensions (largest box length and height scale) and shearing at 50 kPa the average peak stress ratio is 1.23, and when shearing at a normal stress of 150 kPa the average peak stress ratio is 0.98 (Figure 4-2a). The stress ratio is generally inversely proportional to the box length scale, i.e. as the box length scale becomes smaller, the observed stress ratio increases. As an example, when utilizing the greatest box length and height scale the average peak stress ratio is 1.23 (Figure 4-2a), and when conducting tests at the smallest box length and height scale the average maximum peak stress ratio is 3.1 (Figure 4-4a).

Moreover, it would seem that, generally, the applied shear displacement at the peak stress ratio decreases as the box length scale decreases. For example, the average displacement for the greatest box length and height scale, is 6.2 mm (Figure 4-2a) at the peak stress ratio, whereas, for the smallest box length and height scale it is 2.6 mm (Figure 4-4a). Minor variations in peak stress ratios are observed with changes of the box height scales (at constant box length scales). Most often, smaller box height scales returns lower peak stress ratios; indicating a positive correlation. As an example, when considering the intermediate box length scale the average peak stress ratio for the maximum box height scale is 1.35 (Figure 4-3a), whereas for the smallest box height scale it is 2.21 (Figure 4-3c).

Decreasing the box length scale is associated with increased variation of the stress ratio, i.e. the results become less repeatable. For instance, when adopting the smallest height scale and varying the box length scale from the largest to the smallest, the range in resultant stress ratios is greatest for the smallest box length scale (1.43) and greatest for the largest box length scale (0.12). Variations in box height scale, on

Stellenbosch University https://scholar.sun.ac.za

the other hand, show similar behaviour as before; decreased box height scale most often results in the smallest range of stress ratio results, indicating a higher degree of repeatability for smaller box height scales. The model example is shown by the largest box length scale and largest box height scale which produces a range of peak stress ratios of 0.36, which by comparison, is greater than those brought about by the smallest height scale yielding a range of results of only 0.12.

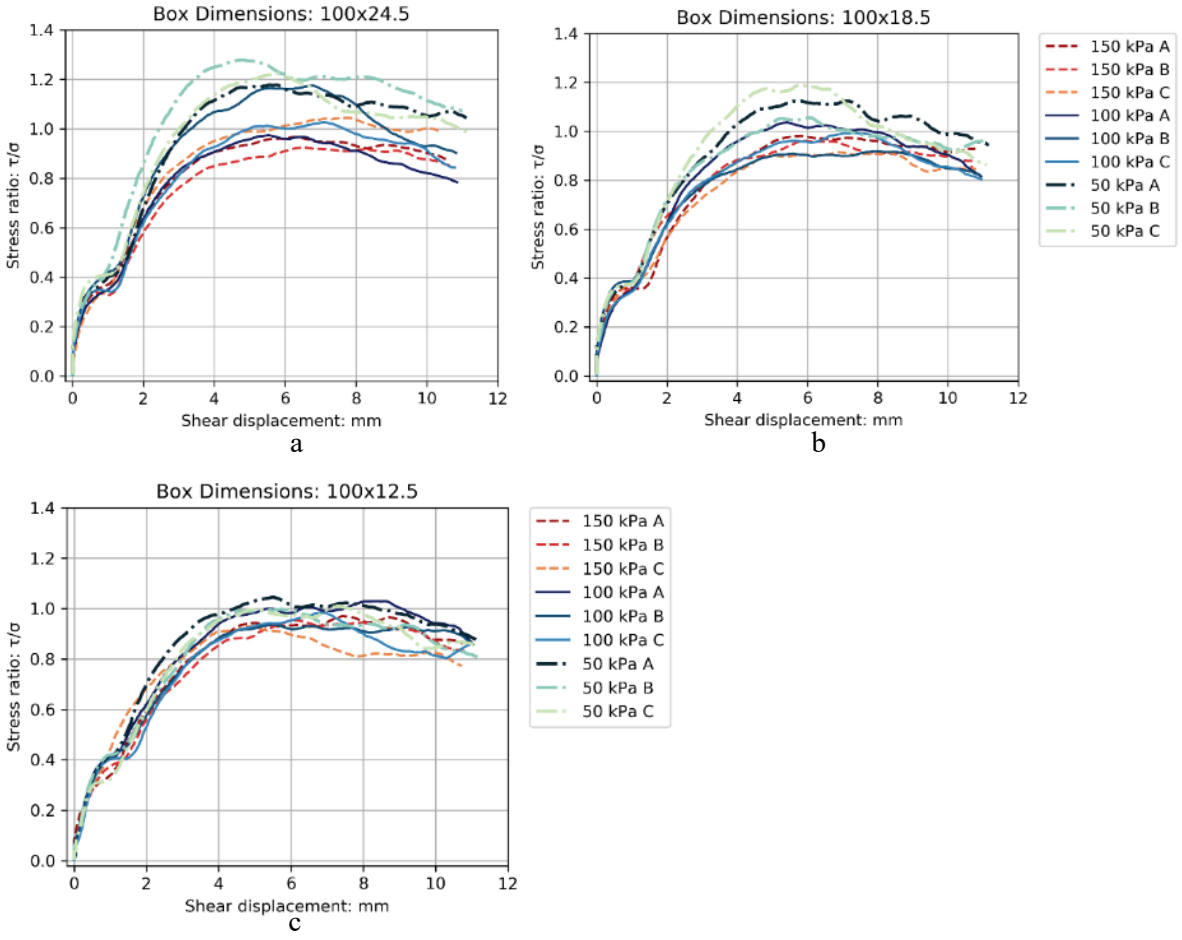

Figure 4-2. Stress ratio-displacement curves for 100 mm [L] box for poorly-graded soil specimens (a to c)

Stellenbosch University https://scholar.sun.ac.za

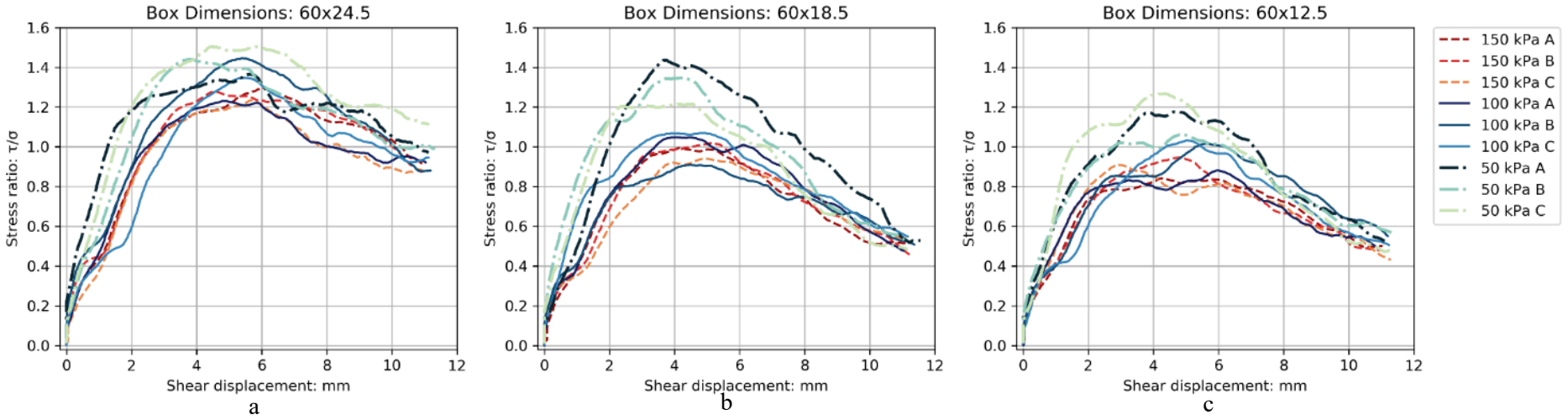

Figure 4-3. Stress ratio-displacement curves for 60 mm [L] box for poorly-graded soil specimens (a to c)

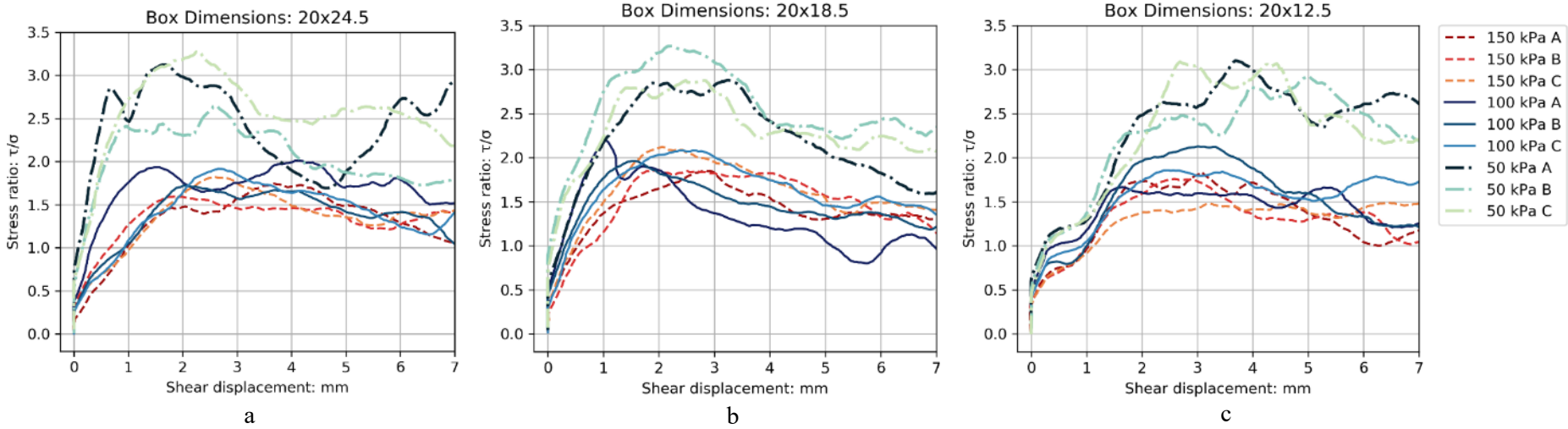

Figure 4-4. Stress ratio-displacement curves for 20 mm [L] box for poorly-graded soil specimens (a to c)

Stellenbosch University https://scholar.sun.ac.za

4.2.2 Stress ratio – applied strain curves

The stress ratio-applied shear strain curves are presented for the poorly-graded specimens in Figure 4-5 to Figure 4-7. As above, the stress ratio increases with decreasing box length scale (with constant height scale). For instance, when a constant height scale of 24.5 mm is adopted, the intermediate box length scale returns an average peak stress ratio of 1.35 (Figure 4-6b), and the smallest box length scale yields an average peak stress ratio of approximately 2.21 (Figure 4-7b). The box height scale is directly proportional to the peak stress ratio; for instance, the smallest box length scale with the largest height scale yields an average peak stress ratio of 2.21, as compared to the smallest height scale with an average peak stress ratio of 2.23. Trends in the applied shear stress at the peak stress ratio, with variation in box scale ratios, are unlike those described for the average peak stress ratio.

Generally, the applied shear strain required at the peak stress ratio becomes smaller as the box length scale reduces. For example, when considering the largest box height scale coupled with the intermediate and smallest box length scales, the average applied shear strain at the peak stress ratio is 5.09% and 2.60%, respectively. For all box length scales, there is no notable effect of height scale variation on the average magnitude of applied shear strain required to reach the peak stress ratio; it can be seen that for the intermediate box length scale with variation in the height scale, on average, the applied shear strain at the peak stress ratio is consistently between 7.89 and 8.66% (Figure 4-6a-c). However, it seems that strain softening is more clearly defined for the smallest height scale as compared to the largest height scale (Figure 4-6a-c). It appears that this observation seems is less apparent for the cases of the largest and smallest box length scales; in fact, the opposite seems to be true for the largest box length scale (Figure 4-5; Figure 4-7).

Regarding the ranges of stress ratios observed with variations in the box length and height scales, similar trends are observed as before (Section 4.2.1 Stress ratio – displacement curves): generally, smaller box height scales produce more repeatable results; and decreased box length scales yield larger ranges of stress ratios.

Stellenbosch University https://scholar.sun.ac.za

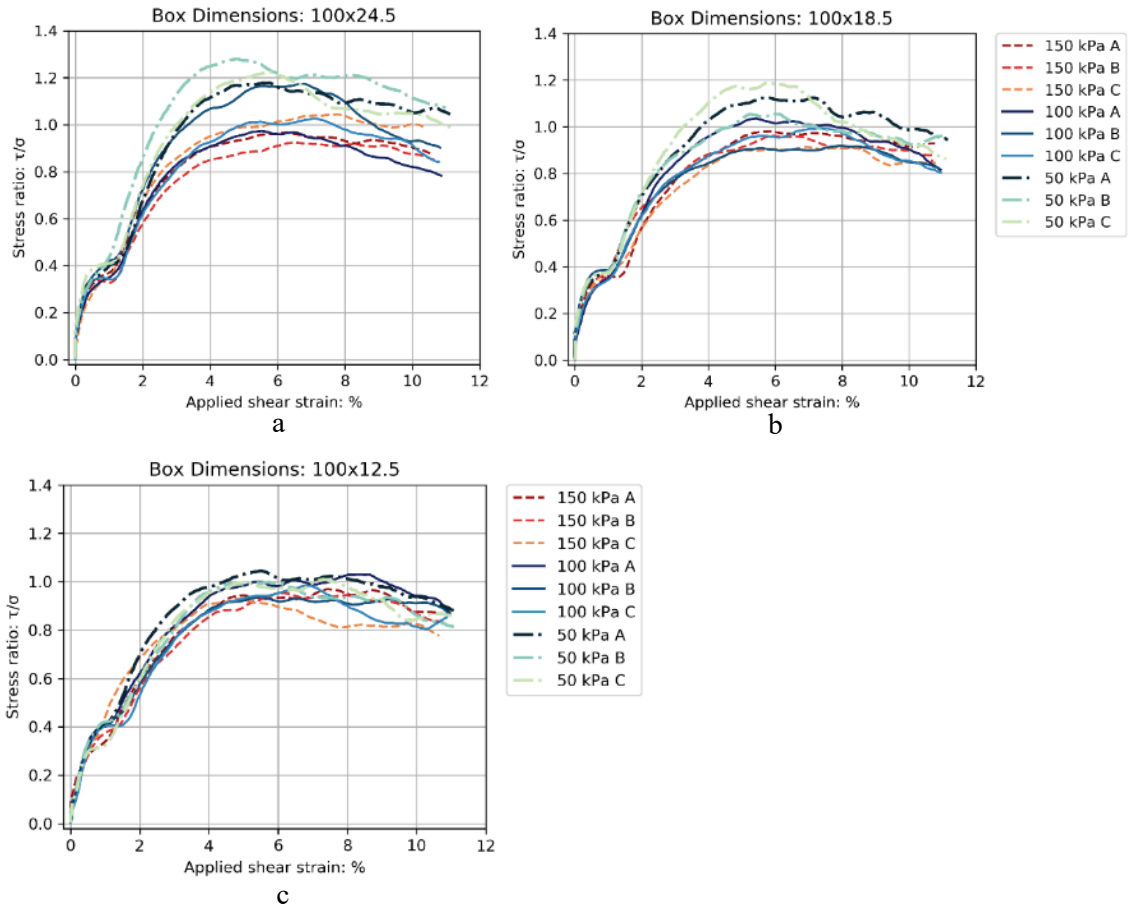

Figure 4-5. Stress ratio vs applied shear strain curves for 100 mm [L] box for poorly-graded test specimens (a to c)

Stellenbosch University https://scholar.sun.ac.za

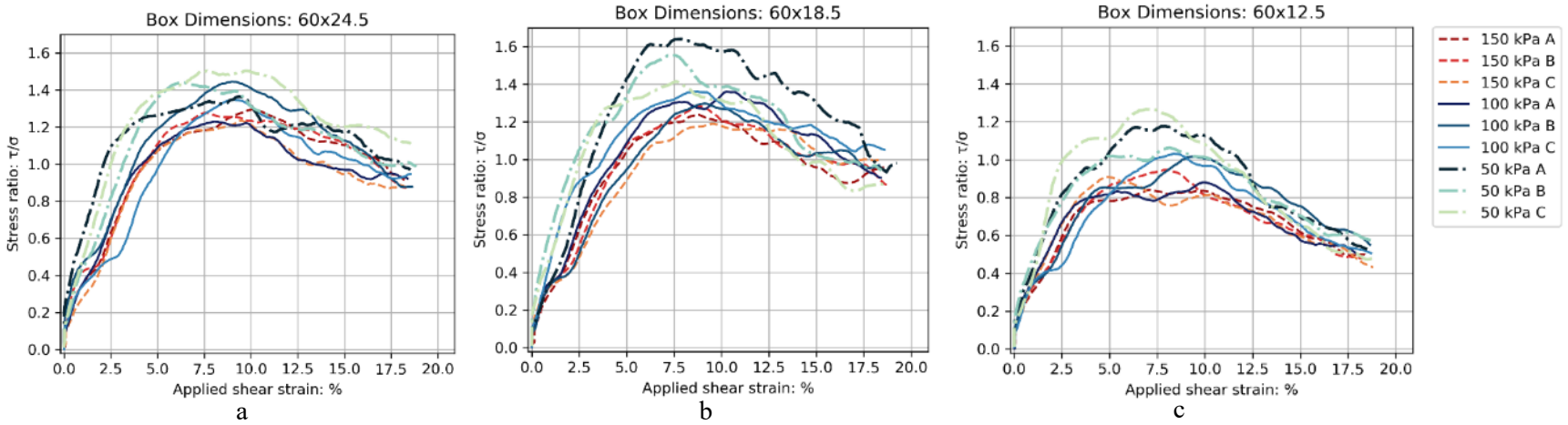

Figure 4-6. Stress ratio vs applied shear strain curves for 60 mm [L] box for poorly-graded test specimens (a to c)

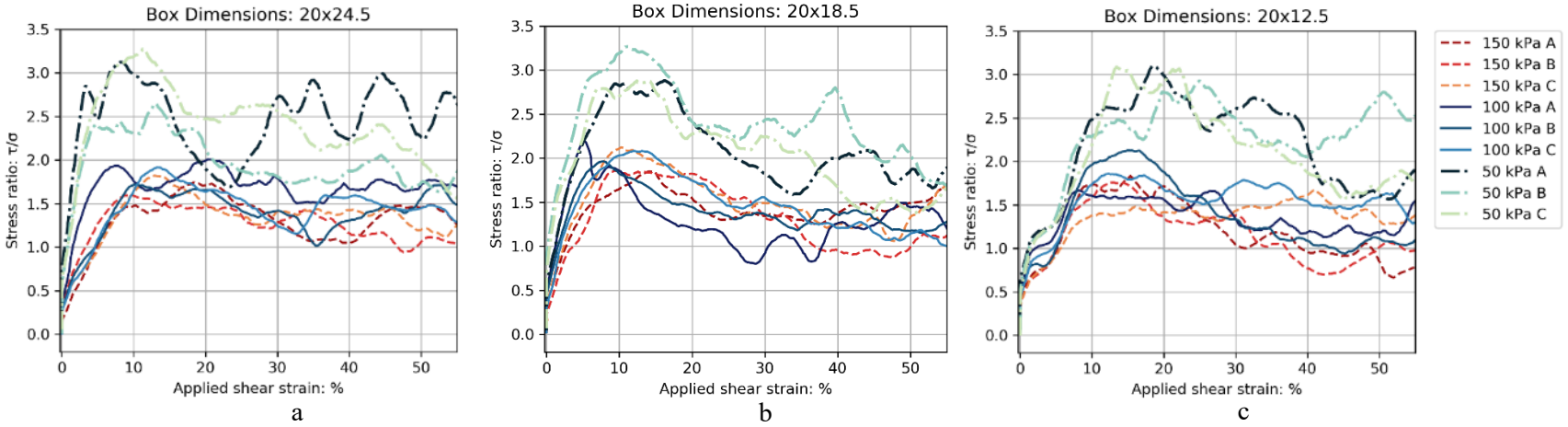

Figure 4-7. Stress ratio vs applied shear strain curves for 20 mm [L] box for poorly-graded test specimens (a to c)

Stellenbosch University https://scholar.sun.ac.za

4.2.3 Top wall vertical displacement - shear displacement curves

The results of the poorly-graded specimens vertical displacement variations with shear displacement are presented in Figure 4-8 to Figure 4-10. As the sample box height scale decreases, the magnitude of the vertical displacement of the Shear Box top wall decreases proportionately. This can be seen most clearly when considering the largest box length- and height scale, which returned a maximum vertical displacement of the Shear Box top wall of approximately 1.8 mm (Figure 4-8a), and the case of the maximum box length- and minimum height scale produced a maximum vertical displacement of approximately 1.0 mm.

Typically, as the length scale of the Direct Shear decreases, so does the average magnitude of the vertical movement of the Shear Box top wall. When comparing the magnitudes of the vertical movement of the Shear Box top wall for the largest box length scale, the final magnitude of the vertical movement is, on average, 1.2 mm (Figure 4-8a), whereas for the smallest box length scale the average final magnitude of vertical displacement is 0.7 mm (constant height scales of 24.5 mm) (Figure 4-10a). Here, it should be pointed out that when assessing the vertical height of the top wall of the DS test with shear displacement, or the associated total volumetric strain, the 'raw' data was used and not the smoothed data, therefore, the trends can be of a more erratic nature (in the present and subsequent sections) (e.g. Figure 4-10).

Higher normal stresses reduce the magnitude of the vertical displacement of the top wall. This is illustrated well by adopting the intermediate box length- and maximum box height scales, e.g. the maximum vertical displacement when testing under a normal stress of 50 kPa and 150 kPa was 1.6 mm and 0.9 mm, respectively (Figure 4-9a). Moreover, the effects of a reduction in length or height scale are less sensitive at higher normal stresses. This is illustrated by the minor differences in the final magnitudes of vertical movement of the top wall of the Shear Box, when comparing results derived from normal stresses of 150 kPa with and 50 kPa, while varying the box length- and height scales. The largest Shear Box mould under a normal stress of 150 kPa returns a final vertical displacement of the Shear Box top wall of 1.0 mm (Figure 4-8a) when the box height scale is reduced (e.g. 100 x 12.5 mm) the final vertical displacement is 0.8 mm (Figure 4-8c). In contrast, when observing the final displacement magnitudes for the same Shear Box height- and length scales for tests conducted under a normal stress of 50 kPa, for the previously mentioned Shear Moulds, the magnitudes are 1.5 and 0.75 mm, respectively.

Stellenbosch University https://scholar.sun.ac.za

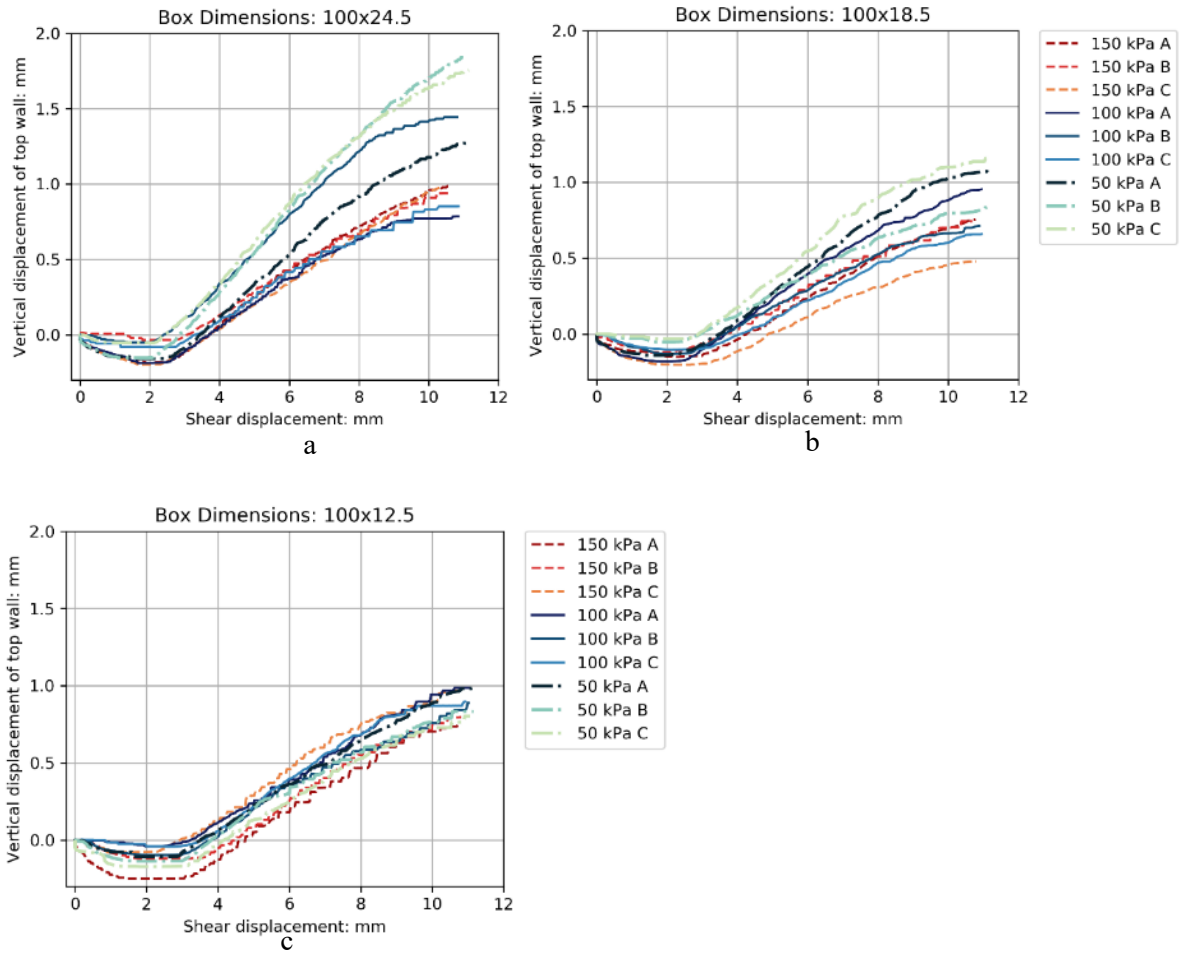

Figure 4-8. Vertical displacements of Shear Box top wall vs shear displacement curves for 100 mm [L] box for poorly-graded soil specimens (a to c)

Stellenbosch University https://scholar.sun.ac.za

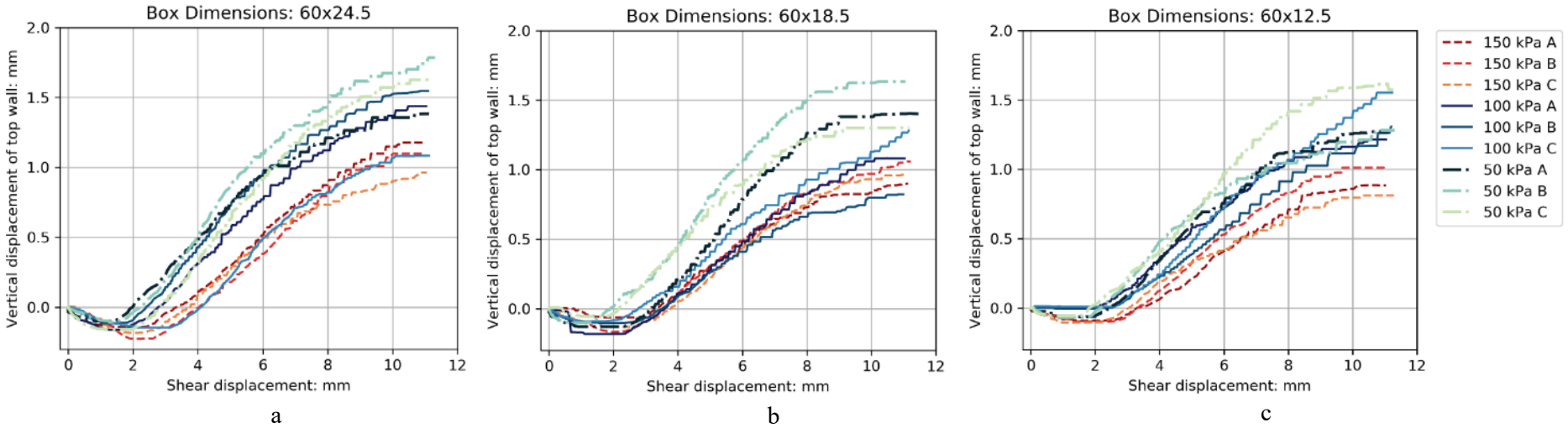

Figure 4-9. Vertical displacements of Shear Box top wall vs shear displacement curves for 60 mm [L] box for poorly-graded soil specimens (a to c)

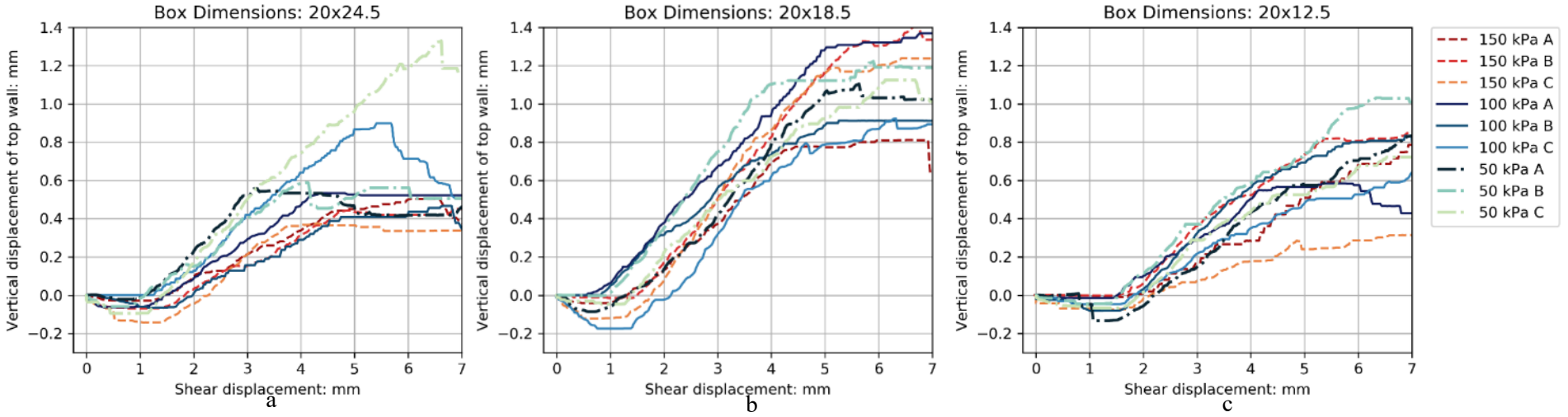

Figure 4-10. Vertical displacements of Shear Box top wall vs shear displacement curves for 20 mm [L] box for poorly-graded soil specimens (a to c)

Stellenbosch University https://scholar.sun.ac.za

4.2.4 Total volumetric strain - applied shear strain

The total volumetric strain-applied shear strain graphs for the poorly-graded specimens are presented in Figure 4-11 to Figure 4-13. Similar trends are observed to those indicated above (Section 4.2.3), with minor variations. For example, although the applied shear displacements are the same, the applied shear strain is largest (at test completion) for the smallest box length scale, which is significantly larger than the intermediate and largest box length scales.

On average, the total volumetric strain at the peak stress ratio is inversely proportional to the box length- and height scales. The effect of the box height scale is typified by the intermediate box length scale; the largest box height scale (on average) generates a total volumetric strain of 0.85% (Figure 4-12a), the intermediate box height scale 1.42% (Figure 4-12b), and the smallest box height scale 2.28% (Figure 4-12c). The effect of box length scale is best illustrated by the smallest box height scale, the average total volumetric strain (at the peak stress ratio) increases from the smallest box height scale at 2.28% (Figure 4-12c) to 3.33% for the intermediate box length scale (Figure 4-13c).

Similarly, the final total volumetric strain (at test completion) is inversely proportional to both the box length scale and box height scale. These trends in final total volumetric strain are most prominent for the intermediate (Figure 4-12b) and smallest (Figure 4-13c) box length scales; furthermore, when comparing the intermediate box length scale with the smallest box length scale (for any constant height scale) the intermediate length scale generates greater maximum and minimum magnitudes of final total volumetric strain. For example, the intermediate box length- and height scale produces a range of final total volumetric strain values between 4.2 % and 9.0% (Figure 4-12b), whereas the smallest box length scale (H = 18.5mm) produces final total volumetric shear strain values between 2% and 7.5% (Figure 4-13b), and the smallest box length- and height scale yields final volumetric strains of between 1.0% and 8.5%.

Contrary to the examples indicated above, the largest box length scale, on average, does not demonstrate these trends by generating smaller final total volumetric strains at the smallest height scale (e.g. smallest- and largest height scales: 6.0% and 2.5%, respectively) (Figure 4-11a-c); as compared to those generated by the intermediate- (e.g. smallest- and largest height scales: 4.2% and 10.0%, respectively); and smallest box length scales (e.g. smallest- and largest height scales: 1.0% and 6.0%, respectively). Interestingly, a decrease in box height scale does not induce a consistent increase in the total volumetric strain, when utilizing the largest box length scale. For instance, when comparing the results of the largest Shear Box length- and height scale average total volumetric strain of 7.0% (Figure 4-11c), with 10.0% brought about by the intermediate box height scale (Figure 4-12c) and 6.0% by the smallest box height scale (Figure 4-13c).

The total volumetric strain is more sensitive to the initial box height scale than the length scale of the specimen. This is demonstrated by comparing each box height scale of the intermediate (Figure 4-12a-c) and smallest (Figure 4-13a-c) box length scale examples, whereafter a comparison is made between

Stellenbosch University https://scholar.sun.ac.za

a single box height scale (e.g. smallest) between the intermediate and smallest box length scales. The range of maximum total volumetric strain is larger when comparing height scales of a single length scale. For instance, when comparing the range of the final total volumetric strain derived from the intermediate box length scale and largest box height scale (4.0% - 7.2%)(Figure 4-12a), with the range of the final total volumetric strain obtained from the intermediate box length- and height scale (4.3% - 8.9%)(Figure 4-12b), the range of final total volumetric strain values becomes larger.

As the box length scale decreases, the range-, minimum and maximum magnitudes of applied shear strain that induce specimen dilation (i.e. positive total volumetric strain) becomes greater. As an example, tests conducted using the largest box length scale, only induced dilation once the applied shear strain was between 2.4% and 5.8% (Figure 4-11a-c), whereas for the intermediate box length scale dilation was induced later at between 2.5% and 6% (Figure 4-12a-c) and later still for the smallest box length scale at between 2% and 10.5% (Figure 4-13a-c).

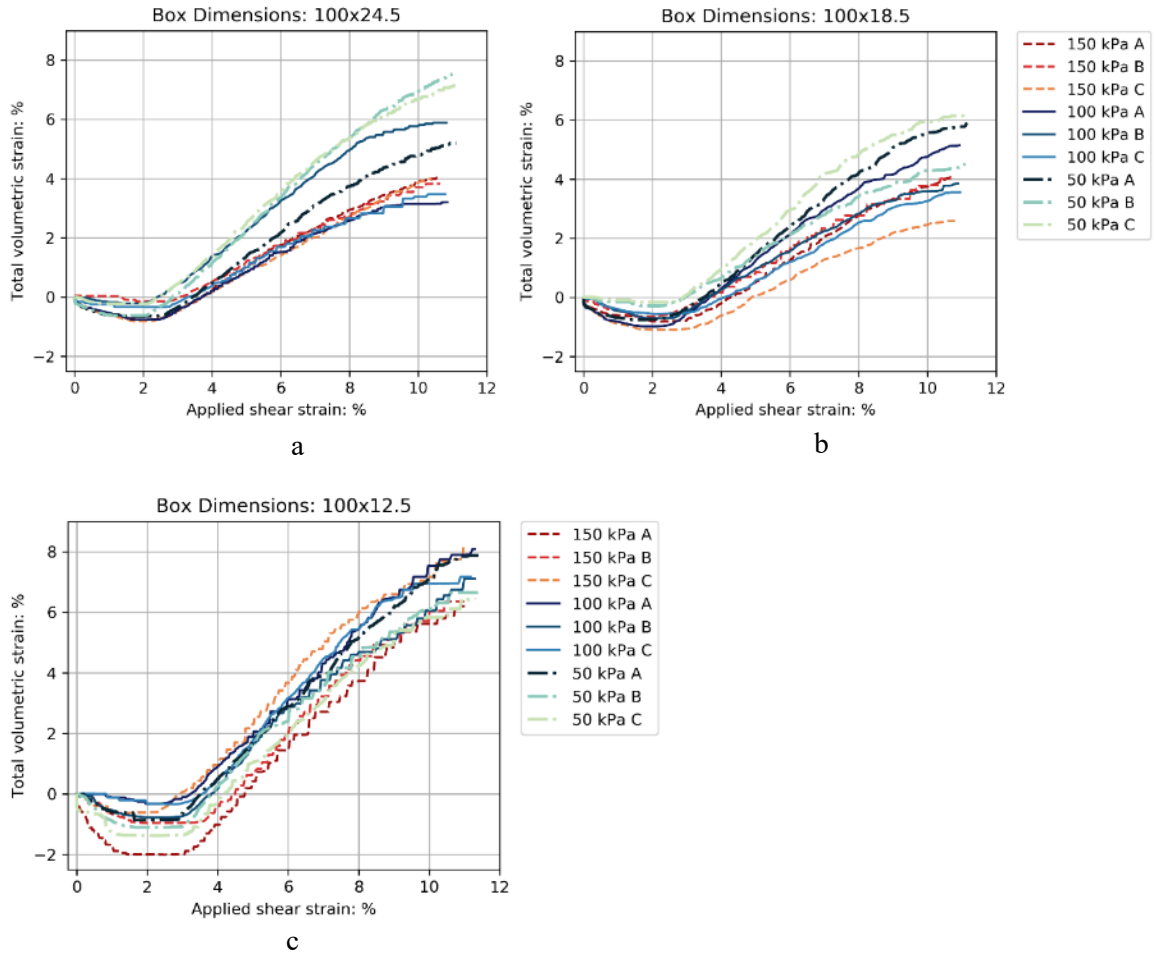

Figure 4-11. Total volumetric strain vs applied shear strain100 mm [L] box for poorly-graded soil specimens (a to c)

Stellenbosch University https://scholar.sun.ac.za

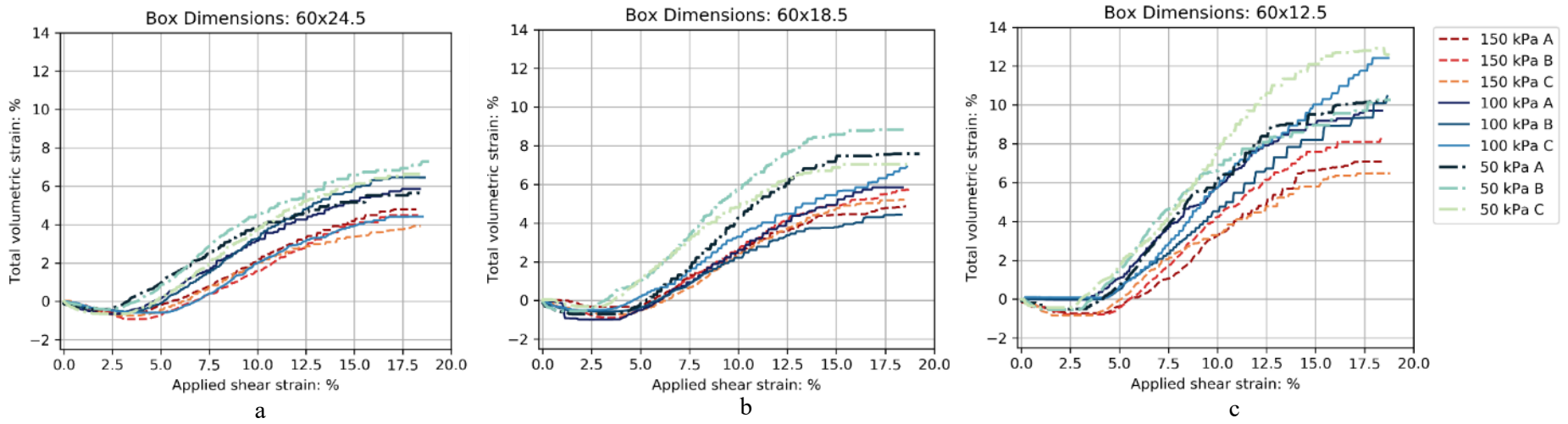

Figure 4-12. Total volumetric strain vs applied shear strain 60 mm [L] box for poorly-graded soil specimens (a to c)

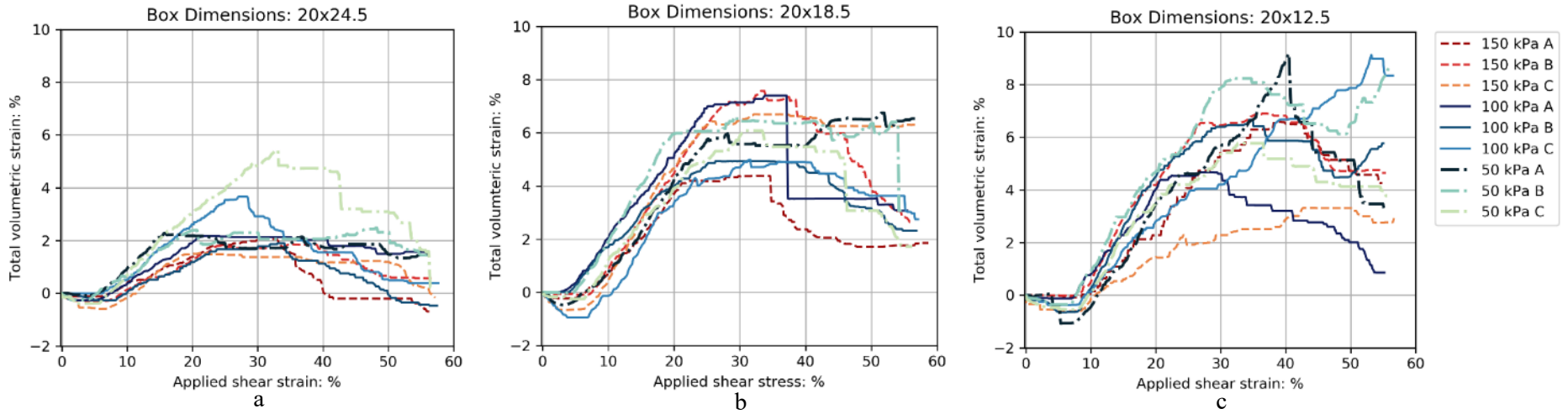

Figure 4-13. Total volumetric strain vs applied shear strain 20 mm [L] box for poorly-graded soil specimens (a to c)

Stellenbosch University https://scholar.sun.ac.za

4.3 Well Graded Specimen Results

4.3.1 Stress ratio – displacement curves

In this section, the results for 81 DS tests conducted on reconstituted well-graded soil specimens are presented; the stress ratio vs displacement results are shown in Figure 4-14 to Figure 4-16. The results presented are similar to those explained in Section 4.2.1. The higher the normal stress, the lower the average peak stress ratio. For example, the average peak stress ratio for the largest box lengths scale and intermediate box height scale is highest at 50 kPa (1.03), lower at 100 kPa (0.93) and the lowest at 150 kPa (0.92; Figure 4-14b). For the largest box length- and height scale the overall trend is similar, however, the average the peak stress ratio is highest (1.06) when testing at 100 kPa (Figure 4-14a).

The general trends are similar to those of the poorly-graded specimens (Section 4.2.1 Stress ratio – displacement curves), in that there is a length scale effect observed in the shear displacement-stress ratio results. As an illustrative example, consider the average peak stress ratio of the greatest box length- and height scale with the tests conducted at the smallest box length scale and largest height scale. The larger Shear Box mould generates a significantly lower average peak stress ratio (0.99; Figure 4-14a) than those derived from the smaller Shear Box mould (2.68; Figure 4-16a).

Furthermore, a height scale effect is present. In general, a directly proportional relationship exists between the box height scale and the peak stress ratio. For example, when considering the intermediate box length scale, the average peak stress ratio is greatest (1.28; Figure 4-15a) when conducting tests at the largest box height scale, and lowest (1.08; Figure 4-15c) when conducting tests at the smallest box height scale. Conventionally, the average peak stress ratio, for the intermediate box height scale lies between the average peak stress ratios of the largest and smallest box height scales, which is the case for the intermediate box length scale (1.20; Figure 4-15b).

Intriguingly, a deviation from the overall height scale effect is observed for the smallest box length scale. The results yielded are atypical, in that on average, an inversely proportional relationship exists between the box height scale and the average peak stress ratio (Figure 4-16a-c). In this case, the smallest box height scale does not represent the smallest average peak stress ratio (2.66; Figure 4-16c) but lies between the average peak stress ratios of the intermediate (2.50; Figure 4-16b) and largest box height scales (2.68; Figure 4-16a), respectively.

Stellenbosch University https://scholar.sun.ac.za

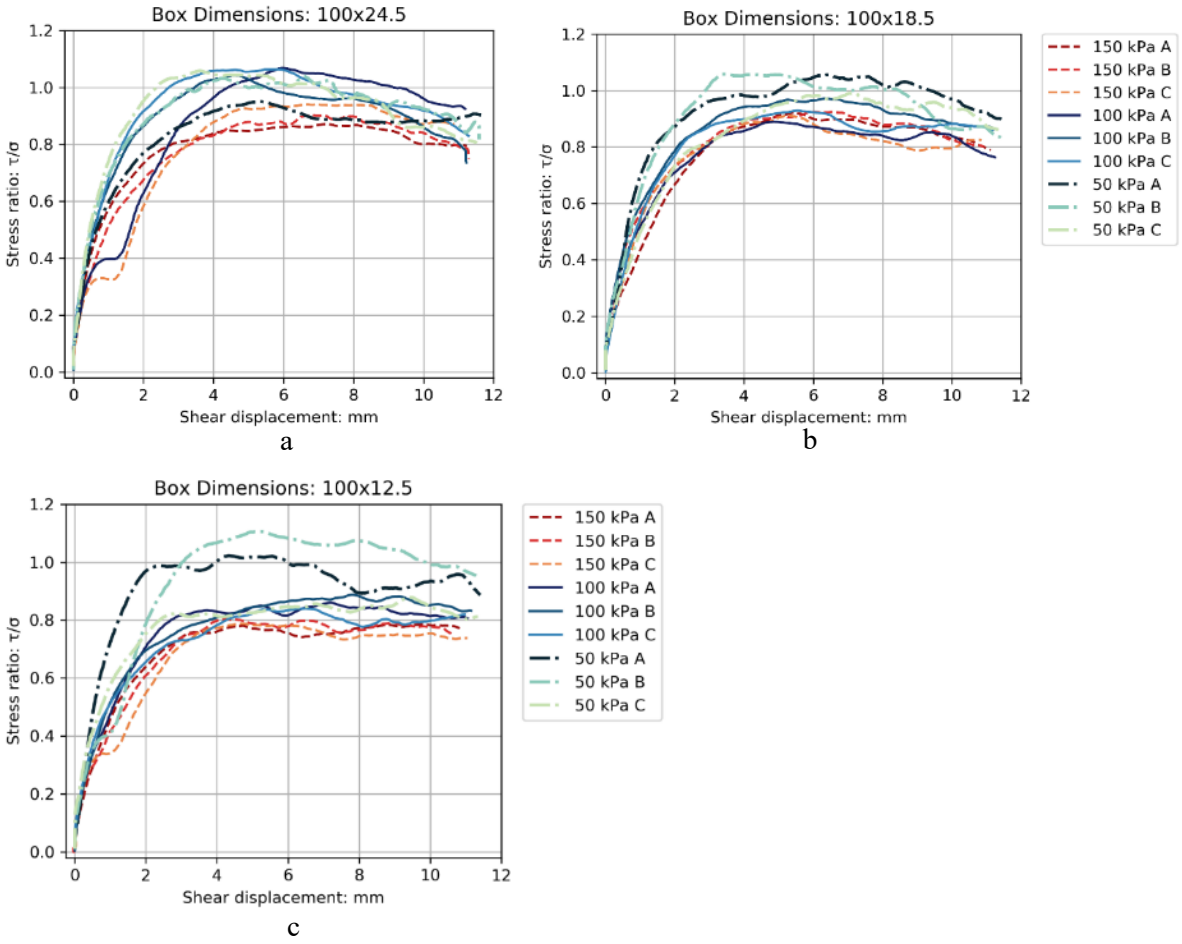

Figure 4-14. Stress ratio-displacement curves for 100 mm [L] box for well-graded soil specimens (a to c)

Stellenbosch University https://scholar.sun.ac.za

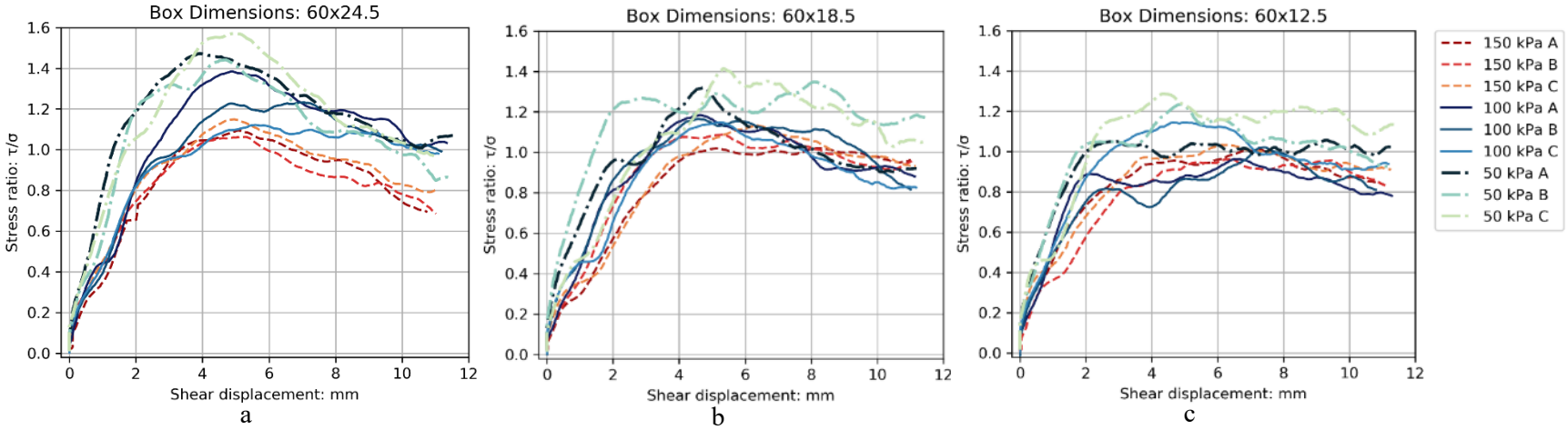

Figure 4-15. Stress ratio-displacement curves for 60 mm [L] box for well-graded soil specimens (a to c)

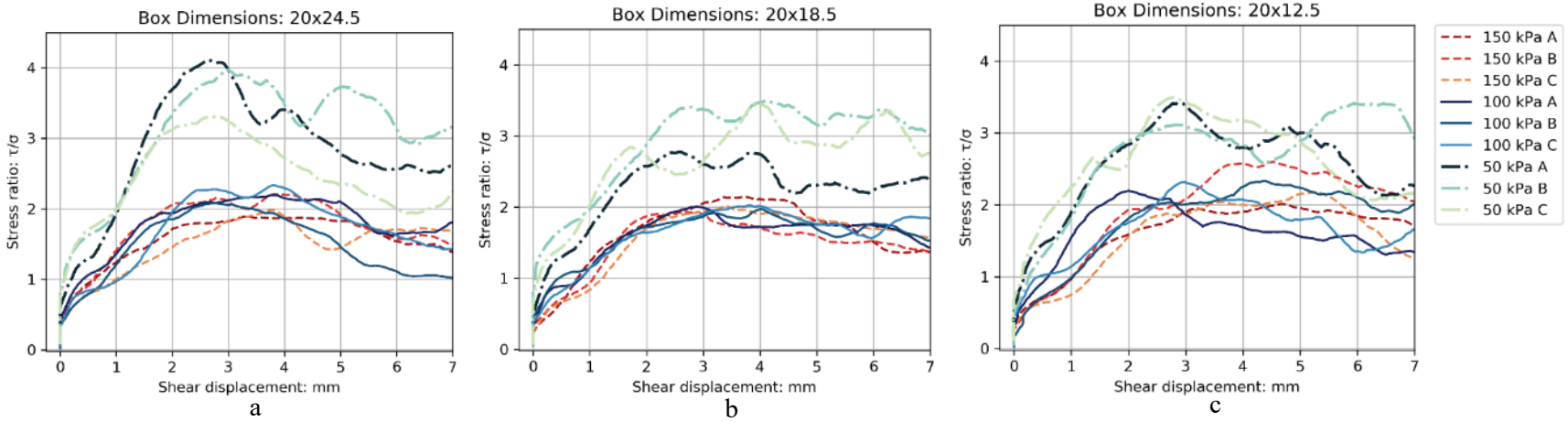

Figure 4-16. Stress ratio-displacement curves for 20 mm [L] box for well-graded soil specimens (a to c)

Stellenbosch University https://scholar.sun.ac.za

4.3.2 Stress ratio – applied strain curves

The stress ratio versus applied shear strain results for the well-graded specimen are presented in Figure 4-17 to Figure 4-19. The results are similar to those of the poorly-graded specimen (Section 4.2.2 Stress ratio – applied strain curves). The applied shear strain, at the average peak stress ratio, increases with reduction in the box length scale. This is apparent when comparing the results of the smallest Shear Box mould, with those of the largest box length scale (and smallest box height scale). The smallest Shear Box mould reaches the peak stress ratio at an average applied shear strain of 21.74% (Figure 4-19c), the largest box length scale reached the peak stress ratio significantly earlier, at an applied shear strain of 5.91% (Figure 4-17c).

For the intermediate and smallest box length scale ratios, an inverse relationship exists between the box height scale and the average shear strain at the peak stress ratio. This is most apparent when considering that the Shear Box mould with the smallest length scale; the average applied shear strain at the peak stress ratio is lowest (16.50%) for the greatest box height scale (Figure 4-19a), significantly higher (20.41%) for the intermediate box height scale (Figure 4-19b), and highest (21.74%) for the smallest box length scale (Figure 4-19c). The effect of height scale is similar for the intermediate box length scale (Figure 4-18a-c), but not for the largest box length scale (Figure 4-17a-c).

Interestingly, the largest Shear Box mould generates an average shear strain value (5.91%), at the peak stress ratio, that lies between those derived by the smallest and largest box height scales (Figure 4-17a). The lowest average applied shear strain, at the peak stress ratio, is reached by the intermediate box height scale (5.66%; Figure 4-17b), and the greatest average applied shear strain, at the peak stress ratio, is highest for the smallest box height scale (6.58%; Figure 4-17c).

Stellenbosch University https://scholar.sun.ac.za

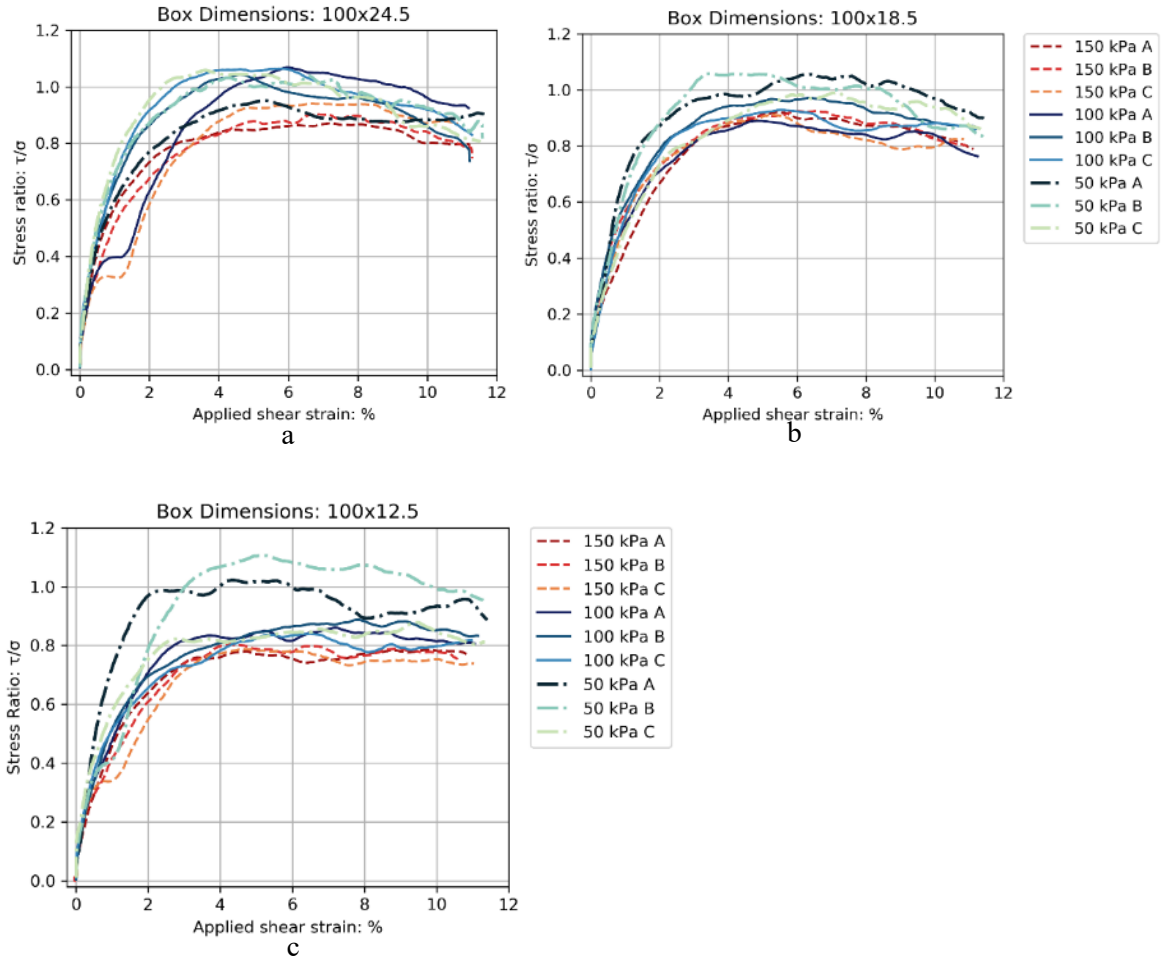

Figure 4-17. Stress ratio vs applied shear strain curves for 100 mm [L] box for well-graded test specimens (a to c)

Stellenbosch University https://scholar.sun.ac.za

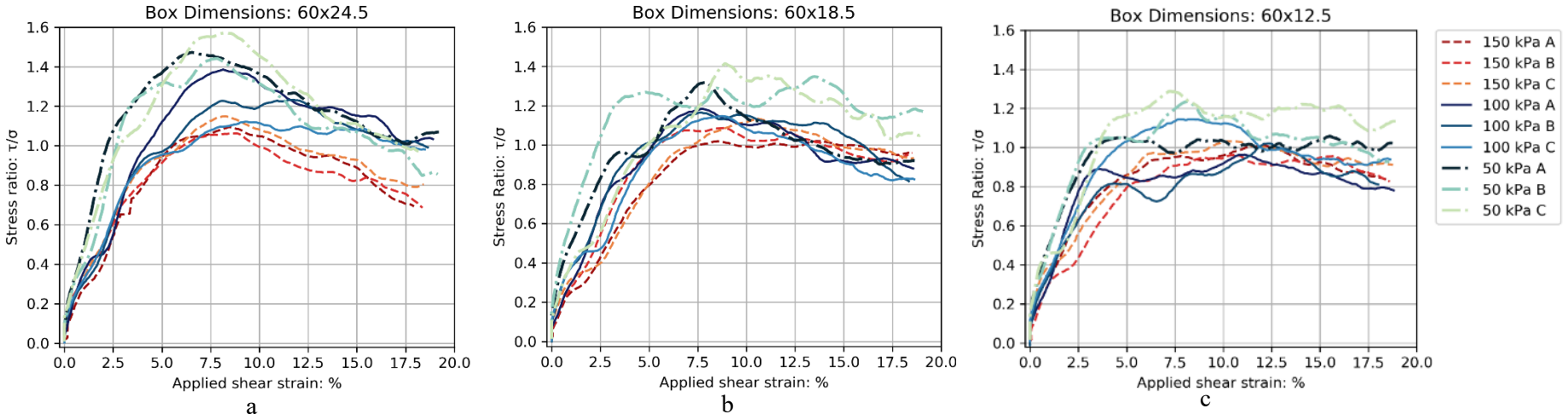

Figure 4-18. Stress ratio vs applied shear strain curves for 60 mm [L] box for well-graded test specimens (a to c)

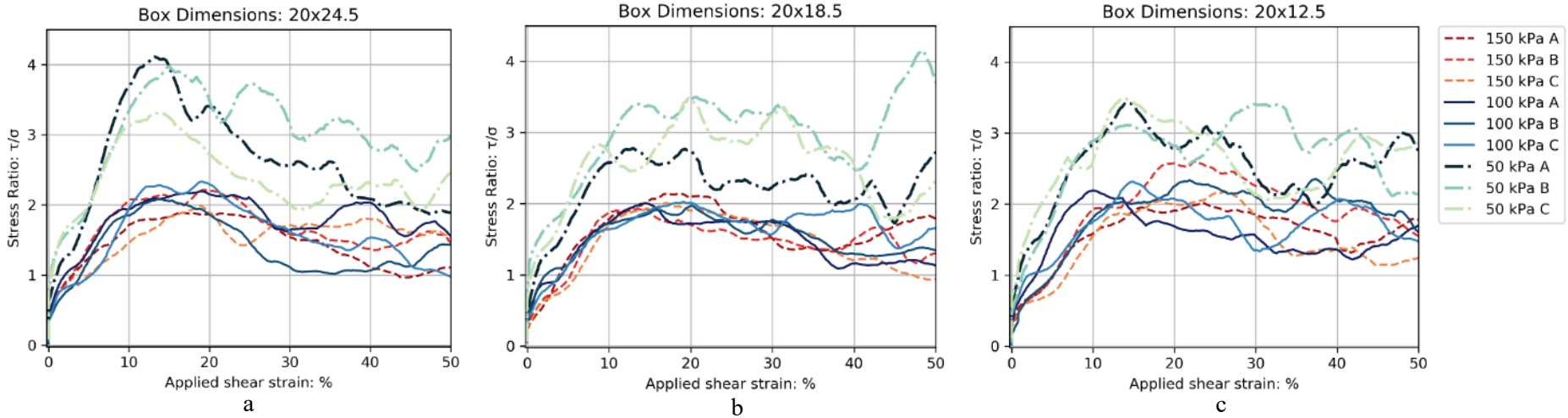

Figure 4-19. Stress ratio vs applied shear strain curves for 20 mm [L] box for well-graded test specimens (a to c)

Stellenbosch University https://scholar.sun.ac.za

4.3.3 Top wall vertical displacement - shear displacement curves

The vertical displacement with applied shear displacement curves are presented in Figure 4-20 to Figure 4-22. Most specimens show an initial decrease, followed by an increase in the vertical displacement of the top wall, this indicates that all of the specimens exhibit dilatancy, apart from two conducted at 150 kPa that only showed contractile behaviour (Figure 4-21a,b). The applied normal stress most often reduces the amount of specimen dilation that takes place. To best illustrate this relationship, compare the results of the maximum vertical displacement of the top wall of the specimens subject to 50 kPa and 150 kPa normal stress, which were derived by the shear mould with the intermediate box length scale and the minimum height scale (Figure 4-21c).

For most of the specimens, at a given length scale, as the box height scale increases from the smallest to the intermediate box height scale, the average magnitude of the vertical movement of the top wall (at the peak stress ratio) decreases proportionately. For example, the average magnitude of vertical displacement of the top wall (at the peak stress ratio) for the smallest box height- and length scale is 0.51 mm (Figure 4-22c), which decreases to 0.34 mm when making use of the intermediate box height scale (Figure 4-22b); and, decreases further to 0.28 mm for the largest box height scale (Figure 4-22a). Similar trends can be observed for the intermediate and greatest box length scales (Figure 4-20 to Figure 4-21).

The trends present in the average vertical displacement of the top wall at the peak stress ratio are less consistent for variations in the Shear Box length scale. Commonly, the well-graded material at the intermediate box length scale (for a given box height scale) represents an ‘inflexion point’, at which, the trend in the average magnitude of the vertical displacement of the top wall (at the peak stress ratio) for variations in box length scale, changes. This is most clearly illustrated when contrasting the average vertical displacement of the top wall, at the peak stress ratio, for intermediate box height scale, which at the smallest box length scale yields an average vertical displacement at the peak stress ratio of 0.51 mm (Figure 4-22b) and decreases to 0.18 mm (Figure 4-21b) for the intermediate box length scale; whereafter, increasing to 0.25 mm (Figure 4-20b) for the largest box length scale. The results of this length scale effect will be elaborated upon in the Discussion.

Stellenbosch University https://scholar.sun.ac.za

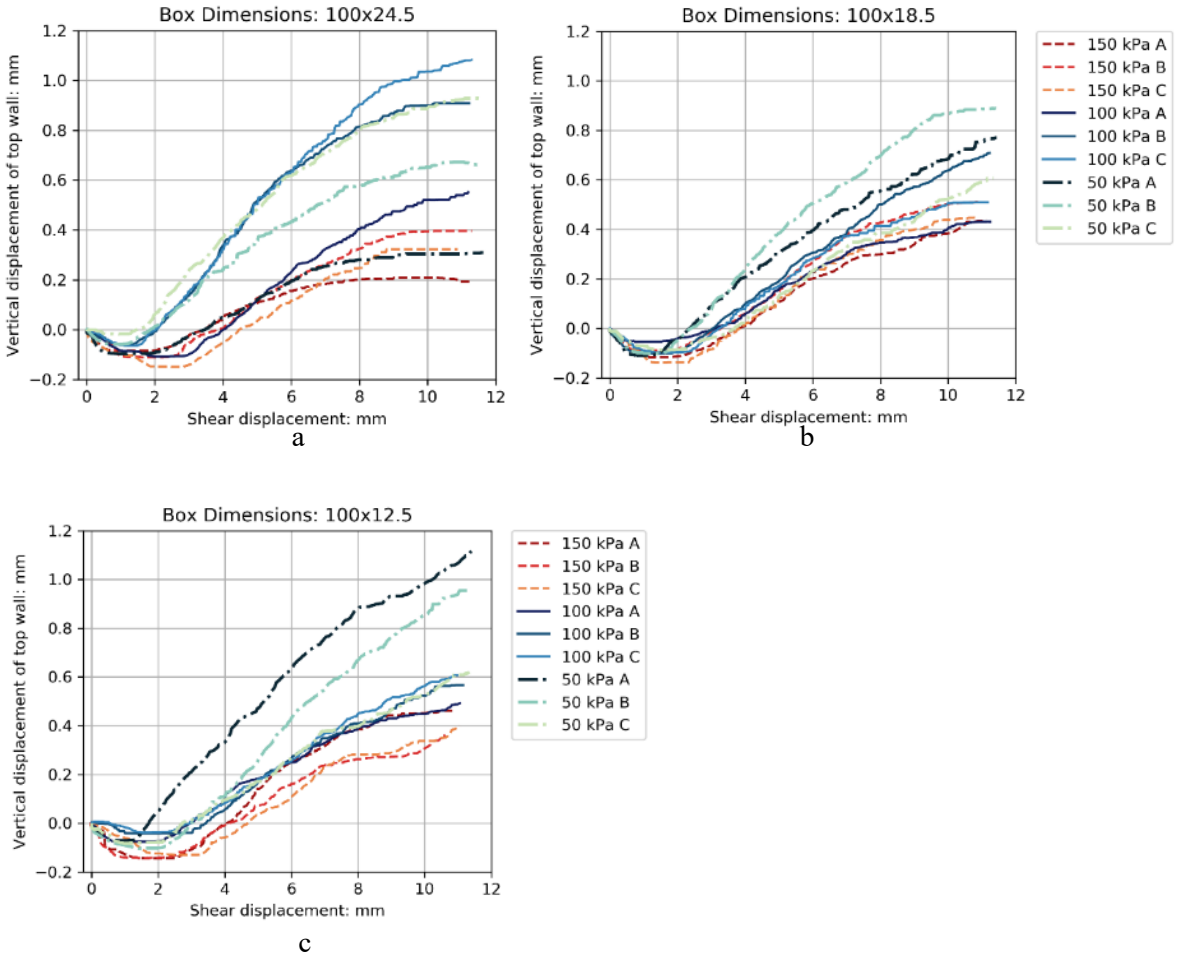

Figure 4-20. Vertical displacements of Shear Box top wall vs shear displacement curves for 100 mm [L] box for well-graded soil specimens (a to c)

Stellenbosch University https://scholar.sun.ac.za

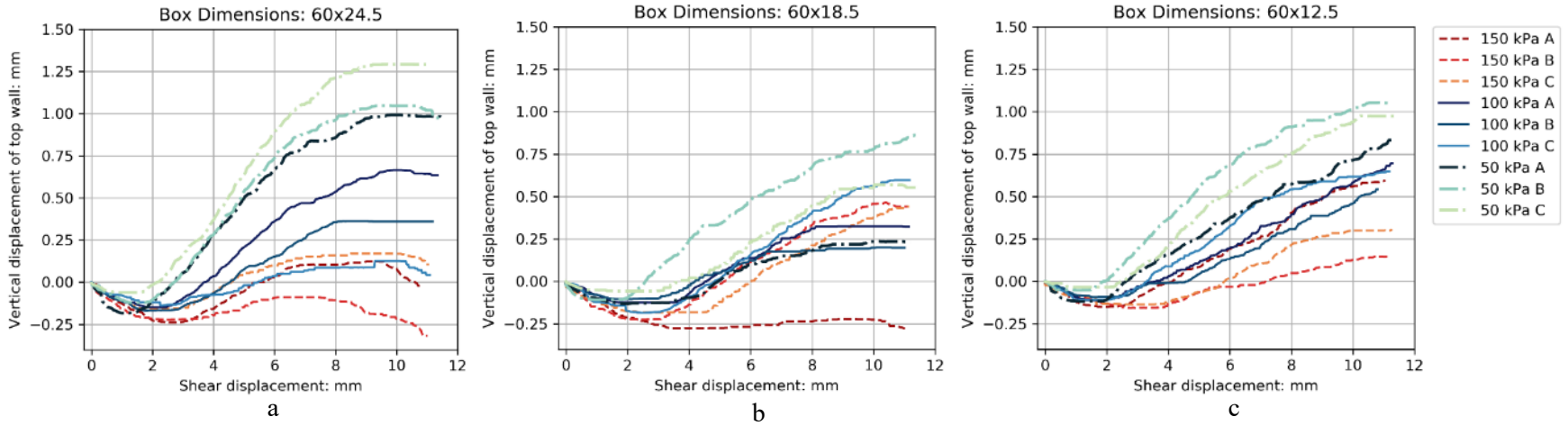

Figure 4-21. Vertical displacements of Shear Box top wall vs shear displacement curves for 60 mm [L] box for well-graded soil specimens (a to c)

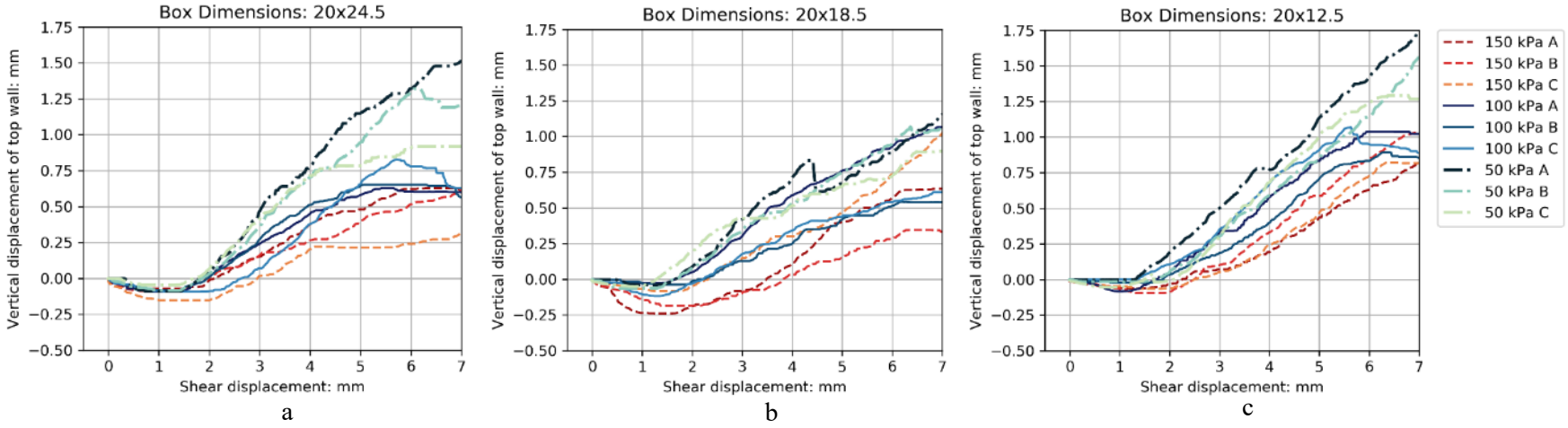

Figure 4-22. Vertical displacements of Shear Box top wall vs shear displacement curves for 20 mm [L] box for well-graded soil specimens (a to c)

Stellenbosch University https://scholar.sun.ac.za

4.3.4 Total volumetric strain - applied shear strain

The total volumetric strain vs the applied shear strain results are presented in Figure 4-23 to Figure 4-25. As indicated above, an inverse relationship exists between the vertical displacement of the shear box top wall and the applied shear displacement (Section 4.3.3); this relationship is reflected in the results of the applied normal stress and the amount of total volumetric strain that occurs. The effect of normal stress is typical for the results presented in this section (Figure 4-23 to 4-25). It is important to note that most of the total volumetric strain vs the applied shear strain results show dilatant behaviour, there are; however, results that are of smaller box length scales that initially display dilatancy and only once the test is nearing completion, display contractile behaviour. As an example, the tests conducted at 150 kPa when using the smallest Shear Box mould display this behaviour of late, or post-peak, contraction of the specimen (20x 12.5 mm) (Figure 4-25c).

The most consistent relationship for the volumetric strain vs applied shear strain is that the box height scale is inversely proportional to the average total volumetric strain, at the peak stress ratio. This is most apparent when considering the average total volumetric strain, at the peak stress ratio, for the smallest box length scale at each height scale. The largest height scale resulted in 1.13% average total volumetric strain (Figure 4-25a); the intermediate box height scale 1.86% (Figure 4-25b), and smallest height scale significantly larger at 4.11% average total volumetric strain (Figure 4-25c). It is noted that a deviation from this trend occurs for the intermediate box length scale. The average total volumetric strain, at the peak stress ratio, for the largest box height scale is 0.77% (Figure 4-24a), the smallest box height scale is 2.17% (Figure 4-24c), and; the intermediate box height scale is lower than would be expected, as compared to the other results, at 0.45% (Figure 4-24b). On the other hand, the variation of the Shear Box mould length scale, particularly at the largest and smallest box height scales, produce divergent trends.

This divergence of trends makes the overall effect of length scale variation more challenging to characterise. One commonality, however, is that the intermediate box length scale consistently produces the lowest magnitude of average total volumetric strain by comparison with the largest- and smallest box height scales. To illustrate this, two examples will be used to display the extremities of the relationship, i.e. the largest and smallest box height scales. First, the smallest box height scale, which for the smallest box length scale yielded an average total volumetric strain of 4.11% (Figure 4-25c), the intermediate box height an average of 2.17% (Figure 4-24c), and the largest box length scale increasing again to an average of 2.43% total volumetric strain (Figure 4-23c). By contrast, the largest box height scale at the smallest length scale, produced an average total volumetric strain of 1.13% (Figure 4-25a), the intermediate box length 0.77% (Figure 4-24a) (again, a reduction for the intermediate box length scale is noted), and the largest box length scale increases to a maximum of 1.33% average total volumetric strain (Figure 4-23a).

Stellenbosch University https://scholar.sun.ac.za

Overall, as illustrated by the examples above, the largest box height scale (with variation in length scale) exhibits a directly proportional relationship between box length scale and the average total volumetric strain, and; by contrast, the smallest box height scale (with variations in length scale) yields an inversely proportional relationship between box length scale and the magnitude of the average total volumetric strain. This will be elaborated upon, in more detail, in the Discussion Chapter.

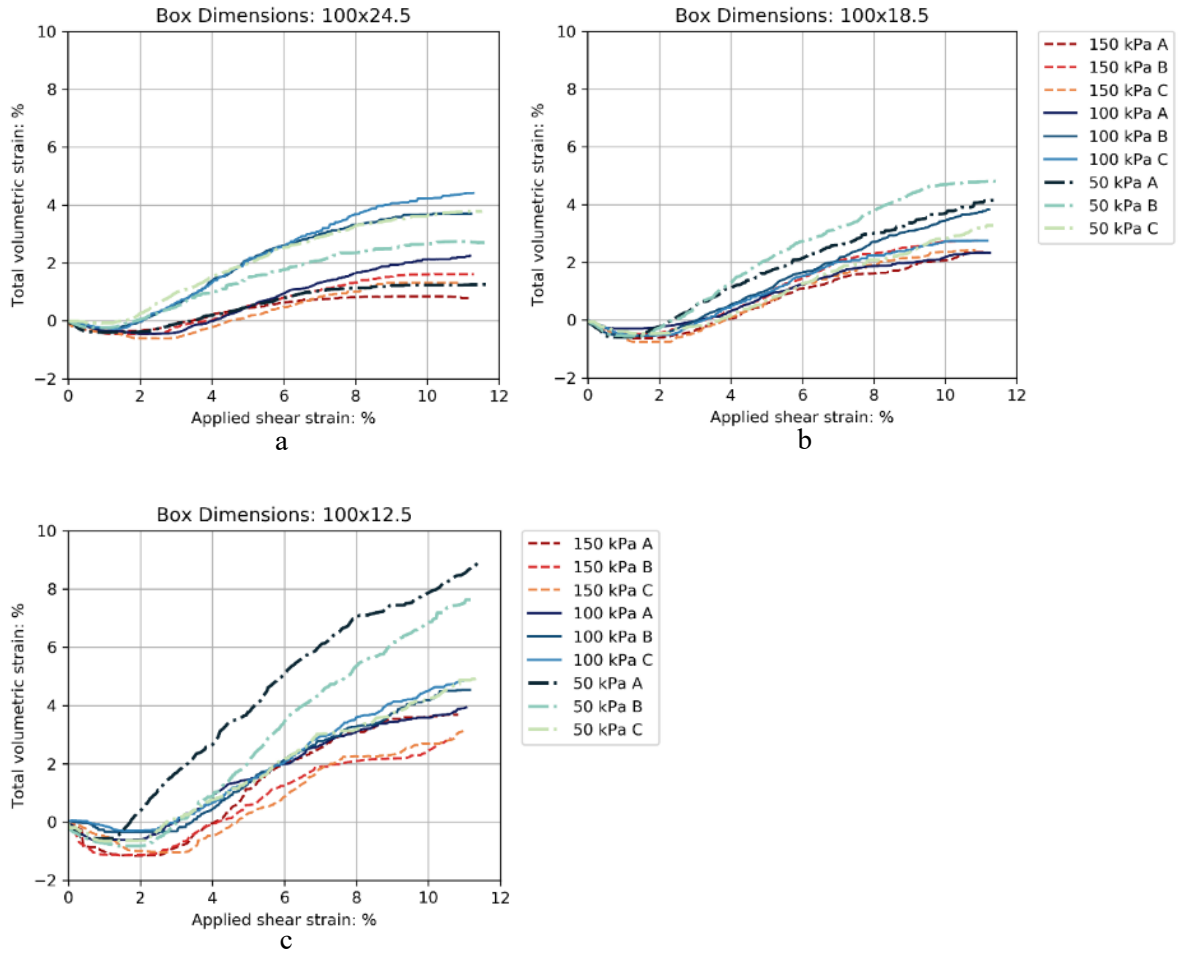

Figure 4-23. Total volumetric strain vs applied shear strain 100 mm [L] box for well-graded soil specimens (a to c)

Stellenbosch University https://scholar.sun.ac.za

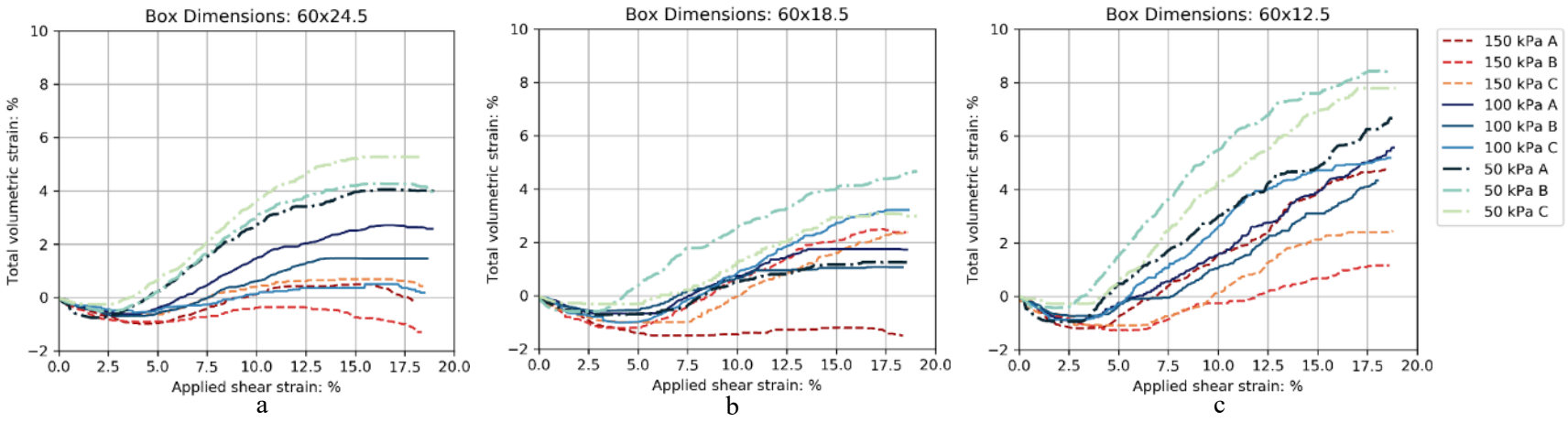

Figure 4-24. Total volumetric strain vs applied shear strain 60 mm [L] box for well-graded soil specimens (a to c)

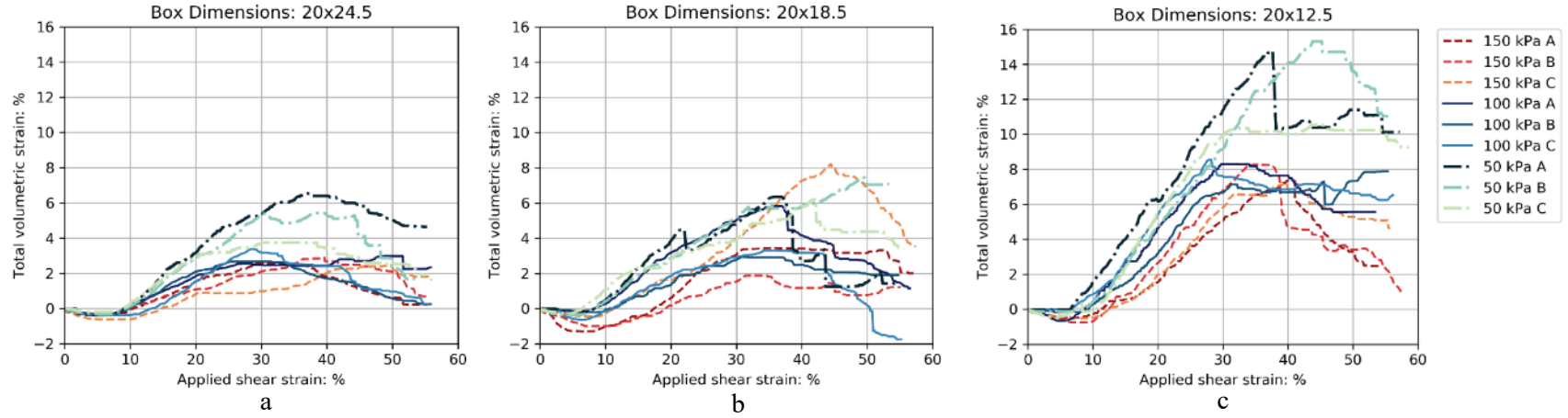

Figure 4-25. Total volumetric strain vs applied shear strain 20 mm [L] box for well-graded soil specimens (a to c)

Stellenbosch University https://scholar.sun.ac.za

4.4 Shear Box Data Summary

For the reader's convenience a summary of the test results, at the peak stress ratio, is contained in Table 4-1. The magnitudes and values used to drive the highlight average trends, at the peak stress ratio, which are described in Sections 4.2 and 4.3 are found here. For example, this summary is useful when pointing out the effect of normal stresses on the results, e.g. the peak stress ratio of the well-graded material, at the smallest box height and length scale is higher at 50 kPa (3.44) than 100 kPa (2.29) and 150 kPa (2.26) (Table 4-1).

This summary also serves for easy contrast and comparison of the results between the well- and poorly-graded grain size distributions. For example, at the smallest box length and height scale, the poorly-graded grain size distribution yields a significantly lower peak stress ratio at 50 kPa (3.04), than that of the well-graded grain size distribution (3.44) (for the smallest Shear Box mould). On the contrary, the average peak stress ratio for the well-graded grain size distribution is lower than the poorly-graded grain size distributions at larger box length scales (i.e. intermediate and largest). This is best indicated when contrasting the average peak stress ratio of the GW (1.36) and GP (1.54) specimens, at 50 kPa for the largest box length scale and smallest height scale.

It is important to draw the readers attention to the differences observed in the peak stress derived from the largest and intermediate box length scales, in conjunction with the largest box height scale (i.e. 100 mm x 24.5 mm and 60 mm x 24.5 mm). The well-graded specimens yield an average peak stress ratio of 0.99 in the largest box length scale and an average peak stress ratio of 1.28 in the intermediate box length scale (Table 4-1). This marks a 29.0% increase in the peak stress ratio for the reduction in the box length scale, while still respecting the ASTM D3080-11 box scale ratios (Table 3-3) (ASTM, 2011). The increase in the peak stress ratio for the poorly-graded grain size distribution, for the same Shear Moulds, was 27.8%.

Stellenbosch University https://scholar.sun.ac.za

Table 4-1. Summary of average results for triplicate tests at the peak stress ratio

L: mm	H: mm	L/H	σ: kPa	Well graded material: SW				Poorly graded material: SP			
				δ: mm	*εv: %*	τ: *kPa*	*(τ/σ)*peak	*δ: mm*	*εv: %*	τ: *kPa*	*(τ/σ)*peak
20	**12.5**	1.60	50	4.05	5.35	214.00	3.44	3.78	3.42	184.15	3.04
20	**12.5**	1.60	100	4.15	3.27	310.09	2.29	2.37	1.28	223.70	1.88
20	**12.5**	1.60	150	4.84	3.72	457.36	2.26	4.61	2.13	358.47	1.76
20	**18.5**	1.08	50	5.40	3.81	254.41	3.47	2.65	2.33	170.05	3.01
20	**18.5**	1.08	100	3.58	1.52	254.28	2.00	1.74	0.80	237.45	2.08
20	**18.5**	1.08	150	3.27	0.25	372.03	2.03	2.30	1.12	336.62	1.94
20	**24.5**	0.82	50	2.81	1.35	216.76	3.80	2.16	0.90	165.62	3.01
20	**24.5**	0.82	100	3.45	1.21	277.97	2.20	2.92	1.12	230.99	1.88
20	**24.5**	0.82	150	3.63	0.84	380.52	2.03	2.72	0.53	305.98	1.72
60	**12.5**	4.80	50	6.18	3.85	66.92	1.19	4.67	4.49	74.75	1.17
60	**12.5**	4.80	100	6.35	1.89	116.65	1.04	5.55	4.51	140.71	0.98
60	**12.5**	4.80	150	6.60	0.75	169.43	1.00	3.99	0.99	172.56	0.90
60	**18.5**	3.24	50	6.05	1.42	76.32	1.36	4.52	2.83	83.71	1.54
60	**18.5**	3.24	100	4.83	0.19	126.92	1.17	5.62	2.32	148.08	1.34
60	**18.5**	3.24	150	6.61	-0.27	182.67	1.08	5.44	1.95	204.70	1.24
60	**24.5**	2.45	50	4.52	1.82	81.52	1.49	4.63	2.49	78.46	1.44
60	**24.5**	2.45	100	5.83	0.63	125.31	1.25	5.22	2.02	147.14	1.34
60	**24.5**	2.45	150	5.11	-0.14	181.30	1.10	5.43	1.42	210.06	1.27
100	**12.5**	8.00	50	6.35	3.25	53.46	1.00	6.19	2.73	54.29	1.02
100	**12.5**	8.00	100	7.17	2.84	92.99	0.86	6.88	4.09	105.76	0.98
100	**12.5**	8.00	150	6.21	1.20	126.81	0.79	6.11	2.47	152.03	0.95
100	**18.5**	5.41	50	5.64	1.64	54.84	1.03	6.30	2.77	59.90	1.12
100	**18.5**	5.41	100	5.59	1.27	98.61	0.93	6.90	2.15	105.53	0.98
100	**18.5**	5.41	150	5.75	1.09	146.29	0.92	6.21	1.30	152.21	0.95
100	**24.5**	4.08	50	5.18	1.28	53.59	1.02	5.37	2.36	64.90	1.23
100	**24.5**	4.08	100	5.46	1.74	112.03	1.06	6.47	2.48	113.25	1.06
100	**24.5**	4.08	150	7.11	0.89	146.18	0.90	6.83	2.16	157.66	0.98

Stellenbosch University https://scholar.sun.ac.za

4.5 Friction Angle Results

4.5.1 Length and Height scale effects

To assess the effects of the box length- and height scales on the peak friction angle of well and poorly graded materials, the average Mohr-Coulomb parameters were derived, i.e. the effective angle of friction (ϕ') was calculated, and the cohesion (c') was set to zero. These results are presented in Figure 4-26. Broadly, as is to be expected and was illustrated by the peak stress ratio, an inverse relationship exists between the peak friction angle and the box-length scale, at a constant height scale. As an example, when the GP specimens were tested using largest box length scale (smallest height scale) the resultant average peak friction angle was 46.10˚, at the intermediate box length scale was 52.84˚, and at the smallest length scale was 67.28˚ (Figure 4-26). The results show that this trend is consistent, i.e. variation in box length scale, at each box height scale, and is in this case, true for a well- or poorly-graded grain size distribution.

Contrary to the typical effects of box length scale on the shear strength parameters, the relationship between the box-height scale and the internal angle of friction is more consistent. Most often an increase in box-height scale is associated with an increase in the peak friction angle. This is most clear when considering the GW specimens, T the greatest box length scale, a distinct increase in the peak friction angle is observed from 41.45˚ for the smallest box height scale, to 44.74˚ for the intermediate height scale, and 46.30˚ at the largest height scale (Figure 4-26). It is also interesting to note that, for the greater box length scales (60 mm and 100 mm), on average, the GP specimens have higher resultant peak friction angles as compared to those derived from the GW specimens; notwithstanding, at lower box length scales GW specimens consistently produced higher resultant average peak friction angle values (Figure 4-26).

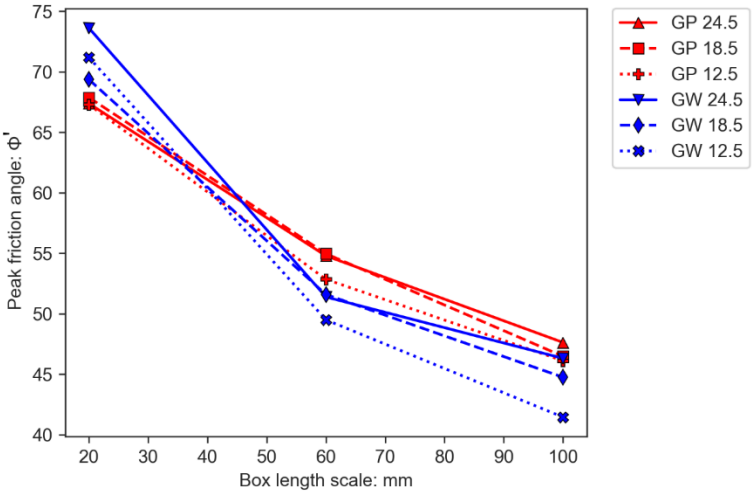

Figure 4-26. Average variations of peak friction angle at different box length scales for the well-graded (GW) and poorly-graded (GP) specimens. Values indicated in the legend refer to the box height scales (mm)

Stellenbosch University https://scholar.sun.ac.za

4.5.2 Aspect ratio results

The variation between the peak friction angles of the well- and poorly-graded samples with a variation in the aspect ratio (L/H) of the Shear Box is presented in Figure 4-27. For both the well- and poorly graded specimen results, an exponential curve was fitted to the laboratory data using the 'optimise curve fit' function based in the 'scipy' package in Python; this function optimises the fitted trend to yield the smallest residual values, i.e. differences between the fitted curve and the experimental results. From the displayed trends, it is clear that an inverse relationship exists between the aspect ratio and the magnitude of the peak friction angle, for both the well- and poorly-graded PSDs. A regression analysis of the fitted curves was performed; the well- and poorly-graded grain size distributions have r^2 values of 0.90 and 0.87, respectively, which indicate that overall the fitted curves perform well, in terms of modelling the experimental results.

The most extreme example of this, is the contrast between the largest and smallest aspect ratios, i.e. when the aspect ratio is lowest (0.82) the peak friction angle for the well-graded PSD is 73.61˚, and at the largest aspect ratio (8.0) the peak friction angle is significantly lower at 41.45˚ (Figure 4-27). Experimentally, however, within this broad inverse relationship, there are localized deviations from the modelled peak friction angles. For example, when increasing the aspect ratio from 4.1, for the poorly-graded PSD, that has an observed peak friction angle of 47.62˚ to an aspect ratio of 4.8, which yields an observed peak friction angle of 52.84˚ (Figure 4-27). This extreme increase in the peak friction angle, from below the model to above the model is much the same for the well-graded PSD. It is important to note that because the aspect ratio is a parameter that is a combination of two parameters (i.e. L and H), small changes in the aspect ratio that cause a large change in peak friction angle are usually induced by a change in box length scale.

It is interesting to note that the results of the well-graded specimens at the lowest aspect ratios (<2), yield greater peak friction angles than those of the poorly-graded specimens, and; the results of the poorly-graded specimens at higher aspect ratios (>2) result in significantly larger peak friction angles than those of the well-graded specimens. This can be demonstrated by the variations of the extremities of the results presented, i.e. the results derived by the largest and smallest aspect ratios. For instance, the well-graded PSD for the largest aspect ratio (8.0) yields an average peak friction angle of 41.45˚, whereas, the poorly-graded PSD resulted in a larger peak friction angle of 46.10˚ (Figure 4-27); yet, the well-graded specimens, when tested at the smallest aspect ratio (0.82), produced a peak friction angle of 73.61˚, which exceeded the average peak friction angle results produced by the poorly-graded specimens at 67.37˚. More information about the deviations from defined trends and the observed (experimental) results can be found in the– Results analysis and Discussion Chapter.

Stellenbosch University https://scholar.sun.ac.za

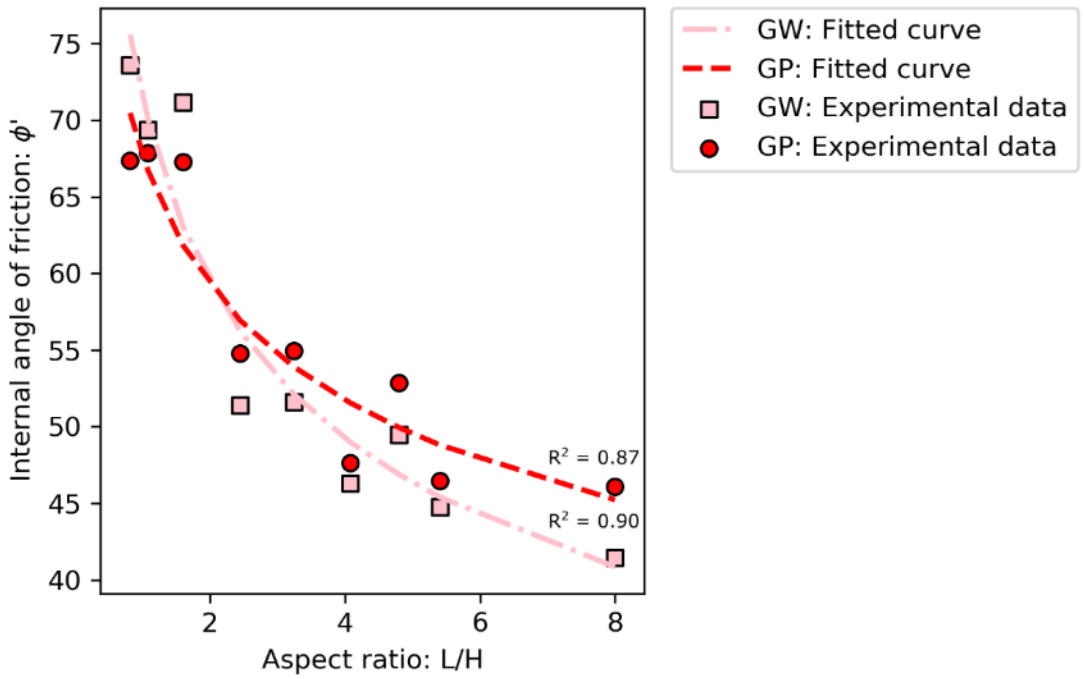

Figure 4-27. Variation the in peak friction angle with a change in aspect ratio

4.6 Particle Shape

In this section, the particle shape data is presented for the field-collected samples, the crushed pre-shear samples, and the crushed post-shear samples for the well- and poorly-graded samples (Table 4-2). The extended results from the grain shape analysis can be found in Appendix B. There is little variation in particle shape data for the groups of particles that were assessed in terms of their grain shape. The mean values for the respective grain shape characters (roundness, sphericity, and grain regularity) does not vary greatly between grain populations (roundness mean range 0.28 – 0.32; sphericity 0.56 – 0.63; and particle regularity 0.44 – 0.47) (Table 4-2).

The spread of grain shape data around the mean values as indicated by the coefficient of variation (COV) of the respective grain shape characteristics for the respective grain populations, is on average highest for the grain roundness (COV ~ 0.51) and lowest for both the grain sphericity and particle regularity parameters (COV ~ 0.27). The range of COV values are highest for grain roundness (0.62 – 0.44) and lowest for grain sphericity (0.28 – 0.25), while the particle regularity lies between (0.30 – 0.22).

The well-graded grain population reflects the highest variability in grain shape characteristics (e.g. Roundness: COV = 0.62 and Standard Deviation = 0.17, Sphericity: COV = 0.27 and Standard Deviation = 0.17) as compared to the other grain populations (Table 4-2). In each case, the waste rock collected in the field (Field WR) grain population represents the highest mean value for each of the grain shape characteristics. Interestingly, the field WR grain population displays the lowest variation in grain shape characteristics (indicating that they are most uniform), which is indicated by their lower COV and

Stellenbosch University https://scholar.sun.ac.za

Standard deviation values, as compared to the crushed grain populations, i.e. the Crushed WR, Well-Graded and Poorly-Graded grain population.

Table 4-2. Particle shape analysis results

Grain Population	Roundness			Sphericity			Particle Regularity		
	Mean	Standard Deviation	COV	Mean	Standard Deviation	COV	Mean	Standard Deviation	COV
Field WR	0.32	*0.14*	0.44	0.63	*0.16*	0.25	0.47	*0.10*	0.22
Crushed WR	0.29	*0.15*	0.52	0.60	*0.16*	0.26	0.44	*0.11*	0.26
Well-Graded	0.28	*0.17*	0.62	0.62	*0.17*	0.27	0.45	*0.14*	0.30
Poorly-Graded	0.30	*0.15*	0.49	0.56	*0.16*	0.28	0.43	*0.12*	0.28

4.7 Summary of Findings

This chapter has highlighted several relationships between several of the tested variables. These relationships can be summarised as follows: i) there is a disproportional relationship between the normal stress and the peak shear stress; ii) the box length scale is directly proportional to the average peak stress ratio; iii) the box height scale is inversely proportional to the average peak stress ratio; iv) on average the shear strain, at the peak stress ratio, increases with a reduction in box length scale or height scale; v) the average magnitude vertical displacement of the shear box top wall increases proportionally with an increase in the box height scale; vi) it appears that the intermediate box length scale (and/or height scale) represent(s) an inflexion point at which the average trend in the total volumetric strain (at the peak stress ratio) changes from a directly proportional relationship to an inversely proportional relationship, and; vii) the well-graded specimens grain shape data displays the greatest variation and is thereby, on average, the most irregularly shaped sample population.

Stellenbosch University https://scholar.sun.ac.za

Chapter 5 – Results analysis and Discussion

5.1 Macromechanical Effects of Shear Mould Size on Peak Stress Ratio

5.1.1 Effect of box length scale (L/D_{max})

In the present study, it has been observed length scale of the shear box has a profound effect on the micromechanical behaviour of granular material. The peak stress ratio of shear test results, with all other parameters fixed, increases significantly as the box length scale decreases (Figure 5-1a,c). For example, the smallest box length scale produces an average peak stress ratio of 1.6 and the largest box length scale results in an average peak stress ratio, which is dramatically reduced, at 0.98 (Figure 5-1a). In addition to this, it is important to point out that a decrease in the box length scale proportionally decreases the magnitude of applied shear displacement required to mobile the peak strength (or stress state) of the material, despite the D_{max} remaining at 4 mm for each test result. This trend is better evaluated by assessing an example, the reduction of largest to the smallest box length scale reduced the required applied shear displacement, at the peak stress state, ie. 6.38 mm was reduced to 2.72 mm (Figure 5-1a,b). On the other hand, the applied shear strain (at the peak stress ratio) increases with decreasing box length scale, this is shown by the Peak Stress state for the largest box scale that occurs at 6.38%, which is less than half of the applied shear strain required to induce failure when utilizing the smallest box length scale at 13.58% (Figure 5-1c).

When analysing the vertical displacement of the shear box top wall, at the peak stress ratio, it is apparent that there a directly proportional increase in the magnitudes of vertical displacement and applied shear displacements with increases in the box length scale (Figure 5-1b). The change in resultant vertical displacement of the shear box top wall appears to be less when reducing the Shear Mould from the largest to the intermediate box length scale; than the change imposed by reducing the Shear Mould from the intermediate to the smallest box length scale. This is clarified when contrasting the results acquired from the largest, smallest, and intermediate box length scales, e.g. the average vertical displacements of, the largest DS box length scale was 0.53 mm, the intermediate box length scale was 0.35 and for the smallest was 0.13 mm; i.e. the difference between the largest and intermediate was 0.17 mm, and the difference between the intermediate and smallest being 0.22 mm (Figure 5-1b). On the other hand, the box length scale is indirectly proportional to the magnitude of the total volumetric strain, the applied shear strain (at the peak stress ratio), on the other hand, increases with decreasing length scale. For example, the largest box length scale yields a total volumetric strain of 1,98% at an applied shear strain of 7,8%, whereas the smallest box length scale yields a total volumetric strain of 1,25% at an applied shear strain of 19,1% (Figure 5-1d).

Stellenbosch University https://scholar.sun.ac.za

Similar observations to those that have been discussed above, were made by Wang and Gutierrez (2010), regarding the DEM shear test results that they presented (Figure 2-18 and Figure 2-19). That is, it was found that with decreases in box length scale (at the peak stress ratio): i) the peak stress ratios were elevated; ii) the applied shear displacement was greater; iii) the applied shear strain increased, and; iv) the magnitude of vertical displacement of the top wall is often larger. Contrary to the observations made in the present study, Wang and Gutierrez (2010), found that the total volumetric strain (at the peak stress ratio) remained largely unchanged with changes in box length scale. Experimentally, no such trends have been highlighted, in the literature, that the resultant vertical displacement of the shear box top wall with changes with variations in the shear box length scale. It is speculated that this phenomenon could be a consequence of one of two mechanisms: i) the imprecise nature of the shear test results presented in the present study. The imprecision of the results will be elaborated upon in subsequent subsections, or; ii) the coarse, inconsistently-shaped granular particles used during the undertaking of this study.

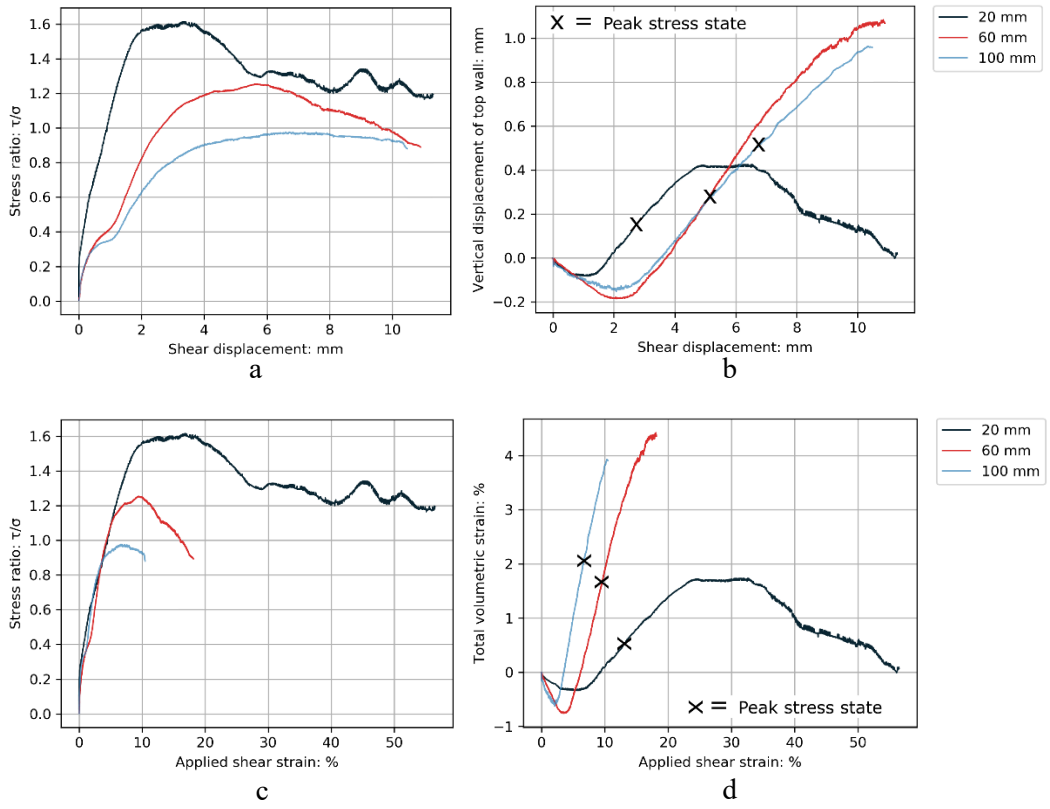

Figure 5-1. Convolved Shear Box results illustrating a variation in length scale for constant box height scale (H=24.5 mm), gradation (GP) and normal stress (150 kPa): a) stress ratio change with shear displacement; b) vertical displacement of the top wall with shear displacement; c) stress ratio change with the applied shear strain; d) total volumetric strain change with variations in applied shear strain

The relationship between the peak stress ratio and the box length scale can be confirmed by plotting the variation in the stress ratio with the variation in box length scale (and height scale) (Figure 5-9). The rate of increase, of the peak stress ratio, is greater between the intermediate and smallest box length scales; as compared to the rate of increase between the largest and intermediate box length scales (Figure 5-9). For example, the peak stress ratio increases, on average, approximately 20% from the largest box length scale to the intermediate box length scale. By contrast, an average increase of approximately

Stellenbosch University https://scholar.sun.ac.za

110% (at the peak stress ratio) is observed from the intermediate to the smallest box length scale (Figure 5-9).

5.1.2 Effect of box height scale (H/D_{max})

A similar approach was adopted to investigate the overall macromechanical effects of the box height scale. In general, as the box height becomes larger the magnitude of the peak stress ratio becomes greater (Figure 5-2a,c). For example, the intermediate box length in conjunction with the largest box height scale yields a peak stress ratio of 1.28, and when the height scale is reduced to the intermediate height scale is 1.20, and at the smallest height scale is further reduced to 1.08 (Figure 5-2a). Moreover, the peak stress ratio also occurs at larger shear displacements for the smallest box height scale as compared to the largest box height scale, e.g. the peak stress ratio occurs approximately 1,3 mm earlier for the largest box height scale (Figure 5-2a,b).

Similarly, the applied shear strain, at the peak stress ratio, also increases inversely with respect to decreases in the box height scale (for constant length scale) (Figure 5-2c). This is made clear when contrasting the results of the smallest and largest box height scales (at the intermediate box length scale), i.e. 10.62% and 8.59%, respectively. The changes in the vertical displacements of the top wall and total volumetric strains do not produce a consistent correlation; that is, the intermediate box height scale does not yield the median magnitude of vertical displacement at the peak stress state, but rather the largest box length scale does (Figure 5-2b).

The maximum vertical displacement of the top wall (at the peak stress ratio) resulted from the smallest box height scale at 0.094 mm and the minimum arose by the intermediate box height scale, which yielded only -0.05 mm. This indicates that the peak stress state was reached, while the specimen still experienced contractile behaviour, during the undertaking of this particular test (Figure 5-2b). This was also the case for the largest box height scale that yielded a vertical displacement of the top wall of -0.04 mm at the peak stress ratio. Only the smallest box height scale reached the peak stress ratio during dilation of the specimen when the vertical displacement was 0.09 mm (Figure 5-2b).

The total volumetric strain displays a similar, i.e. more complex, trend to that of the vertical displacement of the shear box top wall, mentioned above. This is illustrated when contrasting the largest box height scale that produces the median total volumetric strain of -0.14%; the intermediate box height scale produces a greater value of 0.27%, and the smallest box height scale the greatest value of 0.75% (Figure 5-2d).

Similar observations (at the peak stress ratio) were made by Wang and Gutierrez (2010), during the increase of the box height scale with constant length scale: i) the magnitude peak stress ratio increases; ii); the vertical displacement increases and the induced amount by the smallest height scales are most similar; iii) the total volumetric strain decreases, and is inversely proportional. Furthermore, Wang and

Stellenbosch University https://scholar.sun.ac.za

Gutierrez (2010), found that the applied shear displacement increased proportionally with increased box height scale; in the present study, however, the contrary is true.

On average, the applied shear displacement, at the peak stress ratio, is inversely proportional to the shear box height scale. Evidence of the trends present for variations of vertical displacement of the shear box top wall, with changes in box height scale, are not well documented in the literature. Two possible explanations for the behaviour observed in the present study: i) it could be that there is more space for the granular material to deform in, due to the archetype nature of the DS apparatus adopted, and therefore, any deformation in the direct shear test taking place is more pronounced, and; ii) That this is, again, an artefact of the irregularly shaped granular materials which cause for more erratic behaviours during shear. The above macromechanical observations indicate that increased energy is required to rearrange the vertically stacked particles within larger box height scales, pointing toward bulk failure taking place and an increased number of specimen grains being rearranged during failure (Jacobson, Valdes and Evans, 2007; Wang and Gutierrez, 2010).

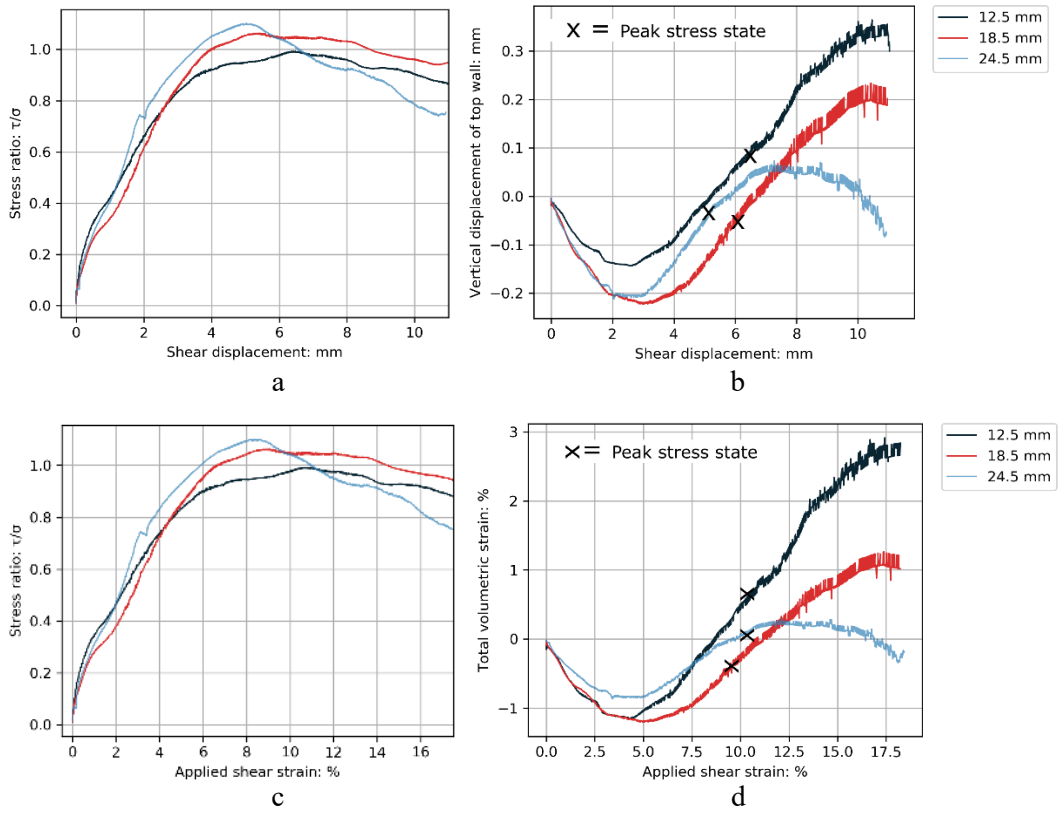

Figure 5-2. Convolved Shear Box results illustrating a variation in height scale for constant box length scale (L=60 mm), gradation (GW) and normal stress (150 kPa): a) stress ratio change with shear displacement; b) vertical displacement of the top wall with shear displacement; c) stress ratio change with the applied shear strain; d) total volumetric strain change with variations in applied shear strain

Stellenbosch University https://scholar.sun.ac.za

Interestingly, when the box length scale is largest, variations in box height scale do not necessarily reflect the trends of those described above, that is, for the intermediate box length scale (Figure 5-3a). For the largest box height scale, it is clear that the peak stress ratio is somewhat proportional to the box height scale; though, it is important to point out that the largest box height scale does not yield the greatest peak stress ratio (Figure 5-3a,c). For example, the maximum peak stress ratio of 0.92, resulted from the maximum length scale and intermediate height scale, and the minimum peak stress ratio was yielded (as expected) by the smallest height scale with an average peak stress ratio of 0.79 (Figure 5-3a).

The magnitude of both the applied shear displacement and applied shear strain (at the peak stress ratio) increases with an increase in box height scale (Figure 5-3b,d). The smallest magnitude of applied shear displacement, at the peak stress ratio, occurred for the smallest box height scale at 4.45 mm of applied shear displacement (Figure 5-3a). The intermediate and largest box height scales, by comparison, yielded the peak stress ratio average applied shear displacements that were notably greater, at 5.50 mm and 7.21 mm, respectively. This dictates that for larger box length scales, the relationship between height scale and the applied shear displacement (at the peak stress ratio) is directly proportional. It is interesting that this relationship, between height scale and the applied shear displacement, is contrary to what was observed when conducting tests at the intermediate box length scale, above.

It is clear that the vertical displacement of the top wall and the total volumetric strain increases (at the peak stress ratio) as the box height scale increases; as an example, when systematically increasing the box height scale from the smallest to the largest scale, the following vertical displacement of the top wall results were obtained: 0.015 mm; 0.2 mm, and; 0.25 mm, respectively (Figure 5-3b). Similar trends are observed for the total volumetric strain; however, there is a distinct difference: the difference in the total volumetric strain for the intermediate and largest box height scales is very small. For instance, the total volumetric strain (at the peak stress ratio) for the largest box height scale is 1.0%, and for the largest box height scale, 1.02% was produced (Figure 5-3d). Compare these values with the much-reduced value yielded by the smallest box height scale, which induced the peak stress state at 0.02% of total volumetric strain. This indicates that as the box height scale systematically becomes larger, the rate of increase in total volumetric strain (for increases in box height) incrementally becomes less (Figure 5-3c). This points toward competition between the effects of box length and box height scale, i.e. there may be a critical height for a particular box length, at a certain maximum particle size, for a given gradation.

An additional significant observation made in the present study is that a decreased box height scale most often produces a smaller range of peak stress ratio results. This indicates that, for smaller box height scales, a higher degree of repeatability is yielded; case in point, is made by the smaller degree of standard error that is usually associated with the smallest box height scale results. For example, the error related to the smallest box height scale, in conjunction with the largest through smallest box length scales are 0.18, 0.027, and 0.029, respectively; as opposed to, the (mostly) larger magnitudes standard error associated with the intermediate box height scale for the same range of box height scales, 0.23, 0.04,

Stellenbosch University https://scholar.sun.ac.za

and 0.017, respectively (Figure 5-4). Despite the diminished nature of the standard error values, at the smallest box height scale, these results likely do not truly reflect the soil strength, due to incomplete development of the shear band in such a small volume for sample deformation to take place (Jacobson, Valdes and Evans, 2007).

On average, variations in box height scale, show similar behaviour to those described above, and those which have been indicated in previous DEM studies (e.g. Jacobson, Valdes and Evans, 2007; Wang and Gutierrez, 2010). However, this behaviour has, to the authors knowledge, not been adequately documented experimentally in the literature in the past.

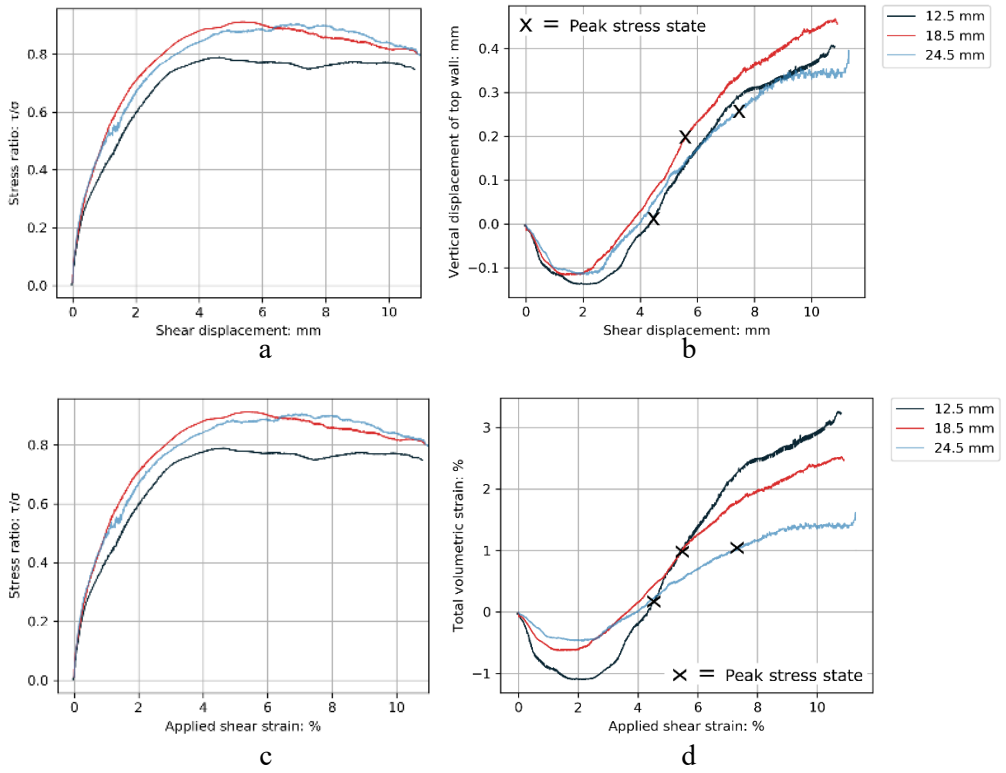

Figure 5-3. Convolved Shear Box results illustrating a variation in height scale for constant box length scale (L=100 mm), gradation (GW) and normal stress (150 kPa): a) stress ratio change with shear displacement; b) vertical displacement of the top wall with shear displacement; c) stress ratio change with the applied shear strain; d) total volumetric strain change with variations in applied shear strain

Stellenbosch University https://scholar.sun.ac.za

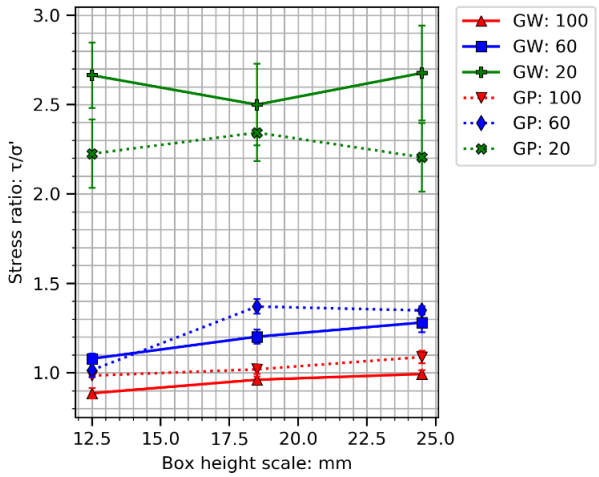

Figure 5-4. Effects of box height scale on the peak stress ratio, error bars display the standard error of triplicate test sets

5.1.3 Pre-shear Porosity

Arbitrary variations, or non-conformation, of several of parameters, and in particular the peak stress ratio, may to a degree be governed by the variations in the pre-shear (or initial) porosity of a test specimen. Bearing in mind that the initial porosity of a shear specimen plays a principal role in the determination of the shear behaviour of a granular material; the following trends in pre-shear porosity, with variations in normal stress and Shear Mould dimensions, were observed during the present study (Figure 5-5):

i) The initial porosity is indirectly proportional to the applied normal stress, for example, the Shear Mould with the largest length scale and smallest height scale, yielded pre-shear porosities of 0.358 at 50 kPa and 0.347 at 150 kPa. (Figure 5-5b).

ii) Well-graded specimens often result in a more consistent reduction of pre-shear porosity with increasing normal stress. For example, the largest box length and intermediate box height scale produced initial porosities of 0.383, 0.376 and 0.71 under normal stresses of 50 kPa, 100 kPa and 150 kPa, respectively (Figure 5-5a); and the poorly graded specimens yielded 0.390, 0.367 and 0.376 (Figure 5-5b).

iii) On average, the poorly-graded specimens have higher initial porosities, for example, the average pre-shear porosity of the Shear Mould comprised of the intermediate length scale and smallest box height scale for the poorly graded specimen is 0.389 (Figure 5-5b), as opposed to 0.377 for the well-graded specimens (Figure 5-5a,b).

iv) The box length scale is generally inversely proportional to the initial porosity, this is illustrated well when considering the well-graded specimens and comparing the average pre-shear porosity of the

Stellenbosch University https://scholar.sun.ac.za

smallest box length scale which is 0.400, and largest box length scale which is 0.358 (both at the smallest height scale) (Figure 5-5a).

v) A direct relationship exists between the box height scale and the initial porosity. For example, when considering the largest box length scale of poorly-graded specimens, the average initial porosity of the smallest box height is 0.358, which increases for the largest box height scale that yielded 0.388 (Figure 5-5a).

vi) The pre-shear porosity of the smallest box length scales are typically the least affected by the any of the above-mentioned trends, that is, their pre-shear porosities fluctuate the least regardless of the subjected normal stress, the specimen gradation implemented, or the box height scale adopted during testing. For example, when considering the poorly-graded specimens, the average initial porosity of the smallest box length and height scale was 0.405 and at the largest box height scale, the pre-shear porosity was 0.406 (Figure 5-5,b).

vii) The largest box length scale in combination with the smallest height scale, and the smallest length scale in combination with the largest height scale, respectively produced the largest and smallest magnitudes of pre-shear porosity. For example, on average when testing the GW specimens in shear moulds of the largest length scale with the smallest height scale produced the smallest pre-shear porosities of between 0.341 to 0.368, and the Shear Mould comprised of the smallest box length scale and largest height scale yielded the highest pre-shear porosities which were between 0.401 and 0.406. A similar observation can be made for the GP specimens.

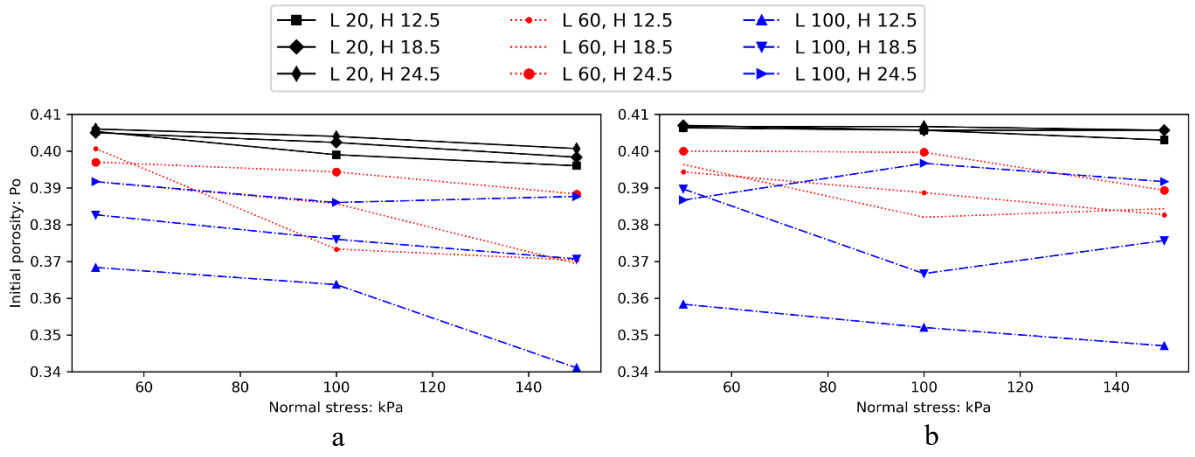

Figure 5-5. Variation in initial specimen porosity as a function of normal stress, Shear Mould size (L, H) and specimen gradation: a) GW specimens; b) GP specimens

The above observations suggest that the effects of variation of box height and length scale produce conflicting trends, in terms of the pre-shear porosity. Similar consequences of the variation in Shear Mould dimensions and normal stresses have been observed in the pre-shear porosity of numerical studies (Wang and Gutierrez, 2010). It is important to point out that in the study conducted by Wang and Gutierrez (2010) special mention was made of the final observation mentioned above (vii); it was

Stellenbosch University https://scholar.sun.ac.za

deemed that this observation was likely a consequence of the competition between the effects of the Shear Box height and length scales, as observed by their conflicting trends.

Moreover, the trends observed during this study are seemingly more linear than those identified in previous studies. Such difference is likely due to the smaller number of applied normal stresses at which tests were undertaken during this study, e.g. Wang and Gutierrez, (2010), conducted tests at four normal stresses. The trends observed in this study were also less regular than those observed in previous studies and, local deviations were observed, especially for the poorly-graded specimens (Figure 5-5). The increase in deviations for the poorly-graded specimens may be explained by the increased variation observed in the angularity of the particles used during the constitution of the poorly-graded sample specimens (Table 4-2). The initial porosity of the sample plays a significant role in the measured peak stress ratio because the porosity is indirectly proportional to the density of the soil which is directly proportional to the resistance to shear of the soil (Holtz & Kovacs, 1981).

The initial porosity is often directly proportional to the magnitude of the peak stress ratio. For example, the peak stress ratio for the well-graded specimen tested using the smallest box length scale and the largest box height scale yielded the largest initial porosity of 0.404 and on average generated a maximum peak stress ratio of 2.68 (Figure 5-6a).On the other hand, the largest box length scale in conjunction with the smallest box height scale produced the smallest initial porosity of 0.358 and yielded a significantly smaller average peak stress ratio of 0.89 (Figure 5-6a).

The range of peak stress ratios and void ratios observed for the GW specimens were widest as compared to the GW specimens. For example, the maximum and minimum stress ratios derived from the GW specimens were between 3.80 and 0.79 (Figure 5-6a) and the GP specimens varied between 3.04 and 0.79 (Figure 5-6b). It is important to note that the GW specimens yielded the greater maximum peak stress ratio, which is contrary to what has historically been indicated in the literature (e.g. Powrie, 1997; Burland, 2012b; Craig and Knappett, 2012). Wang and Gutierrez, (2010) found that the well-graded grain size distribution that they tested yielded larger peak stress ratios than those of the poorly-graded grain size distribution. The observed greater maximum and wider variation of the stress ratio may be due to the greater observed variation (i.e. increased COV and standard deviation) in particle shape characteristics of the grains (Table 4-2). It is also clear that larger the box length scales produce lower the peak stress ratios, regardless of the particle size distribution tested (Figure 5-6).

On average, the GP specimens tested with the smallest box scales yielded lower peak stress ratios than those of the well-graded specimens. It is important to point out, however, that the tests with larger box length scales (60 and 100) allowed for the GP specimens to yield higher average peak stress ratios than those of the GW specimens. These observations contradict typical results which showed that well-graded grain size distributions are characterized by greater degrees of interlocking, which leads to higher

Stellenbosch University https://scholar.sun.ac.za

peak stress states/ratios (Terzaghi, 1943; Terzaghi, Peck and Mesri, 1948; Holtz & Kovacs, 1981; Craig and Knappett, 2012).

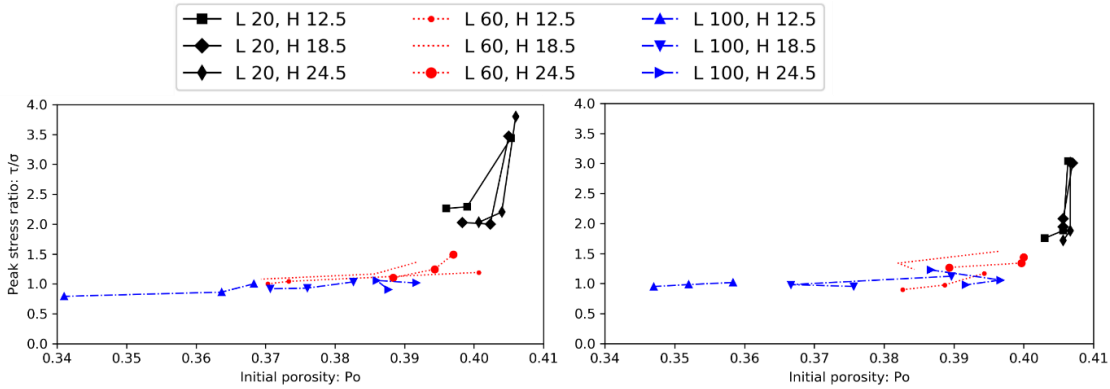

a b

Figure 5-6. Variations in peak stress ratio as a function of initial porosity, Shear Mould size (L, H) and specimen gradation: a) GW specimens; b) GP specimens

5.1.4 Effect of the Aspect Ratio (L/H)

As the effects of the length and box height scales yield conflicting effects of the macroscopic behaviour of granular materials, the combined effects of which, can be studied as a dual parameter, i.e. the aspect ratio (L/H). The combined effects of the Shear Box length and height scales is considered a "critical shape factor" that governs the mode in which a granular material fails (Wang and Gutierrez, 2010). In the present study, it has been observed that there is a directly proportional relationship between the aspect ratio and the peak stress ratio, i.e. smaller aspect ratios induce greater peak stress ratios (Figure 5-7). There is a marked increase in the rate of change in the peak stress ratio when the aspect ratio is reduced to below 4 but is larger than 2. For example, the increase in the average peak stress ratio from an aspect ratio of eight to four showed an 11% increase in the peak stress ratio, from 0.935 and 1.045, respectively, regardless of the box length and height scales, or gradations adopted. When the aspect ratio was decreased from 4.08 to 3.24 the peak stress ratio increased by ~31%, yielding an average peak stress ratio of 1.37 (Figure 5-7; Table 4-1).

It is interesting that significantly greater peak stress ratios were measured for the well-graded specimens (as compared to the poorly-graded specimens) at smaller aspect ratios (L/H<2). The poorly-graded specimens, however, resulted in comparatively higher peak stress ratios when adopting greater aspect ratios (L/H>2) (Figure 5-7). Variations in peak stress ratios, as a consequence of changes in the gradation, are believed to be due to the combination of i) the competition between the length and height scale at which the test is conducted, and; ii) the model error associated with the peak stress ratios at smaller box length scales, this is apparent from the performance of the fitted curves, as illustrated by the residual error (Figure 5-8). More pronounced variations, because of the competitive effects of box length and height scales, can be observed for the variations in the peak friction angles (Section 5.2.3).

Stellenbosch University https://scholar.sun.ac.za

Little information on the trends in the shear behaviour of granular with changes in the aspect ratio has been published in the literature. The models fitted to the experimental data perform reasonably well with coefficients of determination (r^2 values) are both greater than 0.8. It should be pointed out that the residual errors of observations/predictions at aspect ratios below two become greater, indicating that both the models' performance are reduced, i.e. less reliable predictions. This may also be a consequence of the greater error values associated with the smaller box length and height scales.

The macromechanical behaviour observed for similar box scale ratios presented in Wang & Gutierrez (2010), typically displays shear behaviour to that which has been observed in the present study. Based on the micromechanical DEM work conducted by Wang & Gutierrez (2010), light may be shed on modes of failure taking place and explain some of the macromechanical behaviours that have been observed within the present study (Figure 2-26).

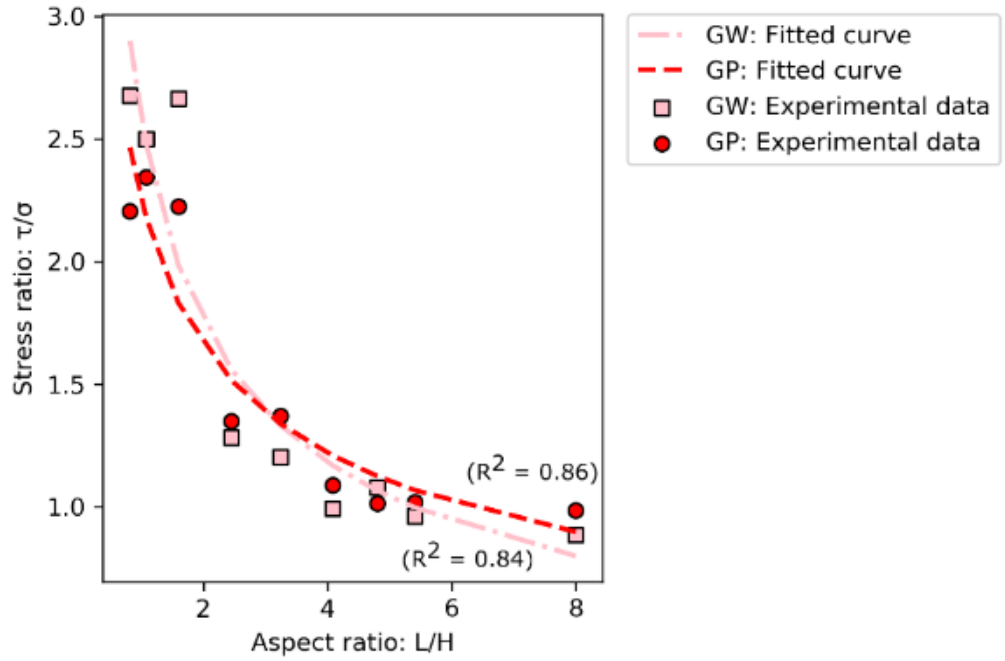

Figure 5-7. Aspect ratio vs peak stress ratio model

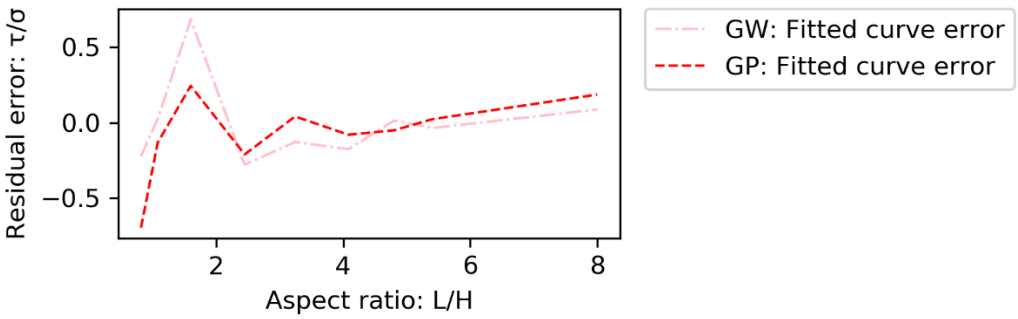

Figure 5-8. Stress ratio residual errors with variation in the aspect ratio

Stellenbosch University https://scholar.sun.ac.za

5.1.5 Effect of Specimen Gradation

The literature indicates that well-graded particle size distributions typically generate higher peak strength parameters than those of poorly graded grain size distributions (e.g. Holtz& Kovacs, 1981) (Table 2-3). In this study, however, the results derived from the largest and intermediate box length scales the well-graded PSD yields lower peak stress ratios; on average, the smallest box length scale the well-graded PSD yields higher peak stress ratios (Figure 5-9). That in mind, it is important to note that the error associated with the smallest box length scale is significantly larger than those of the largest box length scales (Figure 5-9). The large errors related to the smallest box length scale suggest that the results for the smallest box length scale may display the same relationship as those of the largest box lengths, which is still contrary to what is expected based on the literature (Terzaghi, 1943; Burland, 2012b).

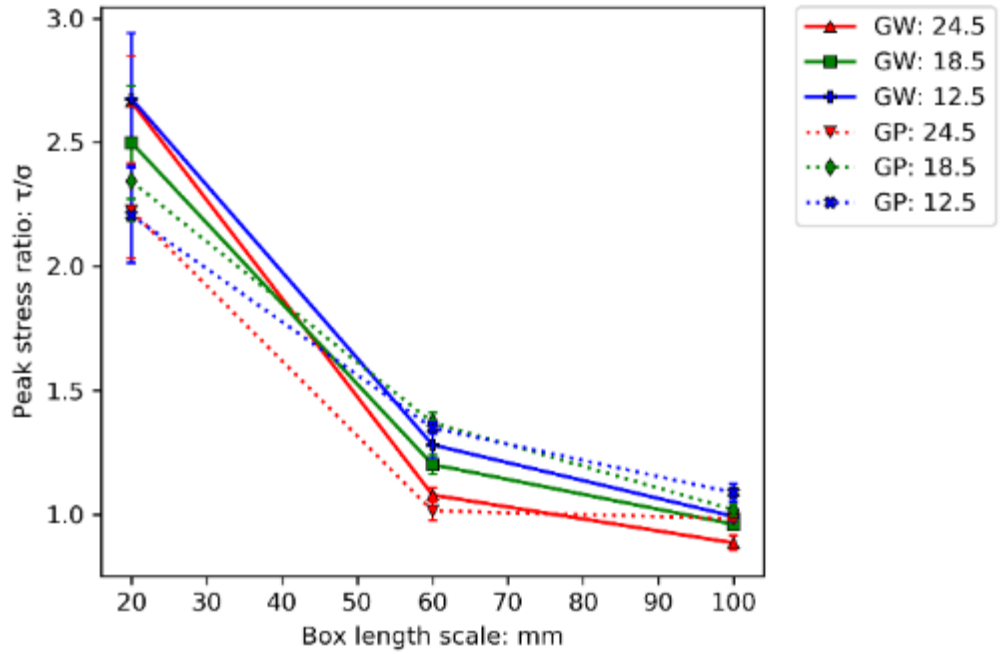

Figure 5-9. Effects of box length scale, height scale and gradation on the peak stress ratio. Error bars display the standard error associated with the combined values for the triplicate test results, at all normal stresses

Stellenbosch University https://scholar.sun.ac.za

5.2 Macromechanical Effects of Shear Mould Size on Peak Friction Angle

The macromechanical effects on the peak friction angles of the shear mould side are similar to those described for the peak stress ratio (Section 5.1 Macromechanical Effects of Shear Mould Size on Peak Stress Ratio): there is an inversely proportional relationship between the peak friction angle and the Shear Mould box length scale; a directly proportional relationship exists between the Shear Mould box height scale and the peak friction angle, and; there is a trade-off between the effects of the box length- and height scales. Little published work on the effects of Shear Box height scale and aspect ratio effects on the peak friction angle of granular materials are found in the literature.

5.2.1 Effects of box height scale

Larger box height scales yield greater peak friction angles. The effects of increasing the box height scale are less pronounced when increasing from the intermediate and largest box height scales, than the increase from the smallest to the intermediate box height scale, this is most pronounced when testing well-graded specimens using the largest box length scales; for example, the peak friction angle is 41.45˚ when adopting the smallest box height scale and 46.30˚, when utilizing the largest box height scale (Figure 5-8).

The smallest box length scale, when testing the GW specimens using the intermediate box height scale, resulted in the lowest peak friction angle (69.36˚), as compared to the smallest (71.18˚) and largest box height scales (73.61˚). Interestingly, this is the opposite is true for the poorly-graded specimens, when testing with the same Shear Mould configurations, yielded peak friction angles of 67.87˚, 67.37˚ and 67.28˚, respectively. Additionally, it is interesting that the peak friction angles of the GP specimens are comparatively smaller and show less variation regardless of the box height scale (Figure 5-8).

Furthermore, it is observed that, contrary to what is indicated in literature and similar to what has been described above, the peak friction angles of the poorly graded specimens are greater when testing at the intermediate and largest box length scales. Case in point is the example of the peak friction angles derived from the smallest box height scale and largest box length scale; the GW specimens resulting in 41.5˚ and the GP specimens yielding 46.1˚ (Figure 5-8).

Stellenbosch University https://scholar.sun.ac.za

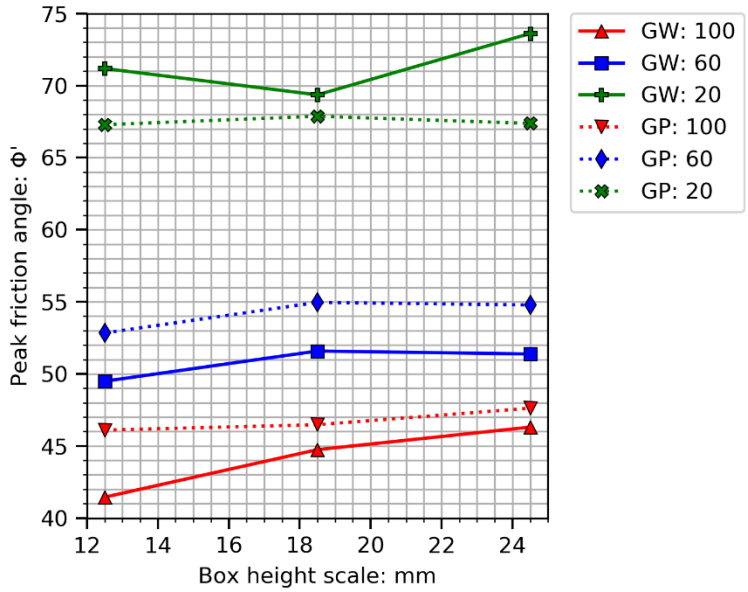

Figure 5-10. Effects of box height scale on peak friction angle

5.3.2 Effects of box length scale

As touched upon in the previous subsection, the box length scale is inversely proportional to the peak friction angle (Figure 5-11). The increase in the peak friction angle, between the largest and intermediate box length scale, is less than the increase between the intermediate and smallest box length scale. For example, the peak fiction angle of the largest box length and height scale was 47.62˚, the intermediate box length scale was 54.78˚ and the smallest box length scale was significantly height at 67.37˚ (Figure 5-11).

Despite the literature pointing toward well-graded specimens yielding great peak strengths (or friction angles) than those of poorly graded specimens, and as alluded to above, the largest and intermediate box length scales, the GW specimens yield lower peak friction angles than those of the GP specimens. For example, the peak friction angle of the GP specimens was greater at the intermediate box length and height scale resulting in a peak friction angle of 54.96˚, as compared to those derived by the GW specimens, generating a peak friction angle of 51.58˚ (Figure 5-11). It was observed that the opposite is true for the smallest box length scale, e.g. the peak friction angle of the GW specimens was 73.61˚, when testing at the largest box height scale and smallest length scale, whereas for the GP specimens the peak friction angle was only 67.37˚ (Figure 5-11).

Stellenbosch University https://scholar.sun.ac.za

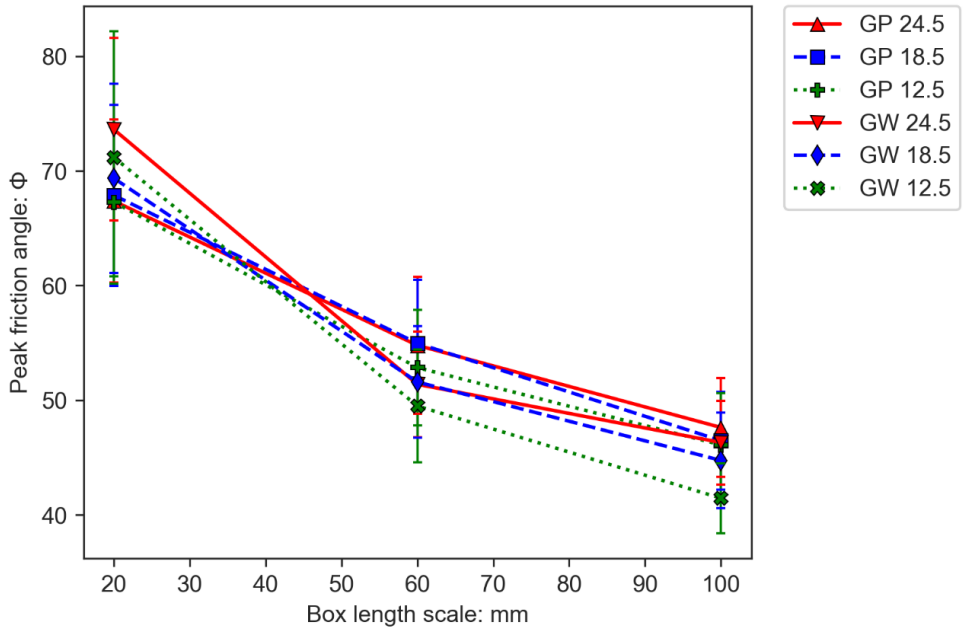

Figure 5-11. Peak friction angle variation with box length, height scale and specimen gradation

5.2.3 Effects of aspect ratio

Similar observations to those made above (Section 5.1.4) for the changes in the peak stress ratio with variations in the aspect ratio can be observed here. The most important observation to be made is that the models derived for the variation in peak friction angle (with changes in the aspect ratio) are more accurate than those derived from the peak stress ratio. The coefficients of determination (r^2 values) are greater, indicating a better 'goodness of fit' as compared to those of the models for the peak stress ratios. For example, consider the GW specimens, the model describing the variation in peak stress ratio with aspect ratio yielded an r^2 value of 0.84, whereas the variation in peak friction angle with aspect ratio yielded an r^2 value of 0.90.

It is important to point out that despite this, the residual error is greater for the peak friction angle models (Figure 5-12). This is attributed to the broader range in magnitude of peak friction angles, as compared to the range values of peak stress ratios, returned from the direct shear test. Although the data is essentially the same, there is a wider variation (or error) associated with the values presented as peak friction angles, as compared to when presented as peak stress ratios.

The competitive effects of the box length and box height scales can more readily be seen in the data presented as peak friction angles (Figure 4-27). This can be illustrated by assessing the variation of the peak friction angles with the reduction of the aspect ratio, particularly from 5.41 (Shear Mould: 100 x 18.5 mm) to 4.80 (Shear Mould: 60 x 12.5) and further still to 4.08 (Shear Mould: 100 x 24.5). On average, the respective peak friction angles associated with the previously described Shear Moulds increased from 45.61˚ to 51.16˚, which reduced to 46.96˚ with an increase in aspect ratio (Figure 5-13). This indicates that notwithstanding a change in the box height scale it will not yield a change as great

Stellenbosch University https://scholar.sun.ac.za

as those derived by a reduction in the box length scale; however, it is important to consider that in the present study, the reduction in the box length scale (i.e. the difference between 100 mm and 60 mm is) far exceeds the reduction in the height scale (i.e. the difference between 24.5 mm and 18.5 mm) of the tested Shear Moulds.

Perhaps the most interesting of the observations was that Shear Moulds implemented with aspect ratios of greater than 2, yielded peak friction angle results (e.g. between approximately 40˚ and 55˚) that fell well within the range of internal angle of friction data observed within several published studies (Table 2-2). The Shear Moulds with aspect ratios of less than 2, however, were of an order higher than those of the former.

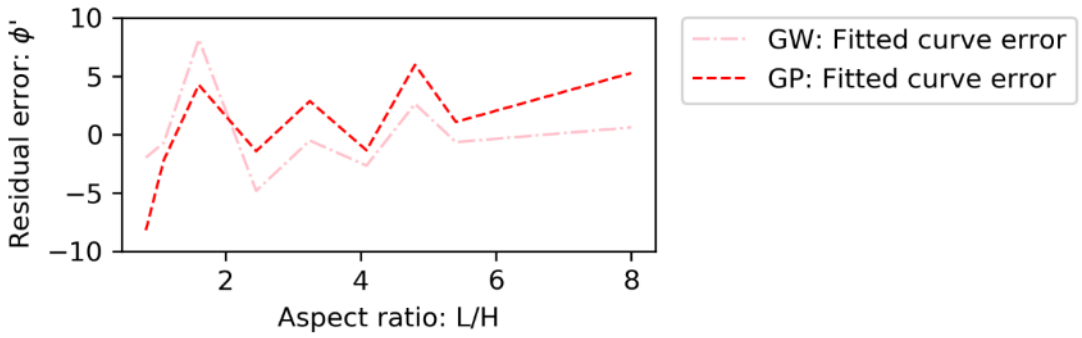

Figure 5-12. Residual errors of friction angle - aspect ratio model

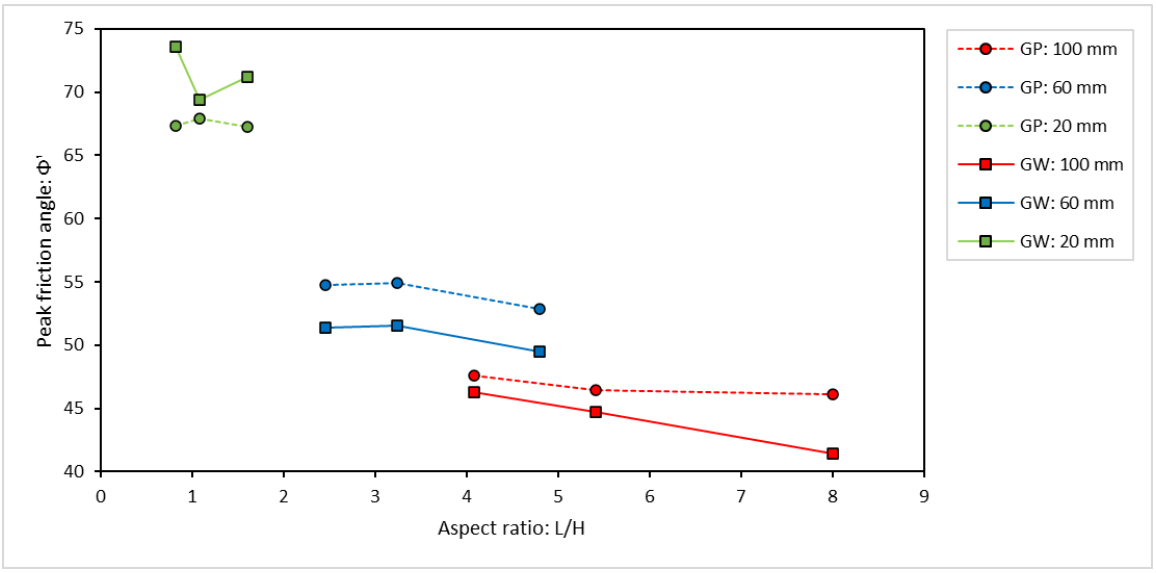

Figure 5-13. Peak friction angle variation with the aspect ratio

Stellenbosch University https://scholar.sun.ac.za

5.3 Effect of Grain Shape

The grain shape plays a crucial role in the behaviour of granular materials (Santamarina and Cho, 2004; Cho, Dodds and Santamarina, 2006; Zhou, Wang and Wang, 2017). During the present study, the grain shapes of several grain populations were studied according to a published grain classification chart (e.g. Krumbein and Sloss, 1963). The grain populations that were assessed by random sampling included: the field-collected waste rock materials; the crushed, but untested (i.e. not shear tested) waste rock particles, and; the crushed grains that the well- and poorly-graded specimens were comprised of.

For all of the grain populations, the sphericity values were highest, the grain roundness was lowest, and the particle regularity was the mean value of the former two grain characteristics (Figure 5-14). For example, the field waste rock (field WR) had average values of sphericity of 0.63, a roundness value of 0.32 and a particle regularity of 0.47 (Figure 5-14). The field derived waste rock (WR) displays the greatest particle regularity and the lowest associated standard deviation (0.22) and smallest standard error (0.011), implying that the material is the most uniform of the grain populations (Table 4-2; Figure 5-14). The particle shape characteristics of the GW grain population is most like those derived from the field WR grain population, e.g. the well-graded sphericity is 0.62 and standard deviation of the mean is 0.17, the roundness is 0.28 and particle regularity is 0.45. This implies that the shape characteristics of the grains used to reconstitute the GW specimens most accurately reflect those the field derived WR particles. However, due to the vastly different PSDs of the field WR and GW specimens, the mechanical behaviour of the respective materials is expected to be very different (Figure 3-5; Figure 3-7).

Interestingly, the poorly-graded grain size distribution produced a roundness value of 0.30, which was the second greatest, only to that of the field derived waste rock which was 0.32. The sphericity and particle regularity of the poorly-graded grain size distribution was found to be 0.56 and 0.43, respectively, which were the lowest of all the grain populations. This may explain the (typically) elevated stress ratios at the peak stress state, of poorly-graded samples, is a consequence of the increased angularity of the particles. Authors have found that increased particle angularity increases the frustration of particle rotation, which in turn increases the shear stress at the peak stress state (Santamarina and Cho, 2004; Shin and Santamarina, 2013).

Stellenbosch University https://scholar.sun.ac.za

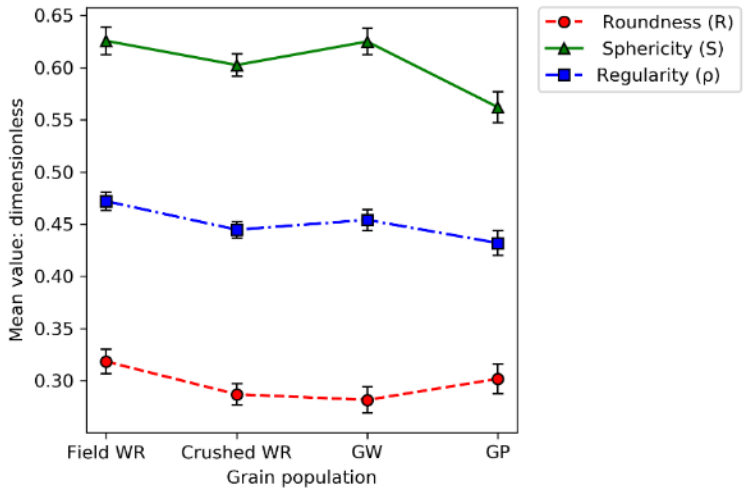

Figure 5-14. Grain shape characteristics according to Krumbien and Sloss (1963), along with standard error (calculated concerning sample size)

5.4 Discussion Summary

The Results and Discussion chapters have highlighted many relationships between several of the tested variables, a brief summary of which, is given by Table 5-1. The trends summarised above have, and in the preceding subchapters, been compared with existing literature, where possible. Some of the relationships present slightly more complex relations with trends which are not entirely linear. As examples, it appears that the intermediate box length scale represents an inflexion point at which the average trend in the total volumetric strain (at the peak stress ratio) changes from a directly proportional relationship to an inverse relationship; and on average the shear strain, at the peak stress ratio, increases with a reduction in box length scale or height scale as opposed to mimicking the trends observed in the peak stress ratios themselves, i.e. a directly or inversely proportional relationship, and have been shown to be opposing.

These opposing effects of length and height have been illustrated in preceding chapters, and the aspect ratio provided a unique lens through which to study these phenomena. In this study, the variation in aspect ratio of the Shear Mould has shown to have a profound effect on the shear behaviour of material tested in the direct shear test, and; this is speculated to be a consequence of the differences in the failure mechanisms taking place within the specimen. When considering the micromechanical studies undertaken by Wang and Gutierrez (2010) it is evident that the aspect ratio plays a crucial role in shear behaviour, and more importantly, seems to govern the manner in which grain on grain interaction takes place. The reduction of box height scale is believed to reduce the shear stress (i.e. peak stress ratio or friction angle) in a sample because less energy is required to displace the shear mould. It is speculated that this is because less means of energy dissipation are available for the individual grains, for example, particle rotation is mechanically hindered by the Shear Mould, leaving more of the shear force to be

Stellenbosch University https://scholar.sun.ac.za

dissipated by, for example, particle contacts, which in the past has been shown to be an efficient means of energy dissipation (Kovalcinova *et al.,* 2018).

An important example to consider, as was pointed out in Section 5.1.4, is the difference in the strength brought about from the maximum and intermediate box length scales, in combination with the largest height scale (i.e. 100 mm x 24.5 mm and 60 mm x 24.5 mm), both fall within the specified ASTM D3080-11 L/D_{max}, H/D_{max} and L/H ratios; yet the intermediate box length scale yielded an average increase of almost 28% in the resultant peak stress ratio (Table 4-1). When considering that this increase is similar to the factor of safety of 1.3 (i.e. 30% more than measured/observed) that is often adopted in geotechnical designs; one can not help but believe that the ratios specified in the ASTM D3080-11 standard are not reasonable in diminishing the scale effects of the direct shear test.

Table 5-1. Summary of effects of tested variables

Variable	Effect	Note
Length (L)	↑L, ↓ϕ	-
Height (H)	↑H, ↑ϕ (and τ/σ)	-
Aspect ratio (L/H)	↑L/H, ↓ϕ	-
Normal Stress (kPa)	↑kPa, ↓n, ↑τ/σ (and ϕ)	-
Porosity (n)	↓n, ↑ϕ (and τ/σ)	-
Grain shape (R, S)	↑R, ↑τ/σ (and ϕ); ↓S, ↑τ/σ (and ϕ)	True for larger box scales
Particle size distribution (Cu, Cz)	↑Cu (or Cz), ↓ τ/σ (and ϕ)	

Stellenbosch University https://scholar.sun.ac.za

Chapter 6 – Conclusions and Recommendations

6.1 Conclusions

The present study sought to investigate whether the box scale ratios specified in the ASTM D3080-11 are reasonable in diminishing the scale effects of the DS test. In doing so, relevant literature, the procedures adopted, the laboratory results obtained as well as their interpretation and significance have been presented in Chapters 1 through 5. The present chapter provides a high-level overview of the pertinent contents of the preceding chapters and highlights many of the findings of the present study.

The adopted testing schedule and procedures were designed to vary the box length and height scales, as well as the aspect ratio of a commercially available DS test. The original design of the Shear apparatus, utilized in this study, included two sets of length scale components, i.e. the largest and intermediate length scales. This allowed for variation length scale of the Shear Mould, by employing these in the experimental setup. In addition, an 'insert' was designed and fabricated that reduced the shear mould length scale further, to fully assess a spectrum of box scale ratios which lay above and below the recommended ASTM D3080-11 guidelines (ASTM, 2011). The particle size distribution was also varied to assess the role (or control) that the particle size distribution has on the scale effects when nearing, and transgressing the ASTM D3080-11 box scale ratios (ASTM, 2011).

This manuscript has aided in the identification of and confirmed several relationships between variables, which are summarised below:

1. When systematically decreasing the box length scale, relative to the maximum particle size, while maintaining the same particle size gradation and box height scale, the strength of the material, i.e. peak stress ratio and/or the peak friction angle, increases.
2. Increasing the box height scale, relative to the maximum particle size, while maintaining the same particle size gradation and box height scale, proportionally increases the shear strength parameters.
3. As the box length scale decreases the scatter (or error) observed in the data increases, regardless of the grain size distribution tested.
4. Typically, as the aspect ratio decreases (i.e. the combined effects of box length and height scale) the shear strength parameters increase following an exponentially and follows a trend that can be modelled by an exponential function with a reasonable goodness of fit ($r^2 > 0.80$).
5. The standard error associated with the functions modelling the variation in peak stress ratio is lower and more regular (with changes in aspect ratio) than those adopted for the peak friction angles. Moreover increased error is associated with the friction angle results as compared to the stress ratio results.

Stellenbosch University https://scholar.sun.ac.za

6. In this study, contrary to what is stated in literature, the poorly-graded gain specimens yielded greater peak shear strength parameters (stress ratio and friction angles), unless testing at small aspect ratios (L/H<2) where the well-graded grain size distribution returns the greater peak strength parameters.
7. All trends observed in the data are typically subdued by higher normal stresses, i.e. trends become less pronounced with increasing normal stress. This is attributed to decreased dilation of specimens.
8. Increased particle angularity increases the stress at the peak stress state.

6.2 Recommendations

This study has focussed on the scale effects and shear strength behaviour of mine waste rock in the standard 100 mm x 100 mm DS Box. Future research could continue this study and explore the following aspects which were not considered here:

1. Adopting a similar approach of systematic length and height box-scale variation starting with a larger initial Shear Mould size, i.e. a Shear Box with a sample mould of 300 x 300 mm and approximately 149 mm in height. This would allow for a greater range in box length and height scales, and a wider range of grain size distributions to be tested, this will allows for a more comprehensive dataset to be obtained. Moreover, where there are large differences in shear box length and height dimensions adopted in the present study, a more rigourous testing shedule could be determined which would reduce the uncertainty associated with larger changes in Shear Mould dimensions.
2. Development and fabriction of an *in situ* Shear Box to test the shear strength of the Witwatersrand mine waste rock in the field, which would allow for a 'true reflection' (or numerical value) of the strength of the Witwatersrand mine waste rock to be determined. This would further shed light on which of the box scale ratios implemented here, resolved the most accurate peak strength parametes.
3. Perform numerical analyses, i.e. Discrete Element Method models, based on the box scale ratios (and grain size distributions) implemented in the present study. A rigourous micromechanical study , i.e. shear band propogation and stress-contact networks, would clarify and possibly untangle the macromechanical behaviour observed in the present study. This may also bring to light, the modes of energy disipation taking place, when a change in the box height and length scales are implemented, which were only speculated upon within the present study.
4. The same approach could be adopted, i.e. grain size distributions and box scale ratios, with a uniformly shaped material, that is manufactured. This would decrease the error associated with the variations observed in the grain shape parameters.

Stellenbosch University https://scholar.sun.ac.za

5. Some of the results, although technically statistically significant (i.e. triplicate tests) yielded a fair degree of uncertainity/error. This error could be reduced by duplicating the same test schedule several times, e.g. seven times, to develop a more statstically robust dataset. Thereby reducing the errors associated with; for example, the test preparation method, grain size distribution implemented and random errors.

Stellenbosch University https://scholar.sun.ac.za

Bibliography:

Adams, R., Ahfeld, D., & Sengupta, A. 2007. Investigating the potential for ongoing pollution from an abandoned pyrite mine, in *Mine Water and the Environment*, 26:2-13.

Agangi, A., Hofmann, A., Rollion-Bard, C., Marin-Carbonne, J., Cavalazzi, B., Large, R. & Meffre, S. 2015. Gold accumulation in the archaean witwatersrand basin, south africa-evidence from concentrically laminated pyrite, *Earth-Science Reviews*. Elsevier B.V., (140):27–53.

Alias, R., Kasa, A. & Taha, M. R. 2014. Particle Size Effect on Shear Strength of Granular Materials in Direct Shear Test, *International* Scholarly and Scientific Research & Innovation 8(11):1144–1147.

Azam, S., Wilson, G. W., Herasymuik, G., Nichol, C. & Barbour, L., S. 2006. Hydrogeological behaviour of an unsaturated waste rock pile: a case study at the Golden Sunlight Mine , Montana , USA. *Bulletin of Engineering Geology and the Environment*, 66:259–268.

Azam, S., Wilson, G. W., Fredlund, D. G. & Van Zyl, D. 2009. Geotechnical characterization of mine waste rock, in *Proceedings of the 17th International Conference on Soil Mechanics and Geotechnical Engineering: The Academia and Practice of Geotechnical Engineering*. Alexandria, Egypt:3421–3425.

Bagherzadeh-khalkhali, A. & Mirghasemi, A. A. 2009. Numerical and experimental direct shear tests for coarse-grained soils, *Particuology,* 7(1):83–91.

Bareither, C. A., Benson, C. H. & Edil, T. B. 2006. Comparison of shear strength of sand backfills measured in small-scale and large-scale direct shear tests, *Canadian Geotechnical Journal*, 45(9):1224–1236.

B. C. Mine Waste Rock Pile Research Committee. 1991. Mined rock and overburden piles. Investigation and design manual: British Columbia Mine Waste Rock Pile Research Committee Interim Guidelines. May.

Bear, J. 1975. *Dynamics of Fluids in Porous Media*. New York: Elsevier.

Bell, F. G. 1996. Dereliction: coliery spoil heaps and their rehabilitation. *Environmental and Engineering Geoscience,* 2(1):85-96.

Bews, B. E. Barbour, S. L., Wilson, G. W. & O'Kane, M. A. 1997. The design of lysimeters for a low flux cover system over acid generating waste rock. Unpublished report.

Blake, G. R. 2008. Particle density, in M. Chesworth (ed.) Encyclopedia of *Soil Science*. Dordrecht: Springer.

Stellenbosch University https://scholar.sun.ac.za

Blight, G. E. 2010. *Geotechnical Engineering for Mine Waste Storage Facilities*. London, UK: Taylor & Francis.

Bolton, M. 1979. *A guide to soil mechanics*. London, UK: Macmillan Education Ltd.

Bolton, M. D. 1986. The strength and dilatancy of sands, *Géotechnique*, 36(1):65–78.

Bracewell, R. 1965. Convolution and Two-Dimensional Convolution, in *The Fourier Transform and Its Applications.* New York: McGraw-Hill.

Brawner, C. O. & Broughton, S. 1991. Recent problems with waste rock spoil dumps, in *15th Annual British Columbia Mine Reclamation Symposium*, 15:85–93.

Brink, A. B. A. 1996. *Engineering Geology of South Africa*. 1st editionn. Pretoria: Building Publications Pretoria.

Burland, J. 2012a. Soils as particulate materials, in Burland (editor in chief), *ICE manual of geotechnical engineering:* vol. 1. London: ICE Publishing. 153-161.

Burland, J. 2012b. Strength and Deformation Behaviour of Soil, in Burland (editor in chief), *ICE manual of geotechnical engineering:* vol. 1. London: ICE Publishing. 175-193.

Cerato, A. & Lutenegger, A. J. 2006. Specimen Size and Scale Effects of Direct Shear Box Tests of Sands, *Geotechnical Testing Journal,* 29(6):1-10.

Chang, C. S., Cerato, A. B. & Lutenegger, A. J. 2010. Modelling the scale effect of granular media for strength and bearing capacity, *International Journal of Pavement Engineering*, 11(5):343–353.

Chevrel, S., Courant, C., Cottard, F. & Coetzee, H. 2003. *Very high resolution remote sensing coupled to GIS-based Environmental Assessment - East Rand Goldfield, South Africa Report BRGMIRP-52724-FR* [Pretoria, South Africa]: Council for Geoscience.

Cho, G. C., Dodds, J. & Santamarina, J. C. 2006. Particle Shape Effects on Packing Density, Stiffness, and Strength: Natural and Crushed Sands, *Journal of Geotechnical and Geoenvironmental Engineering*, 132(5):591–602.

Craig, R. F. & Knappett, J. 2012. *Craig's Soil Mechanics*. eighth edition. New York, NY: Spon Press.

Das, B. M. 2010. *Fundamentals of geotechnical engineering*. Stamford, CT 06902 USA: Cengage Learning.

Dick, J., Shakoor, A., & Wells, N. 1994. A geological approach toward developing a mudrock-durability classification system. *Canadian Geotechnical Journal*, 31(1):17-27.

Stellenbosch University https://scholar.sun.ac.za

Earley, D., III, Kidd, D. A., Shelley, T., Walder, I. & Salvas, E. A. 2003. Slope stability of leached copper stockpiles, in *Tailings and Mine Waste '03*, Swets and Zeitlinger:121-130.

Eddy, C., Tiroyabone, L. & Torrez-Cruz, L. A. 2019. Three dimensional characterisation of the form of sand sized particles, in *Proceedings of the seventeenth African Regional Conference on Soil Mechanics and Geotechnical Engineering*, Cape Town:139-143.

Escario, V. & Saez, J. 1987. The shear strength of partly saturated soils, *Geotechnique*, 37(4):523–524.

Fakhimi, A. Boakye, K. Sperling, D. & McLemore, V. 2008. Development of a modified in situ direct shear test technique to determine shear strength parameters of mine rock piles, *Geotechnical Testing Journal*, 31(3): 269–273.

Fakhimi, A. & Hosseinpour, H. 2008. The role of oversize particles on the shear strength and deformational behaviour of rock pile material, in *forty-second U.S. Rock Mechanics and second U.S.-Canada Rock Mechanics Symposium,* San Francisco, CA: American Rock Mechanics Association.

Fala, O., Molson, J., Dawod, I., Aubertin, M., Bussiere, B. & Chapuis, R. P. 2011. *Simulating Water flow and reactive transport in waste rock piles using stochastic properties.* Ecole Polytechnique Montreal Report: EPM-RT-2011-03.

Filipowicz, P. & Borys, M. 2004. Geotechnical parameters of mining wastes from the Lubelskie coal basin as a material for hydrotechnical embankments. *Journal of Water and Land Development,* 8:163-170.

Filipowicz, P. & Borys, M. 2005. Geotechnical properties of mining wastes and their utilization in civil engineering, in *Proceedings of International Conference on Problematic Soils.* May 25-27, 2005, Eastern Mediterranean University, Famagusta, N. Cyprus: 259-267.

Fredlund, D. G., Morgenstern, N. R. & Widger, R. A. 1978. The shear strength of unsaturated soils. *Canadian Geotechnical Journal*, 15(3): 313–321.

Fredlund, D. G. & Rahardjo, H. 1993. *Soil Mechanics for Unsaturated Soils*. 1st edition. Hoboken, NJ: John Wiley & Sons.

Frimmel, H. E. 2019. The Witwatersrand Basin and Its Gold Deposits, in A. Kröner & A. Hofmann (eds.). *The Archean Geology of the Kaapvaal Craton, Southern Africa. Regional Geology Reviews.* Springer, Cham:255–275.

Frost, R. J. 1973. Some Testing Experiences and Characteristics of Boulder-Gravel Fills in Earth Dams, in *American Society for Testing and Materials*, West Conshohocken, ASTM International:207-233.

Fu, W., Zheng, X., Lei, X. & Deng, J. 2015. Using a modified direct shear apparatus to explore gap and

Stellenbosch University https://scholar.sun.ac.za

size effects on shear resistance of coarse-grained soil. *Particuology* 23:82–89.

Fu, W. & Dai, F. 2015. Scale dependence of shear strength for a coarse granular soil using a superimposition-nest type of direct shear apparatus, *Arabian Journal of Geosciences*, Springer, 8:10301–10312.

Gan, J. K. M., Fredlund, D. G. & Rahardjo, H. 1988. Determination of the shear strength parameters of an unsaturated soil using the direct shear test. *Canadian Geotechnical Journal*, 25(3):500–510.

Gao, S., Wei, Z., Xuyang, S., Qingxiang, C., Garmondyu, C., E., Jr., Shu, J. & Yuejun, H. 2017. Mechanical properties of material in a mine dump at the Shengli #1 Surface Coal Mine, China. *International Journal of Mining Science and Technology*, 27(3):545–550.

Guo, P. & Su, X. 2007. Shear strength, interparticle locking, and dilatancy of granular materials, *Canadian Geotechnical Journal*, 44(5):579–591.

Harehdasht, S. A., Hussien, M. N., Karray, M., Roubtsova, V., Chekired, M. 2019. Influence of particle size and gradation on shear strength–dilation relation of granular materials, *Canadian Geotechnical Journal*, 56(2):208–227.

Hawley, M. & Cunning, J. (ed.) 2017. *Mine Waste Dump and Stockpile Design*. 1st edition. The Netherlands: CRC Press.

Hawley, P.M. 2001. Site Selection, Characterization, and Assessment, in: W.A. Hustrulid, M.K. McCarter & D.J.A. Van Zyl (eds.), *Slope Stability in Surface Mining*. Littleton, Colo: Society for Mining, Metallurgy, and Exploration, Inc (SME):267-274.

Heller, V. 2011. Scale effects in physical hydraulic engineering models. *Journal of Hydraulic Research*, 49(3):293–306.

Hicher, P. Y. (ed.) 2012. *Multiscale Geomechanics: From Soil to Engineering Projects*. New York, NY: John Wiley & Sons.

Hirschman, I. I. & Widder, D. V. 1955. *The Convolution Transform.* Princeton, NJ: Princeton University Press.

Hitch, M., Ballantyne, S. M. & Hindle, S. R. 2010. Revaluing mine waste rock for carbon capture and storage. *International Journal of Mining, Reclamation and Environment*, 24(1):64–79.

Hockley, D. E., Noel, M., Rykaart, E. M., Jahn, S., & Paul, M. 2003. Testing of soil covers for waste rock in the Ronneburg WISMUT mine closure, in *6th ICARD, the Australasian Institute of Mining and Metallurgy.* Australia, Cairns: 273-279.

Stellenbosch University https://scholar.sun.ac.za

Holtz, R.D. & Kovacs, W.D. 2003. *An Introduction to Geotechnical Engineering*. 2nd Edition. Civil Engineering and Engineering Mechanics Series. Taiwan: Pearson Education Ldt.

Hong, Y. H., Byun, Y. H., Chae, J. G. & Lee, J. S. 2015. Shear Behavior of Sands Depending on Shear Box Type in Direct Shear Test. *Journal of the Korean Geotechnical Society*, 31(3):51–62.

Hornbaker, D. J., Albert, R., Albert, I., Barabási, A. L. & Schiffer, P. 1997. What keeps sandcastles standing? *Nature*, 387:765.

Hudyma, M. & Potvin, Y. H. 2010. An engineering approach to seismic risk management in hardrock mines. *Rock Mechanics and Rock Engineering*, 43(6):891–906.

ICOLD. 1996. *Bulletin 106 Guide To Tailings Dams and Impoundments.* Paris, International Commision on Large Dams (ICOLD).

Jacobson, D. E., Valdes, J. R. & Evans, T. M. 2007. A Numerical View into Direct Shear Specimen Size Effects. *Geotechnical Testing Journal,* 30(6):1–5.

Jewell, R. A. & Wroth, C. P. 1987. Direct shear tests on sand, *Géotechnique*, 37(1):53-68.

Kainthola, A. 2011. A Coal Mine Dump Stability Analysis—A Case Study. *Geomaterials*, 13(01):1–13.

Kasmer, O., Ulusay, R., 2006. Stability of spoil piles at two coal mines in Turkey: Geotechnical characterisation and design considerations, *Environmental and Engineering Geoscience*,12(4):337-352.

Kim, D. & Ha, S. 2014. Effects of Particle Size on the Shear Behavior of Coarse Grained Soils Reinforced with Geogrid. *Materials*, 7(2):963–979.

Kovalcinova, L., Karmakar, S., Schaber, M., Schuhmacher, A. L-., Scheel, M., DiMichiel, M., Brinkmann, M., Seeman, R. & Kondic, L. 2018. Energy dissipation in sheared wet granular assemblies. *Physical Review E*, 98(3).

Kroeger, E. B., Huang, S. L. and Speck, R. C. 1991. Spoil pile failure and analysis in interior Alaska. *Society of Mining Engineering, preprint:* 11.

Krumbein, W. C. & Sloss, L. L. 1963. *Stratigraphy and Sedimentation*. 2nd edition. San Francisco and London: W. H. Freeman & Co.

Kyrylyuk, A. V. and Philipse, A. P. 2011. Effect of particle shape on the random packing density of amorphous solids. *Physica Status Solidi (A): Applications and Materials Science*, 208(10):2299–2302.

Lapakko, K. 2002. Metal mine rock and waste characterization tools: An overview. Working Paper No. 16. United Kingdom, London: Mining, Minerals and Sustainable Development, International Institute

Stellenbosch University https://scholar.sun.ac.za

for Environment and Development.

Li, M. 1999. *Hydrogeochemistry of Oxidised Waste Rock From Stratmat Site, N . B . MEND Report 2.36.2a.* [Canada] 555 Booth Street, Ottawa, Ontario: Mine Environment Neutral Drainage (MEND).

Lings, M. L. & Dietz, M. S. 2004. An improved direct shear apparatus for sand, *Géotechnique*, 54(4):245–256.

Lourenço, S. D. N., Gallipoli, D., Augarde, C.E., Toll, D. G., Fisher, P. C. & Congreve, A. 2012. Formation and evolution of water menisci in unsaturated granular media, *Géotechnique*, 62(3):193–199.

Lowe, J. 1964. Shear strength of coarse embankment dam materials, in *Proceedings of the 8th internation congress on large dams,* 8(3):745–761.

Lu, Z., Yao, A., Su, A., Ren, X., Liu, Q. & Dong, S. 2019. Re-recognizing the impact of particle shape on physical and mechanical properties of sandy soils: A numerical study, *Elsevier: Engineering Geology*, 253:36–46.

Lucia, P. C. 1981. Review of experiences with flow failures of tailings dams and waste impoundments. Unpublished PhD dissertation. University of California, Berkley: 234.

Margolis, S. V., & Krinsley. D. K. 1974. Processes of Formation and environmental occurence of microfeatures on detritial quartz grains, *American Journal of Science,* 274(5):499–464.

Marsh, J. S. 2006. The Dominion Group, in Johnson, M. R., Anhaeusser, C. R., and Thomas, R. J. (eds) *The Geology of South Africa*. 2nd edn. Pretoria: Council for Geoscience, pp. 149–154.

Martin, V., Plante, B., Bussière, B., Aubertin, M., Pabst, T., Chen, D., Bréard Lanoix, M., Dubec, J. & Dimech, A. 2017. Controlling water infiltration in waste rock piles: Design, construction, and monitoring of a large-scale in-situ pilot test pile, in *70th Canadian Geotechnical Conference*. Ottawa, ON: Canadian Geotechnical Society.

McCarthy, T. S. 2006. The Witwatersrand Supergroup, in M. R. Johnson, C. R. Anhaeusser, & R. Thomas (eds.) *The Geology of South Africa*. South Africa: Council for Geoscience. 155–185.

Mclemore, V. T., Fakhimi, A., van Zyl, D., Ayakwah, G. F., Boakye, K. A. K., Ennin, F., Felli, P., Fredlund, D., Gutierrez, L. A. F., Nunoo, S., Techie-Menson, S. & Viterbo, V. C. 2009. Literature Review of Other Rock Piles: Characterization, Weathering, and Stability, *Open-file Report.* New Mexico, Socorro: New Mexico Beauro of Geology and Mineral Resources.

Mikasa, M. 1960. New direct shear apparatus, in *Proceedings of 15th Annual Convention Japanense Society of Civil Engineers.* Japan, Tokyo:45-48.

Stellenbosch University https://scholar.sun.ac.za

Mitchell, J. K. & Soga, K. 2005. *Fundamentals of Soil Behaviour*. 3rd edition. United States of America: Hoboken, NJ: John Wiley & Sons, Inc.

Moayed, R., Alibolandi, M. & Alizadeh, A. 2016. Specimen size effects on direct shear test of silty sands. *International Journal of Geotechnical Engineering*, 11(2):198–205.

Morgenstern, N. R. & Tchalenko, J. S. 1967. Microscopic Structures in Kaolin Subjected To Direct Shear, *Géotechnique*, 17:309-328.

Murray, E. J. and Sivakumar, V. 2010. *Unsaturated soils*. 1st edition. United Kingdom, Oxford: John Wiley & Sons.

Nadai, A. 1950. Theory of flow and fracture of solids. New York: McGraw Hill.

Neuner, M., Smith, L., Blowes, D. W., Sego, D. C., Smith, L. J. D., Fretz, N. & Gupton, M. 2013. The Diavik waste rock project: Water flow through mine waste rock in a permafrost terrain. *Applied Geochemistry,* 36: 222-233.

Nichol, C. F. 2002. Transient flow and transport in unsaturated heterogeneous media: field experiments in mine waste rock. Unpublished doctoral dissertation. Vancouver: The University of British Columbia.

Nichol, C. F., Smith, L. & Beckie, R. 2005. Field-scale experiments of unsaturated flow and solute transport in a heterogeneous porous medium. *Water Resources Research*, 41(5):1-11.

Niroumand, H. 2017. *Soil Reinforcement for Anchor Plates and Uplift Response*. 1st edition. United Kingdom, Oxford: Elsevier Science & Technology.

Nolan, Davis and Associates, Limited. 1991. *Heath Steel waste rock study.* MEND project, 2.31.1(a): 187.

Ovalle, C., Frossard, E., Dano, C., Hu, W., Maiolino, S. & Hicher, P. 2014. The effect of size on the strength of coarse rock aggregates and large rockfill samples through experimental data. *Acta Mechanica*, 225(8):2199–2216.

Ovalle, C. Bard, E., Dano, C., Hicher, P., Dorador, L., Campaña, J., Palma, C. & Acuña, G. 2015. A Review of Large Triaxial Tests on Coarse Rockfill Samples, in *Proceedings of the 15th Pan-American Conference on Soil Mechanics and Geotechnical Engineering*. Argentina, Buenos Aires: ISSMGE: 3256–3263.

Palmeira, E. M. & Milligan, G. W. E. 1989. Scale effects in direct shear tests on sand, in *XII International Conference on Soil Mechanics*. Brazil, Rio de Janeiro: ISSMGE:739–742.

Parsons, J. D. 1936. Progress report on an investigation of the shearing resistance of cohesionless soils,

Stellenbosch University https://scholar.sun.ac.za

in *Proceedings of the 1st International conference on Soil Mechanics and Foundation Engineering*. Cambridge, Massachusettes: ISSMGE:133–138.

Piteau Associates, 1991. *Mined rock and overburden piles: Investigation and Design Manual, Interim Guidelines. British Columbia:* British Columbia Mine Waste Rock Pile Research Committee.

Potts, D. M., Dounias, G. T. & Vaughan, P. R. 1987. Finite element analysis of the direct shear box test, *Géotechnique*, 37(1):11–23.

Potvin, Y., Hadjigeorgiou, J. and Stacey, T. 2007. Introduction, in *Challenges in deep and high stress mining*. Perth: Australian Centre for Geomechanics.

Powrie, W. 1997. *Soil Mechanics: Concepts and Applications*. 2nd edition. London and New York: Taylor & Francis.

Powrie, W. 2012. Groundwater profiles and effective stresses, in J. Burland, T. Chapman, H. Skinner & M. Brown. *ICE manual of geotechnical engineering*. London: ICE Publishing. 163–166.

Qin, J. 2007. Investigation of mechanical properties of geomaterials based on DEM simulation and theories for strain localisation analysis. Unpublished doctoral dissertation. Dailian: Dailian University of Technology.

Quine, R. L. 1993. Stability and deformation of mine waste dumps in north-central Nevada. Unpublished masters thesis. Reno: University of Nevada.

Rengach, V. N. 1973. The Theory of Coulomb Aand its Fundamental Significance. *Soil Mechanics and Foundation Engineering*, 10(1):63–67.

Richefeu, V., El Youssoufi, M. S. and Radjaï, F. 2006. Shear strength properties of wet granular materials. *Physical Review E: Statistical, Nonlinear, and Soft Matter Physics,* 73(5):1–11.

Robb, L. J. & Meyer, F. M. 1995. The Witwatersrand Basin, South Africa: Geological framework and mineralization processes. *Ore Geology Reviews,* 10(2):67–94.

Robb, L. J. & Robb, V. M. 1998. Gold in the Witwatersrand Basin, in Wilson, M. G. . and Anhaeusser, C. R. (eds) *The Mineral Resources of South Africa*. Pretoria, Council for Geoscience:294–349.

Roscoe, K. H. 1953. An Apparatus for the Application of Simple Shear to Soil Samples, in *Proceedinga of the 3rd International Society For Soil Mechanics and Foundation Engineering Conference*. Switzerland,ISSMFE:186-191.

Rowe, P. W. 1962 The stress-dilatancy relation for static equilibrium of an assembly of particles in contact. *Proceedings of the Royal Society of London. Series A. Mathematical, Physical and Engineering*

Stellenbosch University https://scholar.sun.ac.za

Sciences, 269(1339):500–527.

Santamarina, J. C. & Cho, G. C. 2004. Soil behaviour: The role of particle shape, in R. J. Jardine & D. M. Potts (eds.) *Advances in Geotechnical Engineering: The Skempton Conference*. Thomas Telford, London.

Saretzky, G. T. 1998. Hydrological characterisation of a sulfide waste rock dump. Unpublished M.S. thesis. Saskatoon, SK: University of Saskatchewan.

Savci, G. and Williamson, A. L. 2002. Hydrologic assessment of waste rock stockpiles: A case study from Ajo mine, Arizona, in *SME proceedings.* Phoenix.

Shakoor, A. & Ruoef, M. A. 1989. Stability of selected coal mine waste embankments in east-central Ohio. *Bulletin of the Association of Engineering Geologists*, 26(3):369-386.

Shibuya, S., Mitachi, T. & Tamate, S. 1997. Interpretation of direct shear box testing of sands as quasi-simple shear. *Geotechnique*, 47(4):769–790.

Shin, H. & Santamarina, J. C. 2013. Role of particle angularity on the mechanical behaviour of granular mixtures. *Journal of Geotechnical and Geoenvironmental Engineering*, 139(2):353–355.

Siemens, G. A. 2018. Thirty-Ninth Canadian Geotechnical Colloquium: Unsaturated soil mechanics — bridging the gap between research and practice. *Canadian Geotechnical Journal.* Ottawa, Canadian Science Publishing, 5:909–927.

Simoni, A. & Houlsby, G. T. 2006. The direct shear strength and dilatancy of sand-gravel mixtures, *Geotechnical and Geological Engineering*, 24(3):523–549.

Smith, L. J. D., Blowes, D. W., Jambor, J. L., Smith, L., Sego, D. C. & Neuner, M. 2013a. The diavik waste rock project: Particle size distribution and sulfer characteristics of low-sulfide waste rock. *Applied Geochemistry,* 36: 200-209.

Smtih, L. J. D., Bailey, B. L., Blowes, D. W., Jambor, J. L., Smith, L. & Sego, D. C. 2013b. The Diavik waste rock project: Initial geochemical response from a low sulfide waste rock pile. *Applied Geochemistry,* 36: 210-221.

Smith, L. J. D., Moncur, M. C., Neuner, M., Gupton, M., Blowes, D. W., Smith, L. & Sego, D. C. 2013c. The Diavik Waste Rock Project: Design, construction, and instrumentation of field-scale experimental waste-rock piles. *Applied Geochemcistry,* 36:187-199.

Skempton, A.W., 1949. Alexandre Collin: a note on his pioneer work in soil mechanics. Géotechnique, 1(4):215-222.

Stellenbosch University https://scholar.sun.ac.za

Skempton, A. W. & Bishop, M. A. 1950. The measurement of the shear strength of soils, *Géotechnique*, 2(2):90-108.

Spitz, K. & Trudinger, J. 2003. *Mining and the environment: From Ore to Metal*.2nd edition. Boca Raton, FL: CRC Press, Taylor & Francis.

Stockwell, J, Smith, L., Jambor, J. L. & Beckie, R. 2006. The relationship between fluid flow and mineral weathering in heterogeneous unsaturated porous media: A physical and geochemical characterization of a waste-rock pile. *Applied Geochemistry*, 21(8):1347–1361.

Stockwell, J. 2002. Investigation of hydrogeological and geochemical properties and spatial relationships of an unsaturated waste rock pile, Key Lake, Saskatchewan. Unpublished masters thesis. Vancouver: The University of British Columbia.

Stormont, J. C. & Farfan, E. 2005. Stability evaluation of a mine waste pile, *Environmental and Engineering Geoscience*, 11(1):43–52.

Sutton, M. W., Galpin, J. S. & Heller, D. 2006. A GIS-based History of Gold Mine Residue Deposits and Risk Assessment of Post-Mining Land-Uses on the Witwatersrand Basin, South Africa, in *1st International Seminar on Mine Closure Conference Proceedings*. Perth, Australian Center Geomechanics. 667–678.

Takada, N. 1993. Mikasa's Direct Shear Apparatus, Test Procedures and Results, *Geotechnical Testing Journal*, 16(3):314–322.

Terzaghi, K. 1943. *Theoretical Soil Mechanics*. United States of America, New York, NY: John Wiley & Sons.

Terzaghi, K., Peck, R. & Mesri, G. 1948. *Soil Mechanics in Engineering Practise*. 3rd edition. United States of America, New York, NY:John Wiley & Sons.

Toll, D. G. 2000. The influence of fabric on the shear behaviour of unsaturated compacted soils', in C.D. Shackelford, S.L. Houston, and N.-Y. Chang. (eds.) *Advances in Unsaturated Geotechnics, Proceedings of Sessions of Geo-Denver 2000.* Denver, Colo, American Society of Civil Engineers: 222–234.

Tynan, M. C. Russel, P. G. L., Perry, V. F., Tynan, M. C., Russell, G. P. & Perry, F.V. 2017. *A Global Survey of Deep Underground Facilities; Examples of Geotechnical and Engineering Capabilities, Achievements, Challenges (Mines, Shafts, Tunnels, Boreholes, Sites and Underground Facilities for Nuclear Waste and Physics R&D): A Guide,* No INL/EXT-17-42285-Rev001. [United States of America, Idaho Falls]: INL Idaho National Laboratory.

URS Corporation, 2003. *Mine rock pile erosion and stability evaluations, Questa mine*. Unpublished

Stellenbosch University https://scholar.sun.ac.za

Report to Molycorp, Inc. 4 volumes.

Valente, T. M. & Leal Gomes, C. 2009. Occurrence, properties and pollution potential of environmental minerals in acid mine drainage, *Science of the Total Environment*, 407(3):1135–1152.

Valenzuela, L., Bard, E., Campaña, J. & Anabalón, M. E. 2008. High Waste Rock Dumps — Challenges and Developments, in *1st International Seminar on the Management of Rock Dumps, Stockpiles and Heap Leach Pads*. Perth, Australian Center for Geomechanics: 65–78.

Vallero, D. A. & Blight, G. 2019. Mine Waste: A Brief Overview of Origins, Quantities, and Methods of Storage, in Letcher, T., Vallero, D. (eds.) *Waste*. 2nd edition. United Kingdom, London, Elsevier Inc: 77-86.

Verma, A. K., Deb, D. & Mukhopadyay, S., M. 2017. Stability of a mine waste dump over an existing dump. *Journal of Mines, Metals and Fuels,* 65(2): 41-48.

Walker, W. K. & Johnson, M. J. 2000. Observational engineering for open-pit geotechnics: A case study for predictions versus performance for the stability of a high overburden embankment over a soft/deep foundation at PT Freeport Indonesia's Grasberg open-pit mine, in *Slope Stability in Surface Mining.* Denver: SME.

Wang, J., Zhang, H., Tang, S. & Liang, Y. 2013. Effects of Particle Size Distribution on Shear Strength of Accumulation Soil. *Journal of Geotechnical and Geoenvironmental Engineering*, 139(11):1994–1997.

Wang, J. & Gutierrez, M. 2010. Discrete element simulations of direct shear specimen scale effects. *Géotechnique*, 60(5):395–409.

Wen-Jie, X., Qiang, X. and Rui-Lin, H. 2011. Study on the shear strength of soil-rock mixture by large scale direct shear test. *International Journal of Rock Mechanics and Mining Sciences*. Kidling, Oxford, England: Elsevier, 48(8):1235–1247.

Williams, D. J. 2001. Assessment of embankment parameters, in Hustrulid, W. A., McCarter, M. C. & van Zyl, D. J. A. (eds.) *Slope Stability in Surface Mining,* Littleton, CA, Society for Mining Metallurgy: (1)1: 275-284.

Wu, P., Matsushima, K. & Tatsuoka, F. 2007. Effects of Specimen Size and Some Other Factors on the Strength and Deformation of Granular Soil in Direct Shear Tests. *Geotechnical Testing Journal,* 31(1):45-64.

Zeller, J. & Wullimann, R. 1957. The Shear Strength of the Shell Materials for the Göschenenalp Dam, Switzerland, in *Proceedings of 4th International Conference on Soil Mechanics and Foundation Engineering*. London, Butterworths Scientific: 2:399–404.

Stellenbosch University https://scholar.sun.ac.za

Zevgolis, I. E. 2018. Geotechnical characterization of mining rock waste dumps in central Evia, Greece. *Environmental Earth Sciences*. Germany, Berlin: Springer, 77(16):1–18.

Zhang, L. & Thornton, C. 2007. A numerical examination of the direct shear test. *Geotechnique*, 57(4):343–354.

Zhou, B., Wang, J. & Wang, H. 2017. Three-dimensional sphericity, roundness and fractal dimension of sand particles. *Géotechnique*, 68(1):18–30.

Zhou, Q. Shen, H. H., Helenbrook, B. T. & Zhang, H. 2009. Scale dependence of direct shear tests. *Chinese Science Bulletin*, 54(23):4337–4348.

Zou, P. Zhao, X., Meng, Z., Li, A. Lui, Z. & Hu, W. 2018. Sample rocks tests and slope stability analysis of a mine waste dump. *Advances in Civil Engineering* [Electronic], 2018:1-17. Available: https://www.hindawi.com/journals/ace/2018/6835709/

Stellenbosch University https://scholar.sun.ac.za

Appendix A - Data smoothing and presentation

A.1 Python Convolution Function

In this Appendix, the code employed to smooth or 'convolve' the data can be found (Figure A-1) as well as the smoothed (stress – displacement) graphics that were used to generate the plots displayed in the Results section if this project. The stress – displacement plots for the poorly graded specimen are shown first, followed by the well-graded specimen. More about the convolution function's derivation and application can be found (among others) in Bracewell, (1965); and, Hirschman and Widder, (1955).

```
import pandas as pd
import numpy as np
import matplotlib.pyplot as plt
from pylab import figure, show, legend, ylabel
import seaborn as sns
from scipy import interpolate
from scipy.interpolate import make_interp_spline


df = pd.read_csv('20x12.5_SP.csv').dropna()
x=df['50_kPa_A_mm']
x=x.to_numpy()
y=df['50_kPa_A_Tau']
y=y.to_numpy()

def smooth(y, box_pts):
    box = np.ones(box_pts)/box_pts
    y_smooth = np.convolve(y, box, mode='same')
    return y_smooth
df['Smooth']=smooth(y,20)
plt.plot(x, y, '.')
plt.plot(x, smooth(y,20), 'r-', lw=2)
df.to_csv('smooth_50_kPaA.csv')
```

Figure A-1 Generic python code employed to smooth raw data.

A.2 Additional Notes on Data Collection and Results

An artefact of 'slip' may be observed in some of the test data, this can be explained as constant stress with a continued increase in the magnitude of shear displacement. This is due to 'play' within the DS apparatus. It was observed that movement could be induced in the shear bath upon the application of a force by one's hand. Where this has occurred, it can be observed within the first 1 – 2 mm of shear displacement of the DS apparatus (Figure A-2). This 'slip' can be seen in test results obtained from any box-length or box height scale. In some of the tests, the smoothing of the test results subdued this artefact (Figure 4-1).

Stellenbosch University https://scholar.sun.ac.za

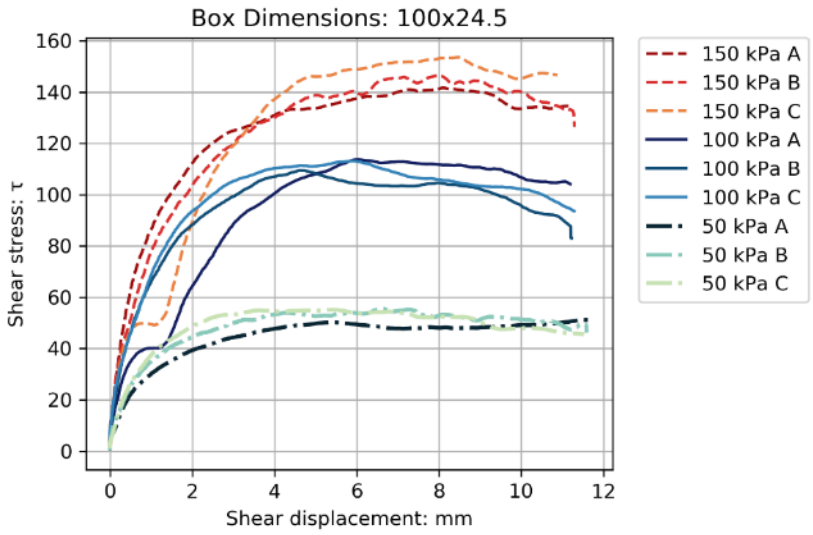

Figure A-2 Observed 'slip' in shear tests

All tests were conducted to the maximum allowable displacement of the DS apparatus. The smallest box length-scale tested was 20 mm and the maximum displacement of the apparatus is 12 mm. The data generated at these large displacements were excluded from the analysis and interpretation from the data as this falls outside of the scope of the present study. Generally, the resultant curves (in the case of the 20 mm box lengths) were clipped to around 6 mm, such that a distinct peak shear stress could be observed. Additionally, this step ensured that the often present secondary rise in shear stress was not captured, as this is assumed to be a function of the area reduction of the specimen; one of the many limitations of the DS test (Craig and Knappett, 2012).

Stellenbosch University https://scholar.sun.ac.za

Appendix B - Additional Laboratory Results and Information

B.1 Specific Gravity

The determination of the specific gravity (Gs) of the crushed waste rock particles was outsourced to a local geotechnical laboratory, Control Geosciences (PTY) LTD. The void ratio results were calculated using the average of Gs values presented in Figure B-1.

CONTROL GEOSCIENCES (PTY) LTD
CIVIL ENGINEERING MATERIAL AND GEOTECHNICAL LABORATORY,
GEOTECHNICAL AND ENVIRONMENTAL SERVICES
A division of ControLab South Africa (Pty) Ltd – Accreditation Number: T0308
1986/091003/07

LABORATORY: 7 Milan Street, Airport Industria, Cape Town, Tel: (021) 934 1114, email: geosci@mweb.co.za
CONTROLAB HEAD OFFICE: 1 Alfred Road, Vincent, East London, Tel: (043) 726 7899, Fax: (043) 726 7426, email: info@controlab.co.za
OTHER CONTROLAB BRANCH OFFICES: East London, Johannesburg, Mthatha, Kokstad, Queenstown, Lusaka - Zambia

CLIENT: Shane Teek **PROJECT:** Witwatersrand Samples

SPECIFIC GRAVITY (ASTM D854)

SAMPLE NO:	1	1	1	2	2	2		
POSITION:								
SPECIFIC GRAVITY	2,698	2,704	2,707	2,708	2,707	2,708		

Figure B-1 Specific gravity results, Control Geoscience.

B.2 Geotechnical Data

Considering the mechanics involved in the dissipation of shear forces in soils, i.e. particle breakage during shear, an indication of the geotechnical parameters governing the particle strength characteristics is considered prudent. Unfortunately, there is limited public knowledge of the geotechnical parameters for the source geology of the waste rock material that was used during the present study. Some general geotechnical information about the quartzites of the Johannesburg and Turffontein groups were published in Brink (1996) (Table B-1).

Table B-1 Strength, deformation and petrographic characteristics of the Johannesburg quartzites (Brink, 1996)

Locality Western Deep Levels Mine (Sample tested 1971)	σ_1/σ_3 ratio	Strength MPa	Number of specimens tested	Standard deviation %
Triaxial compressive strength	20,8	296	10	6,0
	13,3	369	10	5,3
	9,1	488	10	9,1
Uniaxial compressive strength	∞	237	10	4,1
Uniaxial tensile strength	−∞	10,8	10	11,0
Density: kg/m³ 2 710	Modulus of elasticity GPa .		79	
Porosity 1%	Poisson's ratio		0,13	
Moisture content 0,02%				

Petrographic Analysis

Qualitative	Composition (Vol %)		Grain size distribution	
Strongly bonded quartzite, with grains surrounded by thin film of amorphous silica	Quartz	67%	0,1–2,6 mm	
	Muscovite Chlorite Amorphous silica	32%	Quartz	1,2–2,6 60% 0,6–1,2 30% <0,6 10%
	Pyrite	1%	Pyrite: mostly angular grains 0,06 mm (few 1,2 mm)	

Stellenbosch University https://scholar.sun.ac.za

Appendix C - Grain Shape Quantification

This appendix contains the images (or figures) and associated results (tabulated) from the grain shape analysis. It is divided into three sections: i) The uncrushed field-derived waste rock (Appendix C.1); ii) The crushed pre-shearing grains (Appendix C.2), and; iii) The crushed post-shearing grains for both the well- and poorly-graded specimen (Appendix C.3). It is important to note that in each case, the numbers annotating the waste rocks or grains correspond to the particle numbers in the tables.

C.1 Grain Shape Analysis of Field-Derived Waste Rock

C.1.1 Field-Derived Waste Rock Results

Table C-2 Results for the grain shape analysis of the uncrushed, field-collected waste rock specimen

ST02 Bag 8				ST02 Bag 9				ST03 Bag 1				ST03 Bag 4			
Particle	**R**	**S**	**ρ**	**Particle**	**R**	**S**	**ρ**	**Particle**	**R**	**S**	**ρ**	**Particle**	**R**	**S**	**ρ**
1	*0.2*	*0.8*	*0.5*	**1**	*0.5*	*0.7*	*0.6*	**1**	*0.3*	*0.7*	*0.5*	**1**	*0.2*	*0.7*	*0.45*
2	*0.6*	*0.8*	*0.7*	**2**	*0.5*	*0.5*	*0.5*	**2**	*0.1*	*0.6*	*0.35*	**2**	*0.4*	*0.6*	*0.5*
3	*0.2*	*0.5*	*0.35*	**3**	*0.2*	*0.5*	*0.35*	**3**	*0.3*	*0.3*	*0.3*	**3**	*0.2*	*0.6*	*0.4*
4	*0.7*	*0.7*	*0.7*	**4**	*0.2*	*0.6*	*0.4*	**4**	*0.2*	*0.7*	*0.45*	**4**	*0.4*	*0.8*	*0.6*
5	*0.7*	*0.9*	*0.8*	**5**	*0.5*	*0.5*	*0.5*	**5**	*0.2*	*0.5*	*0.35*	**5**	*0.2*	*0.7*	*0.45*
6	*0.3*	*0.7*	*0.5*	**6**	*0.7*	*0.5*	*0.6*	**6**	*0.3*	*0.7*	*0.5*	**6**	*0.3*	*0.7*	*0.5*
7	*0.3*	*0.7*	*0.5*	**7**	*0.3*	*0.7*	*0.5*	**7**	*0.3*	*0.3*	*0.3*	**7**	*0.4*	*0.8*	*0.6*
8	*0.9*	*0.2*	*0.55*	**8**	*0.1*	*0.6*	*0.35*	**8**	*0.3*	*0.8*	*0.55*	**8**	*0.2*	*0.6*	*0.4*
9	*0.2*	*0.9*	*0.55*	**9**	*0.2*	*0.5*	*0.35*	**9**	*0.2*	*0.8*	*0.5*	**9**	*0.2*	*0.3*	*0.25*
10	*0.3*	*0.5*	*0.4*	**10**	*0.5*	*0.7*	*0.6*	**10**	*0.3*	*0.7*	*0.5*	**10**	*0.4*	*0.4*	*0.4*

Stellenbosch University https://scholar.sun.ac.za

ST02 Bag 8				ST02 Bag 9				ST03 Bag 1				ST03 Bag 4			
Particle	**R**	**S**	**ρ**	**Particle**	**R**	**S**	**ρ**	**Particle**	**R**	**S**	**ρ**	**Particle**	**R**	**S**	**ρ**
11	*0.3*	*0.8*	*0.55*	**11**	*0.5*	*0.8*	*0.65*	**11**	*0.3*	*0.7*	*0.5*	**11**	*0.2*	*0.8*	*0.5*
12	*0.5*	*0.3*	*0.4*	**12**	*0.7*	*0.7*	*0.7*	**12**	*0.3*	*0.5*	*0.4*	**12**	*0.2*	*0.7*	*0.45*
13	*0.5*	*0.7*	*0.6*	**13**	*0.1*	*0.7*	*0.4*	**13**	*0.3*	*0.3*	*0.3*	**13**	*0.2*	*0.8*	*0.5*
14	*0.3*	*0.5*	*0.4*	**14**	*0.3*	*0.4*	*0.35*	**14**	*0.2*	*0.4*	*0.3*	**14**	*0.2*	*0.7*	*0.45*
15	*0.3*	*0.8*	*0.55*	**15**	*0.5*	*0.7*	*0.6*	**15**	*0.3*	*0.7*	*0.5*	**15**	*0.3*	*0.7*	*0.5*
16	*0.5*	*0.9*	*0.7*	**16**	*0.3*	*0.6*	*0.45*	**16**	*0.3*	*0.6*	*0.45*	**16**	*0.5*	*0.7*	*0.6*
17	*0.3*	*0.7*	*0.5*	**17**	*0.3*	*0.5*	*0.4*	**17**	*0.3*	*0.7*	*0.5*	**17**	*0.2*	*0.6*	*0.4*
18	*0.4*	*0.3*	*0.35*	**18**	*0.2*	*0.9*	*0.55*	**18**	*0.3*	*0.6*	*0.45*	**18**	*0.3*	*0.7*	*0.5*
19	*0.5*	*0.7*	*0.6*	**19**	*0.2*	*0.7*	*0.45*	**19**	*0.3*	*0.7*	*0.5*	**19**	*0.3*	*0.8*	*0.55*
-	-	-	-	**20**	*0.3*	*0.7*	*0.5*	**20**	*0.7*	*0.6*	*0.65*	**20**	*0.4*	*0.7*	*0.55*
-	-	-	-	**21**	*0.3*	*0.5*	*0.4*	**21**	*0.3*	*0.7*	*0.5*	**21**	*0.3*	*0.7*	*0.5*
-	-	-	-	**22**	*0.5*	*0.6*	*0.55*	**22**	*0.2*	*0.3*	*0.25*	**22**	*0.3*	*0.6*	*0.45*
-	-	-	-	**23**	*0.5*	*0.3*	*0.4*	**23**	*0.3*	*0.5*	*0.4*	**23**	*0.5*	*0.7*	*0.6*
-	-	-	-	**24**	*0.3*	*0.7*	*0.5*	**24**	*0.2*	*0.7*	*0.45*	**24**	*0.2*	*0.6*	*0.4*
-	-	-	-	**25**	*0.3*	*0.5*	*0.4*	**25**	*0.5*	*0.7*	*0.6*	**25**	*0.2*	*0.7*	*0.45*
-	-	-	-	**26**	*0.3*	*0.3*	*0.3*	**26**	*0.2*	*0.7*	*0.45*	**26**	*0.2*	*0.3*	*0.25*
-	-	-	-	**27**	*0.2*	*0.7*	*0.45*	**27**	*0.1*	*0.7*	*0.4*	**27**	*0.3*	*0.7*	*0.5*
-	-	-	-	**28**	*0.4*	*0.7*	*0.55*	**28**	*0.2*	*0.7*	*0.45*	**28**	*0.2*	*0.7*	*0.45*
-	-	-	-	**29**	*0.3*	*0.3*	*0.3*	**29**	*0.1*	*0.7*	*0.4*	**29**	*0.2*	*0.7*	*0.45*
-	-	-	-	**30**	*0.3*	*0.7*	*0.5*	**30**	*0.3*	*0.6*	*0.45*	**-**	-	-	-
-	-	-	-	**31**	*0.3*	*0.9*	*0.6*	**31**	*0.2*	*0.7*	*0.45*	**-**	-	-	-
-	-	-	-	**32**	*0.3*	*0.3*	*0.3*	**-**	-	-	-	**-**	-	-	-

Stellenbosch University https://scholar.sun.ac.za

ST02 Bag 8				ST02 Bag 9				ST03 Bag 1				ST03 Bag 4			
Particle	**R**	**S**	**ρ**	**Particle**	**R**	**S**	**ρ**	**Particle**	**R**	**S**	**ρ**	**Particle**	**R**	**S**	**ρ**
-	-	-	-	**33**	*0.3*	*0.7*	*0.5*	-	-	-	-	-	-	-	-
-	-	-	-	**34**	*0.5*	*0.7*	*0.6*	-	-	-	-	-	-	-	-
-	-	-	-	**35**	*0.3*	*0.3*	*0.3*	-	-	-	-	-	-	-	-
-	-	-	-	**36**	*0.4*	*0.7*	*0.55*	-	-	-	-	-	-	-	-
-	-	-	-	**37**	*0.3*	*0.7*	*0.5*	-	-	-	-	-	-	-	-
-	-	-	-	**38**	*0.7*	*0.7*	*0.7*	-	-	-	-	-	-	-	-
-	-	-	-	**39**	*0.3*	*0.3*	*0.3*	-	-	-	-	-	-	-	-
-	-	-	-	**40**	*0.1*	*0.8*	*0.45*	-	-	-	-	-	-	-	-
-	-	-	-	**41**	*0.3*	*0.7*	*0.5*	-	-	-	-	-	-	-	-
-	-	-	-	**42**	*0.3*	*0.7*	*0.5*	-	-	-	-	-	-	-	-
-	-	-	-	**43**	*0.3*	*0.5*	*0.4*	-	-	-	-	-	-	-	-
-	-	-	-	**44**	*0.3*	*0.5*	*0.4*	-	-	-	-	-	-	-	-
-	-	-	-	**45**	*0.3*	*0.3*	*0.3*	-	-	-	-	-	-	-	-
-	-	-	-	**46**	*0.3*	*0.9*	*0.6*	-	-	-	-	-	-	-	-
-	-	-	-	**47**	*0.2*	*0.8*	*0.5*	-	-	-	-	-	-	-	-
-	-	-	-	**48**	*0.3*	*0.6*	*0.45*	-	-	-	-	-	-	-	-
-	-	-	-	**49**	*0.3*	*0.7*	*0.5*	-	-	-	-	-	-	-	-
-	-	-	-	**50**	*0.2*	*0.5*	*0.35*	-	-	-	-	-	-	-	-
-	-	-	-	**51**	*0.2*	*0.7*	*0.45*	-	-	-	-	-	-	-	-
-	-	-	-	**52**	*0.2*	*0.5*	*0.35*	-	-	-	-	-	-	-	-
-	-	-	-	**53**	*0.3*	*0.5*	*0.4*	-	-	-	-	-	-	-	-
-	-	-	-	**54**	*0.3*	*0.7*	*0.5*	-	-	-	-	-	-	-	-

Stellenbosch University https://scholar.sun.ac.za

ST02 Bag 8				ST02 Bag 9				ST03 Bag 1				ST03 Bag 4			
Particle	**R**	**S**	**ρ**	**Particle**	**R**	**S**	**ρ**	**Particle**	**R**	**S**	**ρ**	**Particle**	**R**	**S**	**ρ**
-	-	-	-	**55**	*0.3*	*0.7*	*0.5*	-	-	-	-	-	-	-	-
-	-	-	-	**56**	*0.3*	*0.7*	*0.5*	-	-	-	-	-	-	-	-
-	-	-	-	**57**	*0.3*	*0.8*	*0.55*	-	-	-	-	-	-	-	-
-	-	-	-	**58**	*0.5*	*0.8*	*0.65*	-	-	-	-	-	-	-	-
-	-	-	-	**59**	*0.3*	*0.5*	*0.4*	-	-	-	-	-	-	-	-
-	-	-	-	**60**	*0.3*	*0.7*	*0.5*	-	-	-	-	-	-	-	-
-	-	-	-	**61**	*0.3*	*0.5*	*0.4*	-	-	-	-	-	-	-	-
-	-	-	-	**62**	*0.3*	*0.6*	*0.45*	-	-	-	-	-	-	-	-

Stellenbosch University https://scholar.sun.ac.za

C.1.2 Field-Derived Waste Rock Images

Below the figures corresponding to the results presented above can be found (Figure C-1).

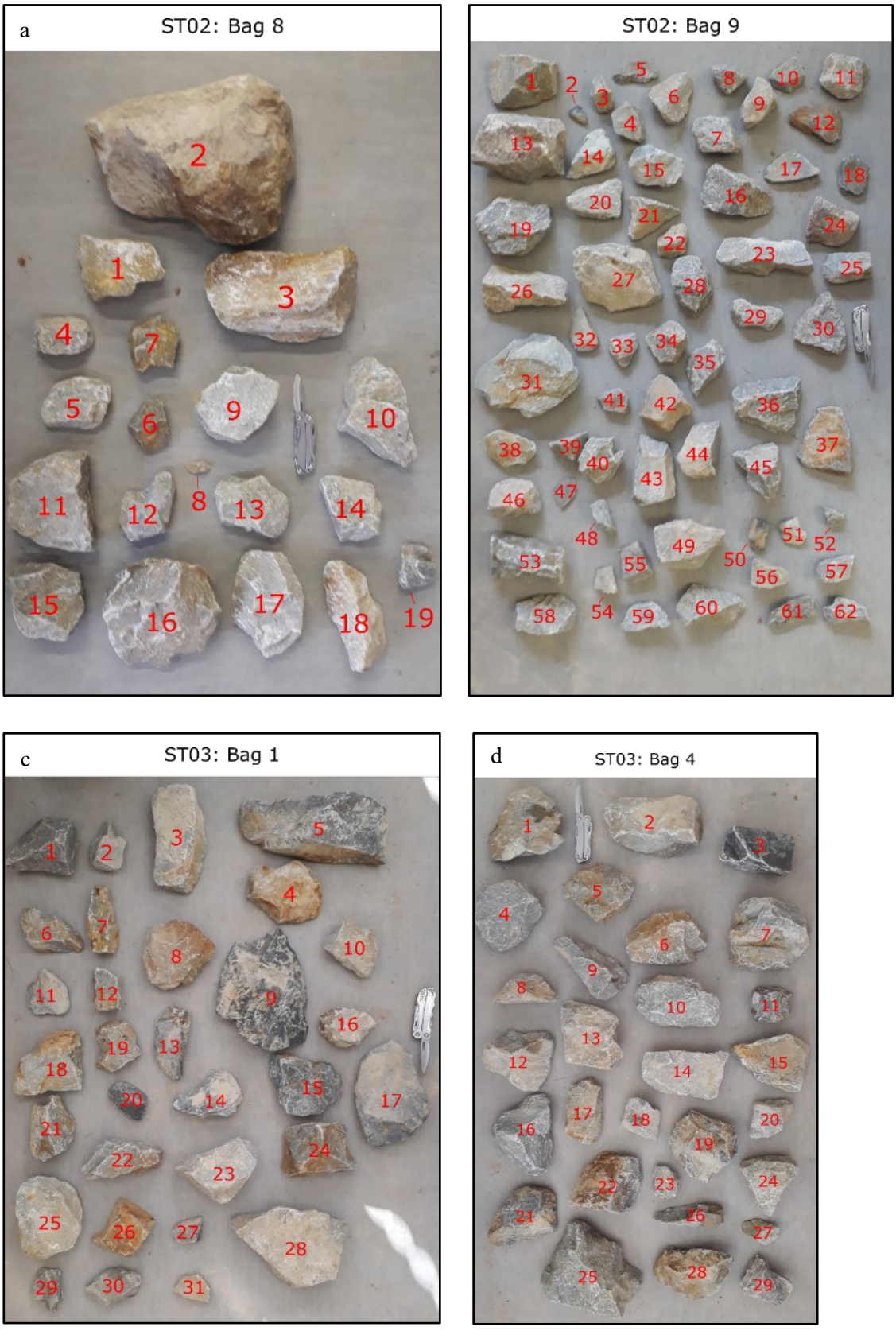

Figure C-1. Images of field-derived waste rock particles analysed for grain shape, split into site localities: a) ST02 [Bag 8]; ST02 [Bag 9]; ST03 [Bag 1], and; ST03 [Bag 4]

Stellenbosch University https://scholar.sun.ac.za

C.2 Grain Shape Analysis of Pre-Tested Waste Rock

C.2.1 Pre-Tested Waste Rock Results

After crushing of the field derived waste rock, the material was sieved into several required size fractions. A minimum of 20 individual grains for each size fraction, that was used during reconstitution of the well- and poorly-graded specimens which were randomly sampled, and assessed. The results of the grain shape analysis are presented below (Table C-3). The summary statistics for the results presented here are presented in Chapter 4, Results.

Stellenbosch University https://scholar.sun.ac.za

Table C-3 Results of grain shape analysis for crushed and un-tested waste rock

Size Fraction:	4,00-3,35 mm			3,35-2,36 mm			2,36-2,00 mm			2,00-1,70 mm			1,70-1.40 mm		
Particle No.	**R**	**S**	**ρ**	**R**	**S**	**ρ**	**R**	**S**	**ρ**	**R**	**S**	**ρ**	**R**	**S**	**ρ**
1	*0.2*	*0.7*	*0.45*	*0.2*	*0.8*	*0.5*	*0.1*	*0.7*	*0.4*	*0.2*	*0.7*	*0.45*	*0.2*	*0.4*	*0.3*
2	*0.2*	*0.7*	*0.45*	*0.3*	*0.6*	*0.5*	*0.2*	*0.3*	*0.3*	*0.1*	*0.7*	*0.4*	*0.2*	*0.6*	*0.4*
3	*0.2*	*0.6*	*0.4*	*0.2*	*0.6*	*0.4*	*0.2*	*0.7*	*0.5*	*0.1*	*0.7*	*0.4*	*0.3*	*0.6*	*0.45*
4	*0.1*	*0.7*	*0.4*	*0.3*	*0.7*	*0.5*	*0.3*	*0.7*	*0.5*	*0.1*	*0.7*	*0.4*	*0.3*	*0.3*	*0.3*
5	*0.2*	*0.8*	*0.5*	*0.3*	*0.6*	*0.5*	*0.1*	*0.5*	*0.3*	*0.2*	*0.6*	*0.4*	*0.2*	*0.6*	*0.4*
6	*0.3*	*0.7*	*0.5*	*0.1*	*0.6*	*0.4*	*0.1*	*0.5*	*0.3*	*0.2*	*0.6*	*0.4*	*0.5*	*0.8*	*0.65*
7	*0.3*	*0.6*	*0.45*	*0.2*	*0.8*	*0.5*	*0.2*	*0.6*	*0.4*	*0.2*	*0.7*	*0.45*	*0.2*	*0.7*	*0.45*
8	*0.2*	*0.5*	*0.35*	*0.5*	*0.4*	*0.5*	*0.2*	*0.6*	*0.4*	*0.1*	*0.7*	*0.4*	*0.4*	*0.7*	*0.55*
9	*0.3*	*0.5*	*0.4*	*0.3*	*0.6*	*0.5*	*0.2*	*0.5*	*0.4*	*0.2*	*0.6*	*0.4*	*0.4*	*0.6*	*0.5*
10	*0.3*	*0.8*	*0.55*	*0.5*	*0.8*	*0.7*	*0.2*	*0.5*	*0.4*	*0.1*	*0.6*	*0.35*	*0.6*	*0.7*	*0.65*
11	*0.3*	*0.7*	*0.5*	*0.5*	*0.7*	*0.6*	*0.1*	*0.8*	*0.5*	*0.2*	*0.3*	*0.25*	*0.3*	*0.5*	*0.4*
12	*0.1*	*0.6*	*0.35*	*0.4*	*0.7*	*0.6*	*0.2*	*0.7*	*0.5*	*0.2*	*0.5*	*0.35*	*0.4*	*0.4*	*0.4*
13	*0.1*	*0.5*	*0.3*	*0.3*	*0.3*	*0.3*	*0.2*	*0.7*	*0.5*	*0.3*	*0.7*	*0.5*	*0.4*	*0.6*	*0.5*
14	*0.2*	*0.5*	*0.35*	*0.2*	*0.3*	*0.3*	*0.1*	*0.7*	*0.4*	*0.2*	*0.7*	*0.45*	*0.3*	*0.7*	*0.5*
15	*0.2*	*0.7*	*0.45*	*0.1*	*0.7*	*0.4*	*0.2*	*0.8*	*0.5*	*0.1*	*0.3*	*0.2*	*0.5*	*0.7*	*0.6*
16	*0.1*	*0.8*	*0.45*	*0.3*	*0.6*	*0.5*	*0.2*	*0.7*	*0.5*	*0.2*	*0.4*	*0.3*	*0.3*	*0.6*	*0.45*
17	*0.2*	*0.8*	*0.5*	*0.2*	*0.7*	*0.5*	*0.1*	*0.7*	*0.4*	*0.2*	*0.3*	*0.25*	*0.1*	*0.3*	*0.2*
18	*0.1*	*0.3*	*0.2*	*0.1*	*0.5*	*0.3*	*0.1*	*0.6*	*0.4*	*0.3*	*0.7*	*0.5*	*0.3*	*0.3*	*0.3*
19	*0.1*	*0.4*	*0.25*	*0.5*	*0.5*	*0.5*	*0.2*	*0.7*	*0.5*	*0.2*	*0.3*	*0.25*	*0.4*	*0.6*	*0.5*
20	*0.3*	*0.8*	*0.55*	*0.3*	*0.8*	*0.6*	*0.1*	*0.4*	*0.3*	*0.2*	*0.5*	*0.35*	*0.3*	*0.2*	*0.25*

Stellenbosch University https://scholar.sun.ac.za

Table C-4 Results of grain shape analysis for crushed and un-tested waste rock (continued)

Size Fraction:	1,40-1,18 mm			1,18-1,00 mm			1,00-0,85 mm			0,85 - 0,60 mm			0.6-0.425 mm		
Particle	**R**	**S**	**ρ**	**R**	**S**	**ρ**	**R**	**S**	**ρ**	**R**	**S**	**ρ**	**R**	**S**	**ρ**
1	*0.5*	*0.7*	*0.6*	*0.1*	*0.9*	*0.5*	*0.2*	*0.7*	*0.45*	*0.3*	*0.5*	*0.4*	*0.5*	*0.8*	*0.65*
2	*0.3*	*0.5*	*0.4*	*0.2*	*0.4*	*0.3*	*0.3*	*0.5*	*0.4*	*0.2*	*0.7*	*0.45*	*0.3*	*0.5*	*0.4*
3	*0.3*	*0.5*	*0.4*	*0.1*	*0.3*	*0.2*	*0.3*	*0.6*	*0.45*	*0.6*	*0.6*	*0.6*	*0.5*	*0.3*	*0.4*
4	*0.2*	*0.7*	*0.45*	*0.1*	*0.7*	*0.4*	*0.2*	*0.8*	*0.5*	*0.4*	*0.6*	*0.5*	*0.4*	*0.8*	*0.6*
5	*0.7*	*0.6*	*0.65*	*0.1*	*0.7*	*0.4*	*0.4*	*0.3*	*0.35*	*0.3*	*0.7*	*0.5*	*0.4*	*0.7*	*0.55*
6	*0.3*	*0.6*	*0.45*	*0.3*	*0.8*	*0.55*	*0.3*	*0.3*	*0.3*	*0.2*	*0.6*	*0.4*	*0.4*	*0.7*	*0.55*
7	*0.4*	*0.7*	*0.55*	*0.1*	*0.8*	*0.45*	*0.2*	*0.5*	*0.35*	*0.3*	*0.5*	*0.4*	*0.2*	*0.5*	*0.35*
8	*0.3*	*0.6*	*0.45*	*0.1*	*0.7*	*0.4*	*0.3*	*0.5*	*0.4*	*0.3*	*0.8*	*0.55*	*0.4*	*0.7*	*0.55*
9	*0.3*	*0.6*	*0.45*	*0.2*	*0.3*	*0.25*	*0.2*	*0.7*	*0.45*	*0.2*	*0.3*	*0.25*	*0.5*	*0.8*	*0.65*
10	*0.4*	*0.7*	*0.55*	*0.2*	*0.7*	*0.45*	*0.5*	*0.7*	*0.6*	*0.3*	*0.7*	*0.5*	*0.5*	*0.5*	*0.5*
11	*0.2*	*0.6*	*0.4*	*0.2*	*0.7*	*0.45*	*0.5*	*0.8*	*0.65*	*0.2*	*0.7*	*0.45*	*0.5*	*0.5*	*0.5*
12	*0.3*	*0.7*	*0.5*	*0.1*	*0.3*	*0.2*	*0.3*	*0.8*	*0.55*	*0.5*	*0.3*	*0.4*	*0.2*	*0.3*	*0.25*
13	*0.1*	*0.6*	*0.35*	*0.3*	*0.6*	*0.45*	*0.2*	*0.6*	*0.4*	*0.2*	*0.3*	*0.25*	*0.5*	*0.7*	*0.6*
14	*0.3*	*0.8*	*0.55*	*0.1*	*0.6*	*0.35*	*0.3*	*0.8*	*0.55*	*0.3*	*0.6*	*0.45*	*0.4*	*0.7*	*0.55*
15	*0.4*	*0.6*	*0.5*	*0.3*	*0.3*	*0.3*	*0.3*	*0.7*	*0.5*	*0.5*	*0.8*	*0.65*	*0.5*	*0.4*	*0.45*
16	*0.4*	*0.7*	*0.55*	*0.3*	*0.9*	*0.6*	*0.5*	*0.5*	*0.5*	*0.3*	*0.3*	*0.3*	*0.5*	*0.5*	*0.5*
17	*0.2*	*0.7*	*0.45*	*0.5*	*0.4*	*0.45*	*0.4*	*0.5*	*0.45*	*0.4*	*0.4*	*0.4*	*0.5*	*0.5*	*0.5*
18	*0.4*	*0.7*	*0.55*	*0.3*	*0.7*	*0.5*	*0.2*	*0.5*	*0.35*	*0.7*	*0.6*	*0.65*	*0.3*	*0.3*	*0.3*
19	*0.2*	*0.7*	*0.45*	*0.1*	*0.7*	*0.4*	*0.3*	*0.7*	*0.5*	*0.7*	*0.8*	*0.75*	*0.7*	*0.8*	*0.75*
20	0.2	0.8	0.5	0.3	0.7	0.5	0.3	0.7	0.5	0.3	0.6	0.45	0.8	0.8	0.8
21	-	-	-	-	-	-	0.2	0.7	0.45	0.2	0.5	0.35	0.8	0.8	0.8
22	-	-	-	-	-	-	0.3	0.3	0.3	0.3	0.7	0.5	0.5	0.7	0.6
23	-	-	-	-	-	-	-	-	-	0.6	0.6	0.6	0.5	0.7	0.6
24	-	-	-	-	-	-	-	-	-	0.5	0.6	0.55	-	-	-

Stellenbosch University https://scholar.sun.ac.za

C.2.2 Pre-Tested Waste Rock Images

Below, the figures corresponding to the results presented in Section C.2.1 can be found. For each of the images, the scale increment represents 500 µm (Figure C-2).

Stellenbosch University https://scholar.sun.ac.za

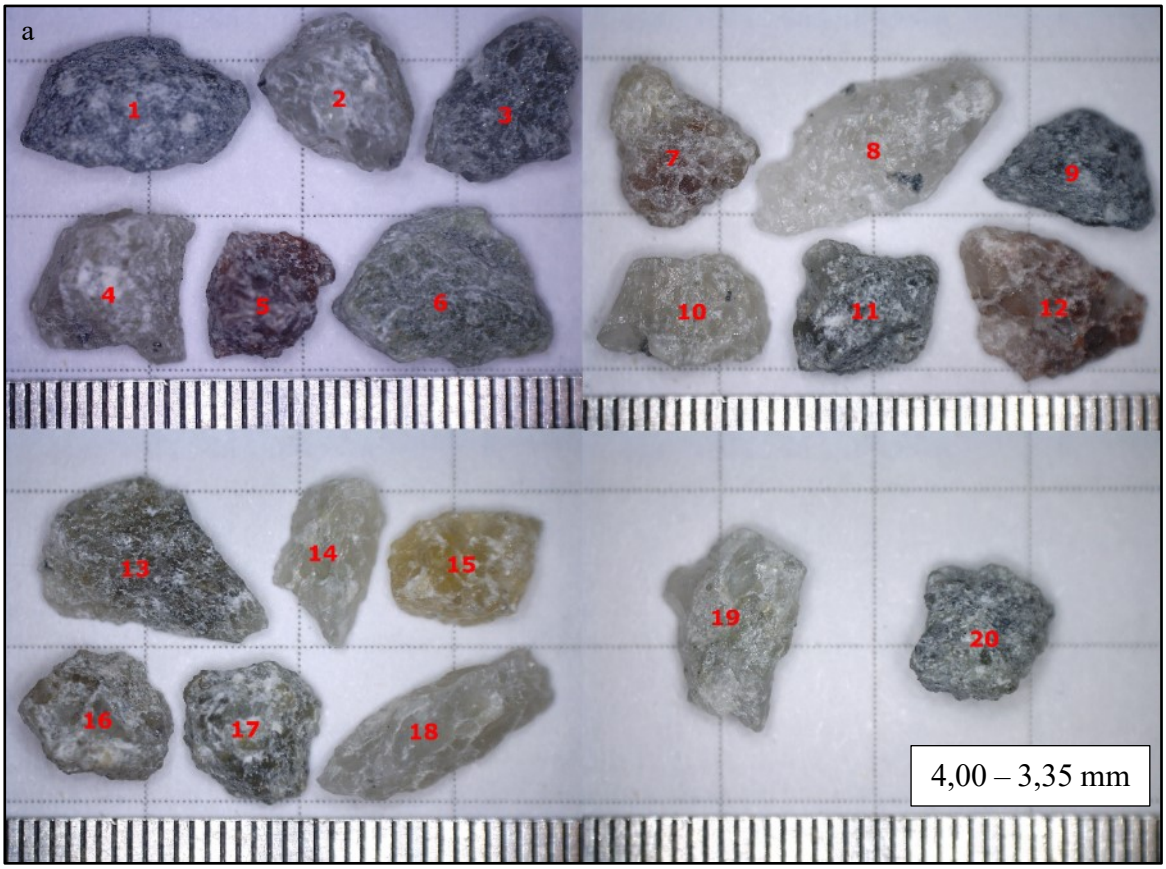

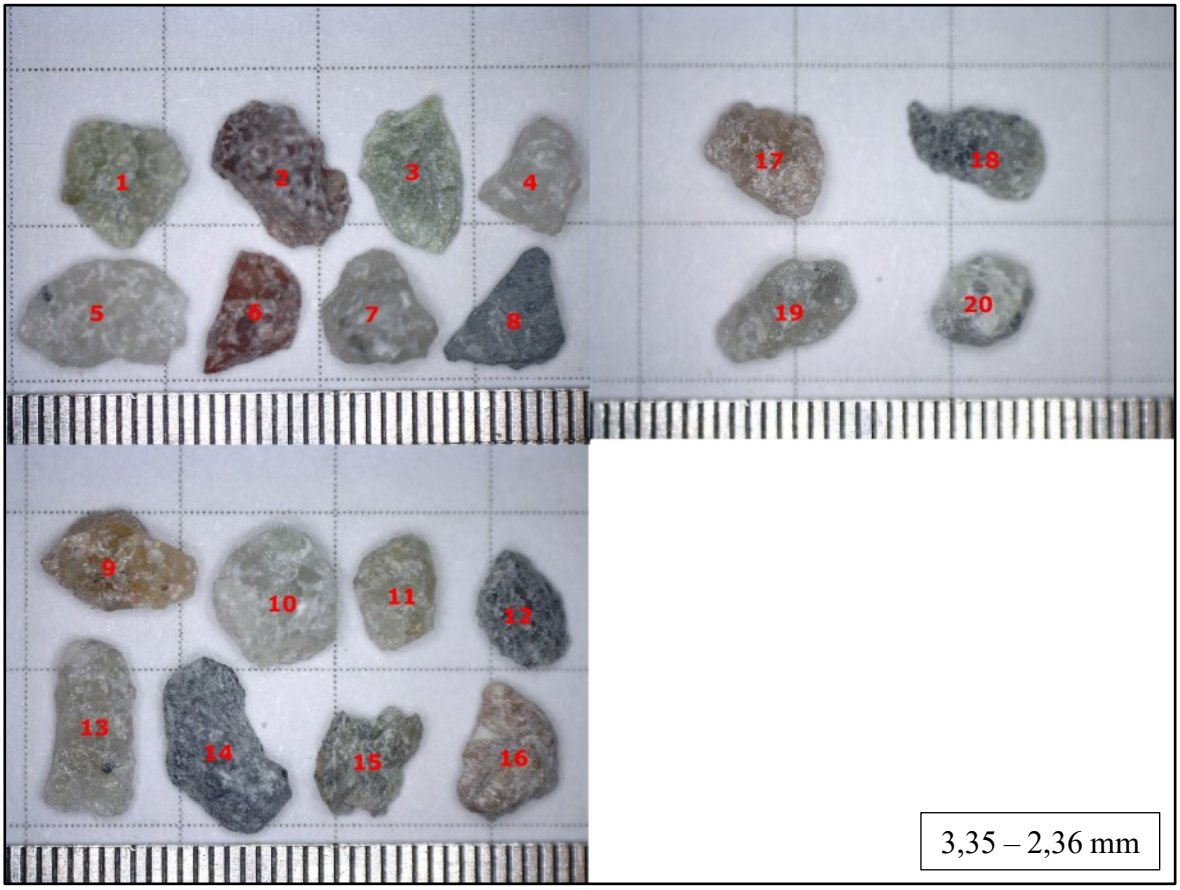

Stellenbosch University https://scholar.sun.ac.za

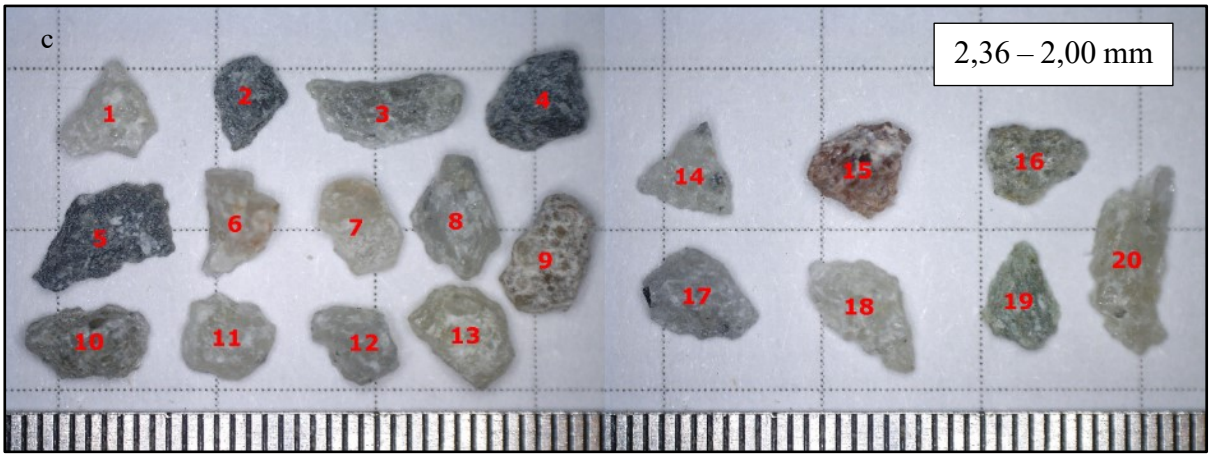

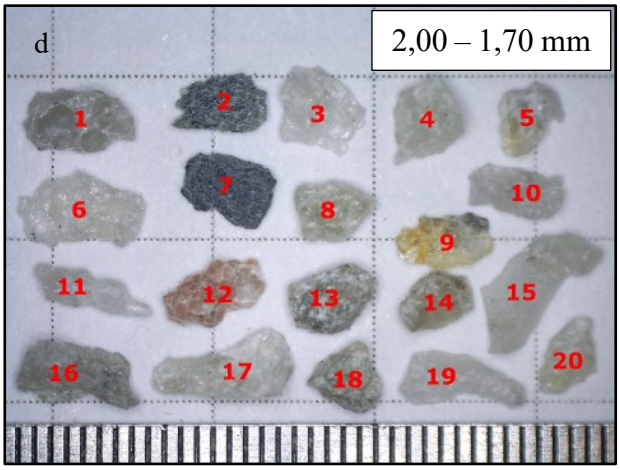

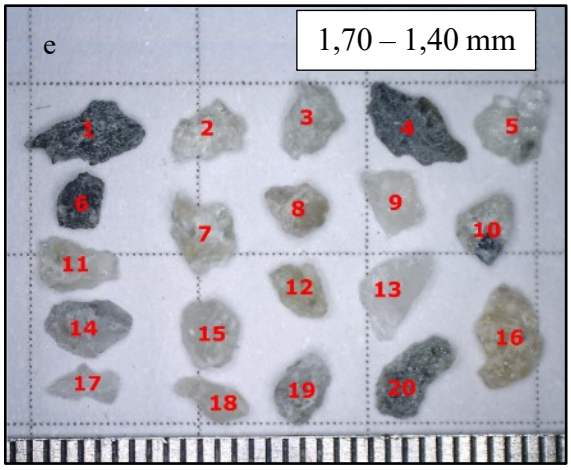

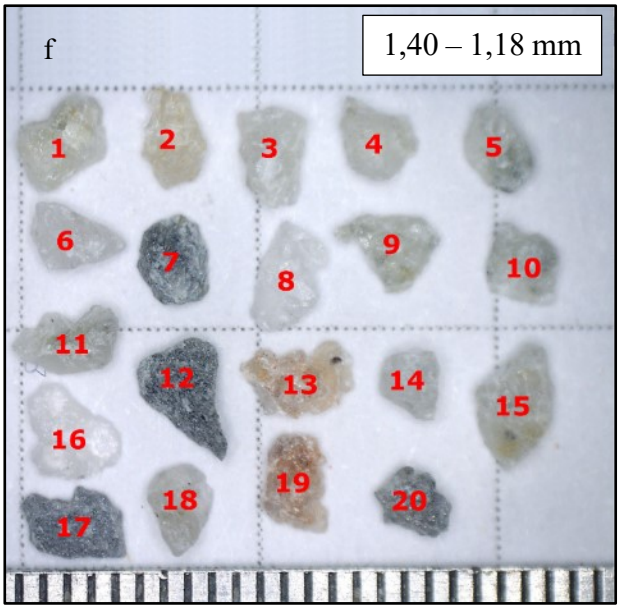

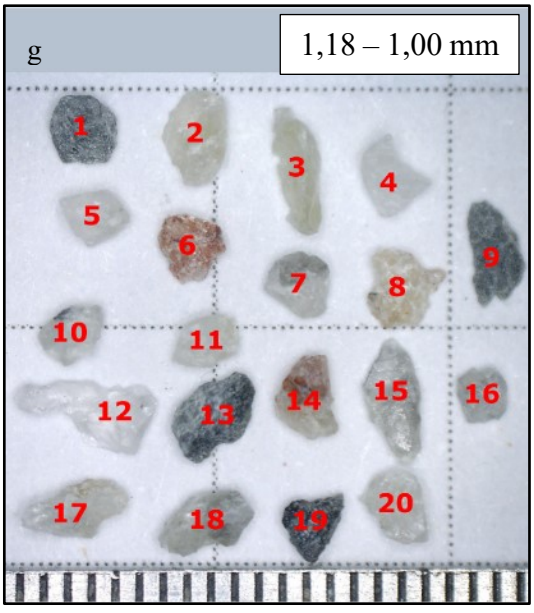

Stellenbosch University https://scholar.sun.ac.za

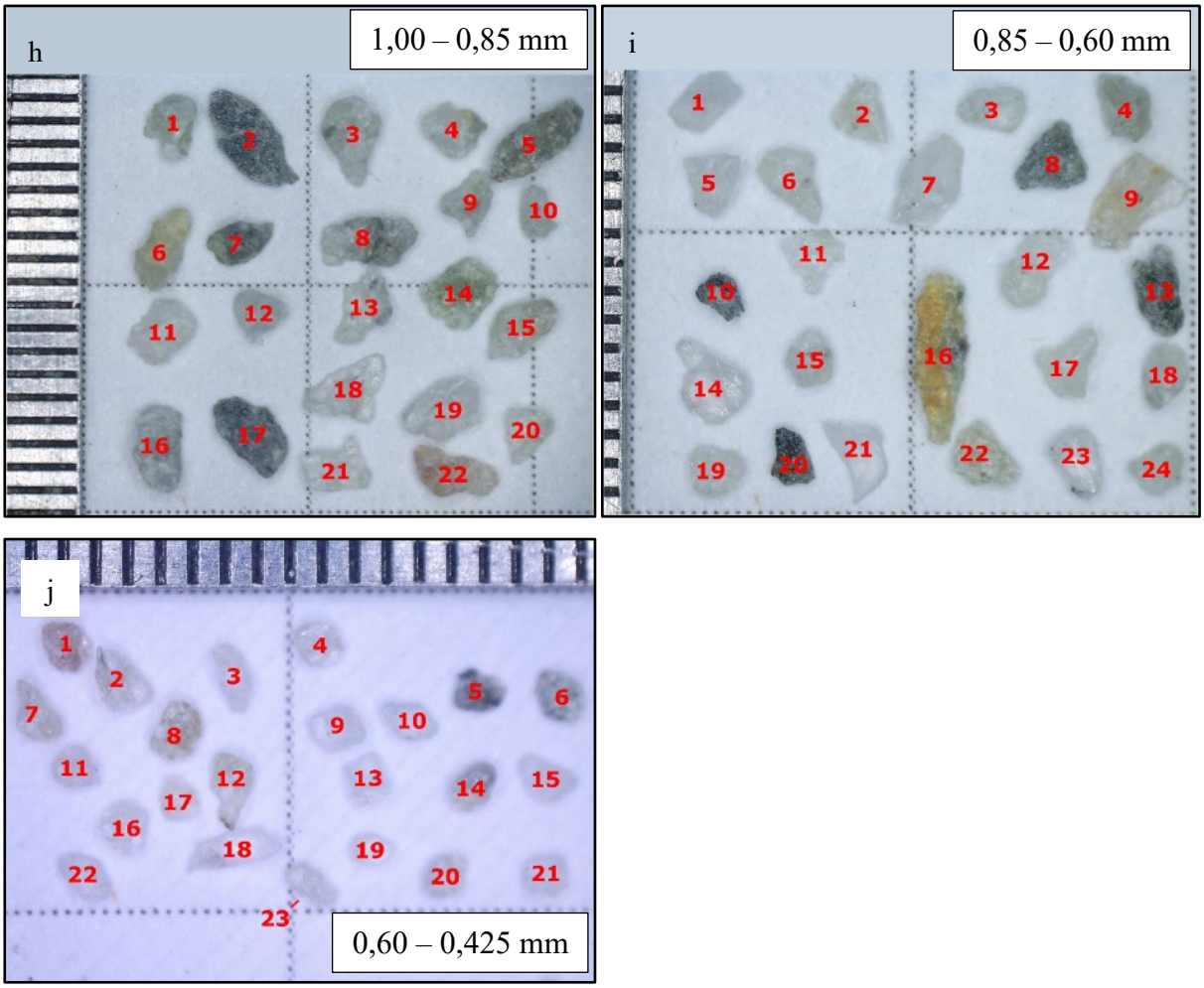

Figure C-2. Images of crushed and untested waste rock, assessed for grain shape parameters, particle diameters: a) 4,0 – 3,35 mm; b) 3,35 – 2,36 mm; c) 2,36 – 2,0 0mm; d) 2,00 – 1,70 mm; e) 1,70 – 1,40 mm; f) 1,40 – 1,18 mm; g) 1,18 – 1,00 mm; h) 1,00 – 0,85 mm; i) 0,85 – 0,60 mm, and; j) 0,60 – 0,425 mm

Stellenbosch University https://scholar.sun.ac.za

C.3 Grain Shape Analysis of Post-Tested Waste Rock

C.3.1 Post-Tested Poorly-Graded Waste Rock Results

Stellenbosch University https://scholar.sun.ac.za

Table C-5 Results of the Post-Tested Poorly-Graded test specimens

Shear Mould:	20x12.5_150kPa				20x18.5_150kPa				20x24.5_150kPa				60x12.5_150kPa				60x18.5_150kPa			
Particle No.	**R**	**S**	**ρ**	**Comment**	**R**	**S**	**ρ**	**Comment**	**R**	**S**	**ρ**	**Comment**	**R**	**S**	**ρ**	**Comment**	**R**	**S**	**ρ**	**Comment**
1	*0.2*	*0.3*	*0.25*	-	*0.3*	*0.6*	*0.5*	-	*0.3*	*0.5*	*0.4*	-	*0.5*	*0.7*	*0.6*	-	*0.2*	*0.7*	*0.5*	-
2	*0.3*	*0.7*	*0.5*	-	*0.3*	*0.8*	*0.6*	-	*0.3*	*0.7*	*0.5*	-	*0.2*	*0.5*	*0.35*	-	*0.3*	*0.5*	*0.4*	-
3	*0.3*	*0.1*	*0.2*	-	*0.3*	*0.3*	*0.3*	-	*0.2*	*0.6*	*0.4*	-	*0.3*	*0.7*	*0.5*	-	*0.3*	*0.6*	*0.5*	-
4	*0.8*	*0.7*	*0.75*	-	*0.3*	*0.7*	*0.5*	*Too small*	*0.6*	*0.7*	*0.65*	-	*0.5*	*0.5*	*0.5*	-	*0.2*	*0.7*	*0.5*	-
5	*0.5*	*0.3*	*0.4*	-	*0.3*	*0.6*	*0.5*	-	*0.2*	*0.6*	*0.4*	-	*0.3*	*0.5*	*0.4*	-	*0.3*	*0.5*	*0.4*	-
6	*0.4*	*0.7*	*0.55*	-	*0.3*	*0.5*	*0.4*	-	*0.2*	*0.4*	*0.3*	-	*0.3*	*0.5*	*0.4*	-	*0.6*	*0.7*	*0.7*	-
7	*0.3*	*0.6*	*0.45*	-	*0.3*	*0.5*	*0.4*	-	*0.3*	*0.4*	*0.35*	-	*0.2*	*0.5*	*0.35*	-	*0.2*	*0.7*	*0.5*	-
8	*0.6*	*0.7*	*0.65*	-	*0.5*	*0.7*	*0.6*	-	*0.2*	*0.5*	*0.35*	-	*0.3*	*0.5*	*0.4*	-	*0.3*	*0.7*	*0.5*	-
9	*0.6*	*0.5*	*0.55*	-	*0.3*	*0.5*	*0.4*	-	*0.2*	*0.6*	*0.4*	-	*0.3*	*0.5*	*0.4*	-	*0.2*	*0.8*	*0.5*	-
10	*0.6*	*0.6*	*0.6*	-	*0.2*	*0.6*	*0.4*	-	*0.1*	*0.3*	*0.2*	*Too small*	*0.1*	*0.3*	*0.2*	-	*0.3*	*0.3*	*0.3*	-
11	*0.5*	*0.5*	*0.5*	-	*0.2*	*0.3*	*0.3*	-	*0.2*	*0.3*	*0.25*	-	*0.7*	*0.8*	*0.75*	-	-	-	-	-
12	*0.3*	*0.5*	*0.4*	-	-	-	-	-	*0.2*	*0.7*	*0.45*	-	*0.5*	*0.3*	*0.4*	-	-	-	-	-
13	*0.6*	*0.7*	*0.65*	-	-	-	-	-	-	-	-	-	*0.5*	*0.6*	*0.55*	-	-	-	-	-
14	*0.3*	*0.7*	*0.5*	-	-	-	-	-	-	-	-	-	*0.1*	*0.7*	*0.4*	-	-	-	-	-
15	*0.3*	*0.5*	*0.4*	-	-	-	-	-	-	-	-	-	*0.5*	*0.7*	*0.6*	-	-	-	-	-
16	*0.6*	*0.6*	*0.6*	-	-	-	-	-	-	-	-	-	*0.3*	*0.3*	*0.3*	*Too small*	-	-	-	-
17	*0.5*	*0.7*	*0.6*	-	-	-	-	-	-	-	-	-	-	-	-	-	-	-	-	-

Stellenbosch University https://scholar.sun.ac.za

Table C-6 Results of the Post-Tested Poorly-Graded test specimens (continued)

Shear Mould:	60x24.5_150kPa				100x12.5_150kPa				100x18.5_150kPa				100x18.5_150kPa			
Particle No.	R	S	ρ	Comment	R	S	ρ	Comment	R	S	ρ	Comment	R	S	ρ	Comment
1	*0.3*	*0.7*	*0.5*	-	*0.4*	*0.7*	*0.55*	-	*0.2*	*0.5*	*0.35*	-	*0.3*	*0.5*	*0.4*	-
2	*0.2*	*0.7*	*0.5*	-	*0.3*	*0.8*	*0.55*	-	*0.2*	*0.4*	*0.3*	-	*0.2*	*0.4*	*0.3*	-
3	*0.3*	*0.5*	*0.4*	-	*0.3*	*0.5*	*0.4*	-	*0.3*	*0.4*	*0.35*	-	*0.2*	*0.7*	*0.5*	-
4	*0.4*	*0.3*	*0.4*	-	*0.2*	*0.4*	*0.3*	-	*0.1*	*0.7*	*0.4*	-	*0.1*	*0.7*	*0.4*	-
5	*0.2*	*0.8*	*0.5*	-	*0.2*	*0.6*	*0.4*	-	*0.1*	*0.3*	*0.2*	-	*0.1*	*0.6*	*0.4*	-
6	*0.3*	*0.5*	*0.4*	-	*0.2*	*0.6*	*0.4*	-	*0.2*	*0.5*	*0.35*	-	*0.2*	*0.5*	*0.4*	-
7	*0.2*	*0.7*	*0.5*	-	*0.3*	*0.5*	*0.4*	-	*0.6*	*0.8*	*0.7*	-	*0.2*	*0.5*	*0.4*	-
8	*0.3*	*0.5*	*0.4*	-	*0.1*	*0.3*	*0.2*	-	*0.2*	*0.6*	*0.4*	-	*0.2*	*0.7*	*0.5*	-
9	*0.5*	*0.8*	*0.7*	-	*0.1*	*0.3*	*0.2*	-	*0.3*	*0.6*	*0.45*	-	*0.3*	*0.7*	*0.5*	-
10	*0.3*	*0.8*	*0.6*	-	*0.2*	*0.4*	*0.3*	-	*0.1*	*0.6*	*0.35*	-	*0.2*	*0.8*	*0.5*	-
11	*0.4*	*0.8*	*0.6*	-	-	-	-	-	-	-	-	-	-	-	-	-
12	*0.1*	*0.4*	*0.3*	*Too small*	-	-	-	-	-	-	-	-	-	-	-	-

Stellenbosch University https://scholar.sun.ac.za

C.3.2 Post-Tested Waste Rock Images

Below, the figures corresponding to the results presented in Section C.3.1 can be found. For each of the images, as before, each scale increment represents 500 µm (Figure C-3).

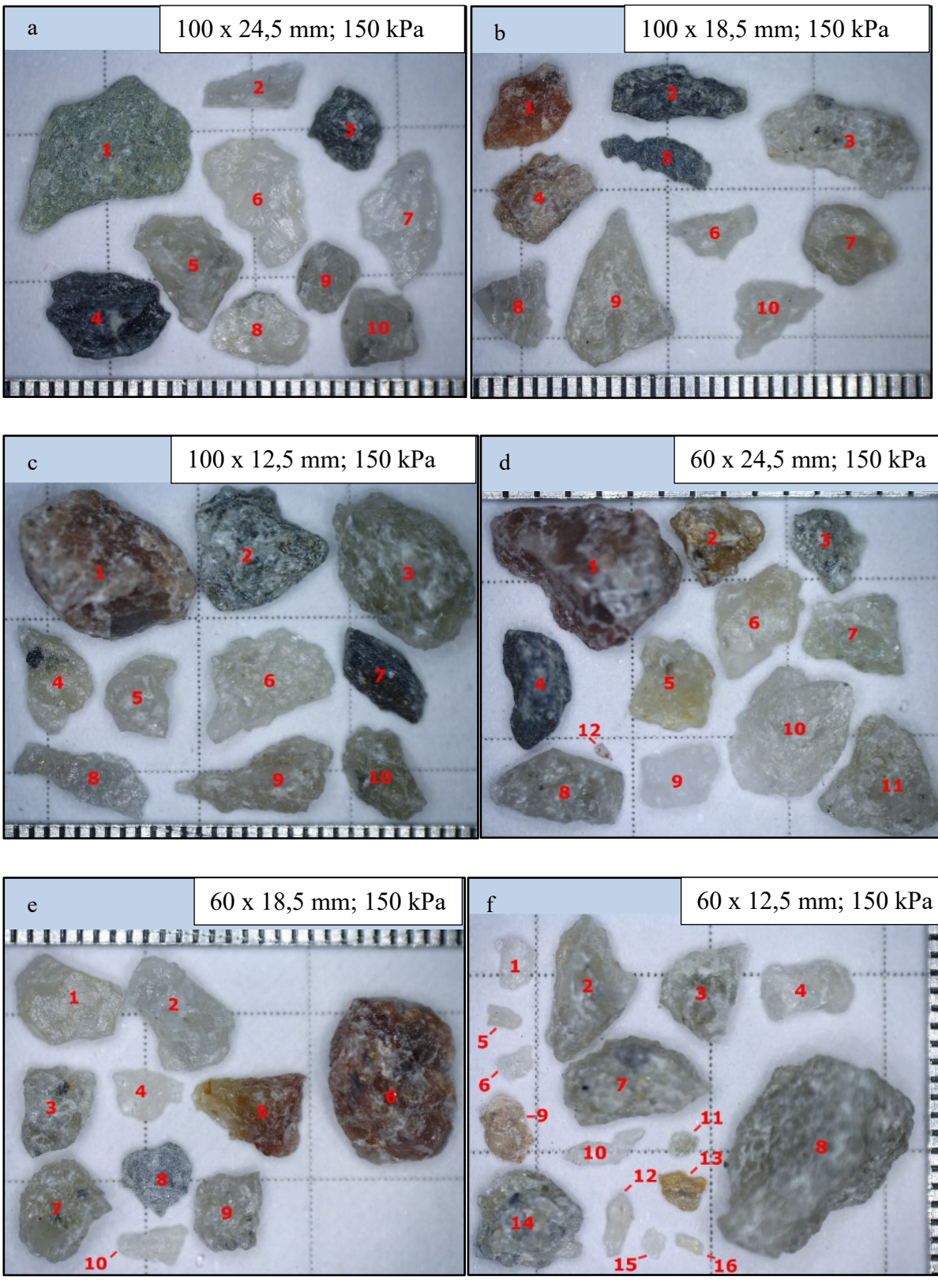

Stellenbosch University https://scholar.sun.ac.za

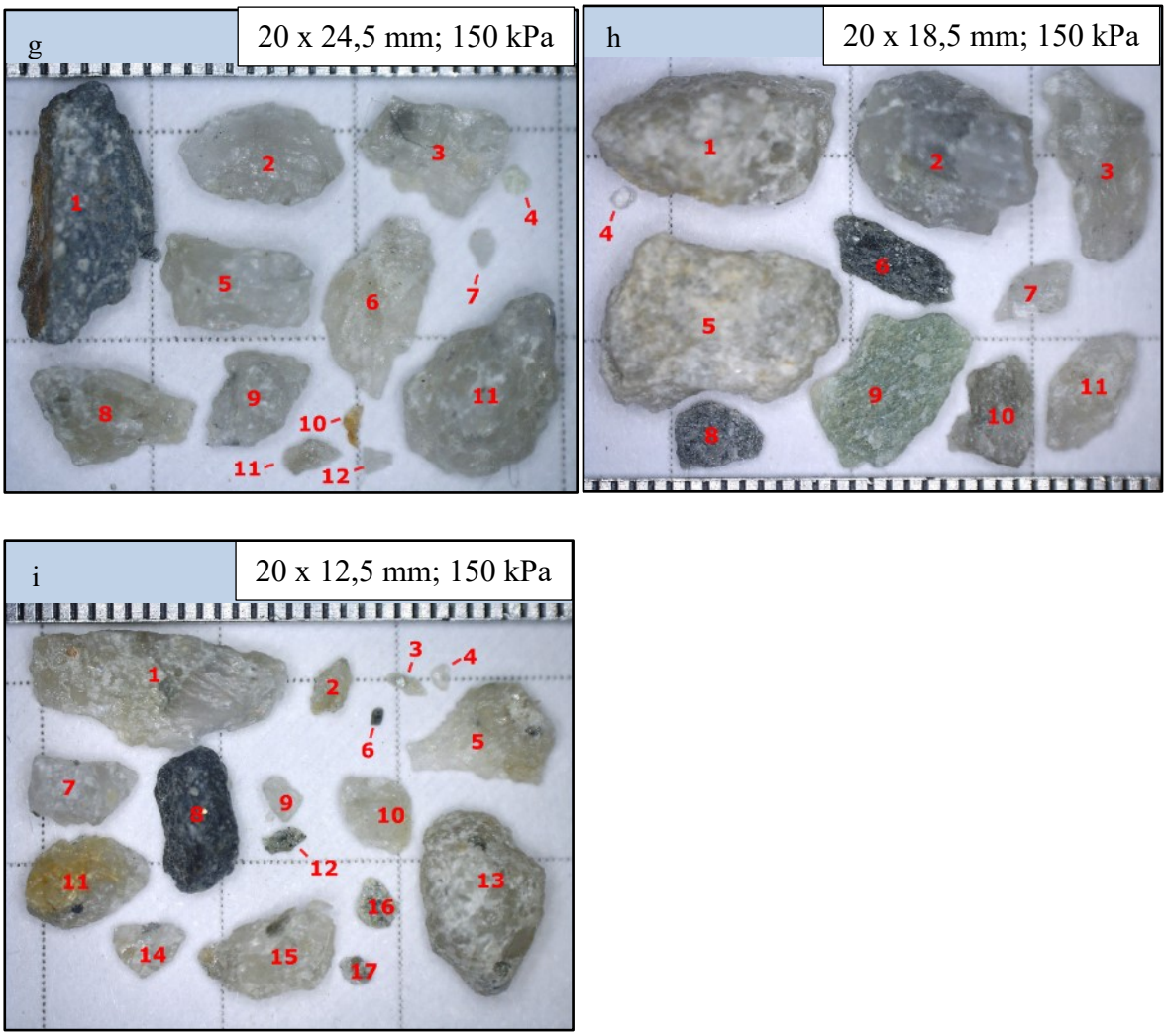

Figure C-3. Images of crushed and tested [at normal stress of 150 kPa] poorly graded waste rock specimen particles, assessed for grain shape parameters, including shear mould dimension: a) 100 x 24,5 mm; b) 100 x 18,5 mm; c) 100 x 18,5 mm; d) 60 x 24,5 mm; e) 60 x 18,5 mm; f) 60 x 12,5 mm; g) 20 x 24,5 mm; h) 20 x 18,5 mm, and i) 20 x 12,5 mm

Stellenbosch University https://scholar.sun.ac.za

C.3.4 Post-Tested Well-Graded Waste Rock Results

Stellenbosch University https://scholar.sun.ac.za

Table C-7 Grain shape analysis results of the poorly-graded specimens

Shear Mould:	20x12.5_150kPa				20x18.5_150kPa				20x24.5_150kPa				60x12.5_150kPa				60x18.5_150kPa			
Particle	**R**	**S**	**ρ**	**Comment**	**R**	**S**	**ρ**	**Comment**	**R**	**S**	**ρ**	**Comment**	**R**	**S**	**ρ**	**Comment**	**R**	**S**	**ρ**	**Comment**
1	*0.2*	*0.7*	*0.45*	-	*0.3*	*0.7*	*0.5*	-	*0.2*	*0.7*	*0.45*	-	*0.3*	*0.7*	*0.5*	-	*0.5*	*0.3*	*0.4*	-
2	*0.1*	*0.6*	*0.35*	-	*0.4*	*0.8*	*0.6*	-	*0.3*	*0.7*	*0.5*	-	*0.2*	*0.6*	*0.4*	-	*0.3*	*0.8*	*0.55*	-
3	*0.1*	*0.5*	*0.3*	-	*0.2*	*0.7*	*0.45*	-	*0.3*	*0.5*	*0.4*	-	*0.4*	*0.8*	*0.6*	-	*0.1*	*0.7*	*0.4*	-
4	*0.3*	*0.7*	*0.5*	-	*0.2*	*0.3*	*0.25*	-	*0.3*	*0.5*	*0.4*	-	*0.2*	*0.7*	*0.45*	-	*0.1*	*0.7*	*0.4*	-
5	*0.2*	*0.2*	*0.2*	-	*0.1*	*0.3*	*0.2*	-	*0.3*	*0.6*	*0.45*	-	*0.3*	*0.7*	*0.5*	-	*0.1*	*0.3*	*0.2*	-
6	*0.4*	*0.7*	*0.55*	-	*0.4*	*0.8*	*0.6*	-	*0.3*	*0.4*	*0.35*	-	*0.3*	*0.7*	*0.5*	-	*0.1*	*0.3*	*0.2*	-
7	*0.3*	*0.7*	*0.5*	-	*0.3*	*0.8*	*0.55*	-	*0.6*	*0.8*	*0.7*	-	*0.2*	*0.6*	*0.4*	-	*0.1*	*0.3*	*0.2*	-
8	*0.2*	*0.7*	*0.45*	-	*0.2*	*0.8*	*0.5*	-	*0.2*	*0.8*	*0.5*	-	*0.3*	*0.5*	*0.4*	-	*0.1*	*0.5*	*0.3*	-
9	*0.4*	*0.7*	*0.55*	-	*0.3*	*0.6*	*0.45*	-	*0.1*	*0.3*	*0.2*	-	*0.2*	*0.5*	*0.35*	-	*0.1*	*0.3*	*0.2*	-
10	*0.3*	*0.5*	*0.4*	-	*0.2*	*0.8*	*0.5*	-	*0.2*	*0.7*	*0.45*	-	*0.2*	*0.6*	*0.4*	-	*0.1*	*0.8*	*0.45*	-
11	*0.2*	*0.6*	*0.4*	-	*0.1*	*0.3*	*0.2*	-	*0.1*	*0.7*	*0.4*	-	*0.4*	*0.7*	*0.55*	-	*0.1*	*0.7*	*0.4*	-
12	*0.1*	*0.6*	*0.35*	-	*0.7*	*0.8*	*0.75*	-	*0.3*	*0.4*	*0.35*	-	*0.3*	*0.7*	*0.5*	-	*0.3*	*0.6*	*0.45*	-
13	*0.1*	*0.3*	*0.2*	-	*0.3*	*0.6*	*0.45*	-	*0.2*	*0.7*	*0.45*	-	*0.2*	*0.5*	*0.35*	-	*0.2*	*0.7*	*0.45*	-
14	*0.7*	*0.9*	*0.8*	-	*0.2*	*0.8*	*0.5*	-	*0.3*	*0.8*	*0.55*	-	*0.4*	*0.5*	*0.45*	-	*0.1*	*0.6*	*0.35*	-
15	*0.2*	*0.4*	*0.3*	-	*0.3*	*0.8*	*0.55*	-	*0.2*	*0.3*	*0.25*	-	0.2	*0.5*	*0.35*	-	*0.1*	*0.8*	*0.45*	*Too small*
16	*0.2*	*0.8*	*0.5*	-	*0.2*	*0.5*	*0.35*	-	*0.2*	*0.3*	*0.25*	-	*0.1*	*0.7*	*0.4*	-	*0.3*	*0.5*	*0.4*	*Too small*
17	*0.2*	*0.8*	*0.5*	-	*0.5*	*0.3*	*0.4*	-	*0.1*	*0.6*	*0.35*	-	*0.1*	*0.8*	*0.45*	-	*0.5*	*0.3*	*0.4*	*Too small*
18	*0.3*	*0.7*	*0.5*	-	*0.4*	*0.5*	*0.45*	-	*0.5*	*0.5*	*0.5*	*Too Small*	*0.2*	*0.7*	*0.45*	-	*0.7*	*0.7*	*0.7*	*Too small*
19	*0.1*	*0.3*	*0.2*	-	*0.1*	*0.3*	*0.2*	-	-	-	-	-	0.1	*0.7*	*0.4*	*Too small*	*0.1*	*0.3*	*0.2*	*Too small*
20	*0.1*	*0.8*	*0.45*	-	*0.5*	*0.6*	*0.55*	-	-	-	-	-	*0.1*	*0.5*	*0.3*	*Too small*	*0.3*	*0.8*	*0.55*	*Too small*
21	*0.7*	*0.8*	*0.75*	-	*0.5*	*0.7*	*0.6*	-	-	-	-	-	*0.1*	*0.3*	*0.2*	*Too small*	*0.3*	*0.8*	*0.55*	*Too small*
22	*0.8*	*0.8*	*0.8*	*Too small*	*0.3*	*0.4*	*0.35*	-	-	-	-	-	*0.2*	*0.8*	*0.5*	*Too small*	*0.2*	*0.7*	*0.45*	*Too small*
23	*0.5*	*0.5*	*0.5*	*Too small*	*0.2*	*0.4*	*0.3*	-	-	-	-	-	*0.1*	*0.8*	*0.45*	*Too small*	-	-	-	-
24	-	-	-	-	*0.2*	*0.7*	*0.45*	*Too small*	-	-	-	-	*0.2*	*0.8*	*0.5*	*Too small*	-	-	-	-
25	-	-	-	-	*0.2*	*0.7*	*0.45*	*Too small*	-	-	-	-	*0.1*	*0.8*	*0.45*	*Too small*	-	-	-	-
26	-	-	-	-	*0.1*	*0.9*	*0.5*	*Too small*	-	-	-	-	-	-	-	-	-	-	-	-
27	-	-	-	-	*0.4*	*0.8*	*0.6*	*Too small*	-	-	-	-	-	-	-	-	-	-	-	-

Stellenbosch University https://scholar.sun.ac.za

Table C-8 Grain shape analysis results of the poorly-graded specimens (continued)

Shear Mould:	60x24.5_150kPa				100x12.5_150kPa				100x18.5_150kPa				100x18.5_150kPa			
Particle	R	S	ρ	Comment	R	S	ρ	Comment	R	S	ρ	Comment	R	S	ρ	Comment
1	*0.2*	*0.7*	*0.5*	-	*0.3*	*0.4*	*0.35*	-	*0.3*	*0.7*	*0.5*	-	*0.3*	*0.7*	*0.5*	-
2	*0.3*	*0.6*	*0.5*	-	*0.3*	*0.4*	*0.35*	-	*0.2*	*0.8*	*0.5*	-	*0.4*	*0.7*	*0.6*	-
3	*0.2*	*0.5*	*0.4*	-	*0.2*	*0.5*	*0.35*	-	*0.1*	*0.7*	*0.4*	-	*0.2*	*0.7*	*0.5*	-
4	*0.1*	*0.5*	*0.3*	-	*0.1*	*0.7*	*0.4*	-	*0.2*	*0.9*	*0.55*	-	*0.1*	*0.6*	*0.4*	-
5	*0.3*	*0.3*	*0.3*	-	*0.3*	*0.8*	*0.55*	-	*0.4*	*0.3*	*0.35*	-	*0.1*	*0.6*	*0.4*	-
6	*0.5*	*0.7*	*0.6*	-	*0.3*	*0.7*	*0.5*	-	*0.1*	*0.7*	*0.4*	-	*0.6*	*0.8*	*0.7*	-
7	*0.5*	*0.7*	*0.6*	-	*0.1*	*0.5*	*0.3*	-	*0.1*	*0.8*	*0.45*	-	*0.6*	*0.8*	*0.7*	-
8	*0.3*	*0.6*	*0.5*	-	*0.2*	*0.5*	*0.35*	-	*0.2*	*0.7*	*0.45*	-	*0.7*	*0.8*	*0.8*	*Too small*
9	*0.2*	*0.7*	*0.5*	-	*0.1*	*0.5*	*0.3*	-	*0.3*	*0.7*	*0.5*	-	*0.7*	*0.7*	*0.7*	*Too small*
10	*0.2*	*0.7*	*0.5*	-	*0.3*	*0.6*	*0.45*	-	*0.2*	*0.8*	*0.5*	-	*0.7*	*0.6*	*0.7*	*Too small*
11	*0.2*	*0.7*	*0.5*	*Too small*	*0.3*	*0.7*	*0.5*	-	*0.3*	*0.7*	*0.5*	-	*0.5*	*0.7*	*0.6*	*Too small*
12	*0.4*	*0.7*	*0.6*	*Too small*	*0.2*	*0.5*	*0.35*	-	*0.5*	*0.7*	*0.6*	-	*0.4*	*0.7*	*0.6*	*Too small*
13	*0.2*	*0.3*	*0.3*	*Too small*	*0.3*	*0.5*	*0.4*	-	*0.2*	*0.8*	*0.5*	*Too small*	*0.7*	*0.8*	*0.8*	*Too small*
14	*0.7*	*0.9*	*0.8*	*Too small*	*0.5*	*0.8*	*0.65*	-	*0.6*	*0.8*	*0.7*	*Too small*	*0.7*	*0.7*	*0.7*	*Too small*
15	*0.1*	*0.9*	*0.5*	*Too small*	*0.1*	*0.4*	*0.25*	*Too small*	*0.6*	*0.8*	*0.7*	*Too small*	*0.1*	*0.3*	*0.2*	*Too small*
16	-	-	-	-	*0.1*	*0.6*	*0.35*	*Too small*	*0.5*	*0.7*	*0.6*	*Too small*	-	-	-	-
17	-	-	-	-	*0.6*	*0.6*	*0.6*	*Too small*	*0.3*	*0.4*	*0.35*	*Too small*	-	-	-	-
18	-	-	-	-	*0.2*	*0.6*	*0.4*	*Too small*	*0.6*	*0.8*	*0.7*	*Too small*	-	-	-	-
19	-	-	-	-	*0.6*	*0.8*	*0.7*	*Too small*	*0.5*	*0.8*	*0.65*	*Too small*	-	-	-	-
20	-	-	-	-	*0.2*	*0.7*	*0.45*	*Too small*	-	-	-	-	-	-	-	-
21	-	-	-	-	*0.3*	*0.5*	*0.4*	*Too small*	-	-	-	-	-	-	-	-

Stellenbosch University https://scholar.sun.ac.za

C.3.4 Post-Tested Waste Rock Images

Below, the figures corresponding to the results presented in Section C.3.1 can be found. For each of the images, as before, each scale increment represents 500 µm (Figure C-4).

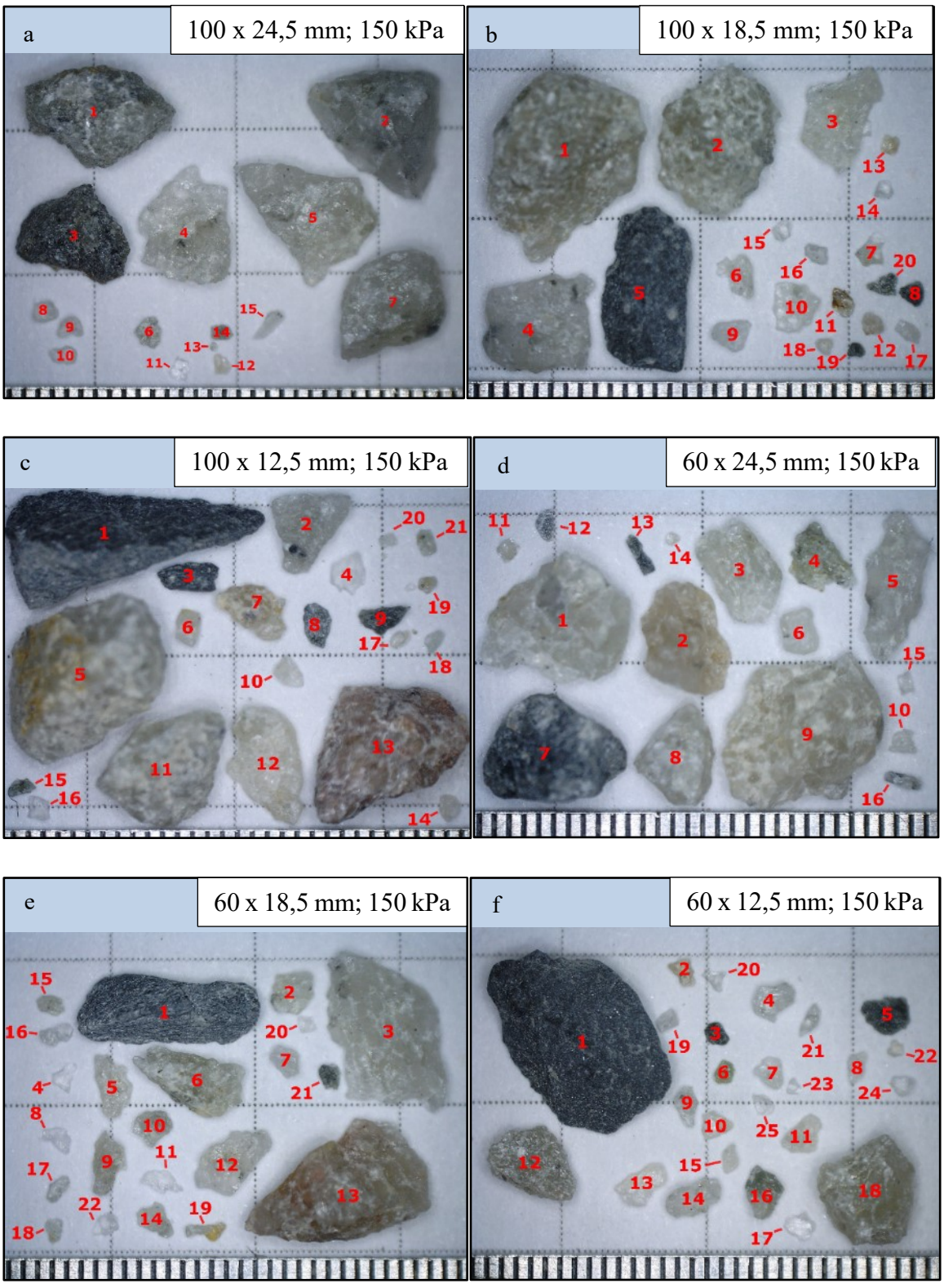

Stellenbosch University https://scholar.sun.ac.za

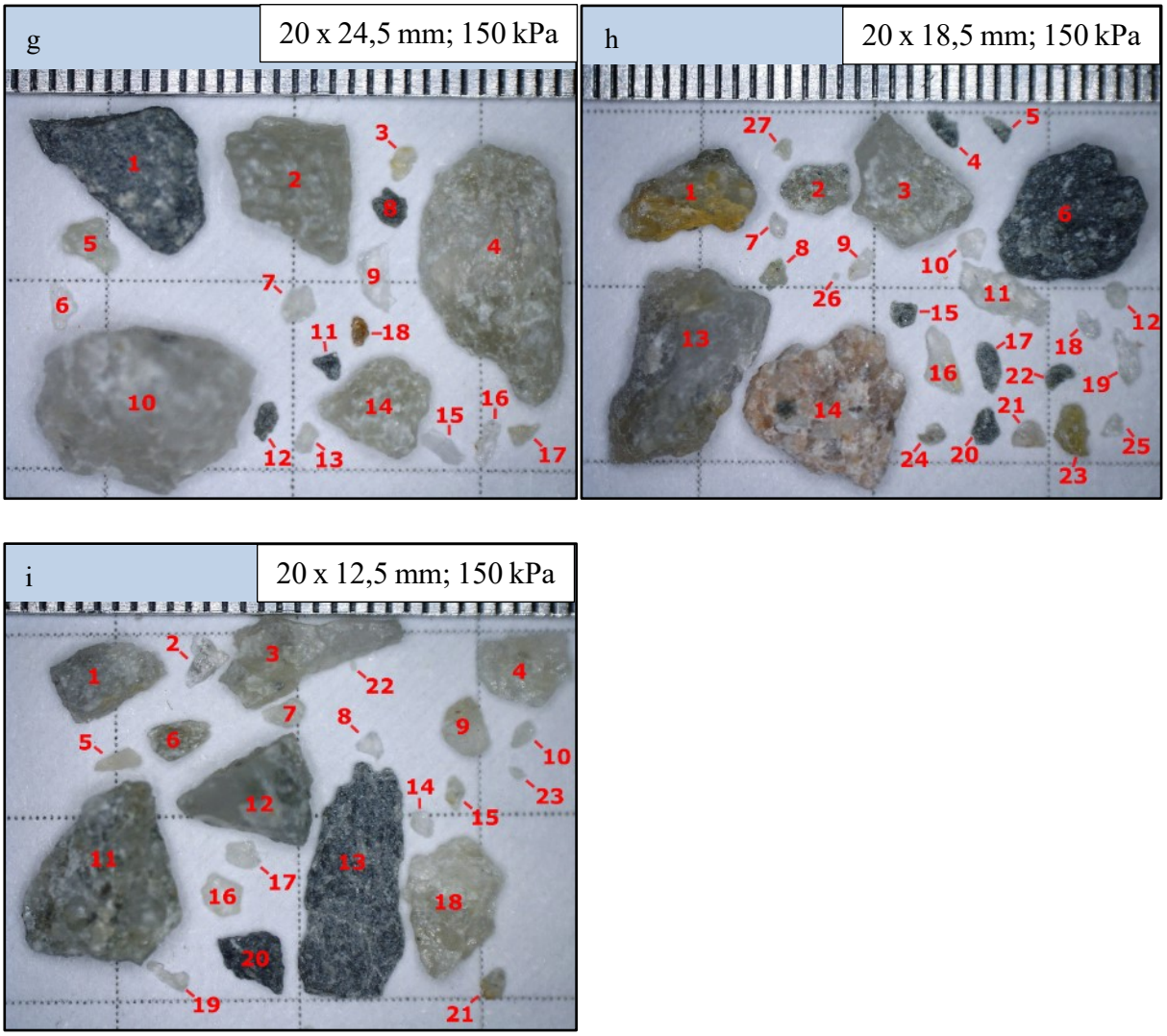

Figure C-4. Images of crushed and tested [at normal stress of 150 kPa] well graded waste rock specimen particles, assessed for grain shape parameters, including shear mould dimension: a) 100 x 24,5 mm; b) 100 x 18,5 mm; c) 100 x 18,5 mm; d) 60 x 24,5 mm; e) 60 x 18,5 mm; f) 60 x 12,5 mm; g) 20 x 24,5 mm; h) 20 x 18,5 mm, and i) 20 x 12,5 mm